

# **FRACTURE CHARACTERISATION OF KAROO AQUIFERS**

by

AHOKPOSSI DEHOUEGNON PACOME

Student number: 2008139541

Dissertation submitted in fulfillment of the requirements for the degree of  
Magister Scientiae in the Faculty of Natural & Agricultural Sciences, Institute for  
Groundwater Studies, University of the Free State, Bloemfontein, South Africa

November 2010

Supervisor: Dr S. R. Rainier Dennis

## DECLARATION

I declare that this dissertation is my own, unaided work. It is being submitted for the degree of Magister Scientiae in the University of the Free State, Bloemfontein. It has not been submitted before for any degree or examination in any other University.

Signed: \_\_\_\_\_

AHOKPOSSI DEHOUEGNON PACOME

\_\_\_\_\_ Day of \_\_\_\_\_ 2010

## **DEDICATION**

This thesis is dedicated to all those who have build and shared knowledge for the protection of the natural resources in general, and water resources particularly.

## ACKNOWLEDGEMENTS

I would firstly, and before all, like to acknowledge the grace of God on me for the experience of life I'm doing in this world.

I would like to thank the director and staff of the Project 'NUFFIC NPT/BEN/151' for giving me a full bursary to complete my Master's degree in groundwater studies.

Special thanks to those responsible of the local coordination the project at 'EPAC', mainly to Dr Bacharou Taoffic of 'EPAC' for encouraging me to pursue an MSc degree in groundwater studies.

I would like to acknowledge the support and supervision of Dr Rainier Dennis, Prof Gerrit van Tonder, and the staff of the Institute for Groundwater Studies at the University of the Free State.

I would also like to acknowledge the assistance of all those who have contributed to the success of the present study but are not mentioned by name.

I would like to thank my wife Corine Islaine, my daughter Benie-Fifa and my parents Marius and Catherine for their continued support.

## CONTENTS

List of Figures .....	8
List of tables.....	11
List of Abbreviation and symbols.....	11
1 Introduction .....	12
1.1 Aim and objectives .....	14
1.2 Thesis Structure .....	14
2 Fractures and Discontinuities in the Geology of the Karoo aquifer.....	16
2.1 General description of fractures.....	17
2.2 Overview of fractures and discontinuities in the geology of Karoo aquifers.....	19
2.2.1 Intrusive and extrusive formations.....	20
2.2.2 Non-intrusive tectonic features .....	26
3 Important fracture's parameters required in Secondary aquifers Characterisation .....	29
3.1 Geological and physical characteristics .....	29
3.1.1 Location .....	29
3.1.2 Orientation .....	29
3.1.3 Fracture connectivity, spacing and length.....	30
3.1.4 Fracture aperture .....	31
3.1.5 Fracture surface roughness .....	32
3.2 Hydraulic and mass transport characters .....	34
3.2.1 Hydraulic characters .....	34
3.2.2 Mass transport characters.....	35
3.3 Variability of fracture characters in time and space .....	38
4 Some properties of Rocks in Relation to fracture characters .....	40
4.1 Electrical properties of rocks .....	40
4.1.1 Archie's law .....	40
4.1.2 Void filling and rock properties .....	41
4.1.3 Bruggeman-Hanai-Sen equation .....	41
4.2 Rocks' hydraulic properties .....	42
4.2.1 Darcy's law .....	42
4.2.2 Hydraulic Conductivity.....	43
4.3 Relationships between rocks' electrical and hydraulic properties .....	44
4.3.1 Hydro-electrical relationships in a primary aquifer .....	45
4.3.2 Hydro-electrical relationships in secondary aquifers.....	46

5	Overview of fracture characterisation methods.....	48
5.1	Fracture characterisation: What is it about?.....	48
5.2	Classification of fracture characterisation methods .....	48
5.3	Review of commonly used methods of fracture characterisation .....	49
5.3.1	Detection of fractures and estimation of their physical characters .....	49
5.3.2	Methods for estimating hydraulic and transport characters .....	60
5.4	Methods commonly used for fracture characterisation in Karoo aquifers .....	74
5.4.1	A decade of fracture characterisation methods testing on the IGS campus test site .....	75
5.5	Summary and recommendations .....	85
6	Theories on Fluid Electrical Conductivity (FEC) and its applicability to fracture characterisation	87
6.1	Definition of Fluid electrical conductivity .....	87
6.2	Fluid electrical conductivity and temperature.....	89
6.3	Borehole fluid electrical conductivity .....	90
6.4	Principles of FEC for aquifer-borehole flow and transport processes analysis .....	91
6.5	Flowing Fluid Electrical Conductivity logging method (FFEC) .....	92
6.5.1	Borehole fluid conductivity logging (field procedure) .....	95
6.5.2	Analysing fluid conductivity logs .....	96
6.5.3	Determination of a fracture transmissivity.....	101
6.6	FEC-based dilution test for fracture characterisation (borehole dilution).....	102
6.6.1	Planning the test.....	103
6.6.2	Field Procedure .....	109
6.6.3	Analysis of the data.....	111
6.7	Discussion.....	113
7	Case studies of FEC-based dilution techniques for fracture characterisation in Karoo aquifer systems	116
7.1	Campus Test Site .....	116
7.1.1	Regional geological setting and site description.....	117
7.1.2	Local geology and geohydrology at the campus test site.....	117
7.1.3	Field work performed .....	118
7.1.4	Tracer tests.....	123
7.2	Paradys Proefplaas Farm.....	131
7.2.1	Site Description.....	131
7.2.2	Local geology and geohydrology at the Paradys Proefplaas .....	133
7.2.3	Local groundwater chemistry at the Paradys Proefplaas .....	135

---

7.2.4	Fieldwork performed .....	135
8	Conclusion and Recommendations .....	156
	REFERENCES .....	159
	APPENDIXES .....	179
	SUMMARY .....	190

## LIST OF FIGURES

FIGURE 2-1 SCHEMATIC AREAL DISTRIBUTION OF LITHOSTRATIGRAPHIC UNITS IN THE MAIN KAROO BASIN (AFTER JOHNSON <i>ET AL.</i> , 1997) .....	16
FIGURE 2-2 GEOHYDROLOGY OF THE LEHMAN'S DRIFT (A) INCLINED SHEET AND (B) DYKE, QUEENSTOWN (AFTER VANDOO LAEGHE, 1980).....	22
FIGURE 2-3 GEOHYDROLOGY OF THE MX4 DYKE / SILL INTERSECTION ZONE, QUEENSTOWN (AFTER VANDOO LAEGHE, 1980) .....	23
FIGURE 2-4: DIFFERENT TYPES OF FRACTURES ASSOCIATED WITH SILL AND RING COMPLEXES (AFTER CHEVALLIER <i>ET AL.</i> , 2001).....	25
FIGURE 3-1 TYPICAL ROUGHNESS PROFILES, DEFINING THE JOINT ROUGHNESS COEFFICIENT RANGE FROM 0 THROUGH 20. (FROM BARTON & CHOUBEY, 1977). .....	33
FIGURE 4-1 ELECTRICAL CURRENT PATH AND FLUID FLOW PATH AFTER BROWN'S MODEL (1989) .....	47
FIGURE 5-1 NATURAL FRACTURE SYSTEMS AND THEIR SIMPLIFICATION INTO SPHERICAL-SHAPED BLOCKS AND SLAB-SHAPED BLOCKS (VAN TONDER <i>ET AL.</i> , 2001) .....	69
FIGURE 5-2 GROUNDWATER FLOW IN AN IDEALISED DOUBLE POROSITY AQUIFER (VAN TONDER <i>ET AL.</i> , 2001) .....	70
FIGURE 5-3 AVERAGE VALUES OF THE HORIZONTAL HYDRAULIC CONDUCTIVITIES, KH, FOR THE MORE IMPORTANT FORMATIONS ON THE CAMPUS TEST SITE AS DETERMINED FROM DOUBLE PACKER TESTS.....	77
FIGURE 5-4 A CONSERVATIVE ESTIMATE OF THE FRACTURE (SHADED) CONNECTIVITY. (AFTER GEBREKRISTOS (2007)).....	84
FIGURE 6-1 LINEAR RELATION BETWEEN FLUID ELICTRICAL CONDUCTIVITY AND ION CONCENTRATION IN GROUNDWATER AT THE CAMPUS TEST SITE. ....	89
FIGURE 6-2 ILLUSTRATION OF FLOWING AND STAGNANT SECTIONS FROM FFEC AND SFEC PROFILES ON PW17 (ADAPTED FROM MORH AND VAN BILJON (2009)) .....	91
FIGURE 6-3 SCHEMATIC PICTURE OF A BOREHOLE WITH N INFLOW POINTS AND, BOREHOLE FLOW W FROM BELOW ADAPTED FROM TSANG <i>ET AL.</i> (1990) .....	94
FIGURE 6-4 FEC LOGGING EQUIPMENT SETUP AT BOREHOLE NC-EWDP-24PB IN THE ARMARGOSA VALLEY. FROM DOUGHTY <i>ET AL.</i> (2006) .....	96
FIGURE 6-5 SCHEMATIC ILLUSTRATION OF ANALYTICAL INTEGRATION .....	98
FIGURE 6-6 SCHEMATIC DIAGRAM OF A WELLBORE WITH SEVERAL INFLOW POINTS. EACH INFLOW POINT IS CHARACTERISED BY A FLOW RATE $Q_i$ , CONCENTRATION $C_i$ , AND POSITION $x_i$ . Q IS THE TOTAL FLOW RATE OUT OF THE WELL; $C_o$ , IS THE INITIAL SALINITY; AND W IS THE INFLOW AT THE BOTTOM OF THE WELL. REDRAWN FROM TSANG <i>ET AL.</i> (1990). ....	99
FIGURE 6-7 EQUIPMENT FOR CONDUCTING A TRANSIENT STATE FEC-BASED DILUTION TEST.....	108
FIGURE 6-8 EQUIPMENT FOR CONDUCTING A TRANSIENT STATE FEC-BASED DILUTION TEST.....	109
FIGURE 7-1 LOCATIONS OF THE BOREHOLES AT THE CAMPUS TEST SITE.....	117
FIGURE 7-2 POSITION OF THE SELECTED FOR BACKGROUND INFORMATION COLLECTION ON THE CAMPUS TEST SITE. ....	118
FIGURE 7-3: GEOLOGY, FEC AND TEMPERATURE PROFILING OF BOREHOLE D5 AT THE IGS CAMPUS TEST SITE (RED CURVE: 2005; BLUE CURVE: 2010).....	119
FIGURE 7-4 GEOLOGY, FEC AND TEMPERATURE PROFILING OF BOREHOLE UO30 AT THE IGS CAMPUS TEST SITE (RED CURVE: 2005; BLUE CURVE: 2010).....	120
FIGURE 7-5 GEOLOGY, FEC AND TEMPERATURE PROFILING OF BOREHOLE UP15 AT THE IGS CAMPUS TEST SITE. ....	122
FIGURE 7-6 RESULT OF SFEC LOGGING ON BOREHOLE UO7. IGS CAMPUS TEST SITE (UFS), THE BLACK ARROW SHOWING THE DETECTED FLOW POINT. ....	124
FIGURE 7-7 RESULT OF FFEC LOGGING ON BOREHOLE UP15. IGS CAMPUS TEST SITE (UFS), THE BLACK ARROWS SHOWING THE DETECTED FLOW POINTS. (PUMPING RATE: 4 L/MIN).....	125
FIGURE 7-8 RESULT OF FFEC LOGGING ON BOREHOLE UP15. IGS CAMPUS TEST SITE (UFS), THE BLACK ARROWS SHOWING THE DETECTED FLOW POINTS. (PUMPING RATE: 10 L/MIN) .....	126



FIGURE 7-9 BULK GROUNDWATER FLOW ESTIMATED ALONG UO7 WITH THE DROSTIAN ANALYTICAL SOLUTION.....	127
FIGURE 7-10 ESTIMATED FORCED GROUNDWATER FLOW AT DETECTED FLOW POINTS IN UP15 UNDER A PUMPING RATE OF 4 L/MIN. ....	128
FIGURE 7-11 ESTIMATED FORCED GROUNDWATER FLOW AT DETECTED FLOW POINTS IN UP15 UNDER A PUMPING RATE OF 10 L/MIN. ....	128
FIGURE 7-12 EXAMPLE OF BORE II RESULTS SIMULATION FOR UO7 (MODEL DATA DO NOT MATCH WITH THE FIELD DATA FOR EARLY AND LATE TIME SIMULTANEOUSLY). ....	130
FIGURE 7-13 LOCATION OF THE CAMPUS TEST SITE ON AN AERIAL PHOTOGRAPH (GOOGLE EARTH).....	132
FIGURE 7-14 COMBINED CONTOURS AND VECTORS MAPS OF GROUNDWATER LEVEL IN THE PARADYS FARM REGION. ....	133
FIGURE 7-15 SURFACE EVIDENCE OF DOLERITE INTRUSIONS IN CLAY AND MUDSTONE FORMATIONS AT THE PARADYS FARM (BLOEMFONTEIN).....	134
FIGURE 7-16 SAR DIAGRAM OF THE WATER QUALITY AT PARADYS (DANIE AND VAN TONDER.,2005). BH3 AND BH1 REPRESENT RESPECTIVELY PD3 AND PD1. ....	135
FIGURE 7-17 MAGNETIC SURVEY TRAVERSES AT PARADYS FARM.....	137
FIGURE 7-18 MAGNETIC SURVEY AT PARADYS FARM (TRAVERSE 2).....	138
FIGURE 7-19 MAGNETIC ANOMALY AND DRILLING POSITIONS AND INTERPRETATION OF THE DIP OF THE DYKE WITH AN INTERPRETED DYKE WIDTH OF ABOUT 24 M.....	138
FIGURE 7-20 MAGNETIC SURVEY AT PARADYS FARM (TRAVERSE 1).....	139
FIGURE 7-21 LOCATION OF THE DYKE (RED LINE) AND TWO SILLS (RED AREA) AT PARADYS FARM; BH3 AND BH4 ARE ALSO SHOWN ON THE MAP. ....	139
FIGURE 7-22 CONCEPTUAL PICTURE OF THE INTRUSION OF THE DYKE INFERRED FROM DRILLING ASSOCIATED WITH THE DYKE RESULTS: BOREHOLES PD6, PD7, PD8, PD9, PD9 AND PD5. ....	140
FIGURE 7-23 POSITIONS OF THE BOREHOLES AT PARADYS FARM.....	141
FIGURE 7-24 PD17 DRILLING CUTS (START FROM THE BOTTOM RIGHT CORNER AND FOLLOW THE NUMERIC ORDER IN THE CELLS AT RIGHT TO RELATE THE CORRESPONDING DEPTH OF EACH CUTS SAMPLING).....	142
FIGURE 7-25 BOREHOLE PD17 GEOLOGICAL LOG WITH THE LITHOLOGY. ....	142
FIGURE 7-26 PD17-CONSTANT PUMPING (5.5 L/S) TEST RESULT ON SEMI-LOG.....	145
FIGURE 7-27 PD17- COOPER-JACOB: $T=20.00 \text{ m}^2/\text{DAY}$ AND $S=0.003$ .....	146
FIGURE 7-28 PD17- $T = 20.2$ FROM RECOVERY: $T'$ AGAINST RISE OF WL FOR SUSTAINABLE YIELD.....	147
FIGURE 7-29 STEADY STATE FEC-BASED DILUTION LOGGING AT PARADYS FARM (BLOEMFONTEIN).....	148
FIGURE 7-30 PUMPING FEC-BASED DILUTION LOGGING (PUMPING RATE: 2.36L/MN) AT PARADYS FARM (BLOEMFONTEIN).....	150
FIGURE 7-31 PUMPING FEC-BASED DILUTION LOGGING (PUMPING RATE: 2.36L/MN) AT PARADYS FARM (BLOEMFONTEIN).....	151
FIGURE 7-32 CONCEPTUAL MODEL OF THE BOREHOLE-AQUIFER SYSTEM SHOWING THE MAIN FLOW PATH INTERSECTED AT THE MUDSTONE-SILL CONTACT ZONE UNDER THE SILL (PARADYS FARM, BLOEMFONTEIN).....	152
FIGURE 7-33 ESTIMATED GROUNDWATER VELOCITY AT DIFFERENT FLOW POINTS (19.5M, 22M, AND 24.5 M), APPLYING DROSTIAN ANALYTICAL SOLUTION TO SFEC PROFILING IN BOREHOLE PD17 (PARADYS FARM, BLOEMFONTEIN). ....	153
FIGURE 7-34 ESTIMATED GROUNDWATER VELOCITY AT DIFFERENT FLOW POINTS (19.5 M, 22 M, AND 24.5 M), APPLYING DROSTIAN ANALYTICAL SOLUTION TO FFEC PROFILING IN BOREHOLE PD17 AT 2.32 L/MIN OF PUMPING. (PARADYS FARM, BLOEMFONTEIN).....	154
FIGURE 7-35 ESTIMATED GROUNDWATER VELOCITY AT DIFFERENT FLOW POINTS (19.5 M, 22 M, AND 24.5 M), APPLYING DROSTIAN ANALYTICAL SOLUTION TO FFEC PROFILING IN BOREHOLE PD17 AT 9.47 L/MIN OF PUMPING. (PARADYS FARM, BLOEMFONTEIN).....	155
FIGURE 0-1PD17- MAGNETIC SURVEY AT PARADYS (TRAVERSE 3).....	179
FIGURE 0-2PD17- MAGNETIC SURVEY AT PARADYS (TRAVERSE 4).....	179
FIGURE 0-3PD17-CONSTANT PUMPING (5.5L/S) TEST RESULT ON LOG-LOG.....	180

FIGURE 0-4PD17-CONSTANT PUMPING (5.5L/S) TEST RESULT ON DERIVATIVE PLOT (S') .....	180
FIGURE 0-5ESTIMATED GROUNDWATER VELOCITY ALONG THE PD17 IN AMBIENT CONDITION, APPLYING DROSTIAN ANALYTICAL SOLUTION. (PARADYS FARM, BLOEMFONTEIN) .....	181
FIGURE 0-6ESTIMATED GROUNDWATER VELOCITY ALONG PD 17 AT 2.32 L/MIN OF PUMPING, APPLYING DROSTIAN ANALYTICAL SOLUTION. (PARADYS FARM, BLOEMFONTEIN) .....	182
FIGURE 0-7ESTIMATED GROUNDWATER VELOCITY ALONG PD 17 AT 9.47 L/MIN OF PUMPING, APPLYING DROSTIAN ANALYTICAL SOLUTION. (PARADYS FARM, BLOEMFONTEIN) .....	183
FIGURE 0-8PD13 BREHOLE LOG .....	183
FIGURE 0-9EXAMPLE OF BORE II INPUT FILE SET UP FOR UO7 .....	184
FIGURE 0-10EXAMPLE OF BORE II DATA FILE SET UP FOR UO7 .....	185
FIGURE 0-11EXAMPLE OF BORE II INPUT FILE SET UP FOR UP15 .....	186
FIGURE 0-12EXAMPLE OF BORE II DATA FILE SET UP FOR UP15 .....	187
FIGURE 0-13EXAMPLE OF BORE II RESULTS SIMULATION FOR UP15 .....	188

## LIST OF TABLES

TABLE 5-1: COMPARATIVE TABLE OF COMMON CONVENTIONAL WELL LOGS .....	57
TABLE 5-2 DEPTH OF THE FRACTURE ZONE IN THE NEW BOREHOLES (M UNDER SURFACE) (AFTER RIEMANN, 2002) .....	80
TABLE 5-3: PARAMETER VALUES FOR UO26-TEST OBTAINED FROM BARKER MODEL (RIEMAN, 2002).....	81
TABLE 5-4: PARAMETER FOR UO5-TEST OBTAINED FROM BARKER MODEL (RIEMAN, 2002).....	81
TABLE 5-5 PUMP TEST RESULTS IN THE CAMPUS SITE (PRETORIUS., 2007).....	83
TABLE 6-1 SUGGESTED TRACERS FOR FEC LOGGING APPLICATIONS .....	106
TABLE 6-2 COMPARATIVE TABLE OF SUGGESTED TRACERS FOR FEC LOGGING APPLICATION .....	106
TABLE 7-1 RANGES OF DISTRIBUTION OF THE READINGS IN INTERSECTING BOREHOLES .....	121
TABLE 7-2 RANGES OF DISTRIBUTION OF THE READINGS IN NON-INTERSECTING BOREHOLES.....	121
TABLE 7-3 SHORT SUMMARY OF THE BOREHOLE CENSUS AT THE PARADYS FARM.....	135
TABLE 7-4 SOME PARAMETERS ESTIMATED FROM SLUG TESTS (VIVIER METHOD).....	143
TABLE 7-5 SOME PARAMETERS ESTIMATED FROM SLUGS TESTS (RULE OF THUMB AND SWENSON EQUATION) .....	144

## LIST OF ABBREVIATION AND SYMBOLS

**FEC:** Fluid Electrical Conductivity

**FFEC:** Flowing Fluid Electrical Conductivity

**SFEC:** Static Fluid Electrical Conductivity

**TDS:** Total Dissolved Salt

**LNAPL:** Light Non - Aqueous Phase Liquid

**DNAPL:** Dense Non - Aqueous Phase Liquid

**TLC:** Water Temperature Level and Conductivity meter

**IGS:** Institute for Groundwater water studies

**EPAC:** Ecole Polytechnique d'Abomey-Calavi

## 1 INTRODUCTION

Life generally depends on water and especially on the availability of freshwater (or non-saline water), to which access has been and continues to be problematic. Industrial developments and new technologies have contributed to upscale the access of water resources, mainly those stored deeper in the subsurface, through the development of exploration techniques, new drilling equipment and fluid conductor appliances (pipes and accessories). These developments in access to groundwater, coupled with the advantages related to groundwater quality (potential natural protection from pollution) increase the interest in groundwater as a water resource. Nowadays, groundwater constitutes an important source of water for vital human needs: drinking, stock-farming, irrigation of plants, ecological requirements and industrial purposes, in many places around the world, mainly in the arid and semi-arid environments. Morris *et al.* (2003) describe groundwater as the largest source of freshwater on the African continent.

This increasing need for groundwater and the development of industries (mines and others), mainly the oil and hydrocarbon industries, has created various other challenges related to the sustainable management of groundwater resources that does not cause long-term deterioration of the overall resource in terms of quality and quantity. For example, the quality of surface water and groundwater has generally declined in recent decades due principally to growth in agricultural and industrial activities (UN, 2006). In South Africa, water resources (fresh water) are already being stressed and the country is becoming a water-scarce country. Alcamo *et al.* (2003a, based on Water-Gap) state that the water stress indicators (withdrawal to availability ratio) for most of South Africa range between 0.4 and 0.8 (indicating high stress). This situation is also due to the effects of climate change and climate variability (drought, floods) associated with global warming. This presents a challenge to all water resource managers to ensure that the basic water needs of all South Africans are met. 'Until recently, groundwater in South Africa has been managed as a separate entity to surface water. Additionally, the status of groundwater as private has led to unsustainable management and subsequent resource degradation, necessitating a new approach' (Wright and Xu, 2000).

The first step for developing politics, strategies, and techniques for the optimum exploitation of groundwater resources is a conceptual understanding of the behaviour of groundwater within different geological environments. A good estimation of aquifer parameters (characterisation) is the basis of managing groundwater resources and understanding groundwater flow and transport processes. In fractured aquifers, fractures constitute conduits through which groundwater flows preferentially, and thus control the main flow of groundwater. More than 90 % of the aquifer systems in South Africa consist of fractured rock, formed of either hard rock or porous media (Karoo aquifers, Table Mountain sandstone aquifers and the dolomitic aquifer systems) (Weaver *et al.*, 1999).

Characterisation of such fractured-rock aquifers in principle requires information on the nature of both the fractures and the rock matrix, although in practice most hydrogeological studies are often reduced to a characterisation of the bulk flow (formation and fracture), as is the case in the Main Karoo aquifer. This is due to the nature (primarily exploration) and the budget (limited) of such studies. Such simplified studies of bulk flow are efficient for general water supply purposes where the position of the fracture (in a borehole) is needed for reasons of sustainability, but become limited for more managerial uses, prediction (modelling) and for mass transport studies like the cases of the LNAPL and DNAPL studies for example.

'The complexity and the physical structure of fracture characterisation were shown to have a significant effect on modelling results, to the extent that the fracture zone should be characterised fully before simulation models are used for DNAPL simulations' (Dennis *et al.*, 2010). The importance of knowing the character of fractures' is gaining more interest in South Africa. Among others, Akoachere and van Tonder (2009) of the Institute for Groundwater Studies, (University of the Free State) have focused on the issue of fracture characterisation and have developed two methods to determine inclined and horizontal fracture apertures in fractured-rock aquifers.

## 1.1 Aim and objectives

The present dissertation aims to study fracture characterisation in the Karoo aquifer system. Based on previous reports and publications, an overview of fractures in the studied aquifer and a critical review of existing characterisation methods will be done with a special focus on common methods used for Karoo aquifers. A promising method of fracture characterisation, namely, Fluid Electrical Conductivity (FEC) logging, developed by Tsang *et al.* (1990, 2002, 2005), and the FEC-based dilution test, an emergent method in South Africa (Lasher *et al.*, 2009; Mohr Samuel and van Biljon, 2009) will receive special attention. The FEC-based dilution technique will be performed on two different experimental sites of the University of the Free State.

From the field results, the benefits and drawbacks of the applied method will be discussed and recommendations will be provided as to the basis for future research on the refinement of the application of the method, particularly for use in Karoo aquifer systems.

## 1.2 Thesis Structure

The present thesis is divided into eight (08) chapters, including this introduction (Chapter 1) which provides the aims and the general structure of this study. In Chapter 2, typical fracturing developed in the geology of Karoo aquifer is reviewed in terms of their hydrological importance. Chapter 3 presents the most common fracture parameters required for aquifer characterisation.

Chapter 4 provides a review of the available literature on the existing methods for fracture characterisation, and serves to outline briefly the fracture characterisation studies previously conducted on the main Karoo Supergroup Aquifers. Chapter 5 discusses the relation between fractures' electrical conductivity and hydraulic conductivity.

In Chapter 6, Fluid Electrical Conductivity and the different ways it can serve for the deduction of accurate fracture parameterisation is discussed. The Flowing Fluid Electrical Conductivity (FFEC) method of fracture characterisation (Tsang *et al.*,

1990) and its simplification (FEC-based dilution technique using NaCl tracer or borehole dilution) for fracture characterisation are also presented. Aspects such as the choice of tracer, the amount of tracer, and typical field methodology are discussed.

Chapter 7 reports on field work conducted at two sites at Bloemfontein, the Campus Test Site and the Paradys Proefplaas Farm. The approach and field methodology developed are presented and the results from analysis and interpretation are discussed. Chapter 8 gives a summary and conclusion for the study and provides some recommendations for further work on fracture characterisation of the Karoo. The references used in the present study are documented after Chapter 9 and before the different annexures.

## 2 FRACTURES AND DISCONTINUITIES IN THE GEOLOGY OF THE KAROO AQUIFER

The Karoo aquifer in South Africa is formed in sedimentary rocks (mudstone, siltstone, shale and sandstone of the Karoo group), which have been fractured, intruded and metamorphosed to varying degrees and which cover much of the interior of the country (Figure 2-1). It forms part of the fractured metasedimentary aquifer type as classified by Colvin *et al.* (2003). In the present dissertation, the Karoo dyke and sill aquifer types as classified by Colvin *et al.* (2003) will be treated as part of the main Karoo aquifer.

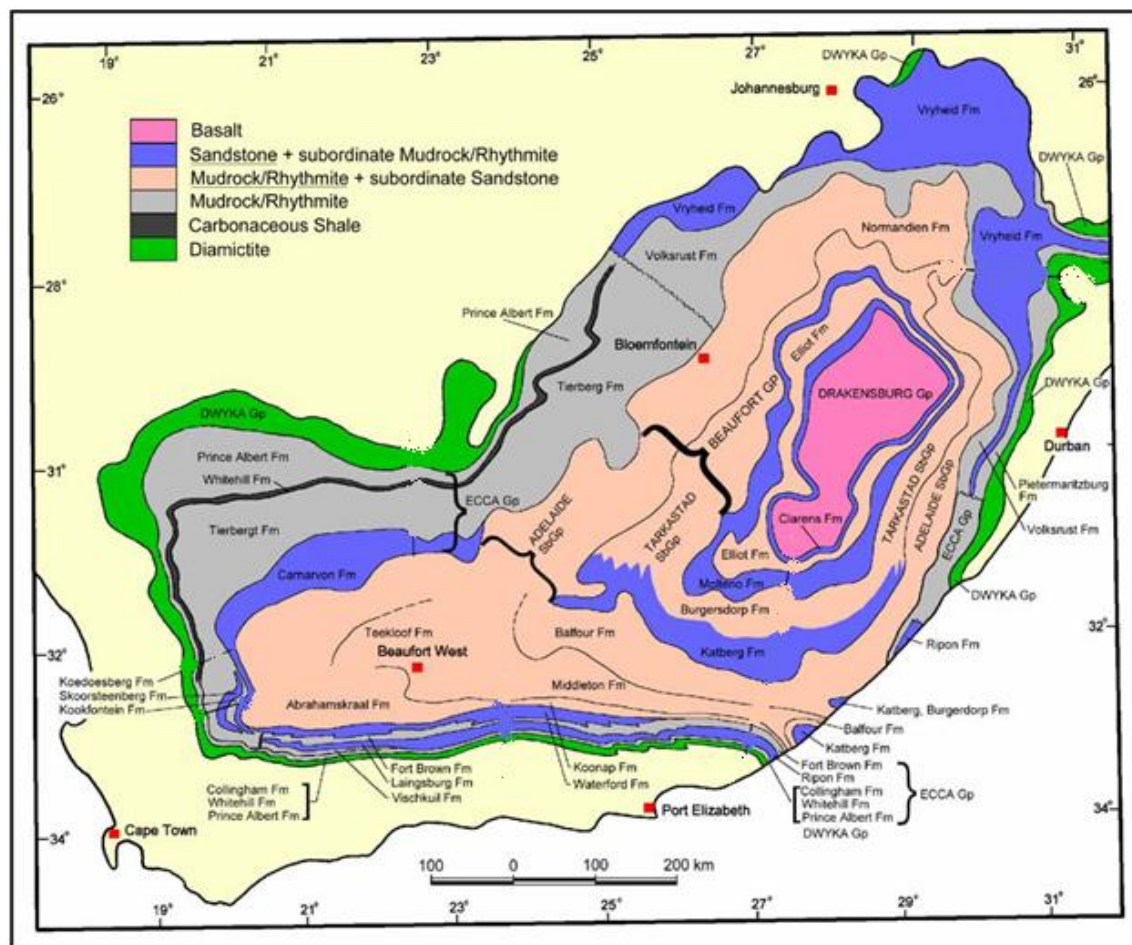


**Figure 2-1 Schematic areal distribution of lithostratigraphic units in the Main Karoo Basin (after Johnson *et al.*, 1997)**

Several tests and reports (on different earth sciences (geology, geography, hydrogeology, environment, hydrology, etc.) provide a good description of the geological and hydrological properties of the Karoo Basin (Botha *et al.*, 1998;



Woodford and Chevallier, 2001, 2002). Since the main issue in this paper is fracture characterisation of Karoo aquifers, the aim in this section of the present dissertation, is an overview of the fracturing associated with the main geological features in the Karoo basin. An understanding of such natural processes may give a better view of the different types of fractures that may be encountered in the basin and so may help to better decide the approach for characterising them. A brief general description of fractures is given first.

## **2.1 General description of fractures**

Generally, fracture is a term used by scientist to describe all types of discontinuities. In heterogeneous geological formations, any variation in the physical and mechanical properties of materials that compose the media, or any stress heterogeneities over a broad range of scales, leads to the existence of discontinuities in displacement across surfaces or narrow zones in the subsurface. Geologically, a fracture is defined as a plane along which lithostatic, tectonic and thermal stresses or high fluid pressure, have caused a relative partial loss of cohesion in the rock. Fractures may occur from microscopic to continental scales, with a variety of geometries, mechanical effects, and flow properties. Three main groups can be distinguished according to the nature of displacement discontinuity:

- a) 'Mode I' fractures: Also called dilating fractures or joints, they can be recognised by any physical sign of dilation between the fracture surfaces. The displacement discontinuity occurs in a direction perpendicular to the fracture surfaces. Joints filled with minerals or clay deposits form 'veins'.
- b) Shearing fractures: Described also as faults, these are relative displacement discontinuities, where the fracture surfaces' movements are predominantly in a direction parallel to the fracture surfaces. A shearing fracture is called a 'mode II' fracture when the movement is perpendicular to the fracture front and a 'mode III' fracture when it is parallel to the fracture front. When a fault is filled with minerals or clay deposits, it is called a 'seam'.
- c) Closing fractures or pressure solution surfaces are also known as stylolites, and are generally formed in sedimentary rock by solution that occurs at the contact

surfaces of grains. The term 'filled pull-apart' is often used to describe a closing fracture that is filled by minerals or clay deposits.

Hydrogeologists are usually concerned with the first two groups. "Conventionally, a fracture or joint is defined as a plane where there is hardly any visible movement parallel to the surface of the fracture; otherwise, it is classified as a fault. In practice, however, a precise distinction may be difficult, as at times within one set of fractures some planes may show some displacement whereas others may not exhibit any movement" (Akoachere and van Tonder, 2009; Cook, 2003). The difficulty of clearly distinguishing one mode from another may also be emphasised by a natural occurrence of a combination of displacement discontinuities (mixed-mode fractures). Distinctive surface features such as 'plumose texture' and 'grooves and striations or slickensides' may be used to identify respectively joints and faults (Bahat, 1988; Patterson, 1958; Suppe, 1985). The conventional definition is the one adopted in the present dissertation.

Different ways of classifying fractures (as joints) exist and can be found in most structural geology textbooks. According to the direction of extending of a fracture front to the regional fold axis, fractures may be subdivided as longitudinal (parallel to the regional fold axis), transverse (perpendicular to the regional fold axis) or oblique (Singhal and Gupta, 1999). The common classification of fractures or joints is based on their geometric relationship with the bedding of the rock. When a joint strikes parallel to the strike of the bedding, it is described as 'strike joint'. When it strikes parallel to the dip direction of the rock, it is described as 'dip joint'. A 'bedding joint' is one that is parallel to the bedding plane and an 'oblique or diagonal joint' strikes at an angle to the strike of the rock. Another approach consists of considering fractures by relating them to the stresses that form them.

Often, groundwater flow in a fracture system is controlled by groups of interconnected fractures (a fracture network) and that may or may not be evenly distributed. In a fracture network, a group of approximately parallel fractures of the same age and type is termed a fracture set. Generally, a fracture network consists of multiple sets of fractures.

## 2.2 Overview of fractures and discontinuities in the geology of Karoo aquifers

Many of the descriptions given in the present section are based on previous works performed in the Karoo, especially the one edited by Woodford and Chevallier (2002). Fracture occurrence in the Karoo aquifer may be associated with different stress (or combined stress) mechanisms in different geological units of formation. The most important of such mechanisms are:

- Magma activities such as extrusive (the Drakensberg lavas) and intrusive features (dolerites, breccia plugs and volcanic vents, Kimberlite and associated alkaline intrusive complexes);
- Non-intrusive tectonic features, which include regional lineaments, folding, vertical jointing and faulting, bedding-plane fracturing and seismotectonic, neotectonic or unloading features;
- Diagenesis, paleo-fluid movement and thermo-metamorphism; and
- Weathering.

Each of these processes is associated with some respective type of fracturing, according to the geological environment in which the processes take place.

The Dwyka Group is mainly characterised by diamictite, shale and a few sandstone deposits (in the glacial valleys of the northern facies), and thus offers very few large-scale exploitable aquifers. The few exploitable aquifers are found mainly in the form of water confined in sand and gravel deposits along beaches or in high fracturing zones like the ones found in folded Dwyka rocks at great depths in the southern Karoo basin by the SOEKOR deep core-boreholes. Water has been struck at 3700 m below ground surface in the Dwyka diamictite (borehole SP1/69), near East London (Rowsell and de Swardt, 1976). The presence of such fractures and the interconnection between them may constitute the main factor that controls water flows and associated mass transports in the folded Dwyka rocks.

The Clarens formation is known as the most homogeneous formation in the Karoo Supergroup, with a relatively high porosity (average 8.5 %) and a very low

permeability (1-73 md<sub>air</sub>) because it is poorly fractured (Beukes, 1969; Rowsell & de Swardt, 1976). This is due to the fine grained action sand.

### **2.2.1 Intrusive and extrusive formations**

The Drakensberg lavas, mainly the basalts, are often associated with open thermal joints with good interconnectivity that are important for hydrogeological studies. The most important geological features associated with fractures in the Karoo Supergroup are the intrusive structures. Intrusive formations in the Karoo Supergroup may be grouped either as dolerite (Karoo dolerite), breccia plugs and volcanic vents, or Kimberlite and associated alkaline intrusive complexes. Detailed information related to the Karoo dolerite can be obtained from Fitch and Miller, 1984 (ages, and geneses); Rogers and du Toit, 1903; du Toit, 1905; Chevallier and Woodford, 1999 (mapping); and du Toit, 1920 and Mask, 1966 (structural aspects). The Karoo dolerite consists of complexes of dykes and sills. Only fracturing associated with dolerite intrusion will be discussed in the present section.

#### **2.2.1.1 Dykes**

The 'en-échelon' pattern along strike exhibited by dolerite dykes is often of concern in groundwater explorations or when attempting to determine preferential flow paths in the fractured Karoo Supergroup. Such a pattern can be detected by mapping. From pumping test analyses in Botswana, Bromley *et al.* (1994) found that dykes that are thicker than 10 m may serve as groundwater barriers, but those of a relatively smaller width are permeable, as they develop cooling joints and fractures. Van Wyk (1963) reported that more than 80 % of the successful boreholes (yield > 0.13 l/s) drilled into Karoo sediments in northern Kwazulu-Natal are directly or indirectly related to dolerite intrusions. Sami (1996) noted that the yield of boreholes adjacent to dolerite dykes intruding the fractured sandstone or mudstone of Karoo aquifers is significantly higher than elsewhere in the basin.

During and after a dolerite dyke emplacement, the country rock is often fractured, leading to a set of master joints parallel to its strike over a distance that does not vary greatly with the thickness of the dyke (between 5 and 15 m). According to van Tonder, numerous case studies show that dykes with a width of between three and

seven meters are the best dykes in terms of water bearing. Cooling fractures called 'contact *oureoles*' develop on the sides of a thin dyke that has cooled quickly, so that fractures with large apertures develop. When dealing with a wide dyke, water-bearing fractures are often located close to the side of the dyke in mudstone or shale formations, but in sandstone formations they develop as bedding-plane fractures along the side of the dyke. The dyke itself is the main target for the investigation of flowing fractures in the eastern Free State. In a number of coalmines in the Vryheid-Dundee area, van Wyk (1963) distinguished three sets of pervasive-thermal, columnar joints approximately 120° apart, and joints parallel to the contact, confined mainly to the host rock alongside the dyke. During his investigation in the area, he showed how the high permeability of the dyke contact zones are related to the joints developed during the cooling of the intrusion. The dolerite dyke itself may be shaped by a set of thermal or columnar jointing, perpendicular to its margins. These thermal joints, originating from the dolerite dyke, also extend into the host rock over a distance not exceeding 0.3–0.5 m from the contact. Vandoolaeghe (1980) described open fractures (sub-horizontal: <50°) or fissures that transgress the dyke and extend some distance (up to 15 m away from the contact) into the country rock, associated with the Lehman's Drift dyke near Queenstown (Figure 2-2 and Figure 2-3). The same author reported similar fractures occurring in the Middelburg district, associated with the Dunblane dyke (Vandoolaeghe, 1979).

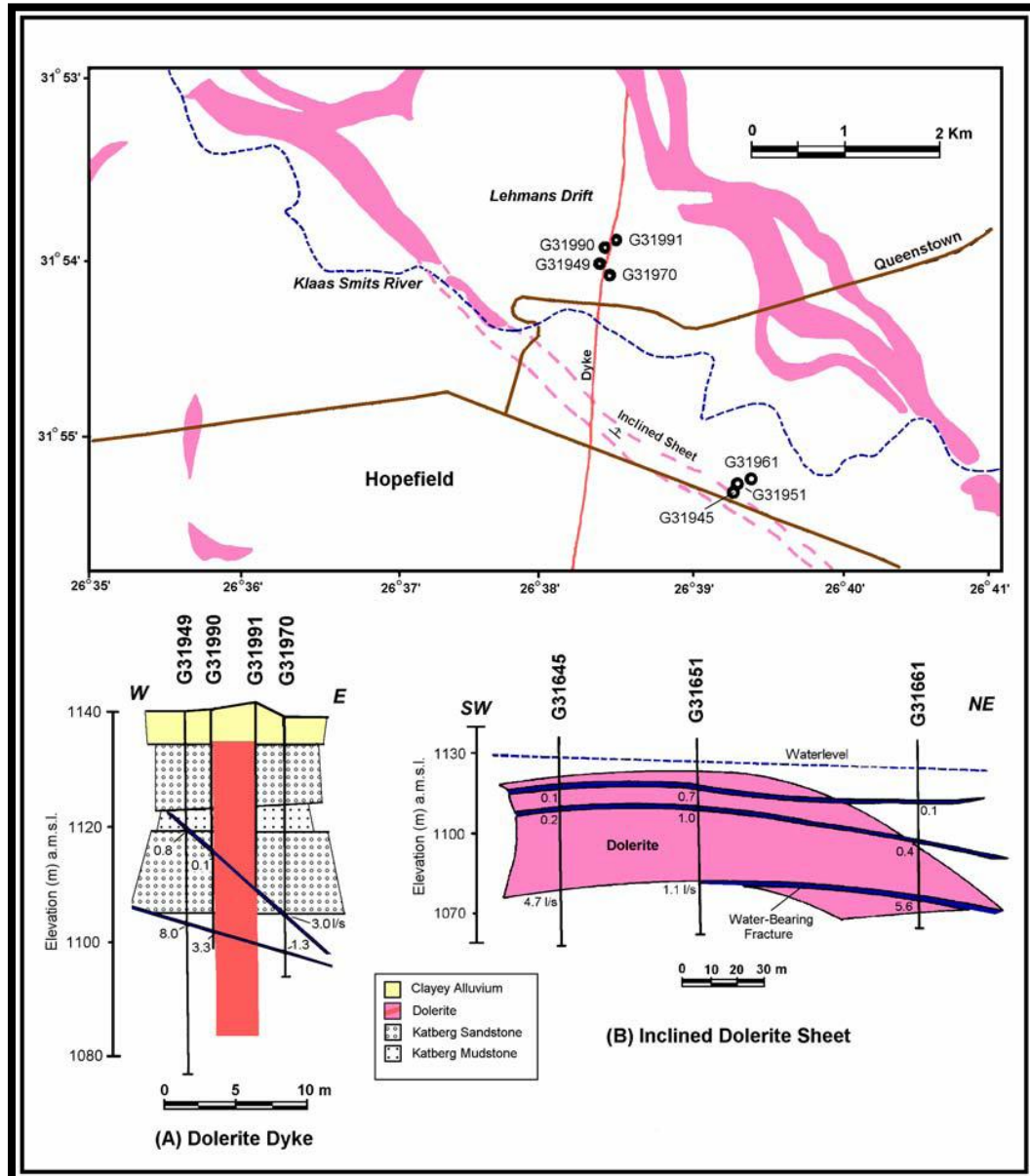
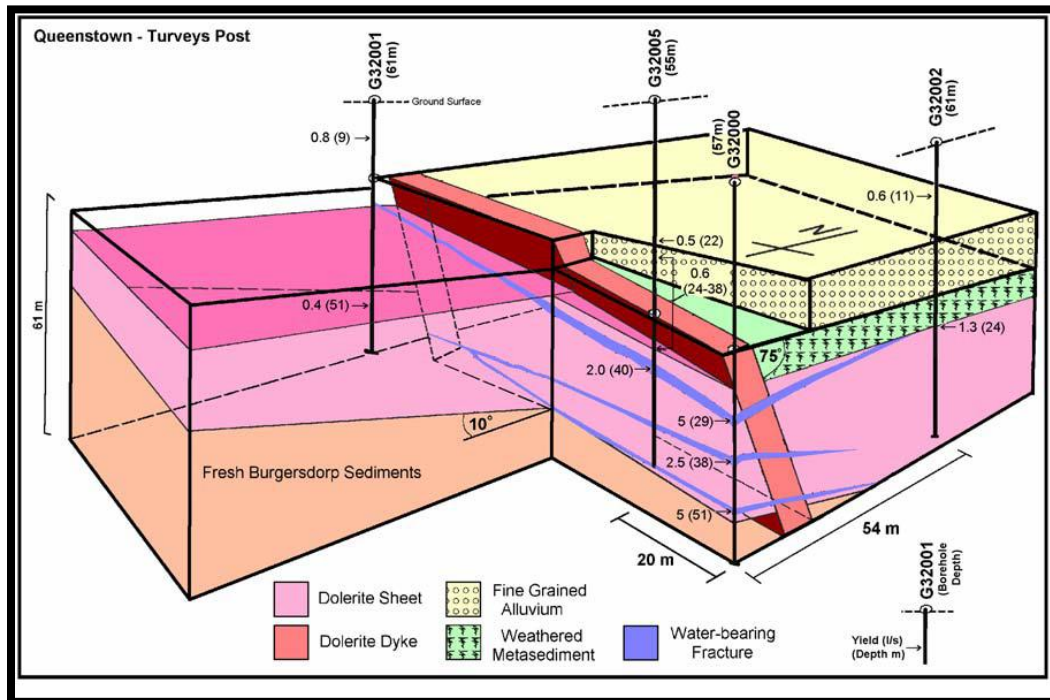


Figure 2-2 Geohydrology of the Lehman's Drift (a) inclined sheet and (b) dyke, Queenstown (after Vandoolaeghe, 1980).



**Figure 2-3 Geohydrology of the MX4 dyke / sill intersection zone, Queenstown (after Vandoolaeghe, 1980)**

Extensive deep and lateral fracturing (shearing and jointing) are associated with wide and extensive dykes such as the E-W Victoria West dyke, the NNW Middelburg dyke and the curved 'gap' dykes near East London. These regional discontinuities could form part of a fracture network wherein deeper-seated groundwater flows on a regional scale. Tectonic reactivation of dolerite dykes is reported by Woodford and Chevallier (2001) in the Loxton-Victoria West area, where there are sub-vertical fissures with a width of up to 150 mm, often filled with secondary calcite or calcrete. Dolerite dykes are also often associated with horizontal, transgressive fracturing.

### 2.2.1.2 Sills

Sills and ring complexes are acknowledged as major features in the Karoo. Du Toit (1905, 1920), one of the first to describe such features, gave explicit reports on their stratigraphy and distribution. He signalled the existence of preferential horizons associated with dolerite sills at the Dwyka-Ecca Group contact, the Prince Albert-White Hill Formation contact, the Upper Ecca-Lower Beaufort Group contact



and other lithological boundaries within the Beaufort Group. The lithology of the country-rock strongly controlled the emplacement of the sills. Satellite images constitute the first tools to identify dolerite sills and ring-complexes, which often display sub-circular saucer-like shapes with rims that are generally exposed as topographic highs and form ring-like outcrops. Such patterns constitute a potential indirect (surface-based) fracture detection tool. Sill intrusion is often followed by vertical jointing in the sediments above the sills or inclined sheet. Botha *et al.*, (1998) reported that sills with laccolith shapes could have contributed to the existence of bedding-parallel fractures in the host rock.

Like dolerite dykes, dolerite sills are also subject to internal fracturing. Chevallier *et al.* (2001) regrouped these fracturing features into three major types (see figure 2-4):

- (a) Vertical thermal columnar jointing that is well developed within the flat-lying sill (*F1*). From aerial photo examination and satellite imagery it appears that the outer sill often displays a very dense system of columnar jointing.
- (b) Fractures parallel to the strike of the intrusion are dominant within the inclined sheet. Aerial photos and satellite imagery show that the actual circular inclined sheet is the most fractured part of the complex (*F2*).
- (c) Well-developed, oblique or sub-horizontal open fractures develop within curved portions of the sill. In the western Karoo, these fractures are often infilled with secondary calcite (*F3*). Vandoolaeghe (1980) made similar observations in the eastern Karoo.

The possibility of recognising columnar joints and fractures parallel to the strike from aerial photo examination and satellite imagery constitutes an advantage for their localisation.



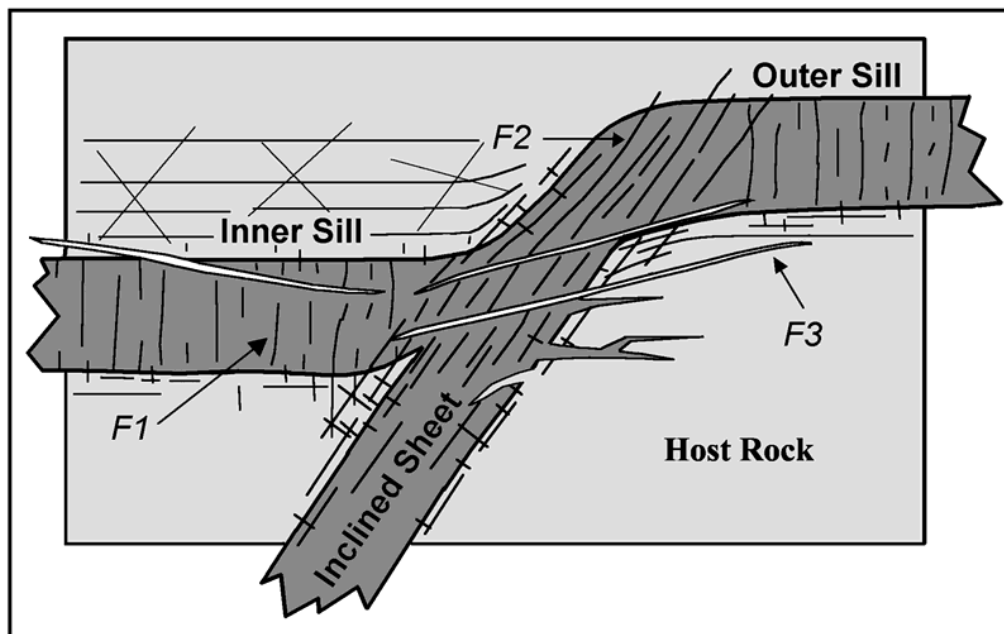


**Figure 2-4: Different Types of fractures associated with sill and ring complexes (after Chevallier *et al.*, 2001)**

When using surface methods to determine fracture location and extent, one should be aware that the dolerite fracturing extending is function of the host rock's material. Fracturing at the junction between a feeder dyke or inclined sheet and a sill is very localised, and thus represents a challenging exploration target that may require drilling of deeper (up to 200-350 m) boreholes (Woodford and Chevallier, 2002). While fracturing in the sediment above an up-stepping sill or at the base of an inner sill can extend some distance from the dolerite contact into the country rock.

### **2.2.1.3 Breccia plugs and volcanic vents**

Breccia plugs and volcanic vents may both be compared to pipe-like structures filled with brecciated and fractured material. The large extent and uniform fractures of volcanic vents, and of breccia plugs with a more limited size, constitute highly permeable, preferential flow targets for groundwater.

Similar to breccia plugs, volcanic vents represent easily locatable, drilling targets for high yielding boreholes because of their shape, size and degree of brecciaing, and they potential association with large, open fractures that control the behaviour of local aquifer systems. In the Clarens formation, where the high porous sandstone

is poorly fractured and has a low permeability, volcanic vent may be the most important groundwater exploration targets (Woodford and Chevallier, 2002).

#### **2.2.1.4 Kimberlites**

Kimberlite fracture swarms consist of parallel fissures and associated joints or fractures. The fissures are always closely spaced (approximately 10 to 50 m apart). This pattern of the fissures allows Kimberlite fissures to be discerned from dolerite dykes on aerial photographs as regularly spaced, narrow, co-linear features with relatively denser vegetation growth along the fissure. This is an advantage for the characterisation of associated joints or fractures (at least in terms of localisation and distinction). Several researchers give good descriptions of the occurrence of Kimberlites and associated fractures in the Karoo Supergroup (Dawson, 1962, Greef, 1968; Nixon and Kresten, 1973; Norman *et al.*, 1977; Nixon *et al.*, 1983; Chevallier, 1997). Mega-joints (parallel) often accompany the emplacement of the Kimberlite, but no transgressive, water-bearing fractures have been developed along Kimberlite fissures and diatreme pipes. The mega-joints that accompanied the emplacement of the Kimberlite form important fractured domains on a regional scale where clusters of Kimberlites occur.

#### **2.2.2 Non-intrusive tectonic features**

Fracture systems (geophysical anomalies) in the Karoo basin may also be associated with non-intrusive tectonic features such as regional lineaments, folding, vertical jointing and faulting, bedding-plane fracturing and seismotectonic, neotectonic or unloading features.

##### **2.2.2.1 Regional lineaments**

Regional lineaments such as deep-seated pre-Karoo structures, geophysical lineaments (Beattie, Williston and Mbashe) magnetic anomalies (e.g. the Kaapvaal Craton margin), major faults (Thomas *et al.*, 1992), and major morphological lineaments detectable from digital elevation models (Woodford and Chevallier, 2002) have been identified in the Karoo, but their influences on the behaviour of groundwater flows have not really been proved. The shallow Tugela (Natal) fault formed by juxtaposition of two different formations (with different hydrogeological

characters) has been identified by Woodford and Chevallier (2002) to be of particular interest for hydrologists. Meyer and van Zijl (1980) reported on the yield potential of these deep-seated structures. The occurrence of flooding in Shaft 2 of the Orange–Fish River Tunnel is evidence of such a structure (Meyer and Van Zijl, 1980). The detection and localisation of such deep-seated structures often constitute geophysical challenges.

#### **2.2.2.2 Folding**

The Karoo Supergroup has been affected by folding processes of varying style and intensity. Campbell (1975), Stear, 1980, Hälbig and Swart (1983), Coetzee (1983), Cole *et al.* (1991), Newton (1993), Woodford and Chevallier (1998), Woodford and Chevallier (2001), among others, have given valuable reports on the occurrence of such tectonic features, and their classification. Six E-W folding zones (zone1 to zone6) with different degrees of structural deformation in " the Cape Orogeny " (Hälbig and Swart, 1983) and a number of NNW and NNE trending oblique lineaments, fracture sets and master joints in the Beaufort West area are the results of folding processes in the Karoo Supergroup. Such features are associated with the development of a dense network (with a high degree of connectivity) of open fractures with different characters (geometry, size and attitude). The high degree of connectivity between fractures should result in more extensive aquifers, and thus give a regional-scale importance to folding features in fracture characterisation.

#### **2.2.2.3 Vertical faulting and master joints**

The geological and structural framework of the Karoo is also marked by vertical faulting and master joints. Campbell (1975), Parsons (1986), and Hancock and Engelder (1989) among others, described such features well. The master joints may be identified on conventional remote sensing imagery by their detectable systematic joint sets, which are dominant in the Karoo and form extensive features (>1 km). Such features are often encountered in the sandstone of the Beaufort Group. They generally have limited vertical extension and are poorly interconnected. However, extensive mega-joints and faults that have considerable

vertical extension and cut through different lithological units, may be encountered in some places in the Karoo.

#### **2.2.2.4 Bedding-plane fracturing**

Horizontal fractures (joints with horizontal-shear patterns) occur generally at local scale in the Karoo aquifer. The southern folded regions provide only one example of regional horizontal fractures in the Karoo. Botha *et al.* (1998) described the occurrence of such bedding-plane fractures in the Karoo. Such features generally extend for some 10 to 20 m and the thickness of the zone affected by this shear deformation is usually in the order of 0.5 m (Woodford and Chevallier, 2002). They serve as lateral conduits for groundwater, but because of their general local scale and discontinuous aspects, cannot control regional aquifer behaviour. Characterisation of such fractures has been carried out by the Institute for Groundwater Studies in the Ecca shale on the Free State University campus test site (Botha *et al.*, 1998).

#### **2.2.2.5 Seismotectonic, neotectonic, and unloading features**

Very few neotectonic activities have been clearly related to seismotectonic stress provinces in South Africa. A fault in a recent deposit on the farm Bultfontein in the Free State, has been attributed to a NNW extensional regime by Andreoli *et al.* (1996). The intercepted 'open' E/W-striking joint system in Shaft 2 of the Orange–Fish River Tunnel in the Eastern Cape was reported as evidence of the eastward extent of the Cape seismic (stress) province by Olivier (1972). Haxby and Turcotte (1976) mentioned that erosional unloading causes isostatic rebound and thermal cooling, and usually creates surface extension that results in a series of recent joint systems. Although fracturing created under the prevailing crustal-stress regime is assumed to significantly affect the occurrence of groundwater, no proof of such effects has been given nor critically tested (Hartnady and Woodford, 1996)

### 3 IMPORTANT FRACTURE'S PARAMETERS REQUIRED IN SECONDARY AQUIFERS CHARACTERISATION

In groundwater studies, the fractures parameters required for a better conceptual understanding of a given aquifer system, vary according to the purposes of the study and the scale of the study area. Kueper *et al.* (2003) and Gebrekristos (2007) among others have described the properties of fractures that are needed for DNAPL site characterisation, for example. The important fracture characteristics needed in a simple groundwater exploration for water supply will not necessarily be the same, as in regional groundwater modelling for risk assessment and aquifer vulnerability management. However, some important characteristics are common in the characterisation of different fractures, and these are generally grouped into two main groups of characters: (1) geological and physical characteristics and (2) hydraulic and mass transport characters. Others like Kornelius (2002) subdivided them into three groups: (1) aquifer geometry, (2) hydraulic properties and (3) transport parameters.

This section of the dissertation reports on different aspects of fractures' parameters needed in hydrogeological studies and their variability in time and space, giving examples from the Karoo Aquifers.

#### 3.1 Geological and physical characteristics

In characterising an aquifer, the geological fracture character describes the geometry of the fracture and its general physical presentation. The main geometrical and physical characters are briefly described below.

##### 3.1.1 Location

In Hydrogeologist investigations, locating hydro-fractures is the basis of fracture characterisation.

##### 3.1.2 Orientation

The orientation of a fracture plane is the measure of the angle it forms with the north direction (dip direction:  $XX^\circ$ ) and its angle with respect to the horizontal plane (dip amount:  $YY^\circ$ ). It is expressed in terms of a pair of numbers, such as  $YY^\circ/N\ XX^\circ$ , implying a plane dipping at  $YY^\circ$  in the direction  $XX^\circ$  measured clockwise

from the north. The dip direction is the direction perpendicular to the fracture strike.

For a set of fractures, Cook (2003) noted that calculation of mean fracture orientation is not as simple as averaging values for strikes, dip directions and dip amounts.

### **3.1.3 Fracture connectivity, spacing and length**

The physical connections between individual fractures greatly influence fluid (groundwater) flow, and are often assessed using information from descriptions of fracture sets (the areal and vertical extent, the spacing or density of individual fractures and the orientation distribution). Fracture connectivity is one of the main fracture characters that control to a relatively important degree the ability of fractures to serve as significant flow paths for groundwater, and is measured as the ratios of three types of fracture termination (Cook, 2003):

1. blind fractures that terminate in the rock matrix;
2. fractures that cross other fractures; and
3. fractures that abut other fractures.

Indeed, fracture connectivity itself is a function of fracture orientation, length and fracture spacing. Singhal and Gupta (1999) described how fracture length and spacing control the connectivity and therefore the main flow process in the subsurface. Generally, the fracture network continuity of a rock volume increases with increasing fracture length and fracture density (Long and Witherspoon, 1985).

Fracture length is one the most difficult characters to determine, since it has to be approached in three dimensions (the fracture's dip and strike). Surface exposures (or channels) sometimes offer the chance to directly observe a fracture (or trace) and measure its trace length. In this case, only the fractures in a certain range of values of length are considered, usually imposed by the limited surface of exposure and the scale of the study (often the lower limit of the range) (Barton, 1996). And, as mentioned by Cook (2003), the observed trace length may be only an apparent value of the true trace length due to various types of bias creeping into the data during measurements of exposures. Gringarten and Ramey (1974), and de Lange

(1999) proposed analytical alternatives for fracture length to be inferred from conventional constant pumping rate tests, but the fracture transmissivity  $T_f$ , and fracture storativity  $S_f$  should be known beforehand. Knowledge of the fracture extent is required for several analytical methods, since they assume finite fracture length.

Fracture spacing describes the average (or modal) perpendicular distance between two adjacent discontinuities of the same set (Singhal and Gupta, 1999), and can be measured averagely, by spreading a tape measure in any convenient direction (not parallel) on an outcrop face (or in tunnels). But this measurement has to be corrected for angular distortion to give the value of true fracture interval, perpendicular to the fracture orientation (LaPointe and Hudson, 1985). Price and Cosgrove (1990) related fracture separations to the lithology and thickness of the beds. Fracture spacing may be used to describe fracture density.

#### **3.1.4 Fracture aperture**

Aperture is the perpendicular distance separating the adjacent rock walls of an open fracture, in which the intervening space is air- or water-filled (Cook, 2003). The term 'mechanical aperture' is used to describe the aperture of a fracture measured directly (on an exposed outcrop, in a channel, or on a core body) using various length determining devices (rulers, callipers, sonar devices). Determination of such a fracture's dimensions is problematic because the original fracture opening is rarely conserved. Early researchers in the field of fracture flow simulated flow through a pair of parallel plates separated by a constant distance,  $b$ , which represented the aperture of the fracture. By doing so, they neglected the roughness of the walls, channelling and closings that affect the hydraulic behaviour of a fracture. The term 'equivalent aperture' was introduced to describe an effective aperture contributing to flow or transport in the fractured rock at a specific time. Such effective apertures are often inferred from hydraulics and tracer tests using fluid flow properties in the fracture. According to the type of test from which the equivalent aperture is derived, three types of equivalent aperture have to be distinguished (Tsang, 1992): (1) mass balance apertures (derived from the mean residence time of a tracer, the flow rate, fracture geometry and the tracer test

breakthrough), (2) frictional loss apertures (derived from the mean residence time of the tracer, the transport velocity), and (3) cubic law or hydraulic apertures.

Steele *et al.* (2006) carried out conventional slug tests and used the results in numerical simulations to estimate fracture apertures (for smaller fractures between 35 and 400  $\mu\text{m}$ ). Akoachere and van Tonder (2009) developed two new methods (a slug-tracer test and a tracer detection method) through laboratory experimentation, to directly determine inclined and horizontal fracture apertures in fractured rock aquifers from 0.04 mm (40  $\mu\text{m}$ ) to 63 mm (63 000  $\mu\text{m}$ ).

Data collected directly at surface for a fracture's apparent apertures should be interpreted with consideration of the potential risk of non-intactness of the rock and the effect of the release of overburden pressures. Such fracture aperture data may be collected with a vernier or gauge (Love *et al.*, 2002). Such a character can also be determined from deep core borehole data, which should also be analysed with caution (considering representativeness and quality of the recovered data). Because of the scarcity of surface exposure, the expense of core-hole drilling, and mainly the nature of the studies, fracture apertures have often been inferred from measurements of fracture transmissivity. Belanger *et al.* (1988) applied a sensitivity analysis method to a guessed fracture aperture value to determine the fracture aperture of the fracture that best fitted field hydraulics test responses.

### **3.1.5 Fracture surface roughness**

The irregularities on a fracture's wall surfaces are an important parameter to take into account, since they affect (reduce) the rate of fluid flow by allowing a local channelling effect of preferential flow. Such irregularities on fracture surfaces have been extensively studied (Brown *et al.*, 1986; Gentier and Ries, 1990, Miller *et al.*, 1990). A rock fracture's surface roughness is measured by comparing its profile with a standard set of profiles. Such a profile is obtained with a mechanical profilometer (Swan, 1981) or by application of optical methods on an exposed, un-weathered fracture surface (Voss and Shotwell, 1990). Thomas (1982) gives a valuable review of surface roughness measurements. He describes more than 20 standards, which include measures such as the average deviation from the mean



(rms: root-mean-square, roughness) and peak-to-valley height. Typical roughness profiles like those described by Barton and Choubey (1977) in terms of 'joint roughness coefficient' (JRC) are usually used. Such a roughness coefficient is defined on a scale from 0 to 20 (

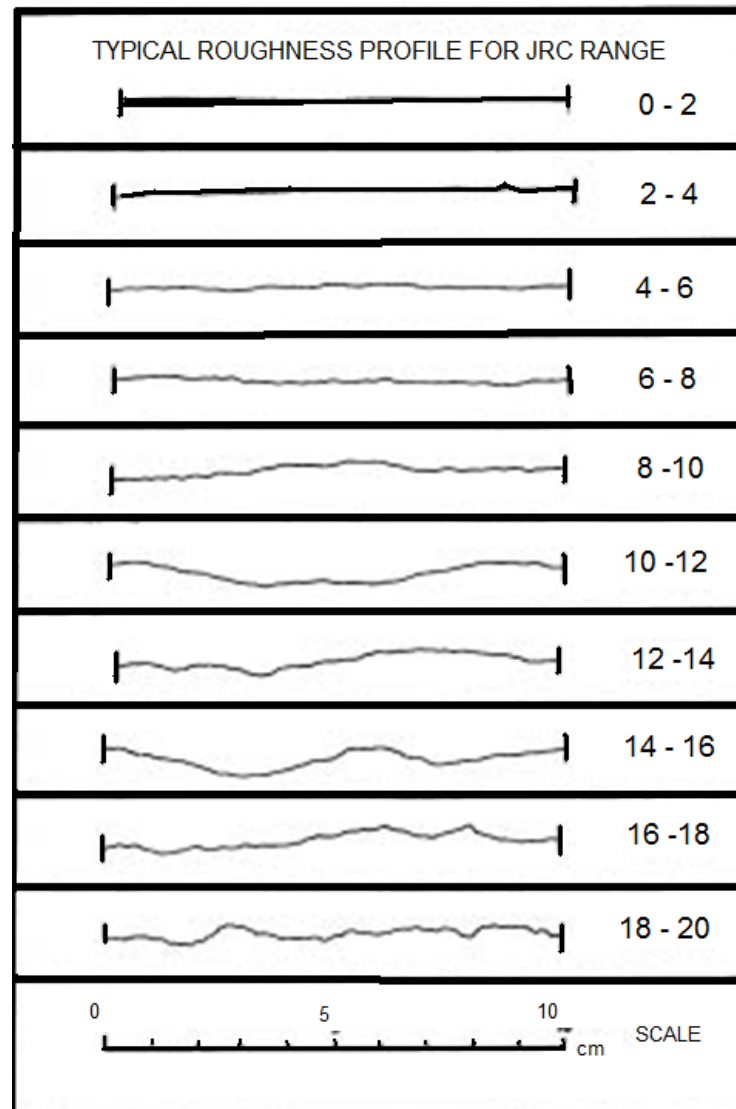


Figure 3-1).

**Figure 3-1 Typical roughness profiles, defining the joint roughness coefficient range from 0 through 20. (From Barton & Choubey, 1977).**

## 3.2 Hydraulic and mass transport characters

Because the processes of flow and mass transport are generally related, water and mass transport characters are often studied together. While the hydraulic characters (transmissivity or hydraulic conductivity, storativity – mainly on a continuum – and effective porosity) control of the flow behaviour under natural or stressed conditions, the transport characters (flow velocity, diffusion, dispersion, advection and others) control the movement of mass (dissolved ions or other rock particles), and are very important for any study of groundwater contamination or in vulnerability and risk assessment of aquifers. Van Wyk (1998) gave proof that contaminant transport predictions based on hydraulic measurements alone are subject to large errors.

### 3.2.1 Hydraulic characters

#### 3.2.1.1 Fracture transmissivity (and hydraulic conductivity)

Transmissivity is a hydraulic parameter that gives a measure of the rate of flow under a unit hydraulic gradient through a cross-section of unit width over the whole saturated thickness of the aquifer. It is expressed as the product of the average hydraulic conductivity **K** and the saturated thickness of the aquifer **D**. In fractured aquifers, when dealing with contamination either in investigation or in scenario testing, the knowledge of the transmissivity (or hydraulic conductivity) of the fracture (or fracture zone) is necessary to evaluate velocities or length of contamination plumes, especially for advective flow. For dispersive flow, in addition of the transmissivity, the dispersivity and a retardation factor may be necessary. The transmissivity of the fracture is expressed as the product of the fracture's hydraulic conductivity  $K_f$  and the equivalent fracture aperture **b**, which can be directly or indirectly measured or estimated from the thickness of the fracture zone  $D_f$  and the intersection angle  $\theta$ .

Hydraulic (flowmeter, packer, etc.) and tracer tests (FEC profiling) have been developed to infer accurately the transmissivity of fractures or fracture zones, and these are reviewed in chapter 5.

### 3.2.1.2 Fracture storativity

The storativity of a saturated confined aquifer of thickness **D** is the volume of water released from storage per unit surface area of the aquifer per unit decline in the component of hydraulic head normal to that surface (Kruseman and de Ridder, 1991). In a fractured system, this storage capacity consists of the storage capacity of both the matrix and fracture storativity. Even if, generally speaking, the storage of a fracture is normally very small compared to the storage capacity of the matrix, and is often neglected in regional aquifer studies, knowledge of the storage capacity of the fracture or fracture network may be important in contaminants studies (investigation and scenario testing) and artificial recharge. A correct estimation is more complicated than for the matrix storativity.

### 3.2.1.3 Effective porosity of fractures (voids that really contribute to the flow)

The effective porosity of a fracture is defined as the ratio of the total volume of interconnected voids in the aquifer (between fracture walls) that really contributes to flow, to the total saturated volume of the aquifer. Sampling for laboratory measurement may be accurate methods to determine such a parameter, if the sampling process does not alter the compaction of the material. This can be problematic and constitutes a real drawback for laboratory measurement. Hall *et al.* (1991) introduced a combination of the point dilution test (Drost *et al.*, 1968) and the injection withdrawal test (Leap and Kaplan, 1988) for measuring effective porosity. This approach has been further developed by van Tonder *et al.* (1999), Riemann (2002), and Gebrekristos (2009) to determine the *in situ* effective porosity of the Karoo aquifer in the vicinity of Bloemfontein.

## 3.2.2 Mass transport characters

Fetter (1999) gave an explicit description of the main phenomena that govern the velocity and particularly the concentration of solutes (mass) in groundwater. Riemann (2002) discussed the key processes that control mass transport in groundwater. In addition to the key processes that control chemical transport in aquifers in general (advection, dispersion, diffusion, and adsorption); others

processes, such as channelized transport and matrix-fracture diffusion, control solute transport in fractured aquifer systems.

### **3.2.2.1 Advection**

Advection (convection) describes the solute transport that occurs with flowing groundwater, and in which the amount of solute that is being transported is a function of its concentration in the groundwater and the rate of groundwater flow. The velocity of the groundwater constitutes the velocity field for such transport. For practical reasons, this velocity field represents an average of different velocity fields over an appropriate volume.

In a heterogeneous aquifer system, particularly in a fractured aquifer where the velocity field varies across the aperture of the fracture, along the fracture, and from one fracture to another, the averaged velocity field may not be representative of the small-scale field.

### **3.2.2.2 Diffusion in the fracture**

Diffusion describes the solute transport controlled by concentration gradient. Fick's first and second laws are often applied to tracer tests in a one-dimensional model to describe such transport respectively for solute concentration and for time-varying concentration.

### **3.2.2.3 Dispersion**

Small-scale variations that are not described by the average velocity field will cause the tracer to spread and mix. When molecular diffusion is added to this spreading and mixing process, the result is what is commonly known as dispersion. Due to the heterogeneity of geologic materials, advective transport in different strata can result in solute fronts spreading at different rates in each stratum (Riemann, 2002).

Dispersion is the transport process that controls the combining processes of spreading of mass solute that is not controlled by advection or diffusion. Generally, Fick's law is used to describe such a transport process, since the data used in such attempts are often from tracer tests conducted over a relatively short distance. But this can lead to an inaccurate consideration of dispersion (heterogeneity) in a

fractured aquifer, where the solute must travel a certain distance before Fickian dispersion is established (Gelhar, 1986). The effect of fracture geometry on the dispersive transport has been clearly shown by Detwiler *et al.* (2000).

#### **3.2.2.4 Channellised transport**

In a fractured aquifer, the groundwater flow normally occurs in a fracture zone consisting of several interconnected fractures, and fluid velocity can vary across the aperture of the fracture, in the fracture plane, from one fracture to another, and from one part of the fracture network to another part. The parallel plate model of a single fracture often used to describe flow through a fracture, because of lack of information on the geometry of the fracture network and of single fractures, assumes a uniform flow along the fracture (or fracture network), neglecting the variations in flow velocity, which are greatly influenced by the flow geometry. Channellised transport arises from the non-uniform velocity of fluid and solute transport in a variable-aperture fracture, resulting in the concentration of flow and transport in narrow regions following pathways of least resistance. This effect has been tested through different developed models (John and Roberts, 1991; Nordquist *et al.*, 1996), basing on assumed fracture network and flow geometry.

#### **3.2.2.5 Matrix-fracture diffusion**

The channellised flow in a fracture leads to the stagnation of groundwater, with its solute in significant portions of the fracture. The presence of such 'stagnant water' may create a retardation effect on the solute's apparent movement, by the occurrence of molecular diffusion processes of solute (tracer): (1) between channels water and the stagnant water, (2) between the mobile water flowing in the connected fractures and the stagnant water residing in unconnected or dead-end fractures, (3) or between fractures and rock matrix (high porosity matrix). Field experimental studies (tracer tests) conducted on the campus test site by Riemann (2002) showed a loss of tracer mass due to matrix diffusion that was found to be up to 30 %. In 2001, van der Voort conducted laboratory experiments on diffusion coefficients for different rock types in South Africa. The matrix diffusion effect becomes difficult to distinguish at a large scale (kilometre scale), because it

emphasises tracer movement retardation due to fractures with large heterogeneity in transmissivities (Shapiro, 2001).

### **3.2.2.6 Adsorption**

The physical properties of some solutes may tend to attach them to solid phases. In fractured aquifer systems, such tracers may adsorb onto fractured surfaces, particularly in the presence of alteration product (clay), and thus be delayed in their movement. This process should be distinguished from reversible matrix–fracture diffusion transport, which is controlled by the physical properties of the aquifer (i.e. velocity in the fracture, porosity of the matrix, diffusivity of the matrix).

## **3.3 Variability of fracture characters in time and space**

The representativeness of estimated (or measured) fractures' parameters, for a given scale and as time passes is an important issues in fracture characterisation, that is usually neglected in different hydrogeological studies, particularly in most studies conducted in the Karoo. Such omission can lead to misunderstandings of the occurrence of the groundwater flow and mineral (or mass) transport at a given scale and at a specific moment.

Due to the degree of heterogeneity and anisotropy in fractured aquifer systems, almost all the fracture characters may change in space (radially in the plane of the fractures or spatially with change of orientation of the preferential flow), either in the same fracture or from one fracture to another, or at different parts of a fracture network. The choice of the fracture characterisation should consider the scale of the study. Shallow fractures characteristics might not be representative of conditions at greater depths. Methods that probe deeply into the subsurface generally have a poor ability to spatially resolve the locations of fractures and those with shorter ranges have correspondingly better resolutions. Even then, some exceptions to this rule exist (NRC 1996, Chapter 40), one should be aware of the range and resolving power of the methods that have to be used for any fracture characterisation study. At regional scales, some information like the locations of major fracture zones and faults may be obtained from aerial photography and remote sensing imagery technology. Information such as orientation, set, aspect, and size can be collected

with direct surface (in-field) observation, like on outcrops. Ground and airborne geophysical surveys may be needed sometimes for more precise resolution purposes. and some fracture characters (geometric and hydraulic) can be obtained only from drilling boreholes or tunnels, either by examination of core material, or by using geophysical logging methods, hydraulics or tracer tests.

If the primitive geometry of a single fracture (or fracture network) is mostly affected by the geological origin of the fracture (Delaney *et al.*, 1986, DeGraff and Aydin, 1993, Chevalier *et al.*, 2002), as time passes, the factors that most affect the geometry of the void space (and subsequent flow characters) are changes in stress brought about by natural processes (groundwater pressure, temperature, general stress state, and others) and artificial processes (human activities) such as withdrawal, artificial recharge, canals, or the charge (weigh/mass) of urban buildings. Generally, fractures are sensitive to changes in temperature, pressure and fluid chemistry, and any slight perturbations of these parameters can result in significant alterations in fracture properties. Stress sensitivity constitutes the greatest distinction in hydrological properties between porous media and fractures. Perkins and Gonzales (1984), Engelder (1993) and the National Research Council Committee on Fracture Characterisation and Fluid Flow (1996) provide clear descriptions of how changes in stress affect a fracture's geophysical characters and the groundwater flow (stress-sensitive flow behaviour) in a fracture. Other no less significant factors are mineral precipitation and dissolution due to fluid (groundwater) flow through a fracture. The fracture's "effective stress" is a concept developed to understand changes in fracture systems owing to variations in pore pressure, and is defined as the difference, between the total stress applied on the fracture face and the pore pressure in the fracture (Warpinski, 1991). An increase in effective stress will close fractures and reduce their permeability; a decrease in effective stress will have the opposite effect. Several models have been developed to attempt to predict the behaviour of stress sensitivity flow (Raghavan *et al.*, 1972; Kafritsas, 1987; Asgian, 1989; Wall *et al.*, 1991; Dvorkin and Nur, 1992). But these models are found to be limited and often require field scale experiments to test them.

## 4 SOME PROPERTIES OF ROCKS IN RELATION TO FRACTURE CHARACTERS

### 4.1 Electrical properties of rocks

One of the main geophysical properties of rocks used to collect sub-surface geological and lithological information is the electrical properties. After seismic properties, electrical properties are found to be most useful in detecting and characterising fluid conductive zones (or fractures) in the subsurface (National Research Council Committee on Fracture Characterisation and Fluid Flow, 1996, Chapter 40).

Originally, the bulk electrical properties of rock were determined based on the properties of its constituents. In the subsurface, rocks are constituted of grain minerals, gases, and fluids (liquid in the saturated zone) that fill the void between grain minerals. The dimensionless ratio of the volume occupied by the fluid to the total volume of the rock mass is defined as porosity. Electrical properties such as conductivity (reciprocally inverse to resistivity) are strongly related to the porosity of the rock mass. In a secondary system (fractured aquifer), and mainly in a densely fractured system (and/or secondary system with low porosity matrix), voids between fractures' spaces contribute significantly to this porosity. This significant contribution constitutes the basis of using electrical methods for subsurface rock mass characterisation in a fractured system.

#### 4.1.1 Archie's law

Archie (1942) described the bulk resistivity of rock, by relating it to pores' fluid resistivity and porosity at low frequencies through the following equation known as Archie's law:

$$\frac{\varphi_r}{\varphi_w} = F = \alpha \phi^{-n} \quad \text{Equation 4.1}$$

Where  $\varphi_r$  is the bulk resistivity of the rock,  $\varphi_w$  is the pore fluid resistivity,  $F$  is the formation factor,  $\phi$  is the porosity,  $n$  is the cementation factor (approximately 1.5), and  $\alpha$  is a dimensionless parameter (approximately unity).



This law allows an estimation of porosity from electrical resistivity measurements, and has been modified for reasons of accuracy to fit certain geologic environment and certain applications studies. Waxman and Smits (1968) extended Archie's law by taking into account the effect of surface conduction along grain boundaries, which may become a significant factor in low porosity rocks with low-conductive pore fluids (or in clay-bearing rocks). This factor's effect was also mentioned by Magnusson *et al.* (1987). The formula developed by Waxman and Smits (1968) also takes into account the relation between the mobility of exchange cations and a pore's water concentration and the clay cation exchange capacity per unit volume.

#### **4.1.2 Void filling and rock properties**

The degree of filling of the voids between the grain minerals by a fluid (water) may in certain conditions have a significant effect on the bulk properties of the rock. In a non-conductive material system, for example, electrical conductivity depends mainly on the fluid saturation in the pores. Simandoux (1963) among others, showed how the bulk electrical conductivity (rock formation filled with fluid) is related to the percentage water saturation and clay concentration.

The effect of the presence of fractures on bulk rock mass conductivity becomes more significant when the fractures are connected and in that sense can constitute a significant path of conduction in the rock mass. Generally, void space connectivity in a rock mass is stress dependent, therefore conduction through fracture paths is stress dependent. For example, any variation in stress on a fracture, changes the geometry of its void space, which in turn changes its global permeability and preferential flow paths (Pyrak-Nolte and Morris, 2000). A fractured rock mass may therefore be visualised as a matrix of one conductivity containing thin sheets of a second stress-sensitive conductivity (National Research Council Committee on Fracture Characterisation and Fluid Flow, 1996, Chap 3).

#### **4.1.3 Bruggeman-Hanai-Sen equation**

One of the multiple theories on electrical properties of rocks at high frequencies is the one developed by Sen *et al.* (1981) and known as the Bruggeman-Hanai-Sen equation. The equation is based on the theory of self-similar systems and hold for a

two-component system. This equation is similar to Archie's law in a direct current conditions. Sihvola (1989) gave experimental proof of reliability of the Bruggeman-Hanai-Sen equation.

## 4.2 Rocks' hydraulic properties

The relationship of geologic materials (rocks) and fluid processes is significantly controlled by the rocks' hydraulic properties and fluid quality. Water in a rock is held and moves through its interconnected voids. The ability of an earth material to hold water and its ability to transmit water constitute its most important hydrogeologic properties. Gehrels and Gieske (2003), by considering the law of conservation and Darcy's law, showed mathematically how flow (both three-dimensional and two-dimensional) in homogeneous, isotropic conditions is mostly driven by two hydrogeologic properties: storage coefficient  $S$  (specific storage " $s_s$ " for an unconfined aquifer) and aquifer transmissivity  $T$ .

These hydrogeologic properties themselves are function of physical properties such as porosity, density, geometry and shape of the void between the grain minerals.

### 4.2.1 Darcy's law

The French engineer Henry Darcy (1856) gave the first acceptable theory for the study of water movement in the subsurface. Through his experience in a porous medium, Darcy found that the rate at which water flows through a given earth material is proportional:

1. to the hydraulic gradient (ratio of the difference in the height of the water between the two ends points of the flow path in material to the length of the flow path),
2. to a coefficient " $K$ ", which depends on the nature of the porous medium,
3. And to the cross sectional area  $A$  of the material.

In general, this relation is termed as follows:

$$Q = -K \left( \frac{dh}{dl} \right) \quad \text{Equation 4.2}$$

Where, the term  $\frac{dh}{dl}$  is the hydraulic gradient.

The coefficient  $K$  was initially referred as the coefficient of permeability, and later as **hydraulic conductivity**.

#### 4.2.2 Hydraulic Conductivity

Hydraulic conductivity is the measure of the ease with which water will pass through the earth's material; and is defined as the rate of flow through a unit cross-section under a unit hydraulic gradient at right angles to the direction of flow. It is expressed in metres per day (m/d). From the general Darcy's equation for flow in porous media, the following mathematical expression determines the hydraulic conductivity:

$$K = \frac{Q}{A(\frac{dh}{dl})} \quad \text{Equation 4.3}$$

But this expression of conductivity does not show how it is a function of the properties of both the earth material and the fluid flowing through this material. This relation is given by the formula:

$$K = K_i \left( \frac{\rho g}{\mu} \right) \quad \text{Equation 4.4}$$

Where  $\rho g$  is the specific weight of the fluid (with  $g$  the acceleration of gravity and  $\rho$  the fluid density);  $K_i$  (is function of the void space shape factor  $C$  and the mean aperture of space  $d$  :  $K_i = C d^2$  ) is the intrinsic permeability of the earth material alone, and  $\mu$  is the dynamic viscosity.

This formula, developed under porous medium conditions, has been found useful in a modified form for modelling fracture flow and associated processes. Gale (1982) reported that 'if fractures are idealised as parallel plates, each having a constant aperture, then, the hydraulic conductivity,  $K_f$ , of a parallel-plate fracture of aperture  $2b$ , is given for smooth laminar flow conditions ( $Re < 2300$ ) by the following equation:

$$K_f = \frac{\rho g}{12\mu} (2b)^2 \quad \text{Equation 4.5}$$

Where  $\rho$  the fluid density,  $g$  is the gravitational constant, and  $\mu$  is the dynamic viscosity.

By using Darcy's law, a first approximation of fluid flow along a fracture has been set. The fluid flow along a fracture is modelled as flow between two parallel plates with constant hydraulic aperture ( $b_h$ ) described by the 'cubic law' (Snow, 1965; Louis and Maini, 1970):

$$q = \frac{w\rho g b_h^3}{12\mu} \Delta H \quad \text{Equation 4.6}$$

Where  $q$  is the flow rate per unit width ( $b_h$ ) and  $\Delta H$  is the hydraulic head (elevation head + pressure head) gradient.

By extension of this formula, the following one has been established with the permeability " $K = \frac{b^2}{12}$ ", by analogy with Darcy's law (National Research Council Committee on Fracture Characterisation and Fluid Flow, 1996: Chap 3):

$$Q = \frac{Kb}{\mu} \nabla P \quad \text{Equation 4.7}$$

Where  $Q$ , is the volumetric flow rate per unit width, and  $P$  is the fluid pressure. Tsang and Tsang (1987), and Brown (1989) demonstrated that the parallel plate model overestimates the volume flow rate through rough-walled fractures.

### 4.3 Relationships between rocks' electrical and hydraulic properties

Because of the connection between electrical property and void volume within a rock, and between hydraulic property (conductivity) and void volume, a close relationship between electrical property and hydraulic conductivity is evident, and this has been studied in different applications. Simultaneous measurement of fluid permeability and electrical resistivity is in fact a well-established practice for core analysis in the oil industry (National Research Council Committee on Fracture Characterisation and Fluid Flow, 1996: Chap 3). The rock's permeability (hydraulic conductivity) and its electrical resistivity (inverse of electrical conductivity) are respectively the key hydraulic and electrical properties that have been used to study the hydro-electrical relationship of rocks. Darcy (1856) described fluid flow as a function of hydraulic conductivity ( $K$ ) through Darcy's equation (Equation 4-8).

$$q = \frac{-K}{\mu} \nabla P \quad \text{Equation 4.8}$$

where  $q$  is the fluid volume and  $\nabla P$  is the pressure gradient.

Ohm (1826) defined rock's electrical resistivity by Ohm's Law (Ohm, 1826):

$$\mathbf{J} = -\sigma \nabla V \quad \text{Equation 4.9}$$

Where  $\mathbf{J}$  is the current flux density and  $\nabla V$  is the potential gradient.

A clear similarity exists between the two distinctive differential equations describing each process (electric and fluid flow). These equations have been related to rock void (space within the rock) through different models. Paterson (1983) and Walsh and Brace (1984) presented the 'equivalent channel model', which explains the relationship between permeability and formation factors. This model describes the transport properties according to 'typical' pore geometries. The equivalent channels assume void space to have a simple geometry (cylindrical tubes for porous media and parallel plates for fractures).

#### 4.3.1 Hydro-electrical relationships in a primary aquifer

In a porous medium, for example, geometrical models (Wyllie and Rose, 1950; Walsh and Brace, 1984) and statistical and percolation concepts (Katz and Thompson, 1986, 1987) have been used to describe relations between void space within an earth material and the two distinctive differential equations cited above. The combination of both relations, assuming no surface conduction, allows a formula that links both rock transport properties (electrical and hydraulic), and in which the rock's electrical conductivity is expressed in terms of the formation factor  $\mathbf{F}$  (see Archie, 1942).

$$\mathbf{K} = \frac{cL^2}{\mathbf{F}} \quad \text{Equation 4.10}$$

where  $c$ , is a shape factor (the ratio between the electrical conductivity of the fluid  $\sigma_{fl}$  at the respective experimental temperature and the measured conductivity of the rock  $\sigma$ ), and  $L$ , is a characteristic length scale.

The length  $\mathbf{L}$  depends significantly on the type model. Milsch *et al.* (2008) recommended to appropriately define and determine  $\mathbf{L}$  for the validity of a model, since it needs to contain all the micro-structural information needed to characterise the interrelationship between both transport properties.

### 4.3.2 Hydro-electrical relationships in secondary aquifers

In fractured rock environments (secondary aquifers), the investigation of hydro-electrical relationships has been conducted in different applications (Kosinski and Kelly 1981; Kelly and Reiter 1984; Yadav and Abolfazli 1998). The flow and mass transport processes in such environments are often concentrated in the conductive fracture networks, mainly when the rock matrix is significantly less conductive. The Fracture is modelled as two parallel plates, and the flow rate per unit width  $Q$  is given by:

$$Q = \frac{Kb}{\mu} \nabla P \quad \text{Equation 4.11}$$

where  $Q$  , is the volumetric flow rate per unit width, and  $P$  is the fluid pressure.

For the same fracture model filled with an electrolyte of resistivity  $\rho$  , the electric current  $I$  per unit width is proportional to the first power of the aperture according to Ohm's law:

$$I = \frac{b}{\rho} \nabla V \quad \text{Equation 4.12}$$

By assuming that topography varies slowly in the plane of the fracture, that the parallel-plate model holds, and that mass and charge are conserved, Brown (1987, 1989) found that Reynolds's equation for fluid flow can be used:

$$\nabla \cdot (b^3 \nabla P) = 0 \quad \text{Equation 4.13}$$

Analogously, the corresponding electrical conduction equation is:

$$\nabla \cdot (b \nabla V) = 0 \quad \text{Equation 4.14}$$

Brown (1987, 1989) used these two differential equations, with generated rough fracture surfaces and pairs of surfaces, to model volume flow rate and electric current fields by using fractal algorithm. Figure 4-1 shows the results of the calculation.

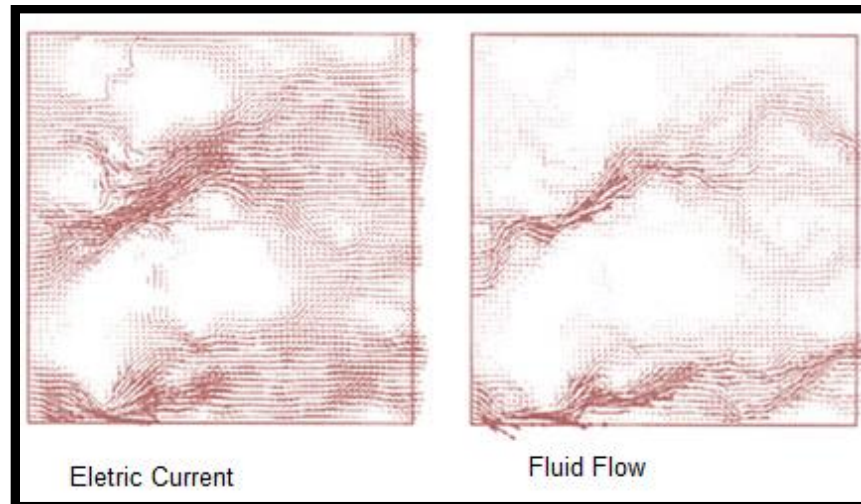


**Figure 4-1 Electrical current path and fluid flow path after Brown's model (1989)**

With this model, Brown confirmed that fluid particles and charged ions take different paths through a fracture and that fluid flow is mostly affected by surface roughness, with the large aperture channels playing the dominant role in transport. Tsang and Tsang (1987) took these considerations into account to build a conceptual model for channel flow through fractures. Brown also demonstrated through this model that the use of an arithmetically average aperture, when using the parallel-plate model, overestimates both the volume flow rate and the electric current through rough-walled fractures. The same model was used by Brown (1989) to compare hydraulic and electrical apertures (respectively  $b_h$  and  $b_e$ ) in a function of a dimensionless aperture,  $bm/hrms$ , where "bm" is the mechanical aperture and "hrms" is the "rms" surface height of the fracture surfaces. The results showed that the relationship between hydraulic and electrical properties changes with deformation ( $bm/hrms$ ). For high values of  $bm/hrms$ , hydraulic and electrical apertures values are the same, but for  $bm/hrms$  close to unity, the electrical aperture  $b_e$  becomes smaller than  $b_h$ . Therefore the use of a fracture's electrical conductivity (inverse of electrical resistivity) may underestimate its hydraulic conductivity. In the final analysis, the results of the Brown model are consistent with the 'equivalent channels model' with simple geometry (cylindrical tubes for porous media and parallel plates for fractures).

## **5 OVERVIEW OF FRACTURE CHARACTERISATION METHODS**

In the present section of this dissertation, the different methods and approaches developed for fractures characterisations will be reviewed with emphases on the commonly used methods. Also discussion on some case studies of characterisation tools used in the Karoo will be made.

### **5.1 Fracture characterisation: What is it about?**

Aquifer's characterisation is important for building up a conceptual understanding of the hydrogeological processes operating in any region and hydrogeological environment, and consists of finding out the main geological and hydraulic parameters that control the groundwater storage and flow at a given scale. In fractured environments (basement complex, younger granites, carbonates, and unconsolidated deposits aquifers) where, a network of flowing fractures cuts through a rock matrix, this requires information on the nature of both the fractures and the rock matrix (Cook., 2003). In most flowing fractures it is generally considered that there is no infilling.

While a rock-matrix's characters can be reliably determined only by using core samples taken from drilling or from surface exposure, reliable methods for determining fracture characters still constitute challenges for hydrogeologists. Characterization of groundwater flow and solute transport through fractures, within such a complex system (with spatial density variability) like in most cases in the Karoo aquifers, requires estimation on both, the fractures' geological and physical characteristics (locations, dimensions, surface roughness), and hydraulic and mass transport characteristics (hydraulic conductivity, porosity, advection, ect...), and the matrix diffusion coefficient, as listed in chapter 3.

### **5.2 Classification of fracture characterisation methods**

Fracture characterisation methods can be classified in different ways according to:

- the fracture's characters, which are able to help to determine physical characters, flow characters and mass transport characters;
- the zone of survey (surface, subsurface) or the impact of methods on the natural condition (invasive, non-invasive).



In practice, classification of the fractures characterization methods accommodates for all above-mentioned considerations (Lasher et al., 2009; Zhou et al., 2002).

### **5.3 Review of commonly used methods of fracture characterisation**

Different approaches have been developed for fracture, and vary according to the type of site and the scopes of the studies. Techniques and methods for the identification, location and characterisation of permeable zones in the subsurface are based on geological mapping, geomechanical and geochemical analysis, and also on geophysical and hydrological field measurements. Most of the fracture characterisation methods are firstly designed to detect fractures indirectly. Since fractures are a typical feature of rocks (associated with distinctive patterns), fracture properties (aperture, density, length, etc.) can be indirectly deduced from the rock mass properties by analysing the inverted rock mass properties and by idealising the fracture geometry. Other properties of fractures cannot be indirectly deduced, and must be estimated from interpretations of deduced fracture properties. Such interpretations rely not only on collected data, but also on experience and good knowledge of the study area on the part of the researcher. Recently, significant improvements in characterisation techniques and the detection of subsurface conductive zones have been done, and the results from assessments of these new methods show a promising future for appropriately detecting and characterising such preferential flow zones (fractures or fracture zones) in the subsurface. However, there is still a need for theoretical research on methods, new instrumentation, and algorithms for data interpretation.

Methods for detecting fractures and estimating their physical characters will be firstly reviewed, followed by a review of methods to estimate their hydraulic and mass transport characters.

#### **5.3.1 Detection of fractures and estimation of their physical characters**

##### **5.3.1.1 Surface methods**

###### ***Geological observation***

The most detailed information can be collected from surface (outcrop) exposures, but the availability of outcrops and the risk that they may be affected by

weathering can sometimes constitute real limitations for this characterisation approach. Without these limitations, surface exposures constitute an often reliable source of information such as the orientation, sets and apparent apertures of fractures.

### ***Seismic reflection methods***

Seismology is one of the most widely used techniques to explore deep subsurfaces. The approach is based on the elastic properties of rocks. Two waves are generally used in such investigations, the P-wave (compressional wave) which tends to deform the rock in the direction of wave travel (longitudinal), and the S-wave (shear wave) which tends to deform the rock in the direction perpendicular to the wave travel (transversal). The technique consists of transmitting energy into the ground by means of a controlled seismic source (a single or closely spaced array of sources) and collecting at many other points (receivers) the reflected energy from subsurface features where the rock properties change suddenly, such as fractures and lithological boundaries. With these methods, fractures zones (or lithological boundaries) position, size and orientation can be deduced. Crampin (1991) described the different field procedures and summarised recent advances in using such methods. The seismic reflection methods are found limited to characterise vertical fractures (Garotta., 1989) and low dense fractures zones or single fractures (Willis *et al.*, 1986; Tomsen., 1998).

### ***Electrical methods***

Electrical methods for fracture detection in the subsurface rely on the Laplace equation. Direct current (DC) is introduced into the ground at low frequency via two electrodes and two other electrodes are used to register the voltage caused by the current. An 'apparent resistivity' is then estimated by multiplying the ratio of the measured voltage to the injected current by the geometry factor, which depends on the configuration (sounding mode or the profiling mode) of the electrodes during the survey (Binley *et al.*, 2002; Zhou *et al.*, 2001; Robain *et al.*, 1996 Dahlin, 2001). Changes in apparent resistivity are given in a function of depth for the sounding mode (Schlumberger), whereas lateral changes in apparent resistivity are given by the profiling mode (gradient). Zhou *et al.* (2002) carried out an ERT

(Electrical resistivity tomography) survey to map enlarged fractures in Nashville, Tennessee, and the findings were confirmed by geological logs from two directional boreholes drilled across the location of the two interpreted fractured zones. Ngeleka (2010) used the ERT to characterize a site for LNAPL investigation in the East London Karoo formation (fractured aquifer). He concluded that the ERT method is applicable to delineate the geological units, to locate the aquifers as well as weathered and fractured zones which are considered as preferential pathways for LNAPL; and he recommended that the method be used for three-dimensional resistivity distributions for a more accurate delineation of LNAPLs plumes and that a time-lapse survey be considered to monitor the changes and progress of LNAPLs contaminant in the subsurface.

Generally, the resolution and the depth of exploration vary proportionally to electrode separation (Dey *et al.*, 1975; Barker., 1989), and the sounding mode resolution becomes problematic in deep subsurfaces (Johansen., 1977; Ward., 1990). In addition to the resolving power limitation in the sounding mode, the effects of overburden (often with the same electrical properties as the fractures) often compromise an accurate estimation of the dip. Like any other geophysical methods, the ERT results need to be complemented by other field testing results for a full subsurface characterisation.

### ***Electromagnetic methods***

Electromagnetic (EM) methods use earth's electrical and magnetic fields that satisfy the diffusion equation, at a few hundred Hertz of frequencies. The EM method responds to high conductivities, therefore can detect small changes in conductivity in a conductive terrain by the correct selection of technique and array (National Research Council Committee on Fracture Characterisation and Fluid Flow, 1996, Chap 4). The field procedure involves a couple of source-receiver circuits, which are used to induce magnetic fields (primary and secondary) in earth materials. The source may be active (alternating current) or passive (sun radiation).

In active EM methods, a time-varying source (primary) current is made to flow in a source loop. A magnetic field associated with the primary current is a primary time-

varying magnetic field. This causes a time-varying magnetic flux through a body (geological unit) in the vicinity of the source loop. This time-varying magnetic flux sets up a time-varying electromagnetic force (emf) in the body. The time-varying emf drives electrical current flows (eddy currents) through the geological unit. The behaviour of the induced eddy currents and their associated (secondary) magnetic fields is dependent on a number of parameters, including the conductivity of the geological unit. The emf induced in a receiver loop by the time-varying magnetic flux of the secondary magnetic field through the receiver loop can be measured. The measured emf contains information on the conductive properties of the geological unit. The subsurface conductivity distribution, as determined from the EM survey, can now be interpreted in terms of local geological conditions by incorporating known information on the geology of the site. As with resistivity methods, the electromagnetic method may be used in sounding and/or profiling modes. Measurement can be made through the use of multiple fixed frequencies (frequency domain) or by sampling the real-time response of a transmitted pulse (time domain). The choice of the mode of measurement depends on practical considerations. Further description and discussion of EM methods are given by Ketola and Puranen (1967).

### ***Ground-penetrating radar (GPR)***

The ground penetration radar method uses electromagnetic energy (at high frequencies: 10 to 1000 MHz) of fields that considers 'displacement current'. The principle of the method is similar to the principle of seismic reflection described above, but electromagnetic energy that suits the wave equation is the energy concerned in the GPR context. The method has the particularity of being able to provide information on structures situated deep in the subsurface. The radar range is roughly proportional to the first power of the resistivity of the rock (National Research Council Committee on Fracture Characterisation and Fluid Flow, 1996, Chap 4). The more resistive the subsurface media, the greater is the probing range. Therefore, the GPR method becomes limited to highly conductive media. As in the cases of the electrical and electromagnetic methods, conductive overburdens

constitute a barrier for the energy to penetrate to greater depths. The use of the method in boreholes or tunnels may help to overcome the effect of overburden.

### **5.3.1.2 Underground based methods**

Many of the surface-based methods have been modified to fit the geometries of boreholes and tunnels, and their principles are valid in underground measurements. Underground measurement of subsurface properties constitutes a good tool for validating surface measurements, which are generally affected by overburdens that do not allow for a deep and clear scanning of the subsurface. Two main types of underground-based methods need to be distinguished: remote sensing techniques (borehole-borehole or surface-borehole), which may determine rock properties along transects, at considerable distances from the site of measurement, and single-hole based methods, which may provide near-borehole measurements of subsurface rock properties (National Research Council Committee on Fracture Characterisation and Fluid Flow, 1996, Chap 4).

#### ***Remote sensing techniques***

In these techniques, waves (seismic or electromagnetic) are propagated from a source, through the subsurface rock, and the response of the rock is recorded by a receiver, in transmitted mode (transmission tomography), reflected mode (cross-hole seismic reflection, borehole radar), or a combined mode (coupled inversion of transmission and reflection data).

- ***Vertical seismic profiling (VSP)***

The VSP survey is essentially a surface-borehole method and is carried out by using a surface seismic source and receivers located in the wellbore (Balch and Lee, 1984). This approach offers a greater spatial resolution advantage over the typical conventional surface seismic methods. However, its measurements are restricted to the vicinity of a borehole.

Different forms of field surveys have been developed, and their descriptions (drawbacks and advantages) are reported by Cosma *et al* (1991), Majer *et al* (1992) and Paillet (1991a). The simplest is the zero offset, in which the source is placed as close to the wellhead as practicable. When the source is placed at some offset

(distance away from the wellhead) in a line, the configuration is called a walkway VSP survey. The reserve VSP survey places the source in a borehole and the receivers are on the surface.

- **Transmission tomography**

Transmission measurements are generally feasible in either cross-boreholes, surface-boreholes or both. Transmission tomography measurement and reconstruction are based on the idea that information about the properties of the interior of a volume can be obtained through measurements performed at the boundary. Multiple source and receiver locations are combined to probe the volume of investigation with multiple crossing rays, each a source-receiver combination. The travel time and amplitude data for each transmitter-receiver pair are recorded, and by a tomographic inversion process, the velocity distribution in the interior of the investigated volume is inferred (Bregman *et al.*, 1989; Olsson *et al.*, 1991). Olsson *et al.* (1992) gave some field applications of cross-borehole measurement to infer fracture position in a mine in the United States. Practical applications of tomography measurement (Dyer and Worthington, 1988a,b; Bregman *et al.*, 1989) show some resolution limitations, which depend mainly on dominant wavelength, on the ray pattern (density and angular coverage), geological structure, noise levels, and suitable positioning of the source-receiver. The high heterogeneity in fractured aquifer systems distorts the assumption of isotropic conditions on which tomographic inversion relies (Olsson *et al.*, 1991). On the other hand, tomographic surveys can be repeated (difference or alteration tomography) to indicate some change of state in the rock occurring between the initial and subsequent surveys (Olsson *et al.*, 1991).

**Reflection**

The subsurface heterogeneity yields to spatial differences in rock properties. Reflection techniques (Cross-Hole Seismic Reflection; Borehole Radar) infer rock properties from these differences and the corresponding distances over which such differences occur (Cosma, 1991; Sattel *et al.*, 1992; Sandberg *et al.*, 1991). The technique has been adapted to openings in the subsurface (borehole to surface, borehole to borehole, borehole to tunnels).

- ***Acoustic emissions***

This technique is based on the measures (at frequencies of 10 to 1,000 Hz) of microseismic events (acoustic emissions or AEs) that are generated during and/or after hydrofracture processes. Lacy and Smith (1989) reported that the method can be used to detect such events at ranges of several hundred feet in competent rock. The main advantages of the technique are found in complex geothermal reservoirs, where the environment is hostile to the downhole transducers, and where transmission losses from remote seismic sources can be severe. Acoustic emissions can be used to locate and describe the geometry of fractures in the reservoir, to interpret the nature of reservoir deformation.

***Single borehole methods***

Generally, boreholes and channels are the only direct means of access to the subsurface for measurements of different permeable layers and fracture properties. Although measurements from boreholes can be significantly affected by drilling damage surrounding the borehole (especially in the fractured aquifer system) and are representative of a restrictive volume of the aquifer at the vicinity of the borehole, some borehole methods have been developed and have proved to be useful in characterising fractures (single or zone) and fluid flow through fractures in a number of case studies, especially where multiple boreholes are often rare.

- ***Core inspection***

By means of conventional rotary coring, the sequential subsurface layers and features (fractures and permeable rock) at a single point can be logged. Bunker in 1998, qualified core drilling as an effective tool where detailed structural geologic analysis is necessary to identify and quantify contaminant migration pathways. The physical (geological) characteristics of fractures, such as location, density (of fractures zone), orientation and their ability to conduct fluids may be described from a core inspection, but it is recommended that such descriptions fracture (or fracture zone) locations in cores be compared with the results of images of the borehole wall derived from down-hole geophysical logging (LaPointe and Hudson, 1985).

Core drilling is a relatively slow process (compared to other methods) and very expensive. The core samples show only intercepted fractures that are not necessarily representative of the fracture network in the local aquifer system, far less of the regional and entire aquifer system. Further, the core samples are often affected during the drilling process and sample recovery may be poor (i.e. it does not give much information) in the intensely fractured and weathered parts of the rocks (rubble) that provide most of the hydraulic conductivity. The core inspection method has been found to be fit for hard crystalline bedrock aquifer systems. In softer formations such as sedimentary formations, shale bits are recommended rather than diamond bits for coring, or the sampling barrel may be directly introduced into the formation to recover samples in relatively natural (intact) state (National Research Council Committee on Fracture Characterisation and Fluid Flow, 1996, Chap 4).

- **Conventional well logs**

Conventional geophysical techniques normally used in borehole logging investigations are summarised in Table 5-1. The techniques are generally based on physical effects indirectly related to contrasts in the subsurface such as fractures, changes in rock properties, and layer contact zones (Sharma, 1997). Generally, the well logging method consists of lowering a combination of logging tools that do not interfere with one another and that are connected by a multi-core cable to a probe-control surface module and recording unit. The recording unit is habitually equipped with a strip chart and digital tape for computer processing (National Research Council Committee on Fracture Characterisation and Fluid Flow, 1996, Chap 4). They provide *in situ* measurements of some rock properties, for correlating laboratory test data on discrete rock samples at specific depths. Their ability to make several different physical (nuclear acoustic, electric, ect...) measurement in a borehole constitute their main attribute (Howard., 1990a,b; Woodford and Chevalier., 2000). But the estimated aquifer parameters (either matrix or fracture) by well logging techniques, often represent some average values of the rock properties affected by the borehole and associated fluid and walls (drilling, casing, screens, etc.) within a given relatively small radius surrounding the studied



borehole (Daniels and Keys., 1990). Usually, the geophysical loggings are recorded before the new borehole (open-hole) devices have been cased. Cased holes permit the use of only a few logging devices such as those based on radioactive emission and detection (Sharma, 1997).

**Table 5-1: Comparative table of common conventional well logs**

Type of Log	Borehole Requirement	Specific Advantages	Drawbacks	References
Caliper	Most conditions	show vertical variation of BH diameters; detect highly weathered zone	Probe performance often affected by borehole deviation; ignore discrete fractures	Miroslav et al ., 2005; NCR., 1996;
Self Potential	Uncased, mud filled only	Identification of thickness of permeable zone, water quality.	Needs contrast in solutes in borehole versus formation; effect of reduction-oxidation	Miroslav et al ., 2005; NCR., 1996; Gomo., 2010
Resistivity	Uncased, fluid filled only	Formation bondaries, fractures detection	Influenced by fluid resistivity and bed boundaries	Miroslav et al ., 2005; NCR., 1996; Gomo., 2010
Natural gamma	Most conditions	Stratigraphy	Unusual lithology interpretations in arkose and phosphate sands	Keyes, 1989, Telford et al, 1990
Gamma-gamma (Density)	Wide range	Bulk density, porosity,moisture, lithology, correlation, well construction	Mineralogy may influence calibration through Z effect	NCR., 1996; Gomo., 2010
Neutron	Wide range	Saturated porosity,moisture, lithology, fractures positon	Ineffective porosity of clay minerals included in total porosity	Miroslav et al ., 2005;
Acoustic waveform	Uncased, fluid filled only	Saturated porosity, lithology, Fracture position	Measures primary or matrix porosity rather than total porosity	Hardin et al. (1987)
Acoustic borehole tele-viewer	Uncased, fluid filled, water or mud	Character and orientation of fractures, fractures openings, and bedding	Fracture interpretation may be affected by drilling damage to borehole wall	Zemanek et al. (1970), Keys (1990), and Maki et al. (1991)
Video logging	Uncased or cased, air or clear fluid	Well construction, secondary porosity, fracture detection; lost objects	No information in cloudy or muddy fluid; dark mineral bands mimic fractures	Howard (1990a,b); Woodford and Chevalier (2000)

- **Fluid electrical conductivity logs**

This method may also be classified as a geo-chemical or hydro-chemical method and has been widely used, mostly in water related sciences, to get a first, general idea of water qualities (surface and groundwater), and how it varies with time and in space. In geohydrology, for example, groundwater electrical conductivity logs have become a common tool for locating fractures or permeable zones in a borehole, and getting an initial idea of the variation of water quality in the subsurface. The fluid conductivity log known as 'Fluid Electrical Conductivity logging' (FEC) or 'electrical conductivity' (EC) for short, is an inexpensive and easy method for locating conductive fracture zones and other physical and hydraulic features that control water quality. Changes in fluid electrical conductivity along a borehole may indicate an inflow or outflow point (or zone) that creates contrast in total dissolved salt in the borehole. The method has been found to be more reliable when the borehole is not yet cased. Gebrekristos (2007) recognised that the FEC logs may also allow the determination of hydraulic variation within the vertical profile of the subsurface and identification of important features in the system.

The fluid electrical conductivity may be logged in ambient conditions, or in stressed (pumping at a relatively low rate) conditions. Either in ambient or pumping conditions, the EC logging may be made on the natural borehole water or on altered borehole water. The borehole water is altered by introducing a tracer into a measured borehole or into a borehole situated upstream that intersects the same flow paths (conductive zones) as the measured borehole. The entire measured borehole water may be also replaced with very low conductive water (de-ionised water).

In addition to their ability to detect contrasting features related to water salinity, the EC logs may be used as a measure of salinity for *in situ* determination of the effective diffusion coefficient of the matrix (Gebrekristos., 2007), the porosity of the matrix (Gebrekristos., 2007) and Darcy's velocity at a fracture position (Gomo, 2009).

In the past two decades, the applicability of borehole fluid electrical conductivity logs in subsurface flow characterisation has improved significantly. The method demarcates itself from other methods by the fact that it can detect which of the intersected fractures or permeable zones really contribute to the fluid flow in the borehole. Tsang *et al.* (1990) gave proof that the method may also be used to measure the hydraulic properties of detected fractures (or conductive zones) in a borehole. Dynamic wellbore electrical conductivity logs provide a valuable means to determine the flow characteristics of fractures intersecting a wellbore, in order to study the hydrologic behaviour of fractured rocks (Doughty and Tsang, 2000, 2004). The same authors set up a computer programme called BORE II (a modification of an older code BORE) that can calculate the evolution of fluid electrical conductivity (FEC) profiles in a wellbore or wellbore section, which may be pumped at a low rate, and compares model results to log data in a variety of ways. More detail and discussion on the present method is given at chapter 6.

- **Temperature logs**

At equilibrium state, it has been proved that the temperature log accurately reflects the local formation temperature. When water is circulating along the wellbore, departures from the geothermal gradient indicate where water is entering or exiting from the borehole (National Research Council Committee on Fracture Characterisation and Fluid Flow, 1996, Chap 4; Malard and Chapuis, 1995). Trainer (1968), traced laterally continuous bedding plane fractures in a carbonate rock aquifer by correlating inflections in open-hole temperature profiles. Field experiences show that the method is subject to limitations such as the inadequacy of certain temperature probe sensitivity (low resolution) and the influence of vertical flow in open boreholes (Bidaux and Drogue, 1993; Robison *et al.*, 1993). The limitation related to the sensitivity of the temperature probe has been overcome (Green-House and Pehme, 2002; Genthon *et al.*, 2005). Several approaches (sealing, pvc pipes, water columns, fiber optic, liner) have also been developed to overcome the effect of vertical flow in open boreholes (Keys and Brown, 1978; Ferguson *et al.*, 2003; Henninges *et al.*, 2005; Wisian *et al.*, 1998; Pehle *et al.*, 2009). Although these two limitations have been overcome, the

method still has some significant disadvantages. For example, Pehle *et al.* (2009) concluded that the temperature profiling method applied in a lined borehole has the following limitations:

1. In some unusual hydrogeologic circumstances, extreme hydraulic head variations over short intervals can cause inadequate sealing of liners along parts of the hole;
2. The method is not sufficiently sensitive to identify all hydraulically active fractures, and therefore the number of fractures identified in a given hole should be regarded as a minimum;
3. The method is effective only when the temperature of the water in the fracture is in disequilibrium with the surrounding rock. Pehme *et al.* (2007a) described a technique for overcoming this limitation.

- **High-resolution flow-meter methods**

The borehole flow-meter logging is a useful method developed to estimate the magnitude of inflow or outflow between borehole and surrounding rocks. It consists of passive measurement of water flow velocity along a borehole. In the first attempts (in conventional boreholes) at flow-meter logging, the sensitivities of the tools were low, and it was difficult to quantitatively estimate hydraulic properties from the velocity profile obtained. Recently, developed logging techniques have allowed improvement from the conventional flow-meter to a high resolution flow-meter, which is sensitive enough to detect minor flow, to investigate fractures population and associated flow in the rock surrounding the borehole. Hess (1986), Molz and Young (1993), Momii *et al.* (1993), and Kazumasa *et al.* (2006) among others, gave examples of field applications using flow-meters in a well for fracture characterisation. A cross-hole flow-meter survey is possible, which consists of pumping one well and measuring vertical velocity in an observation well (Shapiro and Hsieh, 1994).

### **5.3.2 Methods for estimating hydraulic and transport characters**

In groundwater studies (exploration, investigation, modelling) the estimation of fluid flow and chemical transport parameters is done by field investigation (tests), where subsurface responses are measured and data collected after certain

artificially induced perturbations. There are two main groups of such tests: (1) hydraulics tests and (2) tracer tests. Nowadays, estimation of the hydraulic and transport parameters of some aquifers is determined by a combination of both hydraulic and tracer tests (van Tonder, 1999; Rieman 2002).

Generally, when performing either a hydraulic or a tracer test for aquifer characterisation, one should be aware that the analysis of the resulting data consists of two main steps. The first step requires conceptually modelling the flow and transport in the rock mass, based on knowledge of the mass rock and the behaviour of the test response. The model has to be an adequate representation of the hydrogeological system studied. The second step consists of parameter estimation, which is done by matching the field responses (field data) with model-computed responses (model data) that follow a determined mathematical model (that well describes the chosen model). These two steps in practice are iterative processes, since difficulties during the fitting procedure may lead to reconsideration of the initial conceptualised model for a better matching between field data and model data (NCR, 1996, Chap 5).

The generalised radial flow model or the fractal reservoir model may be used to solve flow and chemical transport studies' problems (Rieman 2002), with the inherent risk of estimating inaccurate fractures parameters due to the drawbacks (unknown geometry of the fracture network) of such models.

#### **5.3.2.1      *Hydraulics tests***

In hydraulics tests, the induced perturbation may be created by injecting (artificial recharge) or withdrawing (pumping) fluid from a borehole, and the aquifer responses (the change in fluid pressure, hydraulic head) are collected in the same or nearby observation boreholes. Hydraulics tests may be conducted on one single borehole (slug test, constant discharge test, etc.), or on multiple boreholes.

For different purposes and different geological structures, several hydraulics test set-ups have been developed. The most commonly used hydraulics tests are slug tests, multi-rate tests, constant head tests and constant discharge tests. Descriptions of such tests are given in many textbooks (Kruseman and de Ridder,

1994; van Tonder *et al.*, 2001). The constant discharge test (or constant rate test) is the most common hydraulics test, where water is abstracted from a borehole at a constant discharge rate and the drawdown (change in pressure) in the same single borehole or multiple observation boreholes is measured and can be related to the aquifer's hydraulic properties. The test is popular because it offers multiple possibilities for data analysis, and is often time and cost effective, depending on the purpose of the test. Van Tonder *et al.* (2001) state that, a few hours of abstracting can be sufficient in certain investigations. Also, the constant discharge test has been found to fit in combination with other tests (tracer tests). The major disadvantage of conventional constant rate tests is that the observed water level always represents an average over the aquifer thickness (Verwey and Botha, 1992).

Hydraulics test data in fractured systems may be interpreted for estimation of hydraulic parameters, either analytically or numerically. The availability of analytical solutions is highly advantageous for gaining insight into how well model parameters can be estimated from field data (NCR, 1996, p.257). Either with the analytical method or the numerical methods, a correct interpretation of pumping test data relies on a clear definition of the following points:

- Adequate conceptual model for the hydrogeological system, which, as stated above, should be based on a knowledge of geology of the system and the behaviour of the response of the aquifer (diagnostic plots);
- The geometry of the aquifer, which is often unknown in fractured reservoirs;
- Inner boundary conditions (such as well bore storage, skin effects), which can be depicted on traditional diagnostic plots;
- Outer boundary conditions (no-flow boundaries, etc.), which can be depicted on traditional diagnostic plots;
- Characteristics of the flow conditions (steady, transient, uniform, etc.).

In the following section, different models and subsequent analysis methods for fracture characterisation will be discussed, according to the type of hydraulics tests.

***Single borehole hydraulics tests***

Single borehole hydraulics tests are generally the most commonly used field tests performed in the field of geohydrology for site characterisation, particularly in South African aquifer systems, where most of the investigations do not reach the detailed phase and are often constrained by time and for economic reasons. Broadly, single borehole hydraulics tests are performed in an open borehole (uncased and/or not equipped) or with packers. The NCR (1996) recommended conducting open-borehole tests prior to packer tests.

- ***Open-borehole hydraulics tests***

In an open-borehole test, the entire uncased portion of the borehole is tested. Such tests are easy to conduct and may provide information on the hydraulic properties of the tested rock mass as a whole. Still, in an open-borehole hydraulics test, the pressure head response of the aquifer-borehole system is controlled by the most conductive zone, and that is the real drawback of this type of hydraulics test configuration for fracture characterisation, since the real contribution of each fracture intersected by the borehole (particularly the less conductive fractures when multiple fractures are intersected) cannot be directly inferred from interpretation of the test data. Also, in rock of low transmissive environment, the hydraulics test responses in an open borehole may be influenced by wellbore storage effects (Kruseman and de Ridder, 1994).

- ***Straddle packer tests***

Like the common open-borehole hydraulics test, the straddle packer test is another configuration for performing a single borehole hydraulics test. It differs from the open-borehole approach in the fact that it allows one to perform hydraulic measurements (transmissivity and hydraulic head) of the different fractures (isolated or grouped) or permeable zones by using two or more packers to isolate a portion (interval) of the borehole for testing, which often depends on the application. When the test interval is constant, the borehole is tested in consecutive sections throughout its length to obtain a hydraulic conductivity profile. In the other case (variable intervals) the hydraulic measurements are just concentrated on the more permeable zone that intersects the borehole. By testing the borehole's

different straddle sections, the straddle packer approach overcomes some of the limitations associated with the open-borehole approach. For example, the water inflow zone can be located and the hydraulic contribution of each test section to the total averaged hydraulic properties through the entire length of the borehole can be deduced. Two types of packer test are often applied in practice: the double packer (single borehole) and the cross-borehole packer tests. The double packer test may be used to determine horizontal hydraulic parameters, whereas the cross-borehole packer tests may be used to determine both horizontal and vertical hydraulic parameters. Botha *et al.* (1990) successfully used cross-borehole packer tests in the Malmesbury formation at Atlantis, but the method is found to be unsuited for the Karoo aquifer at the Institute for Groundwater Studies campus test site (Botha *et al.* 1998). It was realised that cross-borehole packer tests do not appear to be useful in studies of highly heterogeneous aquifers, since positive results can only be expected from such a test if the spacing of the borehole takes the geometry of the aquifer into account. Generally, wellbore storage can be neglected when analysing packer test data, since, in packer tests, the change in hydraulic head is not associated with a change in water level. But in very low transmissivity environments the equipment compliance could induce a wellbore storage effect that needs to be taken into account (NCR, 1996, p.262).

### ***Multiple borehole (cross-borehole) hydraulics tests***

Multiple borehole tests involve one perturbation borehole and at least two observation boreholes (for responses) in the same aquifer system. Like single-borehole tests, multiple-borehole tests can be performed on open boreholes, where groundwater is pumped from one well and drawdown is observed in the pumped well and nearby observation wells; or on packer-isolated intervals, where the groundwater is pumped from a 'pumped interval' in one borehole, and drawdown is monitored in 'observation intervals' in nearby boreholes. Basically, the multiple borehole tests have the advantage over single borehole tests to sample a larger volume of the aquifer, and therefore leave less uncertainty on the inferred hydraulic parameters. Multiple borehole hydraulics tests are known as good tools to provide information on the connectivity of fractures (flow zone) and aquifer anisotropy.



When correctly designed, some information on their spatial variability may be collected (Pretorius., 2007).

Correct design of a multiple borehole test depends on the geological condition and the purposes of the test, and becomes more challenging when packers have to be installed. The NCR (1996, p.265) gave the set-ups of multiple boreholes for the different most commonly encountered conditions (bedding-plane fracture in low permeable rock matrix; bedding-plane fracture in permeable rock matrix; multiple bedding planes in sedimentary rocks; high densely fractured rock; mixed of horizontal and inclined fracture zones in a fractured rock mass). For each set-up, they gave the corresponding models, and the different ways to estimate parameters of both fracture and matrix blocks. Botha *et al.* (1998) and van Tonder *et al.* (2001) reported on multiple borehole pumping tests performed in the Karoo aquifer.

### ***Common models for hydraulics test interpretation in a fractured aquifer***

Different type of models and corresponding methods of analysis have been developed and yield acceptable estimated hydraulic parameters in primary aquifer systems, but their direct application in secondary (fractured) aquifer systems generally leads to ambiguous results, mainly because most developed models for interpreting hydraulics tests assume a homogeneous, isotropic porous medium, and one of three basic flow geometries (spherical, radial and linear) described by the NCR (1996). For a simple system comprising identical, planar, parallel and evenly spaced fractures of infinite length, simple analytical equations relating groundwater flow and solute transport to fracture characteristics, have been developed by considering flow through aquifers comprising more than one set of parallel fractures, by allowing the matrix to have some permeability, and by allowing fractures to have a finite length (Van der Kamp, 1992; Cook *et al.*, 1996; Cook ., 2003).

The famous analytical porous models developed by Theis (1935) and Cooper-Jacob (1946), have been shown to estimate hydraulic parameters (transmissivity and storativity values) that represent, a mixture of the matrix and fracture properties.

Botha *et al.* (1998) and van Tonder *et al.* (2001) gave illustrative demonstrations of this reality. Because the geometry of the fracture network is not initially known, usually three kinds of analytical models are applied in fractured-rock aquifers for the analysis of the constant discharge hydraulics test data: (1) the single fracture model, (2) the double porosity model, and (3) the generalised radial acting flow models.

- ***Single fracture model***

A single fracture model conceptualises the aquifer system as a homogeneous confined aquifer of large extent formed by a very low hydraulic conductivity matrix, in which a pumped well intersects an embedded major fracture (horizontal or vertical), fault or dyke (of infinite length). Generally in such an ideal system, the time drawdown response of the entire aquifer may be significantly influenced by the intersected major fracture (or fracture zone). Several types of single fracture models have been developed in different earth science fields. Three of the main types adapted for groundwater studies, deserve attention: (1) the infinite conductivity fracture, (2) uniform flux fracture, and (3) finite conductivity fracture (Verweiji and Barker, 1999). The dyke model is another common single model that has been developed especially for groundwater purposes, and has been successfully applied in the Karoo aquifer (Chiang and Riemann., 2001).

The infinite conductivity model assumes a major fracture (horizontal or vertical) embedded in a confined, infinite, homogeneous, horizontal matrix and that has anisotropic radial and vertical conductivities. Verweiji and Barker (1999) acknowledged that the infinite hydraulic conductivity for a single borehole model is not realistic for highly conductive fractures in hard rock aquifers with low permeable rock matrices. In the infinite conductivity single fracture model, the pumped fluid (groundwater) will initially flow linearly from the matrix towards the fracture (and the well), and later, after a transition period, will flow toward the well by radial-acting flow (Gringarten and Ramey, 1974; Gringarten *et al.*, 1974). In the case of a vertical fracture, the flux distribution may be uniform and homogeneous (*uniform flux*) along the fracture during the test phases; or uniform along the fracture during the linear flow phase, but not in the transient and radial-acting flow phase (*infinite*

*flux*). In infinite flux, flux distribution varies with time until the radial-acting flow phase is reached. Cinco and Samaniego (1981b) affirmed that the flux distribution along a fracture may approach uniformity only if there is a skin or a low permeability layer between the fracture and the aquifer matrix. Gringarten *et al.* (1974) presented two analytical solutions that resolved the drawdown  $s$  in the fracture, at earlier and at later stages of the constant rate test, by relating it with the abstraction  $Q$  rate, the transmissivity  $T$ , and the elapsed time  $t_d$  of pumping:

*At earlier stages:*

$$s = \frac{Q}{2\pi T} \sqrt{\pi t_d} \quad \text{Equation 5.1}$$

with:  $t_d < 10^{-2}$  for uniform flux;  $t_d < 2 \cdot 10^{-1}$  for infinite flux. Because the fracture has infinite conductivity, there is an infinitely small pressure gradient along the fracture that can be neglected ( $\Delta p / \Delta x_f = 0$ ). Therefore, in the early stages, the same drawdown is observed along the entire length of the fracture, and an observation well located in the fracture will show the same curve as the pumped well.

*At later stages:*

The long-term solution describes the radial-acting flow phase on the fracture as:

$$s = \frac{Q}{2\pi T} \left[ \frac{1}{2} \ln(t_d) + 1.1 \right] \quad \text{Equation 5.2}$$

In the case of a horizontal fracture, Gringarten and Ramey (1974) gave an analytical model that describes the drawdown in a bedding plane fracture with infinite conductivity and finite extension with constant and uniform flux.

The finite conductivity model assumes a major fracture (particularly the vertical one) embedded in a confined, infinite, isotropic, homogeneous, horizontal matrix. In the finite conductivity single fracture model, the flow (groundwater) is considered to be bilinear (flow from fracture and formation) toward the fracture, and therefore only generalised solutions should be expected. After a certain period of pumping, the radial acting flow phase starts, during which the flux distribution stabilises (stabilised flux distribution). Cinco-Ley *et al.* (1978) proposed a semi-analytical model that resolved the drawdown in such a model. The gradient along the fracture is not neglected like in an infinite conductivity model, due to its finite

conductivity, and the solution requires knowledge of the flux distribution along the fracture in time. Their solution uses the concept of relative conductivity  $C_r$  to relate the permeability of the fracture ( $T_f$ ) and of the matrix ( $T$ ), and the fracture's width or aperture ( $w$ ) and half length ( $x_f$ ) as follows:

$$C_r = \frac{T_f w}{\pi T x_f} \quad \text{Equation 5.3}$$

They found through this semi-analytical solution that when  $C_r \geq 100$ , the response curve corresponds to the infinite flux solution of Gringarten *et al.* (1974). By using a straight-line method (lin-log plot) and a type curve method (log-log plot) the following parameters can be determined:

- Reservoir transmissivity,
- Reservoir storage coefficient,
- Fracture half-length,
- Fracture transmissivity,
- Fracture storage coefficient.

The finite conductivity fracture model offers a real advantage to solve developed analytical models that relate the fracture extent (half length:  $x_f$  or radius of extend:  $r_f$ ), the fracture transmissivity  $T_f$ , and fracture storativity  $S_f$ ; to a pumping rate  $Q$  and its corresponding drawdown  $s_f$  after a given time  $t$  (Gringarten and Ramey, 1974; de Lange, 1999).

#### • **Double porosity model**

In a double porosity model, the response of the aquifer is controlled initially by the fractures during a certain period, followed by a second period during which the blocks begin to supply water to the fractures and the head in the fractures stabilises, which in turn is followed by a third period during which both the fractures and the porous matrix provide water to the well with a relatively higher contribution from the blocks matrix. The concept was introduced by Barenblatt *et al.* (1960), assuming homogeneously distributed conductive fractures embedded in a homogeneously distributed blocks matrix. Two types of double porosity model are distinguished according to the type of matrix adopted (Figure 5-1 and Figure 5-2).

(1) The spherical-block matrix (Warren and Root, 1964; van Tonder *et al.*, 2001), used to represent aquifers like quartzite, and the layered matrix (Kazemi, 1969) or slab-shaped blocks (van Tonder *et al.*, 2001) adopted, for example, for sandstones with bedding planes.

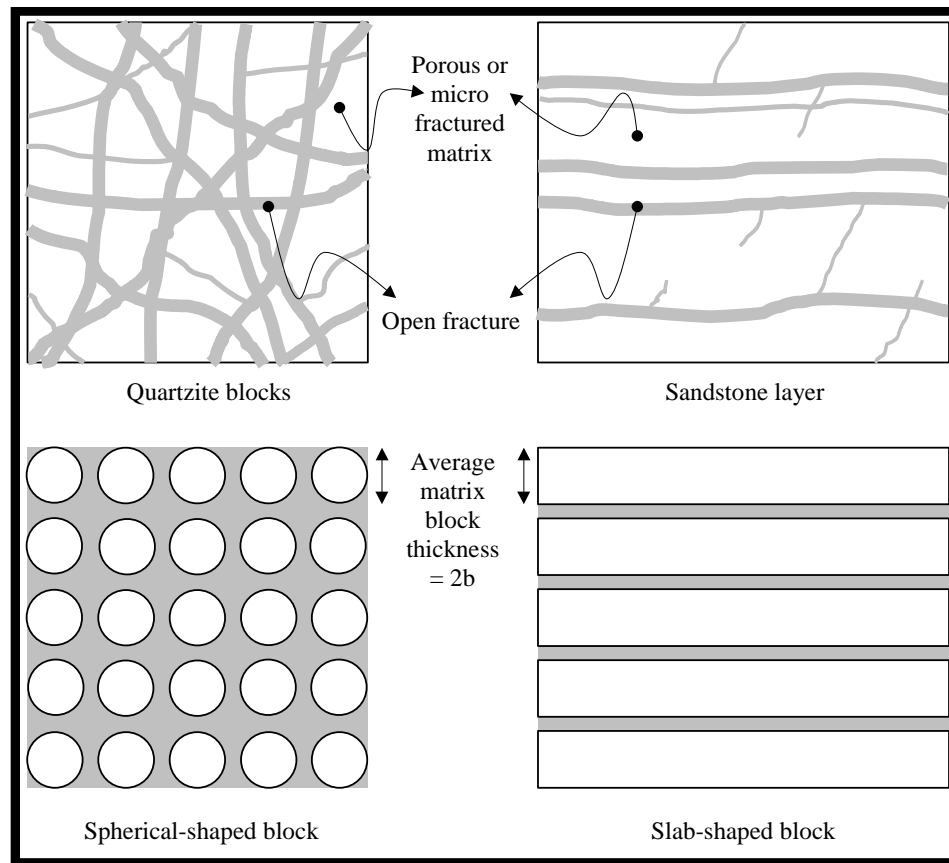


**Figure 5-1 Natural fracture systems and their simplification into spherical-shaped blocks and slab-shaped blocks (van Tonder *et al.*, 2001)**

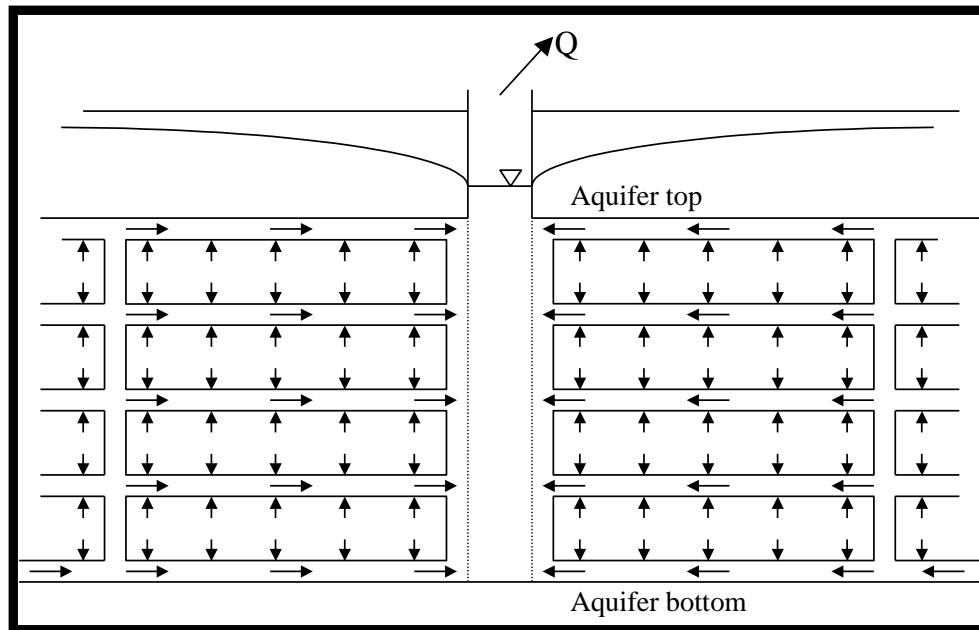


**Figure 5-2 Groundwater flow in an idealised double porosity aquifer (van Tonder *et al.*, 2001)**

Warren and Root (1964), by assuming a pseudo-steady block-to-fracture flow, used the straight line approach (like the Cooper-Jacob straight-line method) to fit field data. With this approach, Warren and Root attempted to determine the transmissivity  $T$  of the fracture system, and the storage coefficients  $S_f$  and  $S$  for the fracture system and the matrix respectively (Riemann., 2002). Both straight lines (early and late part of the response curve on the lin-log plot) must have the same slope, as they reflect the transmissivity of the fracture system, and one should insure that the influence of the wellbore storage and borehole skin are negligible before the Warren and Root approach is applied. Kazemi (1969) and Wei *et al.* (1998), by using numerical models, found that flow is of transient block-to-fracture nature, and proposed also a straight line method that is applicable even in the presence of a skin at the well. Moench (1984) considered the effects of wellbore storage, well skin and fracture skin, and proposed a type curve approach for the analysis of double porosity data, which is able to calculate different drawdown scenarios after model calibration to find the optimal abstraction rate for a particular well. Nowadays, with progress in computer science, a combined approach of straight line and forward modelling is possible. Kirchner and Van Tonder (1995), among others, demonstrated from applications in a fractured Karoo aquifer that the

estimated S-values with the Moench model have the same distance dependency as those estimated with the Theis method (using real observation distances). Also, the numbers of parameters that have to be fitted make the solution from the model non-unique.

- **Generalised radial flow model for fractured reservoirs**

In analytical approaches, the generalised radial flow model for fractured reservoirs deserves particular attention for fracture characterisation. The model describes the drawdown in a fractured aquifer for various flow dimensions  $n$  (linear:  $n=1$ , radial:  $n=2$ , and spherical:  $n=3$ ), and is sensitive to fracture connectivity rather than aquifer dimensions. The model assumes a confined, homogeneous and isotropic fractured medium, with Darcian flow, finite storage, infinite matrix, and negligible fracture skin. Barker (1988), was the first to introduce the concept of the fractional flow dimension for hydraulics test analysis (NCR, 1996) by attempting to describe the power relationship between the distance from the test interval and the area available for flow. He stated that the fractional flow dimension describes a fracture network that exhibits fractal geometry and may be related to the fractal dimension of the fracture network. The flow dimension  $n$  may take non integral values. Leveinen *et al.* (1998) explained that the non-integer values of  $n$  describe excess or lack of fracture connections compared to fracture networks with perfect connections in 1, 2 and 3 dimensions. Barker (1988) proposed a type curve method (similar to that of the Theis type curve method) to determine the hydraulic conductivity  $K_f$  and the specific storage  $S_{sf}$  of the fracture system, if the fracture thickness (aperture) is known. This method is applicable to single borehole data only if the wellbore storage and the wellbore skin are negligible, but if not, it is applicable to observation borehole data (multiple boreholes).

- **Numerical models**

Based on the analytical solutions, several numerical models have been developed for analysing hydraulics tests. Bardenhagen (1999) designed the 'Test Pumping Analysis' (TPA) for fractured primary and secondary (fractured) aquifers. The TPA software can analyse step test data, multi-rate test data, constant discharge test and recovery data, and consider all the analytical solutions listed above. Roberts *et*

*al.* (2001) developed the 'n-dimensional Statistical Inverse Graphical Hydraulics test Simulator' (nSIGHTS) for hydraulics test interpretation in low permeable aquifers (primary and secondary). With the nSIGHTS software, fracture networks can be simulated as a continuum, or as double porosity, in which case a differentiation between fracture and matrix parameters is not possible. The nSIGHTS software can be used to solve the case of a single horizontal fracture or a horizontal fracture zone, but features like single vertical fractures or faults cannot be simulated with this approach, because they are not homogenous in areal extent (radially centred).

### **5.3.2.2 Artificial Tracer tests**

Generally, tracer tests can be used to explore connectivity in the subsurface and to determine transport properties (e.g. kinematic porosity and dispersivity) and chemical reaction parameters. Generally, they consist of introducing one or more chemicals (tracers) into the groundwater and measuring their concentrations over a certain period of time at various sampling points downstream from the tracer introduction point.

'The natural gradient' and the 'forced gradient' are the two main classes of tracer tests that exist for field measurement of these transport parameters. Natural gradient tracer tests in fractured aquifer systems are seldom conducted because it is expensive, and the large scale of heterogeneity associated with secondary aquifers make them difficult to apply. Also, according to some researchers such as Tsang and Tsang (1989), Abelin *et al.* (1991a,b), the tracer travels along channels that occupy small portions of the fracture planes. Therefore, natural gradient tracer tests may not be an effective tool for accurately determining mass transport parameters in fractured aquifers, since the grid of sampling wells may not be designed adequately to sample the full extent of the tracer plume. Forced gradient tracer tests, on the other hand, are commonly used in fractured formations. The NCR (1996, Chap 5) described other problems with conducting a natural gradient tracer test in fractured rocks. They recommended the development of specialised packer equipment as developed by Novakowski and Lapcevic (1994), when implementing natural gradient tests in fractured aquifer systems. The NCR (1996, Chap 5) and van Wyk (1998) have given illustrative descriptions of case studies of with the



existing forced gradient tracer tests when measuring the mass transport parameters of fractures. These forced gradient tracer tests are named according to the induced flow fields: radial convergent, radial divergent, and injection withdrawal or two-well tracer tests. Radial convergent and divergent flow fields are created by pumping water from or into the aquifer, respectively. The convergent tracer test is easier to conduct in the field while the radial divergent test has the advantage that the tracer arrival can be observed at several observation points, using a single tracer (van Wyk, 1998). The injection-withdrawal test involves pumping from one well, while another well is recharging (by recirculation mode or not) at the same rate of pumping until a steady state field is reached. Then the tracer is introduced (as a pulse or step increase) into the recharging borehole and monitored from the pumping borehole by sampling the pumped water. The NCR (1996, pp.276-280) explained that the injection-withdrawal test may be less sensitive to dispersion in fractured aquifers compared to either divergent or convergent tests. Welty and Gelhar (1989) recommended that a pulse injection of tracer be used in this test, rather than a step rise in concentration, to improve the sensitivity of the injection-withdrawal test to dispersion.

Other tracer tests restricted to a single borehole have been developed for field measurements of mass transport. Drost *et al.* (1968), assuming horizontal flow and absence of diffusion/dispersion along a borehole, developed an analytical solution for the concentration observed in the borehole at a specific point (or borehole test section). Based on this analytical model, the Darcy velocity is computable from a dilution test (Drost and Neumaier 1974). The point dilution test is a common tool in the Karoo aquifer for site characterisation mainly of LNAPL and DNAPL contaminated aquifers (van Wyk, 1998; Rieman *et al.* 2002; Gebrekristos 2007; Gomo, 2009). The borehole dilution technique was developed to measure the groundwater velocity under natural conditions and can be successfully applied in both aquifer types (Freeze and Cherry, 1979). When applied to a fractured rock formation, the borehole dilution test yields the volumetric rate of groundwater flow through a packed-off interval of a wellbore (NCR, 1996, p.282). The packed-off

interval allows one to isolate the fracture flow response (dilution), and therefore to characterise major flowing fractures.

#### **5.4 Methods commonly used for fracture characterisation in Karoo aquifers**

Aquifer characterisation is particularly challenging in Karoo aquifers, due to their complex lithological character and igneous intrusions. Rare are Groundwater exploration projects that characterise fractures in detail. Since water supply has often been and still the most important purpose for groundwater exploration in South Africa, characterisation of aquifers tends to be focussed on locating sources of water (water-bearing fractures or fracture zones) and testing how much water they can yield (seeking of high yielding boreholes), rather than developing a conceptual understanding of the aquifers at hand. Therefore, groundwater investigations in the main Karoo basin, usually involved the following actions:

- Locate any indication of dykes and other hydrogeologically significant features (or discontinuities) for targeting potential zones of preferential flow, by examining aerial and/or satellite photography of the study area;
- Basing geophysical survey or aerial/satellite photography, and site characteristics and requirements, implant a borehole and equip it after successful drilling;
- Then, perform different tests (slug test, step-rate test, constant discharge test) on the single newly drilled borehole (or on multiple boreholes if observation boreholes exist) to determine the sustainable yield of the new borehole, and bulk aquifer parameters (often hydraulic conductivity and storativity).

Several studies reporting on groundwater exploration in the Karoo mention the limitations of such standard approaches (Van Tonder, *et al.* 2002; Weight 2008; Van Tonder, pers. comm. 2010) and how they can lead to an inadequate understanding of the occurrence of groundwater flow and associated transport (Sami, *et al.*, 2002) in the studied areas. Such approach gives very few characters on the main fractures (or fractures zone). Only the location of the main fractures (or fracture zones) intersected by the boreholes can be determined, as follows:

- During the drilling process, by observing the main water strikes positions, and the size of the cut-offs,
- By profiling electrical conductivity,
- Or by inferring from pumping test data analysis (often constant discharge).

By the end of the last century, a number of studies (Verwey and Botha, 1992; Botha *et al.*, 1998; ect...) had been initiated by the Water Research Commission of South Africa, to better understand the behaviour of the Karoo aquifers systems. The results of these studies show the importance of the main fractures parameters. Owing to limited access to efficient and precise tools often assisted by computer sciences, and due to budget constraints, only fractures associated with intrusive formations such as dolerite dykes and sills, have been and are still targeted during aquifer characterisations in the Karoo. The direct effect of this approach is that only tools and techniques related to locating and identifying doleritic dykes are generally employed or given any great importance in aquifer characterisation. Usually, magnetic or electro-magnetic techniques are used to locate doleritic intrusions. In recent years, however, electrical resistivity based surveys have been introduced to locate faults and fracture zones (weathered zones) not associated with dykes that may also act as preferential flow-paths (Gioa *et al.*, 2008).

#### **5.4.1 A decade of fracture characterisation methods testing on the IGS campus test site**

Developed by the Department of Geohydrology to serve as an experimental field site for post-graduate students, five original boreholes were drilled on the campus test site by the Department of Geohydrology in 1989. Situated on the Karoo aquifer area, the site has been used as an experimental field site for many studies (often initiated by the Water Research Commission Projects and the Department of Geohydrology), such as the behaviour of the Karoo aquifer (Botha *et al.*, 1998), tracer tests in fractured aquifers (Van Wyk *et al.*, 2000), and parameter estimation with computer models (Chiang and Riemann, 2001), among many others.

The campus test site is mainly characterised by bedding-parallel fractures (one of the features in Karoo aquifers) situated about 21 m below the surface, along the contours of a sandstone unit. Other less extended and less conductive fractures are

also present in the site, but they do not greatly affect the general behaviour of the aquifer system. From the geological outcrops around the Campus Site, the existence of extensional fractures (mode I) and shearing fractures (mode II) has been observed. The dominant type of fractures recognised in the sediments include sub-horizontal bedding-parallel fractures and orthogonal and diagonal fractures with dominant north-west, north-east and east-west trends (Riemann 2002). Several field tests have been conducted on this site to characterise flow and transport through this fractured aquifer. The present section focuses only on previous works related to fracture characterisation.

Botha *et al.* (1998) studied the behaviour of the Karoo aquifer as a secondary aquifer. The campus test site was one of the five experimental sites used for their studies. In sum, twenty-six (26) additional boreholes have been drilled on the campus test site during their studies, with nineteen (19) percussion boreholes, five (5) vertical core-boreholes and two (2) 45° inclined core-boreholes. Multiple constant rate tests performed on the first sixteen boreholes (UO1-UO16) allowed Botha *et al.*, (1998) to group boreholes UO4, UO5, UO6, UO7, UO8, UO9, UO11, UO13, UP15, and UP16 as were classified as those which intersect the main fractures, with consistent and regular draw-downs responses to the stress from UO5. The results from these constant rate tests confirmed how in Karoo aquifer, the hydraulic parameters (mainly the transmissivity **T**) obtained with the Theis model depend on the depth at which the pump is installed, as previously observed by Verwey and Botha (1992). That was later confirmed by van Tonder *et al.* (2001), who concluded that most pumping test data are evaluated using analytical solutions such as Theis or Cooper-Jacob with assumptions that cannot be applied to fractured rock environments. Botha *et al.* (1998) attempted in vain to clarify the behaviour of the Karoo aquifer on the campus test site with cross-borehole packer tests failed due to the geometry of the aquifer, which is highly heterogeneous. However, they use double packer tests on the campus test site to yield average values of horizontal conductivities ( $K_h$ ) for the more important formations (Figure 5-3). An average value of  $2.754 \cdot 10^{-4}$  m/s was determined for the mode I fracture. They

underlined the importance of the presence of bedding-parallel fractures in the Karoo for borehole productivity.

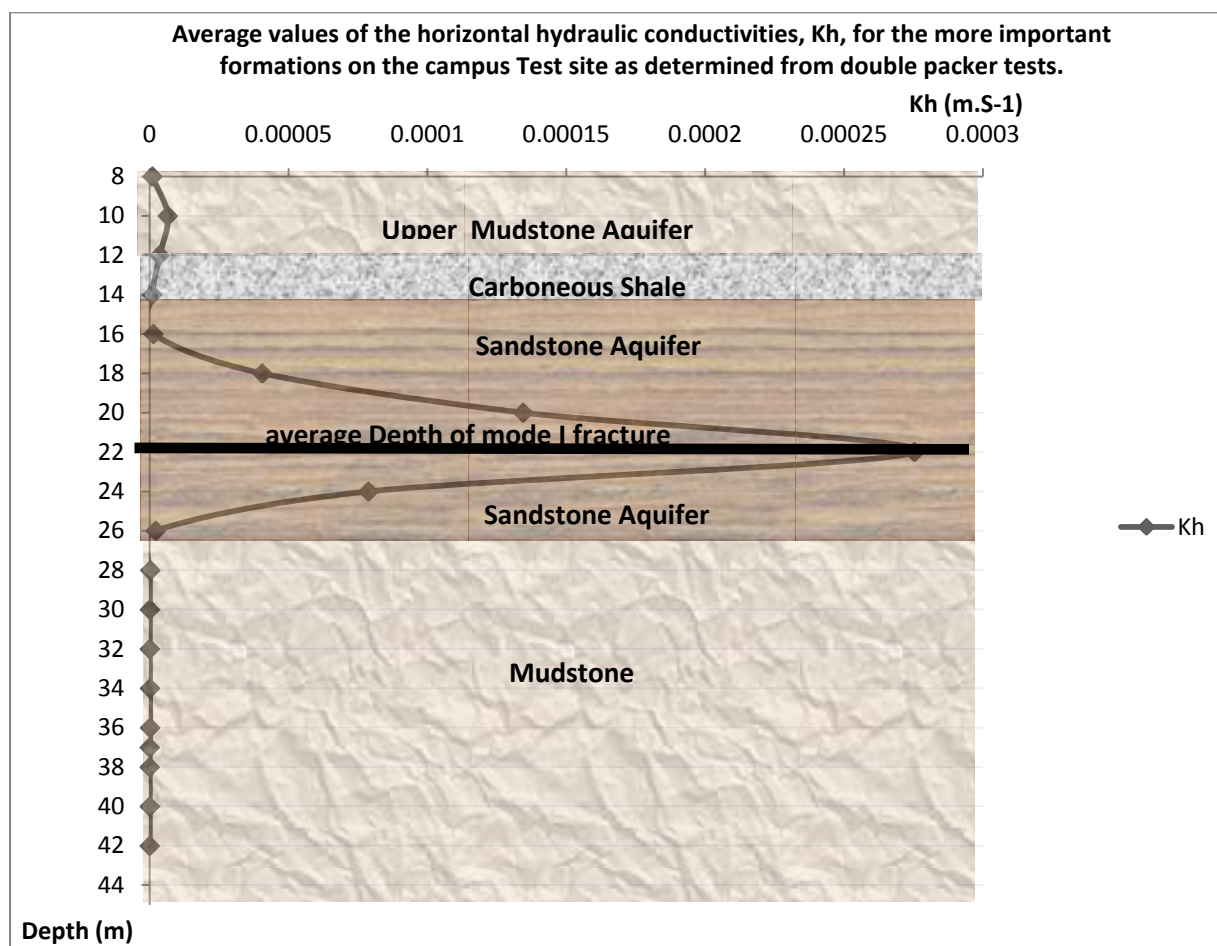


**Figure 5-3 Average values of the horizontal hydraulic conductivities,  $K_h$ , for the more important formations on the campus Test site as determined from double packer tests.**

Groundwater flow in the Karoo is mainly controlled by these fractures, and water pumped from a borehole that intersects such fractures is assumed to move first from the matrix (as a reservoir) to the fractures and then from the fractures (as conductors) to the borehole. The possible abstraction rate over a short term is determined by the fracture. The longer term flow rate to the borehole is determined by the flow from the matrix to the fracture, which is function of the matrix  $T$  and the Area. The possible abstraction rate from such a borehole is controlled by the bedding-parallel fractures and the layered nature of the formations. Three-dimensional models are therefore required for the study of such a system. A three-

dimensional model has been developed on the campus test site in studies, using the three-dimensional computer programme SAT<sub>3</sub> (Verwey and Botha, 1992). Results from this three-dimensional model revealed two important findings:

1. Water level in open boreholes in the Karoo is representative of the average piezometric level in the main fracture and the aquifer, weighed in favour of the piezometric level in the main fracture;
2. The flow velocities in the fractures are very high.

The campus test site model showed that groundwater flows mainly vertically in stressed Karoo aquifer. This allowed Botha *et al.* (1998) to derive a two-dimensional vertical model from the three-dimensional model. This model yields hydraulic parameters that are more realistic than the conventional two-dimensional horizontal model (which neglects the aquifer geometry) used in primary aquifer characterisation. Botha *et al.* (1998) gave insight also on deformation in Karoo aquifer.

In the context of the utilisation of tracer experiments for the development of rural water supply strategies for secondary aquifers, a series of tracer tests (point dilution, radial convergent) have been conducted on the campus test site (UO5, UO6, UO7, UO8 and UO20) to provide information on the travel times of water in the aquifer, aquifer parameters, the geometry of fractures and the role of fractures of different apertures in contaminant migration. It has been found that natural groundwater velocities in a sedimentary rock can be as high as 27 m/day, and at the scale of the fracture zone, the calculated effective porosity is 30 % (van Wyk, 1998). The main outcomes of this work are summarised as follows:

1. Velocity estimates from the borehole dilution test are in agreement with the results of the radial convergent tracer tests, and the method is regarded as valid if the value of the effective porosity is known.
2. Equivalent apertures are not regarded as valid for velocity estimations with the dilution test method.

3. Since the effective porosity cannot be derived from hydraulics tests, porosity estimation involves a tracer migration test in the aquifer between two boreholes (porous model).
4. The derivation of the K-value from slug test data in fractured aquifers is scale related, and often misinterpreted since the actual aquifer thickness,  $b$ , is not known. In the case of pollution studies, it is recommended that a tracer test be conducted to derive the K-value.
5. The peak of a tracer breakthrough curve does not represent the mean pore velocity of the fluid in the medium. This is called "the dominant flow velocity".

Van Wyk (1998) recommended a radial flow field tracer test, as a field method for velocity estimation (under stressed condition). The outcome of the recommended test should be the measurement of the rate of the tracer recession in the injection borehole, the tracer breakthrough in the abstraction borehole, and the hydraulic head between the boreholes.

The project 'Guidelines for Aquifer Parameter Estimation with Computer Models', initiated by the Water Research Commission of South Africa (Chiang and Riemann, 2001), five additional boreholes (UO26, UO27, UO28, UO29, UO30) were drilled on the campus test site. Borehole fluid conductivity logs, hydraulic (abstractions from UO5 and UO26) and tracer tests were conducted on the campus test site's boreholes to locate the accurate positions of the intersected fractures and to estimate the hydraulic parameters of the aquifer system (Riemann 2002). The fractures' depths determined from the field tests (Table 5-2.) were in agreement with the previous averaged fracture depth (22 meters) determined by *Botha et al* (1998).

**Table 5-2 Depth of the fracture zone in the new boreholes (m under surface) (After Riemann, 2002)**

Borehole	Depth of fracture	Method of estimation
UO23	21 m	Borehole video
UO26	24 m	Tracer test, borehole conductivity log
UO27	21 m	Tracer test, borehole conductivity log
UO28	20.5 m and 22 m	Tracer test, borehole conductivity log
UO29	21 m	Tracer test, borehole conductivity log
UO30	21 m	Tracer test, borehole conductivity log
Average value	21.66 m	Arithmetic mean

The analysis of the constant rate test (UO26 was pumped and UO27, UO28, and UO29 was observed) data using different analysis methods (Theis, Cooper-Jacob, drawdown-distance and the GRF model) showed different results, and Riemann (2002) concluded that the porous media models estimate hydraulic parameters values for the whole aquifer thickness; while the GRF-model estimates averaged values (Table 5-3) over the fracture zone flow domain, and the Cooper-Jacob II method relates to a single fracture ( $T = 755 \text{ m}^2/\text{d}$  and  $S = 5.87 \cdot 10^{-7}$ ). Riemann (2002) said that early time drawdown (less than 3 minutes) data of a constant rate pumping test, could be used to estimate the transmissivity of the fracture zone using the Cooper-Jacob 2 (CJ2) method. This method (CJ2) known also as drawdown-distance method involves at least two observations boreholes. At a specific time of constant pumping at rate  $Q$ , the semi-log plot of drawdown versus distance (of observation boreholes) shows a straight line with slope (drawdown difference  $\Delta s_m$  per log cycle of distance) equal to  $\frac{2.3 Q}{2\pi T}$ . Hence, the transmissivity "T" is then deducted as follow:

$$T = \frac{2.3 Q}{2\pi \Delta s_m} \quad \text{Equation 5.4}$$

After Riemann (2002) the transmissivity value, estimated with the distance-drawdown method is close to the value ( $700 \text{ m}^2/\text{d}$ ) obtained for the fracture zone in



March 1994 (UO5 was pumped at constant rate and UO6, UP15 and UP16 was observed). Different constant rate tests (UO5 was pumped, and piezometers in UO27, UO28, UO29 and UO23 were observed), to assess separately the responses of fracture zone and the matrix, confirmed for the fracture zone a transmissivity of 743 m<sup>2</sup>/d with the Cooper-Jacob II method (Riemann 2002). And the results (Table 5-4) of Barker model on this data (UO5-test) are in argument with

**Table 5-3: Parameter values for UO26-test obtained from Barker model (Rieman, 2002).**

Borehole	Kf (m/d)	Ssf	N
UO26	199	2.7E-3	1.85
UO27	187	1.7E-2	1.80
UO28	201	2.4E-3	1.84
UO29	200	1.1E-3	1.85

**Table 5-4: Parameter for UO5-test obtained from Barker model (Rieman, 2002).**

Borehole	Kf (m/d)	Sf	N
UO5	653	2.6E-3	1.75
UO6	645	1.1E-3	1.75
UP15	651	1.5E-3	1.75
UO16	657	1.7E-3	1.74

Chiang and Riemann (2001) constructed a numerical model constructed for the site by using the 3D Modflow program PMWIN (Chiang and Kinzelbach, 2001) and using twenty layers of thickness of 0.5 m and 1 m respectively above and below the main fracture layer with a thickness of 0.2 m. They used the inverse model PEST (Doherty, 2000) to calibrate the data (of UO5 March 1994). The estimated horizontal hydraulic conductivity value (3600 m/d) for the fracture for a fracture zone of about 0.2m is in agreement with fracture zone transmissivity estimated with the analytical drawdown-distance method. But strangely, a numerical model simulation with data from the constant rate discharge tests performed on UO5 in July 2000, resulted lower values (3080 m/d) for the fracture zone. The difference in the estimated Kf-value with the Barker method and the numerical model for the

UO5-tests, illustrates that there might be a hierarchy of smaller fractures present that possibly form a fractal system with a lower effective hydraulic conductivity than that of the main fracture (Riemann, 2002). Van Tonder and Vermeulen (2005) estimated the transmissivity of the fracture to be about  $580 \text{ m}^2/\text{d}$ , whereas the transmissivity of the sandstone matrix was approximately  $3 \text{ m}^2/\text{d}$ .

Point dilution and injection withdrawal tests conducted by Riemann (2002) showed special variation of the fracture kinematic porosity, which vary between 0.02 and 0.18 at UO20 and between 0.07 and 0.49 at UO28. The two tests resulted in different fracture seepage velocities values ( $10.0 \text{ m/d}$  for injection withdrawal, and  $23.1 \text{ m/d}$  for point dilution). Riemann (2002) compared estimated fracture seepage velocities values using different flow dimensions ( $n=1.75$  and  $n=2$ ) and noticed that higher values are estimated by the flow dimension  $n=1.75$ . Radial convergent tests conducted on the campus test site showed a forced flow velocity of  $51 \text{ m/d}$  for the fracture zone, which thickness is found to vary from  $0.15 \text{ m}$  at UO5 to  $0.16 \text{ m}$  at UO26 (Riemann., 2002). In his experience he combined hydraulic and tracer tests to estimate the campus test site's aquifer parameters. The main advantage of this combined method is that it enables one to estimate important hydraulic and transport parameters from the results of one test rather than conducting different tests.

Gebrekrstos (2007) and Pretorius (2007) reported on field experimentations for determining critical factors for the fate and transport of DNAPL contaminants in (porous) fractured aquifer systems in South Africa. Additionally, six percussion boreholes (D1, D2, D3, D4, D5, D6) and two core holes (DC1 and DC2) were drilled for this purpose at the campus test site, which was selected for the characterisation of fractures, particularly for the accurate investigation of the bedding-parallel fracture. Blow yield ( $>3\text{L/S}$ ), slug tests, pump tests, video camera logging, borehole geophysics, geochemical profiling, down-hole techniques and tracer tests were used together with comprehensive integration of the data, and the results showed that boreholes D2, D3, and D4 intersect the same main fracture (located between 20-22m bgs) as the 'class 3' boreholes initially identified. Pump tests were done especially to determine the aquifer parameters, the connectivity and

heterogeneity of the mode 1 fracture between boreholes, and the subsequent response of the fracture system during pumping. The results of the pumping tests (Table 5-5) showed smaller fracture transmissivity values (with the Barker method) compared to the values estimated on previous boreholes. This could be due either to the difference in analytical and numerical methods used for estimation or the fact that the transmissivity is smaller at the DNAPL mini-test, caused by spatial variability across this site (Pretorius, 2007).

**Table 5-5 Pump test results in the Campus Site (Pretorius., 2007).**

Pumped Borehole	Tf (m <sup>2</sup> /d)	Tfm (m <sup>2</sup> /d)
UO23	149	17
UO23	150	15
D3	83	16
D3	178	17
D2	149	16

Tf = fracture, Tfm = formation

Gebrekrastos (2007) showed based on field experiences that estimated transmissivities using CJ2 as stated previously by Rieman (2002), did not give any physical meaning. In Gebrekrastos experimentation, the semi-log plot of drawdown versus distance (of 05 observations boreholes) showed widely scattered boreholes, and it was not possible to fit a single line on them. Different sets of observation boreholes result in different values of transmissivity. In another case, he found that the estimated transmissivity by boreholes that do not intersect the fracture was higher than that estimated by the boreholes intersecting the fracture. These limitations are due to the fact that the standard approach does not consider the geometry of the aquifer as stated by Botha *et al.* (1998). According to Pretorius (2007), the reason for this lies in applying the wrong conceptual model to the interpretation and analysis of the data results. The water level responses in some observation boreholes (D1 and UO30) when pumping from UP16 showed also that the conceptual model previously developed by Botha *et al.* (1998) is a simplified form of the site and cannot explain

the behaviour of the boreholes satisfactorily. The tracer tests (point dilution, injection withdrawal and radial convergent) analysis resulted approximately the same parameters values as those of Riemann (2002). The estimated conservative fracture connectivity is shown in Figure 5-4 (Gebrekristos ., 2007).

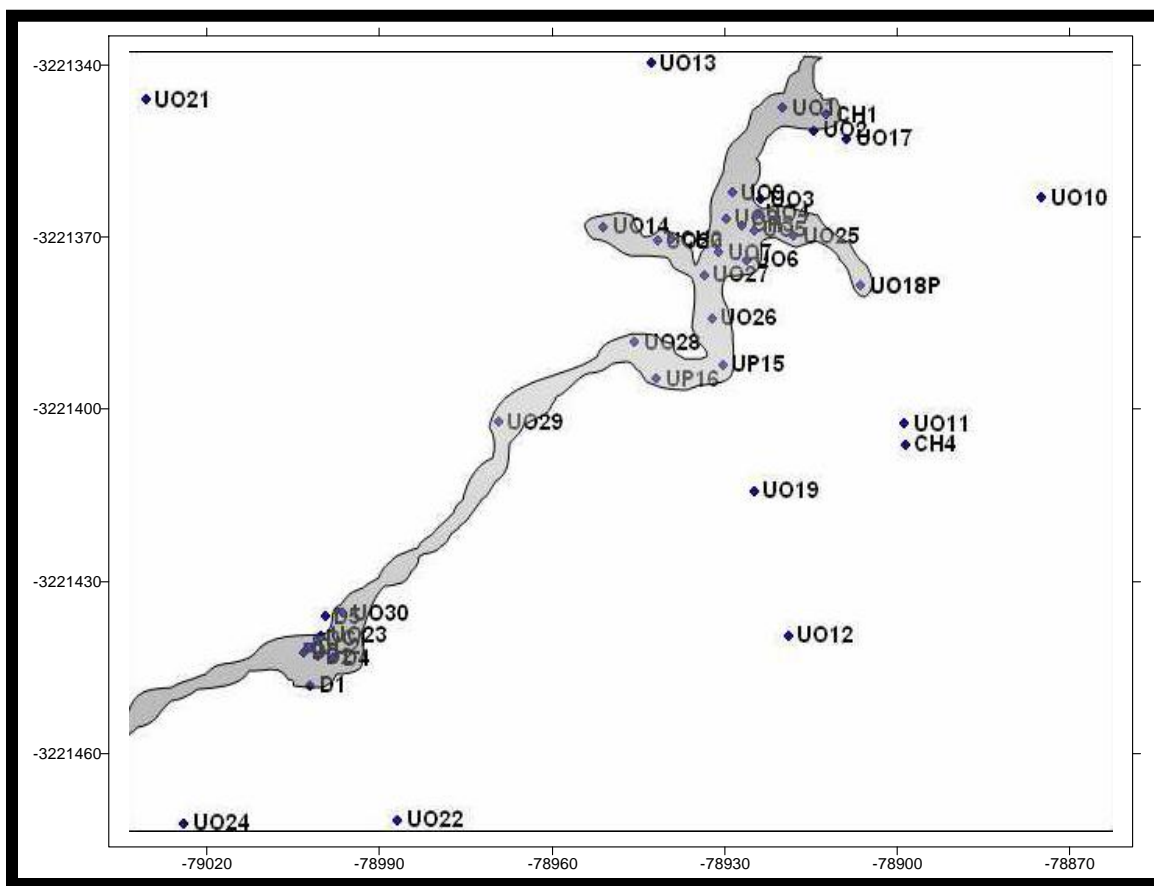


**Figure 5-4 A conservative estimate of the fracture (shaded) connectivity. (after Gebrekristos (2007))**

From the present perspective, it is clear that the campus test site is an appropriate field site for geohydrological assessment tools. The different projects conducted on the site confirm the existence of a horizontal bedding plane fracture between approximately 21 and 22 meters below subsurface that governs the main behaviour of the aquifer system.

The newly developed borehole Fluid Electrical Conductivity method has not yet been applied on the campus site for fracture characterisation. Its application may yield

better and additional information on the flow and solute transport through the characteristic bedding plane fracture present on the site.

## 5.5 Summary and recommendations

The issue of fracture characterisation in a fractured aquifer system can be summarised into three main groups of investigation:

- Laboratory and field studies of fracture properties,
- Geophysics,
- Hydraulic and tracer testing.

But the success of these three steps is strictly dependent on the geological and fracturing mechanism, which needs to be understood before any attempt is made at characterisation. The kinds of fractures that tend to form in a given setting and their commonly associated patterns are always key information that helps in decision making when flowing fractures have to be identified, located and quantitatively appreciated (geometry, flow and transport).

In the Karoo, significant efforts have been made to build up knowledge about geology and fracturing mechanisms, and few studies have been conducted on fracture properties. Most geophysical techniques (surface or underground based) are design to detect fractures remotely (where not visible), based on knowledge of fracture properties (mechanical and elastic anomalies, especially in shears; electrical resistive and electromagnetic anomalies; and permeability). Different geophysics tools have been successfully applied in the Karoo, mainly the electrical (tomography) and electro-magnetic techniques, to depict fractures related to anisotropy (anomalies), combined with other information. But there is a need for more multiple field studies of hydrologically significant fractures for indexing the specific signatures of such fractures. Geophysical methods trace mechanical, electrical, and electromechanical but not hydrological properties, and are subject to limitations such as low resolution (<100 m) and are fruitless in inherently anisotropic environments.

A large range of borehole logs specifically designed for fracture systems have also shown their benefits for characterising fracture flow systems, mainly when used in conjunction with other types of information. Such logs provide multiple measurements of physical properties along the borehole and, although available, their measurements are often restricted to a small volume of the drilling-disturbed formation surrounding the borehole. Flow and transport properties in the fractures are directly inferable for hydraulic and tracer tests, but lack of knowledge of the geometry of the fractures and the flow geometry restrict the solutions of hydraulics testing based on simplified models that do not always represent the hydrogeological system.

Solutions that allow the flow dimension to be in a range of non-integer flow values between 1 and 3, have been demonstrated to be useful in the Karoo aquifer, in combination with additional information, to diagnose its geometry system. The co-interpretation of multiple well tests has shown advantages in determining critical aspects of fracture flow systems. Tracer tests remain effective tools for assessing fractures' connectivity and some mass transport parameters, mainly in simple fracture geometry environments (dominant fracture zones). In complex fractured systems, approximation of flow geometry and boundary conditions become problematic and limit the capacity of tracer test data to yield valuable transport parameters.

Most of the existing characterisation tools are limited in their resolution and cannot be used to evaluate fracture properties at scales as large as kilometres.

## 6 THEORIES ON FLUID ELECTRICAL CONDUCTIVITY (FEC) AND ITS APPLICABILITY TO FRACTURE CHARACTERISATION

The measurement of a fluid electrical conductivity with an “electric conductivity probe” to produce an FEC log is a simple technique that does not require novel equipment or procedures, and has long been used to characterise subsurface heterogeneity (Ward *et al.*, 1998; Cook *et al.*, 2001a; Love *et al.*, 2002).

The present section of this dissertation focuses on aspects related to the link between the FEC and ion concentration, temperature, some subsurface conditions (in a borehole and depth); introduce the principle on which FEC may be based for aquifer-borehole flow and transport processes analysis. Also, the FEC logs technique as developed by Tsang *et al.* will be introduced, and the FEC-based dilution technique (borehole dilution) using salt tracers (particularly NaCl) will be presented. Aspects of the methodology related to the choice of tracer, preparation of FEC logging (contrasting the water’s salinity), and the analysis of such FEC profiles data for weighting the contribution of individual fractures or fracture zones to the total transmissivity of the borehole, will be discussed.

### 6.1 Definition of Fluid electrical conductivity

The term ‘electrical conductivity’ is the common designation of fluid electrical conductivity, which may not be confused with geo-electrical conductivity. Fluid electrical conductivity is also called specific conductance (conductivity of water at 25°C), and is defined as a measure of a fluid's ability to conduct an electrical current. Fluid electrical conductivity ( $\sigma$ ) is the inverse of fluid electrical resistivity ( $\rho$ ), and has the System International (SI) units of Siemens per meter ( $\text{S}\cdot\text{m}^{-1}$ ). But, generally, natural water (rain, surface water, and groundwater) have such low conductivities (rainwater:  $0.5 \text{ mS}\cdot\text{m}^{-1}$ ) that sub multiples of  $\text{S}\cdot\text{m}^{-1}$  such as  $\mu\text{S}\cdot\text{cm}^{-1}$  (micro-Siemens per centimeter) or  $\text{mS}\cdot\text{m}^{-1}$  (milli-Siemens per meter) are used.

$$\sigma = \frac{1}{\rho} \quad \text{Equation 6.1}$$

Related to electrical current density  $J$  and electrical field  $E$  strength, the following equation can be written:

$$\sigma = \frac{J}{E} \quad \text{Equation 6.2}$$

Generally, a material's ability to conduct electrical (conductivity) increases with increasing of the impurity in this material (doping). Pure water by example has a very low conductivity and may be regarded as non-conductor. The purer the water, the lower its conductivity. The conductivity of a fluid depends on the concentration of the charged species (ion strength), the ability of the ions to move, and sometimes other ionised chemical species. Electrical conductivity of water samples may be used as a measure of how ion-free the samples are.

The dependency of the electrical conductivity on charged species' concentrations (ion strength) in a fluid have been used for estimating the concentration of ions in fluid solution. Shedlovsky and Shedlovsky (1971) reviewed the relationship between ion concentration and fluid electric conductivity, and gave graphs and tables relating them. Fluid solution EC is a measure of the total ion concentration. Each ion has its own specific ability to conduct current. Hale and Tsang (1988) expressed at low concentrations (less than 6 Kg/m<sup>3</sup>; 11S/m) the relationship between total sodium chloride (NaCl solution) ion concentration  $C$  (in Kg/m<sup>3</sup>) and corresponding electrical conductivity  $\sigma$  (in S/m), at 20°C, as follows:

$$\sigma = 0.187C - 0.004C^2 \quad \text{Equation 6.3}$$

For NaCl solution concentrations of up to 4 Kg/m<sup>3</sup> and corresponding electrical conductivities of up to 7 000 S/m, they observed a linear relationship between  $\sigma$  ( $\mu\text{S}/\text{cm}$ ) and  $C$  (Kg/m<sup>3</sup>):

$$\sigma = 1870C \quad \text{Equation 6.4}$$

Gebrekrastos, (2007) reported from experimental studies on the campus test, that the concentration of "NaCl" (in mg/L), is four times the EC value (in mS/m). Using chemistry data (from IGS laboratory) collected on few boreholes on the campus test site between 1990 and 1995, the following linear relation can be deducted (Error! Reference source not found.):

$$C = 1.6966\sigma - 73.815$$

Where, the FEC  $\sigma$  is expressed in mS/m and the NaCl ion concentration  $C$  in Kg/m<sup>3</sup>.



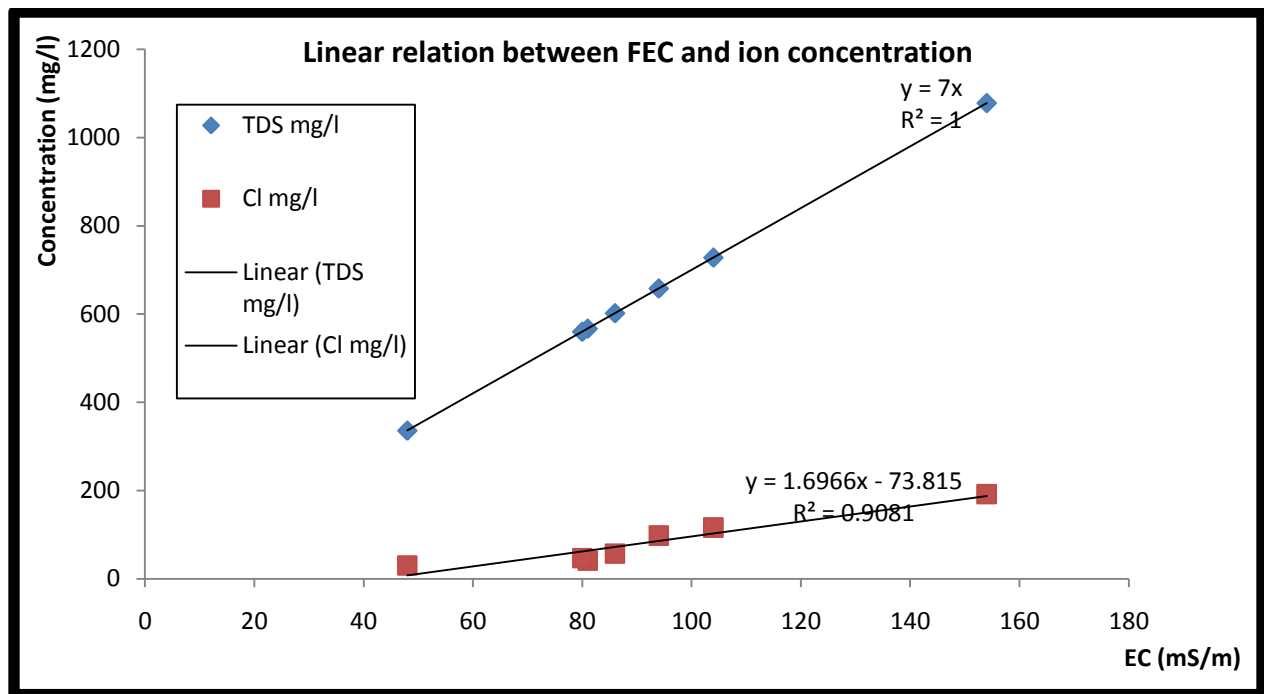


**Figure 6-1 Linear relation between Fluid Electrical Conductivity and ion concentration in groundwater at the campus test site.**

At low concentrations ( $\text{FEC} < 10\,000\ \mu\text{S}/\text{cm}$ ), another linear relation between FEC and ion concentration was expressed through the empirical equation that relates total dissolved salt (TDS) to FEC as follows:

$$\text{TDS} = k\sigma \quad \text{Equation 6.5}$$

Where,  $\sigma$  is in  $\mu\text{S}/\text{cm}$ , TDS is in mg/l, and  $k$  is the slope of the curve TDS versus  $\sigma$ . Experimentally,  $k$  has been found to range between 5 and 10, depending on the dominant anion. For bicarbonate or chloride dominated waters  $k$  is close to 7 as proved on the campus tests site (Figure 6-1).

## 6.2 Fluid electrical conductivity and temperature

Because electrical current is carried in the fluid by ions, chemical changes occur in the solution and an increase in temperature decreases the resistance, unlike in metal, where the electrical current is transported by electrons without changing any chemical properties of the substance and an increase in temperature increases the electrical resistance. Schlumberger (1984) give a formula for fluid FEC conversion from logging data collected at any temperature  $T$  in  $^{\circ}\text{C}$ , to FEC at  $20^{\circ}\text{C}$  (for calculation of ion concentration):

$$FEC(20^{\circ}C) = \frac{FEC(T)}{1+s(T-20^{\circ}C)} \quad \text{Equation 6.6}$$

Where, S is a parameter with value  $0.024^{\circ}C^{-1}$ .

### 6.3 Borehole fluid electrical conductivity

A borehole constitutes an induced local point of shortcutting (interaction) of different flow systems occurring in the subsurface. One of the main concerns, when considering the fluid electrical conductivity logs from a single borehole is the understanding of the vertical variation (natural or induced) of the EC values in the borehole. Yet, the considerations for understanding the fluid electrical conductivity along a borehole vary from ambient condition to pumping condition.

In ambient condition, differences in hydraulic head at feed points (fractures or flow zones) intersected by a borehole, creates an internal borehole flow (from the highest hydraulic head points to the lowest hydraulic head points). This internal borehole flow is associated with chemical and transport processes (dispersion, diffusion, advection, etc...). The effect of density gradient (if exist) need also to be considered to understand the vertical FEC distribution in a borehole. Therefore, the quality (concentrations distribution) of a fluid in a borehole may not be necessary representative of water from just one system, and cannot be directly associated with the formation's FEC. In uniform head formation (absence of internal borehole flow), the natural groundwater flow in an open borehole is horizontal from an inflow point to a corresponding outflow point located approximately at the same elevation. In the present dissertation, a section through which an internal borehole flow occurs is called "flowing section", and the one which no internal borehole flow is observed is called "stagnant section". Although ambient condition imply no pumping occurrence in the borehole, measured responses (FEC logs) could be influenced by pumping from another borehole that intersects the same flow zones.

In pumping condition, the water movement in the borehole is from all the existing feed points to the pump position, skewing the curve toward the pump position, and eliminating the natural occurrence of borehole internal flow. This movement of the water is associated with mainly advection and diffusion. The effect of density gradient in the borehole can be significantly reduced, but not necessary eliminated.

For a hole of large radius, the FEC electrical conductivity may considerably vary from one point to another at the same depth. In the hydrogeological investigations, the borehole's radiuses are small compared with their total lengths. Salinity is assumed to be uniform at each depth in a borehole.

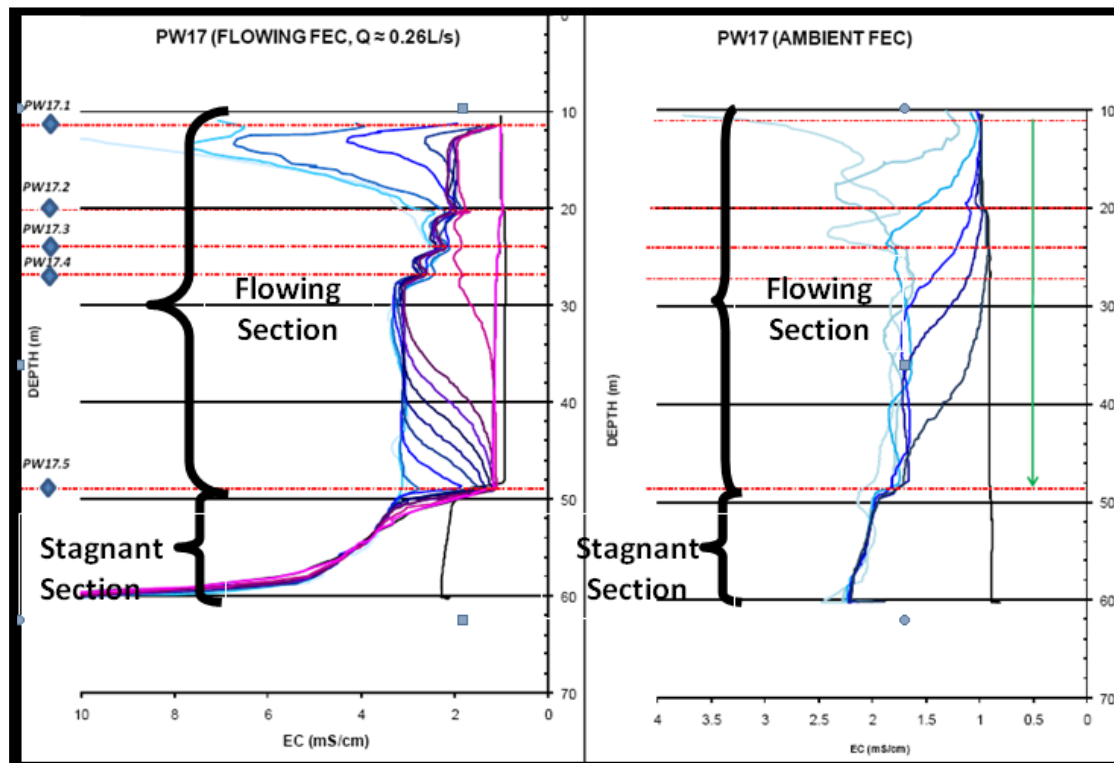


Figure 6-2 Illustration of flowing and stagnant sections from FFEC and SFEC profiles on PW17 (adapted from Morh and van Biljon (2009))

#### 6.4 Principles of FEC for aquifer-borehole flow and transport processes analysis

The FEC based method considers uncased sections of a wellbore that intersect a number of flowing fractures or conductive zones in the borehole. Generally in ambient (without pumping) conditions, salinity increases continuously with depth in a borehole, and the FEC is constant in the stagnant sections and varies in flowing sections. Erratically distributed salinity along a borehole's section may be the effect of feed points. In the flowing sections, the water quality is affected by the quality of the water from feed points (permeable layers or fractures); while in the stagnant sections, the water quality is more affected by the quality of water stored in the formation (diffusion) according to the residence time of the water. This principle

has been used to determine in-field conditions the effective diffusion coefficient of a formation (Gebrekristos, 2007).

The FEC at a flowing section may be higher or lower than the FEC at stagnant water sections, according to the quality of water entering the borehole. In non-contaminated environments, fresh water from feed points with relative lower electrical conductivity circulates through flowing sections; while in stagnant sections, water with relative higher electrical conductivity stills. In Contaminated environments, groundwater is often associated with high electrical conductivity, and feed points, in such environment are often identified by relatively high fluid electrical conductivity on a borehole FEC profile in natural conditions. Atekwana *et al.* (1998) mentioned that groundwater hydraulically conductive zones associated with the biodegradation of LNAPLs in the subsurface can provide a window into the biogeochemical processes ongoing at such sites.

According to the type of flow zone properties needed, the borehole's FEC log data needed. Natural stratification of electrical conductivity in a borehole can be assumed to equal to that in the aquifer (Love *et al.*, 2002) and may be used in fractured aquifers, to detect the potential location of the main conductive points of the aquifer that draws waters to the borehole. But for confirming the conductive points position and for the determination of the rate of the groundwater flow through these conductive points, time sequence of measured FEC logs are required. The measured time sequence FEC logs are assumed to constitute the subsurface responses to induced changes in the concentration of the water in the borehole. The changes can be made by simply disturbing (recirculation) the natural stratification (Love *et al.*, 2002) or by changing the bore fluid water with significantly different salinity water (Cook *et al.*, 2001a; Gomo., 2010; Tsang *et al.*, 1990; Pedler *et al.*, 1992; Bauer and LoCoco, 1996; Mohr *et al.*, 2009).

### **6.5 Flowing Fluid Electrical Conductivity logging method (FFEC)**

A method called the 'flowing fluid electric conductivity logging method' (FFEC) has been developed by Tsang *et al.* (1988, 1989, 1990) to identify depth locations of feed points and evaluate the transmissivity and the salinity of the fluid at each

inflow point. Changes in the borehole FEC are by substituting the borehole water with de-ionised or constant low salinity water. In this method, each feed point is characterised by the time  $t_i$  when the flowing fluid emerges from the feed point to the fracture, the location  $x_i$  of the inflow point, the volumetric inflow (or outflow) rate  $q_i$ , and the solute mass inflow rate  $q_i C_i$ . In these conditions, the conductive zones intercepted by the borehole are constantly stressed by a very low pumping rate (generally lower than 10 L/min), and the general flow along the borehole is toward the pump position (often at the top of water column). The time  $t_i$  may be different from one feed point to another, due to possible differences in initial values of hydraulic heads and pressure history, which results in the entering of de-ionised water into the feed points during borehole washout.

Figure 6-3 below shows a schematic picture of a wellbore with inflow  $n$  points, with a vertical borehole flow rate  $w$  from below (Tsang *et al.*, 1990).

The entering of the groundwater into a borehole results in peaks' areas on the curve, at particular feed point depths. The area under each peak of the curve increases with time as a function of the feed point flow rate  $q_i$  and its salt mass rate " $q_i C_i$ ". Without any overall upward flow, and by neglecting density effect, the distribution of the salinity curve at each feed is supposed to be symmetrical at the feed point location. The overall up-flow due to pumping skews the salinity curves. This effect becomes more significant as the feed point is located closer to the pumping position. Therefore, by analysing the sequence of FEC profiles, which depicts dynamic flow and transport responses, it is possible to obtain the flow rate and salinity of groundwater inflows from each individual feed point.

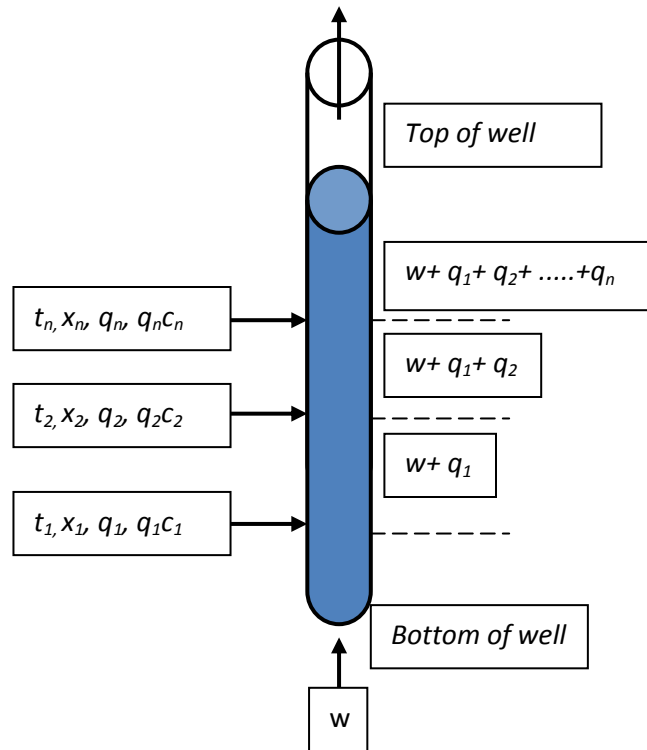


**Figure 6-3 Schematic picture of a borehole with  $n$  inflow points and, borehole flow  $w$  from below adapted from Tsang *et al.* (1990)**

As time passes, the salinity will increase at each feed point and will finally reach a saturation value. The salinity saturation value  $C_{max_i}$  for each single feed point, assuming negligible diffusion, is given by:

$$C_{max_i} = \frac{wC_0 + q_i C_i}{w + \sum_{n=1}^i q_n} \quad \text{Equation 6.7}$$

Where  $w$  is the borehole flow rate from below the studied section,  $C_0$  is the initial concentration of the borehole water, and  $q_i$  is the volumetric inflow rate with  $i = 1$  for the deepest feed point.

In the case where successive feed points show peaks on the FEC profile that overlap at or before saturation time, the salinity saturation of the " $(i + 1)th$ " feed point is given by:

$$C_{max_{i+1}} = \frac{wC_0 + q_i C_i + q_{i+1} C_{i+1}}{w + \sum_{n=1}^{i+1} q_n} \quad \text{Equation 6.8}$$

At the limits of a very long time period, Tsang *et al.* (1990) mentioned that the saturation concentration between " $ith$  and  $(i + 1)th$ " feed points as:

$$C_{max_i} = \frac{wC_0 + \sum_{n=1}^i q_n C_n}{w + \sum_{n=1}^i q_n} \quad \text{Equation 6.9}$$

### 6.5.1 Borehole fluid conductivity logging (field procedure)

Firstly, the existing water in the study well is changed with de-ionised water or water of a constant salinity, distinct from that of the surrounding formation water. The de-ionised water is pumped via a tube to the bottom of the wellbore at a given rate, while the water in the wellbore is pumped out simultaneously from the top of the borehole at the same rate. The main objective of replacing the existing borehole is to create in the borehole an initial condition that will allow a better analysis of the FEC log (quasi-homogeneity, no density gradient, etc.). Secondly, the well is pumped out at a constant flow rate (usually at low rate), which can be adjusted to optimise borehole flow conditions. When pumping at a constant low rate, an electric resistivity probe is lowered into the borehole to scan flowing fluid electrical conductivity (FFEC) as a function of depth down the borehole. The variation of vertical electrical conductivity profile (down the borehole) versus time may be used to identify inflow and outflow points on the wall of the borehole. This variation is recorded by a series of five or six FEC loggings obtained at time intervals over a one or two day period. In fact, at a specific time, the vertical FEC profile shows peaks at the depth levels where water enters the wellbore. This is due to the fact that, in general, fractures (or more transmissive layers) contain fluids with different ion concentrations from each other and therefore different electrical conductivities. During the logging procedure, care should be taken to reduce as much as possible the scale of induced disturbance of the borehole fluid. The analysis of such time sequential profiles may provide information on the permeability and salinity of each hydrologic transmissive layer.

The method is applicable either in primary or secondary aquifers, as well as shallow or deep aquifers, and is cost effective. Tsang *et al.* (1990) when comparing other single hole methods, described it as much more accurate than flow meters and much more efficient (much cheaper) than packer tests, particularly in low permeability formations.

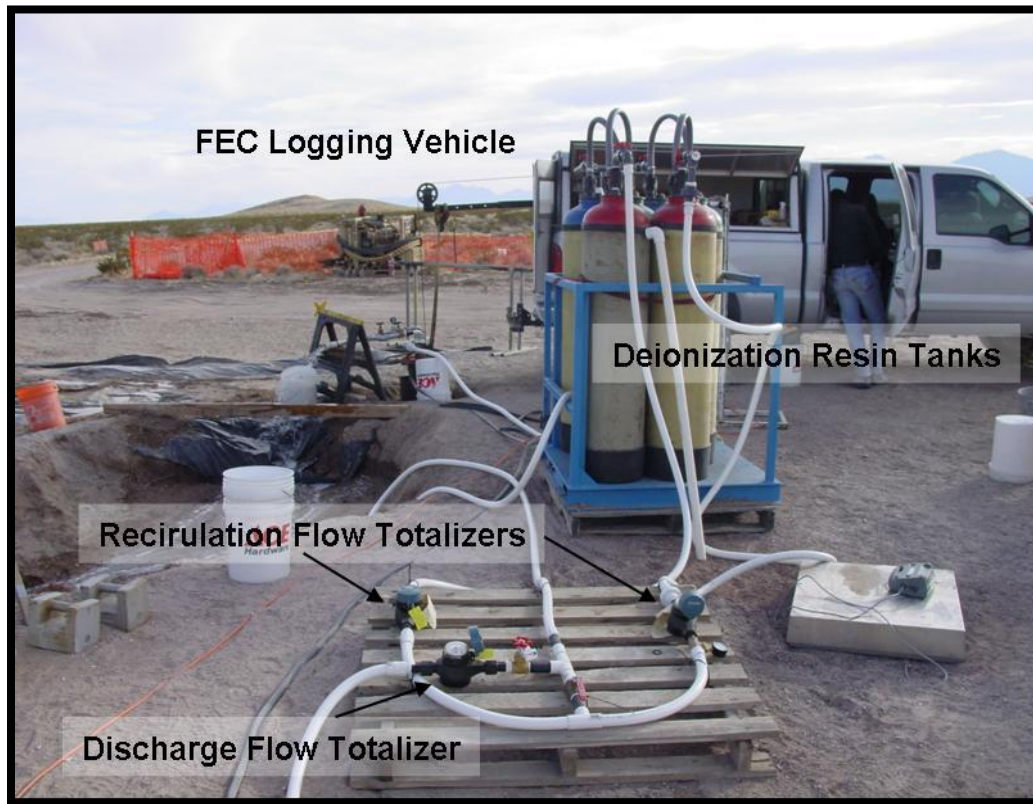


**Figure 6-4 FEC logging equipment setup at Borehole NC-EWDP-24PB in the Armargosa Valley. From Doughty et al. (2006)**

### 6.5.2 Analysing fluid conductivity logs

As explained above, fractures (or more transmissive layers) contain fluids with different ion concentrations from each other and therefore different electrical conductivities. The FEC profiles may give qualitative or quantitative information on flow and processes in the borehole. Locations where fluid enters the wellbore, show peaks in the FEC logs which can be analysed to infer inflow points' strengths and salinities (Doughty *et al.*, 2005). At each feed point detected by the FEC method, a distinctive peak is depicted on the FEC profile at a specific time  $t_i$ . At first (until adjacent peak curves start to overlap), the area under this peak extends with time as a function of the inflow rate  $q$  and the salinity  $c$  of the fluid flowing into the borehole. By considering the extent of this area, and the boundary conditions (early and late), one can infer analytically and/or numerically the volumetric inflow rate  $q_i$ .



and the salinity associated with each feed point  $i$  at depth  $C_i$ . The estimated volumetric inflow rate  $q_i$  can be combined with other information (drawdown in the well, change in head of each feed point, total length of pumping, well section radius) to calculate the transmissivity of each fracture, feed point or zone.

#### 6.5.2.1 Analytical Approaches for FEC analysis

By assuming for each feed point, constant volumetric inflow rate  $q_i$  and constant feed point water concentration  $C_i$ , Tsang et al (1990) related the area under each feed point located at  $x_i$  (m) to the solute mass inflow rate  $q_i C_i$  over time  $t$ . The following simple mathematical equation describes this relation, and may be used to determine analytically the flow rate  $q_i$  and salinity  $C_i$  at each detected feed point, by using early and late time readings.

$$\int_{x_i+\delta_1}^{x_i+\delta_2} \pi r_w^2 (\sigma(x, t) - \sigma_0) dx = \alpha(q_i C_i) t \quad \text{Equation 6.10}$$

Where  $\delta_1$  and  $\delta_2$  are appropriate distance from the peak axis, for bracketing the peak area;  $r_w$  is the average borehole radius over the section between  $x_i + \delta_1$  and  $x_i + \delta_2$ ;  $\sigma_0$  is the initial electrical conductivity of the water in the borehole,  $\alpha$  is a constant that relates salinity to electrical conductivity, and  $t$  is the time since the feed point water started to flow in to the borehole.

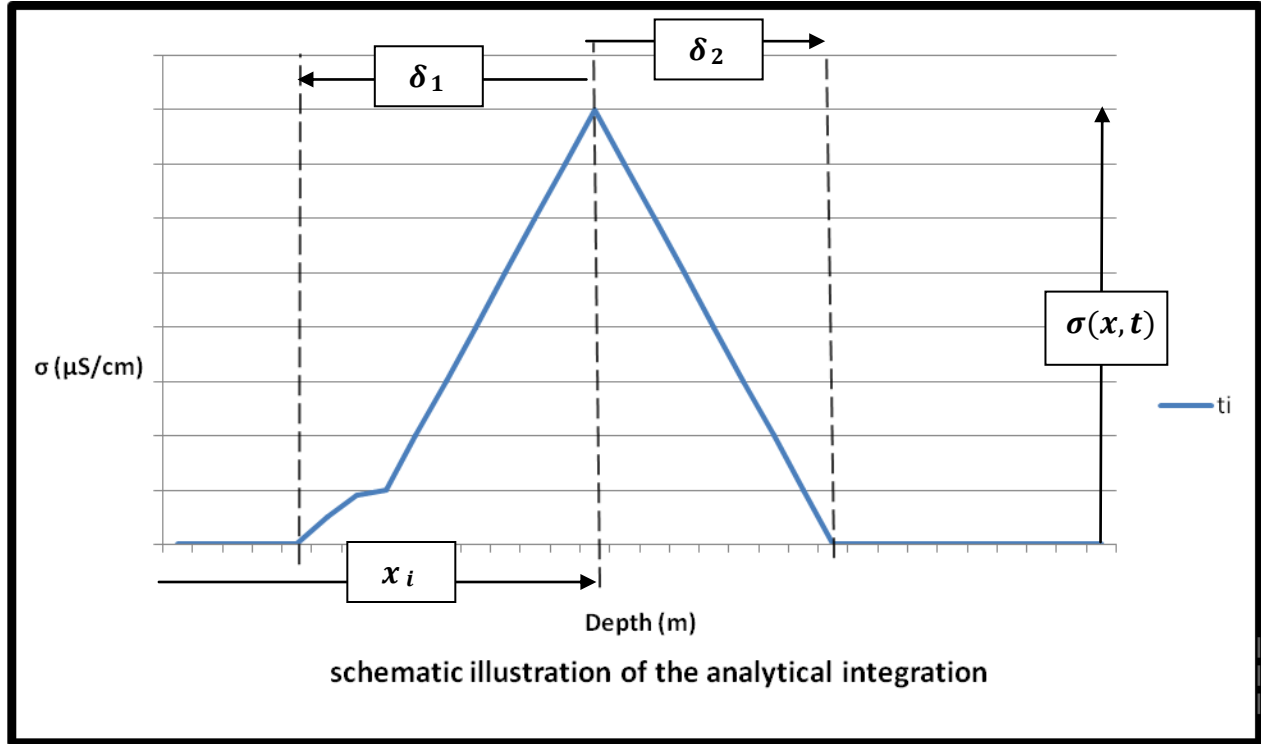


**Figure 6-5 Schematic illustration of analytical integration**

This expression may be arranged as follows:

$$\frac{\int_{x_i+\delta_1}^{x_i+\delta_2} (\sigma(x,t) - \sigma_0) dx}{t} = \frac{\alpha(q_i C_i)}{\pi r_w^2} \quad \text{Equation 6.11}$$

In this formula, the term  $\int_{x_i+\delta_1}^{x_i+\delta_2} (\sigma(x,t) - \sigma_0) dx$  is representative of the area under the peak at  $x_i$  at a given time  $t$ , and should be evaluated at early time, before curves of adjacent peaks start to overlap each other. For a sequence of a few FEC profiles, the plot of  $\int_{x_i+\delta_1}^{x_i+\delta_2} (\sigma(x,t) - \sigma_0) dx$  over time will give a curve with slope  $slp$  that is numerically equal to  $\frac{\alpha(q_i C_i)}{\pi r_w^2}$  and the slope line will intersect the time axis at  $t_i$  when the feed point water started to flow into the borehole.

$$slp = \frac{\alpha(q_i C_i)}{\pi r_w^2} \quad \text{Equation 6.12}$$

$q_i C_i$  and  $t_i$  can be deducted from this relation and used with late time result, in the equations 6-8 and 6-9 described at above, to determine for each feed point located at depth  $x_i$ , the constant volumetric inflow rate  $q_i$  and constant feed point water concentration  $C_i$ .

The same authors (Tsang et al., 1990) proposed another analysis method, based on the principle of mass conservation that does not require late time reading, therefore reduces significantly the duration of the FEC logging test. Considering the illustration in Figure 6-6, and by assuming a constant electrical conductivity  $\sigma_0$ , at the bottom  $L_0$  of the studied section of the borehole, the method consist of determining for each vertical position  $L$  along the borehole, the sum  $Q_L$  of all volumetric inflow rates  $q_i$  between  $L_0$  and  $L$ . To simplify the analysis, the up flow rate  $w$ , at the bottom of the borehole, is neglected and the water is assumed to start flow from all the considered inflow points into the borehole at the same  $t = 0$ .

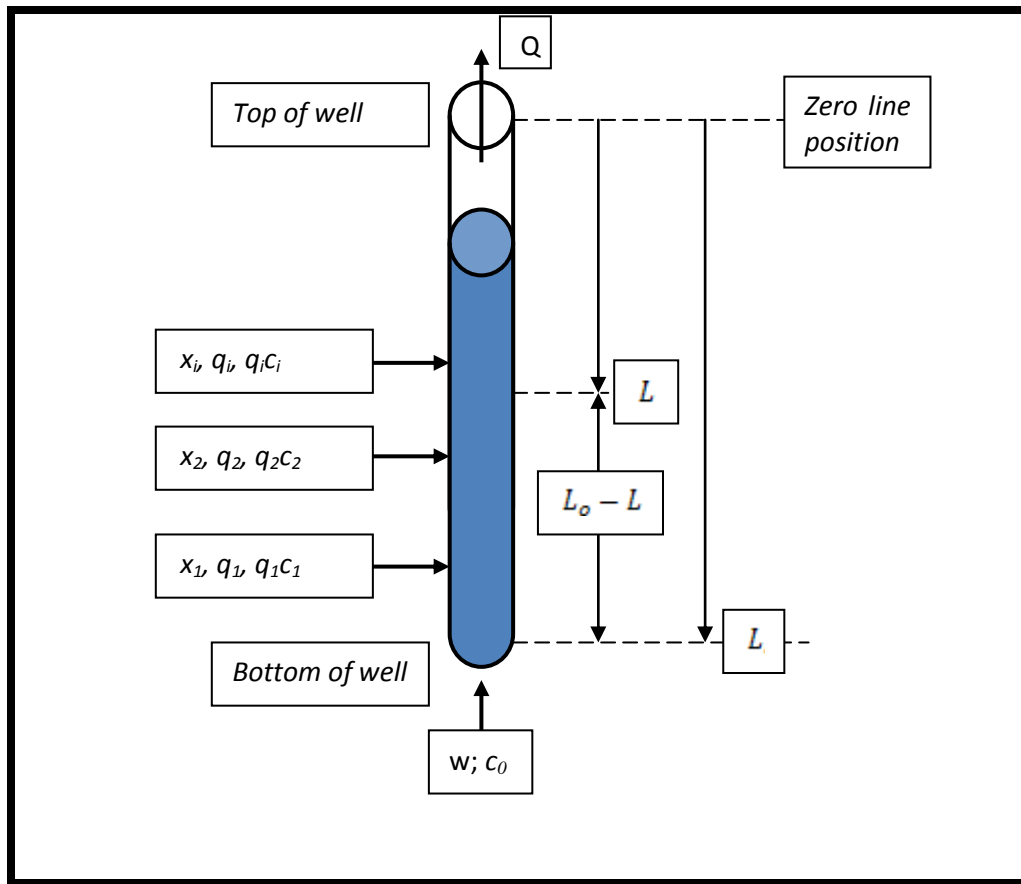


**Figure 6-6 Schematic diagram of a wellbore with several inflow points. Each inflow point is characterised by a flow rate  $q_i$ , concentration  $C_i$ , and position  $x_i$ .  $Q$  is the total flow rate out of the well;  $C_0$  is the initial salinity; and  $w$  is the inflow at the bottom of the well. Redrawn from Tsang et al. (1990).**

By assuming a linear relationship between electrical conductivity and salinity (concentration) in the borehole,  $Q_L$  is expressed as follow:

$$Q_L = \frac{\alpha t \sum_{L < x_i < L_0} q_i C_i - [(L_0 - L) \pi r_w^2] [\sigma_{L(t)} - \sigma_0]}{\int_0^t (\sigma(L, t) - \sigma_0) dt} \quad \text{Equation 6.13}$$

The only term of this equation that cannot be directly obtained from the measurement of the electrical conductivity of the water in the borehole, is the first term of the numerator, which may be deduced as follows:

$$\alpha q_i C_i = \frac{\int_{x_i + \delta_1}^{x_i + \delta_2} \pi r_w^2 (\sigma(x, t_2) - \sigma(x, t_1)) dx}{t_2 - t_1} \quad \text{Equation 6.14}$$

Then, the real time  $t_i$  when feed point water started to flow into the borehole can be deduced from Equation 6.14:

$$t_i = t_1 - \frac{\int_{x_i + \delta_1}^{x_i + \delta_2} \pi r_w^2 (\sigma(x, t_1) - \sigma_0) dx}{\alpha q_i C_i} \quad \text{Equation 6.15}$$

Further developments of Equation 6.13 that take into account time varying of  $q_i$  and  $C_i$ , have been undertaken, and all these analytical formulas have been programmed in a simple code called PRE (Tsang et al., 1990). Assessment of the analytical method using Equation 6.11 showed a dispersion effect in its results, mainly at or near the position  $L$ . The analytical solution is also not applicable when  $q_i$  varies with time. To overcome this limitation, Tsang *et al.* (1990) introduced a numerical code to adjust the analytical results to match the field data.

The main advantage of these developed analytical methods is that because of the integration form that governs their mathematical expression; their results are not affected by borehole radius.

#### 6.5.2.2 Numerical Approach for FEC analysis

The FEC analytical analysis method is conducted according to a code called BORE (Hale and Tsang., 1988; Tsang, 1985 and Tsang and Doughty, 1985) that carries out a forward calculation to produce wellbore FEC profiles given different inflow characteristics (positions, inflow rates, and inflow concentrations). The code allows analysis of solute dilution in a borehole for determination of ambient horizontal flow velocity in the formation, as proposed by Drost *et al.* (1968), and can analyse the combination of horizontal flow across the wellbore and vertical diffusion or dispersion along the depth of the wellbore.

With the development of computer science, the code has been improved to run under current operating systems, to provide interactive modification of model parameters and produce graphical comparisons between model and field data. In addition to these capabilities, the revised code BORE II allows: the salinity of the fluid at any feed point (either inflow or outflow), and the ambient far field pressure head to be determined; even in non-uniform initial salt concentrations along the section of an open borehole (Tsang et Doughty, 2003; Doughty et Tsang, 2005; and Doughty *et al.*, 2008).

The code uses the finite difference method to solve the advection/diffusion equation along the section studied, by considering equal height cells along the borehole. Given the pumping rate of the well, the inflow or outflow rate of each feed point, its location and starting time, and, for inflow points, its ion concentration, BORE II calculates time and space varying FEC (along the borehole) in a wellbore containing multiple feed points. Analysis of the code, based on a one-dimensional model and assuming a generally ideal condition for the field procedure, shows the following (Hale Tsang, 1988):

- A simple polynomial correlation between ion concentration,  $C$ , and FEC;
- Ion transport occurs by advection and diffusion along the wellbore;
- Instantaneous mixing of feed-point fluid throughout the wellbore cross-section.

### 6.5.3 Determination of a fracture transmissivity

By considering each water-producing fracture (feed point) “ $i$ ” , as a single confined aquifer, the general approximated solution of unsteady flow of water to a well in a confined aquifer (Cooper Jacob., 1946) has been generalized to yield a relationship between the pressure head drawdown  $s_i$  at each flowing zone in the well, its volumetric inflow rate  $q_i$  , its transmissivity  $T_i$  , its storativity  $S_i$  , and the well radius  $r_{wi}$  at the flowing point , as follows (Tsang et al 1990):

$$s_i(r_{wi}, t) = h_{0i} - h_i(r_{wi}, t) = \frac{q_i}{4\pi T_i} \ln \left( \frac{2.25 T_i t}{r_{wi}^2 S_i} \right) \quad \text{Equation 6.16}$$

Where  $h_0$  is the initial head at a given fracture (or feed point) position and  $h(r_w, t)$  is the transient head in the well at the inflow zone.

From Equation 6.16, each flowing zone transmissivity can be calculated, but the other components of the equation should be known. The volumetric rate  $q_i$  can be determined from the results of fluid electrical analysis, and the elapsed time  $t$  from pumping test data. The borehole radius is often considered to be constant along a borehole, but more accurate borehole radius values along the borehole may be obtained with a calliper log. Fracture storativity is known to be very small, but cannot be systematically neglected in this equation. Since fractured rock is conceptualized as an equivalent porous medium in the present analysis, the product of fracture storativity ( $S_i$ ) with the fracture aperture  $b$  (aquifer thickness), called specific storativity ( $S_{sf}$ ) is used instead of storativity. The specific storativity is a function of the fluid and rock-fracture compressibility and the fracture porosity, which need to be determined using other approaches (field and laboratory). Also, the fracture aperture has to be determined. Belanger *et al.* (1988) guessed some values and applied a sensitivity analysis method on these guessed values to determine the specific storage of the fracture that fitted field hydraulics test responses (head pressure change). They noticed in their experience that the transmissivity is not significantly sensitive to change in the storage of the fracture. The last needed parameter value in the equation for calculating the transmissivity of a flowing fracture is the pressure head drawdown  $s_i$  associated with each flowing point in the well. This drawdown is the difference between the initial head  $h_{0i}$  and the transient head  $h_i(r_{wi}, t)$ . In absence of internal borehole flow (uniform head along the borehole), pressure head equilibrium prevail, and the steady state head may be taken as the initial head. The transient head  $h_i(r_{wi}, t)$  is function of the drawdown in the borehole, but is also function of the time varying density (salinity and temperature effect) in the borehole, which can be taken into account using the pumping test, FEC and Temperature profiling data.

## 6.6 FEC-based dilution test for fracture characterisation (borehole dilution)

The 'FEC-based dilution technique' technique is also known as "borehole dilution" technique (Cook *et al.*, 2001a; Love *et al.*, 2002; Cook, 2003) and is a modification (no isolation, no mixing of the fluid) of point dilution test (Riemann., 2002). Here,

the time sequence FEC logs shows a rate of dilution rather than the rate of concentration increasing as observed with the FFEC test. Also, the technique allows determining the natural groundwater flow rates at the feed points, rather than hydraulic conductivities (or transmissivity). In South Africa the well dilution methods has gained interest in South Africa. Mohr and van Biljon (2009) have used the method to refine a site conceptual model for an LNAPL-affected fractured rock aquifer in the Karoo. Lasher *et al.* (2009) used a NaCl in the FEC method to characterise hydraulic properties in the quartz arenite Table Mountain Group aquifer. They used the numerical model BORE II (Doutgthy *et al.*, 2008) to study the time evolution of the salinity in the borehole during their tests. They concluded that the technique is suitable to distinguish clearly the transmissive (flowing) fractures, between different fractures intercepted by a borehole, and is relatively cheap and practical.

### **6.6.1 Planning the test**

The planning phase is the most important and most difficult part of conducting any kind of tracer test, and helps to avoid collecting useless data for analysis. The planning phase should be based on the purposes of the test, and should yield a clear idea of the type of tracer to be used, the pumping flow rate (for the transient condition test) during FEC logging and the required equipment.

#### **6.6.1.1 Choice of tracer**

Tracers (artificial and natural) are identifiable substances that may be used to deduce the general behaviour of a subsurface formation from assessment of their activities in a flowing formation. Artificial tracers are site specific, and are introduced only in the region of interest. The use of any artificial tracer requires its physical compatibility with the medium, and the interpretation should be a function of the medium and not of the tracer. Discussions on tracers for investigation related to water science are presented by Betson *et al.* (1985). Evans (1977) presents a review of artificial tracers used to study groundwater movement. According to the scope of the present study, only artificial tracers are discussed. Van Wyk (1998) mentioned that there is no universal ideal tracer, since an ideal groundwater tracer has the following characteristics:

- It should have good solubility even in cold water;
- It is conservative and will follow the movement of the water without loss from the flow (same velocity as the groundwater) due to physical or chemical processes, like adsorption on sediments or equipment, radioactive decay;
- It is non-toxic, and can be applied with no administrative or legislative requirements;
- It is detectable with a high degree of sensitivity and can be measured accurately *in situ* in the field;
- It does not contaminate the terrain of investigation and will not affect results of further tests;
- It is inexpensive and analysis costs are low.

Also, the naturally occurrence of the tracers' molecular compounds in the groundwater (water column in the borehole) has to be considered in the choice of the tracer. Pitrak *et al.* (2006) concluded that no tracer can be used when natural concentration of it is so high that additional increase of tracer concentration would cause unfavourable attenuation of the flow or density movement of water.

Evans (1977) distinguished different categories of artificial tracers (radioactive, activatable, chemical, and particulate) according to their method of analysis. In the context of the present study, chemical tracers (Dyes and salt) are indicated, with the advantage that they can be used without authorisation, and that field detection equipment is readily available (Van Wyk., 1998).

#### **Dye tracers:**

Organic dyes (Sulphorhodamine G, Na-Fluorescein, etc.) have the advantage to be easily detectable in very low concentrations on field (reducing the amount needed) compared to salt tracers. Conversely, some of the dye tracers are not conservative, and their use may become very expensive (compared to salt tracers), since they generally require suitable analytical equipment (van Wyk, 1998).

#### **Salt tracers:**

Salt tracers are commonly used in groundwater studies. Anions such as chloride  $Cl^-$  (NaCl) and Bromide  $Br^-$  (NaBr, KBr) can be traced in groundwater movement, while



the cation compounds are lost by ion exchange. Chloride salts are acknowledged to offer a more or less good solubility with acceptable sensitivity, and their detection is cheap and easy. Potassium chloride ( $KCl$ ), sodium chloride ( $NaCl$ ), lithium chloride ( $LiCl$ ) and calcium chloride ( $CaCl_2$ ), are the common salt tracers used in groundwater studies. The dissolution of some inorganic salts may be problematic with a high discharge rate from the well or at very low temperatures.

Because of its effective availability and the existence (at relative low cost) of different means of measurements in the field, sodium chloride ( $NaCl$ ) is especially popular in groundwater studies. Radulovic *et al.* (2008) described common salt ( $NaCl$ ) as the most suitable choice of tracer, since it can be easily procured and is also easily traceable using conductivity meters.

Other groups of salt exist and have their advantages and drawbacks. The background concentration of iodide salts are generally less than  $10\text{ }\mu\text{g/l}$  in groundwater, and would fit if they were as conservative as the bromides or chlorides, which have relative high background concentration in groundwater ( $100\text{ }\mu\text{g/l}$  for bromide and  $30\text{ mg/l}$  for chloride).  $NaNO_3$  is easy to dissolve and to detect with ion-selective electrodes, but background concentrations of  $NO_3$  may be a problem. Some salt tracers require sample treatment for analysis and have to be transferred to the laboratory when they cannot be detected in the field.

In consideration of all that has been mentioned above about tracers, the tracers suggested for application in the present study are summarised in the following table:

**Table 6-1 Suggested tracers for FEC logging applications**

Tracer	Measurement	Range of Concentration	Other Applications
<i>NaCl</i>	EC-Meter	2 orders of magnitude	Single-well test Natural flow test Point-Dilution test
<i>KCl</i>	EC-Meter	2 orders of magnitude	Single-well test Natural flow test Point-Dilution test
<i>CaCl<sub>2</sub></i>	EC-Meter	2 orders of magnitude	Single-well test Natural flow test Point-Dilution test
<i>NaBr</i>	EC-Meter Ion-sensitive Sensor	4 orders of magnitude	Single-well test Multiple-well test
Fluorescein	Fluorometer	5 orders of magnitude	Single-well test Multiple-well test

**Table 6-2 Comparative table of suggested tracers for FEC logging application**

Tracer	Solubility at 20 °C	Cost per Kg (ZAR) from Sigma-Aldrich	SANS for drinking water (mg/L)		Availability
			Class1	Class 2	
<i>NaCl</i>	Very good	537.52	200	400	Easy to be procured
<i>KCl</i>	39 at 17°C	699.11	50	100	with accredited suppliers
<i>CaCl<sub>2</sub></i>	74.5	283.16	150	300	with accredited suppliers
<i>NaBr</i>	63.4	-	200	400	with accredited suppliers
Fluorescein	-	-	-	-	with accredited suppliers

### 6.6.1.2 The amount of tracer

The estimation of total tracer mass to be injected is the crucial point during the planning process of tracer experiments. The boundary conditions for the amount of salt, depend on the type of the test (SFEC, FFEC), the available measurement equipment, the type of tracer used, the type of aquifer, the quality of the standing

borehole column water and the total rate of discharge (for the FFEC logs). In the FFEC the effect of abstraction rate on the rate of dilution has to be considered. The length and the quality of the test data depends in a certain way, on the amount of added tracer. The amount of added salt should increase the salinity of the standing column water in the borehole by a certain number of magnitudes that will allow a clear and rapid observation of the responses of the aquifer in term of rate of dilution of the borehole water at the position of flow zones or fractures.

First, an equivalent fluid electrical conductivity  $\sigma_{well}$  (average of discrete FECs) is determined for the natural standing water column (background) in the well. For a sodium chloride ( $NaCl$ ) tracer, an order of magnitude two (02) is accepted for the equivalent FEC  $\sigma_{well}$  increasing. Experimental observations have shown that a tracer amount that increases the background concentration by 50 to 300 % may be sufficient (Gebrekristos, 2009). The equivalent FEC  $\sigma_{well}$  can be converted to equivalent salt concentration by using one of the different equations listed in chapter 6 (section 6.1). The maximal equivalent FEC value " $2\sigma_{well}$ " for the entire water in the studied borehole may be then expressed as:

$$2\sigma_{well} = \frac{M_T}{kV_{water}} \quad \text{Equation 6.17}$$

Where,  $M_T$  (g) is the total mass of salt to reach, and  $V_{water}$  ( $m^3$ ) the volume of water in the borehole (or studied section of the borehole), and  $k$  is the slope of the curve of FEC versus salt (NaCl) mass concentration.  $\sigma_{well}$  is considered in mS/m.

$M_T$  is the sum of the initial salt mass  $M_{in}$  in the borehole and the mass of salt that need to be added  $M_{add}$ :

$$M_T = M_{in} + M_{add} \quad \text{Equation 6.18}$$

$$M_{in} = \frac{k\sigma_{well}}{V_{water}} \quad \text{Equation 6.19}$$

By changing Equation 6.17 and Equation 6.19,  $M_{add}$  may be deducted:

$$M_{add} = \frac{k\sigma_{well}(2V_{water}-1)}{V_{water}} \quad \text{Equation 6.20}$$

### 6.6.1.3 Field equipment needed

The FEC-based dilution test is a simple technique which does not require huge and expensive equipment. The equipment needed when using a salt tracer, consists of the following:

*For both steady state and pumping tests (Figure 6-7)*

- A couple of socks (or any permeable container that can enter easily and safely into the borehole);
- A rope that is long enough to lower the slug (sock) of salt (tracer);
- An EC-meter (the Solinst TLC is the common one).

*For just the pumping test (Figure 6-8)*

- A low-rate pump (less than 20 L/min);
- A source of electricity for the pump.



**Figure 6-7 Equipment for conducting a transient state FEC-based dilution test**



**Figure 6-8 Equipment for conducting a transient state FEC-based dilution test**

The Solinst TLC meter displays accurate measurements of conductivity and temperature on an LCD display, and water-level (and probe depth) measurements are read from the accurate flat-tape, marked in millimetres.

## **6.6.2 Field Procedure**

### **6.6.2.1 Introduction of the tracer**

The field procedure differs from the FFEC logging method (Tsang *et al.*, 1990) by the quality of the water that is used to replace the natural borehole water. Here, the induced changes in water quality involve relatively higher concentration before the measure of time sequence FEC logs. Cook *et al.* (2001a) accomplished this by inserting a pump near the base of the bore, with the outlet of the pump located immediately above the water table, so that the pump does not remove water from the well (steady state condition), but re-circulates it from the top to the bottom, and at the same time (during pumping), slowly pouring a concentrated salt solution into the top of the well. This approach has the advantage of insuring a better mixing of the tracer in the borehole (or in the tested section of the borehole), and so may help to reach a closer degree of homogeneity (to avoid diffusion and density gradient along the borehole). But its implementation in the field is complicated and involves equipment that can make the method expensive.

Mohr and van Biljon (2009) introduced the tracer into the borehole, by lowering and raising a permeable salt-filled pouch up and down the well. Lasher *et al.* (2009) used a double layered injection sock that was slowly lowered down the borehole so that there was a significant change in the salinity of the water along the borehole. Borehole water salinity may be increased by repeating for a certain number of cycles the movement (up and down) of the slug of salt, along the water column. The term cycle of slug of salt movement is used here to refer to a complete up and down movement of a slug of salt along a borehole water column. This approach may not be ideal to create homogeneous conditions along the borehole, but is simple and does not required expensive equipment. This approach is the one adopted in the case studies of the present dissertation.

#### **6.6.2.2      *EC measurement***

The type of EC-meter that has to be used, can greatly affect the efficiency (mainly in term of cost) of the entire dilution test. The EC measurement may be done by any kind of EC-meter designed to be lowered into a borehole. Field experiments have indicated that repeating logging in four to six inch (101 to 154 mm) of diameter wells should be done using a small probe of one (01) inch of diameter, with an average velocity of the probe less than 3 meters per minutes, to avoid disturbance of concentration distribution. The well known TLC is easy for use in field conditions and is cost effective compared the multi-probe, which involves a complicated set-up. But the multi-probe offers better measurement resolution.

A first log representing ambient background conditions is done to state a background condition. This first log is not a requisite for flow computation, but may give a first idea of the general main flow zone along the borehole. This first log is termed "base line". The time sequence of tracer concentration (FEC) logs is recorded after tracer application. It is recommended to run as many successive logs as possible in the first thirty (30) minutes after the application, because the first logs are often affected by the combined effect of diffusion and density in the borehole. Dilution logs run directly after tracer application tend to react more to diffusion than to flow transport; therefore, velocity computation should omit these first logs (Pitrak *et al.*, 2006).

The first log considered after tracer application is termed 'initial condition' and is considered to have been run at  $t_0$  equal to zero (0). Time intervals are a function of local hydraulic conditions (flow rate into and out of the borehole). Shorter time intervals should be observed at the beginning (in the first two hours) of the time sequence profiling. The faster the flow (high dilution rate), the shorter the intervals required, and the lower the flow the larger the intervals required.

The time sequence FEC logging can be stopped when the dilution process is well documented, and reaches at least 60 % of the total dilution of the tracer. Riemann (2002) suggested at least 50 % of dilution of the starting concentration value. Logging speed depends basically on the type of measurement equipment. With the TLC, runs are in the range of 3 to 5 m/min, while with an automatic multiprobe, runs are more than 10 m/min.

Dilution logs may be run together with other logging methods, which can help to investigate flow in borehole such as temperature logs and other geochemical parameters (pH, ORP, etc.).

### **6.6.3 Analysis of the data**

The analysis of FEC-based test data can be subdivided into three main steps:

- Detection of feed point locations and their nature (inflow or outflow);
- Building of a conceptual model of the borehole-aquifer system;
- Quantification of flow parameters from time evolution of concentrations in the borehole.

#### **6.6.3.1 Detection of feed points**

The detection of the feed points constitutes the fundamental step in the analysis of FEC profile data. This can be done by using the baseline (natural condition) profile, or the ambient condition (no pumping) concentration profile, or the transient condition (pumping) concentration profiles.

Analysis of the time sequential FEC profiling data starts with analysis of the natural distribution of the FEC in the open borehole. A natural stratification of FEC in an open well may also be used to confirm the main geological lithology in the



subsurface. Love *et al.* (2002) gave evidence of that in a well, drilled into fractured metasediments in the Clare Valley (South Australia). The 'baseline' FEC profile is the first means to detect the main flow points in a borehole, by looking at the nadirs in the curve (the effect of fresh water entering the borehole) if the test is performed in a non-contaminated aquifer system, or the peaks in the curve (the effect of polluted water entering the well) if the test is performed in high TDS aquifer system.

On the time sequential FEC profiles, feed points are generally more localisable on the early time profile, particularly when pumping at very low rates. But first logs should not be used for velocity computation (Pitrak *et al.*, 2006).

Doughty *et al.* (2005) gave description on the different signature of feeds points for the case of de-ionised water or very low water concentration in a borehole. Such knowledge needs to be built for the case of dilution tests. A clear distinction between inflow points and outflow points pose a big challenge when analysing a dilution test.

#### 6.6.3.2 Conceptual model

The conceptual model depends mainly on the type of parameters that one is seeking. The analysis methodology developed in this dissertation focuses mainly on the case where groundwater flow is horizontal through a borehole.

#### 6.6.3.3 Quantitative analysis

Drost *et al.* (1968) developed an analytical solution for horizontal flow in the absence of diffusion and dispersion along the borehole that resolves the change in concentration observed in a borehole as a function of time as follows:

$$C(t) = C_i - [C_i - C(0)] \exp\left(\frac{-2t}{\pi r_w} V_d \alpha_h\right) \quad \text{Equation 6.21}$$

Where  $C_i$  is the formation (inflow) water concentration,  $t$  is time left,  $V_d$  is the Darcy velocity through the aquifer (m/s),  $\alpha_h$  is the aquifer-to-wellbore convergence factor, and  $r_w$  is the wellbore radius (m).



By considering that the natural distribution of the FEC along a borehole is representative of the real water concentration distribution in the host formation, and by using the linear relation between EC values and the tracer (NaCl) concentration, the formation's water concentration can be deduced from the baseline log; otherwise, a non-naturally occurring tracer should be selected or in the worst case assumed. In the case of non-naturally occurring tracer, the above equation is simplified to:

$$\frac{C(t)}{C(0)} = \exp\left(\frac{-2t}{\pi r_w} V_d \alpha_h\right) \quad \text{Equation 6.22}$$

Therefore, Darcian velocity may be inferred from one of these equations (Equation 6.21 and Equation 6.22). Cook *et al.* (2001a) applied this analysis approach to estimate groundwater flow rates of flow zones along a borehole using well dilution test data. The data was collected in basalt and metamorphic aquifers on the Atherton Tablelands, Queensland. The natural groundwater salinity at the site is approximately  $0.1 \text{ mS cm}^{-1}$ , whereas after injection, the electrical conductivity of the test zone ranged between  $3000$  and  $6500 \text{ }\mu\text{S cm}^{-1}$ . Groundwater flow rates have been estimated to range between  $0.4$  and  $1.2 \text{ m day}^{-1}$  within the basalt, whereas within the metamorphic rocks, the horizontal flow rate is between  $0.05$  and  $0.1 \text{ m day}^{-1}$ . This approach has also been suggested by Love *et al.* (2002), who described the estimated values as semi-quantitative estimates.

## 6.7 Discussion

The FFEC technique has been acknowledged as very sophisticated, but it unfortunately requires an elaborate set of equipment to deionise the fluid column in the borehole, as was mentioned (Pitrak *et al.*, 2006). The availability of deionised or constant saline water may be problematic for the application of this technique, particularly in non-developed countries. Also, the replacement of the entire borehole's water requires huge apparatus (a deioniser water truck, injection and extraction pumps, etc.) and literate operators for the FEC logging preparation. Su *et al.* (2006) solved some of those drawbacks by a 'miniaturisation' of the flowing fluid electric conductivity logging technique. In addition to all these drawbacks, replacement of the borehole water may cause a long-term disturbance to the chemical condition around the borehole (Kazumasa *et al.* 2006). The method offers

great advantages in flowing fracture characterisation (detection, volumetric flow determination, fracture fluid solute concentration, fractures transmissivity, far field pressure head determination), but its resolution remains a concern as a single borehole based method. And its utilisation for large-scale aquifer characterisation will need a grid of holes that may make the project really costly. But for local site characterisation, results from a few well located boreholes may be used in combination to accurately infer the local fractures' characters. This approach may be very efficient for contamination studies (investigation and prediction) like in mining environments and deserves to be tried in South-Africa, particularly in the meta-sediments of the Karoo environment.

The Drost solution for groundwater flow rate (at feed points) requires an ideal condition that the FEC-based dilution test (well dilution) does not guarantee. The ideal condition for the application of the Drost solution consists of:

- Homogenous mixing of the tracer in the test section (borehole column water),
- No density gradient by the tracer along the borehole,
- steady groundwater flow during the test,

The first assumption of concern is the 'homogenous mixing of the tracer'. The recirculation system used by Cook *et al.* (2001a) has been demonstrated in the laboratory to be efficient in creating an initial homogenous tracer concentration in a borehole (Lamontagne *et al.*, 2002). Even though in field conditions this cannot be assured at 100 %, the recirculation approach offers an advantage over the 'release of a slug of saline water' (Patten and Bennet, 1962) and the 'up-down movement of a salt-filled pouch' (Mohr and van Biljon, 2009). Mass transport within the borehole, induced by the combined effect of density variation (with time) and density gradient, can be reduced by limiting the increase in solute concentration, but cannot be eliminated. Thus movement within the borehole, can affect the interpretation, particularly where horizontal flow rates through the well are low. In a point dilution test, a packer is used to suspend such effects (Halevy *et al.* 1967; Drost *et al.* 1972). In absence of packers, flow-meter measurement can be used to detect intervals with vertical flow and the vertical flow rate (Michalsky and Klepp, 1989), and then excluding the effect on horizontal flow computation.

The assumption of steady groundwater flow during the test may also be difficult to guarantee in field conditions. In riparian zones, for example, flow recession in rivers with flash hydrographs or tidal cycles in estuaries may distort this assumption (Lamontagne *et al.*, 2002.) Also, pumping from other boreholes surrounding the study area also may affect the test. Despite these drawbacks associated with well dilution tests, the test data can be used qualitatively and quantitatively to appreciate flow in the vicinity of the borehole. The analytical solution developed by Drost *et al.* (1968) will be used to semi-quantitatively determine flow from the flow points (fractures or fracture zones) into the borehole and to weight the contribution of each feed point intersected by a borehole (or the section studied) to the whole borehole-aquifer system's main hydraulic parameters (transmissivity and sustainable yield). Semi-quantitative estimates of flow at all depths can be obtained from well dilution data (Love *et al.*, 2002). The velocity estimated with this analytical solution will be used in combination with data from the conventional pumping test to infer a relative contribution of fractures or flow zones intersected by a given borehole.

## **7 CASE STUDIES OF FEC-BASED DILUTION TECHNIQUES FOR FRACTURE CHARACTERISATION IN KAROO AQUIFER SYSTEMS**

The main objective of the field experiments to evaluate the potential of the FEC-based dilution technique for fracture characterisation. The campus test site (bedding horizontal plane fracture) at the University of the Free State (Bloemfontein) and the Paradys Proefplaas farm (dyke and associated weathering and fracturing) outside Bloemfontein were used for this purpose. Note that although the regional geology seems to be the same for the two sites, they are characterised by different fractures.

This chapter presents the geological setting and a description of the fieldwork sites, the different fieldworks, their results, and the analysis and interpretation of the results.

### **7.1 Campus Test Site**

As an experimental site for IGS, the campus test site offers the advantage that the conceptual model of the general groundwater flow and associated solute transport has been well studied and understood (Botha *et al.*, 1997; Botha *et al.*, 1998; van Wyk *et al.*, 2000; Chiang and Riemann, 2000; Riemann 2002; Dennis *et al.*, 2010). The site is equipped to date with thirty percussion boreholes and seven core-boreholes that have been drilled.

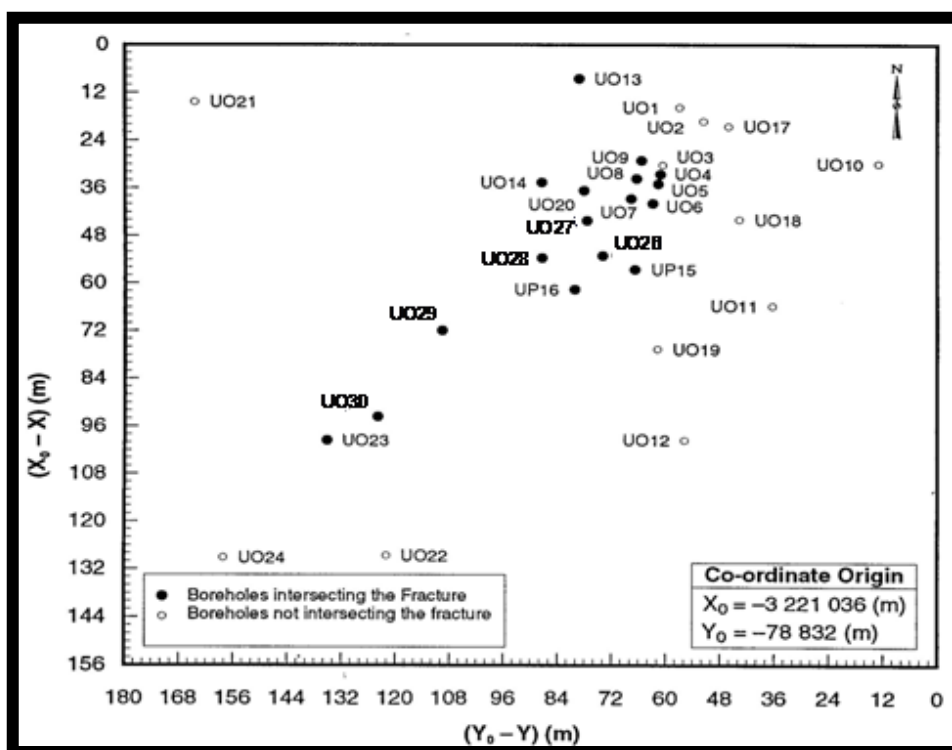


Figure 7-1 Locations of the boreholes at the campus test site

### 7.1.1 Regional geological setting and site description

The campus test site is underlain by a series of Karoo sandstones, mudstones and shales, deposited under fluvial environments of the Adelaide Subgroup of the Karoo Supergroup (Botha *et al.*, 1997; Botha *et al.*, 1998; van Wyk *et al.*, 2000; Chiang and Riemann, 2000; Riemann 2002; Dennis *et al.*, 2010).

### 7.1.2 Local geology and geohydrology at the campus test site

The local geology and geohydrology conditions of the campus test site have been well described in previous studies (Botha *et al.*, 1998; van Wyk *et al.*, 2000; Chiang and Riemann, 2000; Riemann 2002). Three (3) aquifers have been distinguished at the campus test site (see Figure 5-3, Chap5). After Dennis *et al.* (2010) the piezometric level of the upper mudstone aquifer is approximately at 5 m below ground surface, where as the sandstone aquifer and the bottom mudstone aquifer (aquifer 3) piezometric levels are 7m and 9.5m respectively.

### 7.1.3 Field work performed

In order to have a background idea on the water level and general values of EC, and to understand how EC values vary on the site, a survey has been conducted profiling water levels, EC and temperature.

#### 7.1.3.1 Background Information on the FEC at the campus test site

Previous work has already distinguished existing boreholes that intersect the main fracture (mode I) from those that do not intersect it, according to their yield, and using hydraulics tests.

Water levels, temperature and EC profiling were measured on selected boreholes on 1 June 2010. Six boreholes (D3, UO5, UO7, UP15, UO20 and UO23) that intersected the mode 1 fracture, and three boreholes (D5, D6, and UO30) that do not, were selected for the purpose.

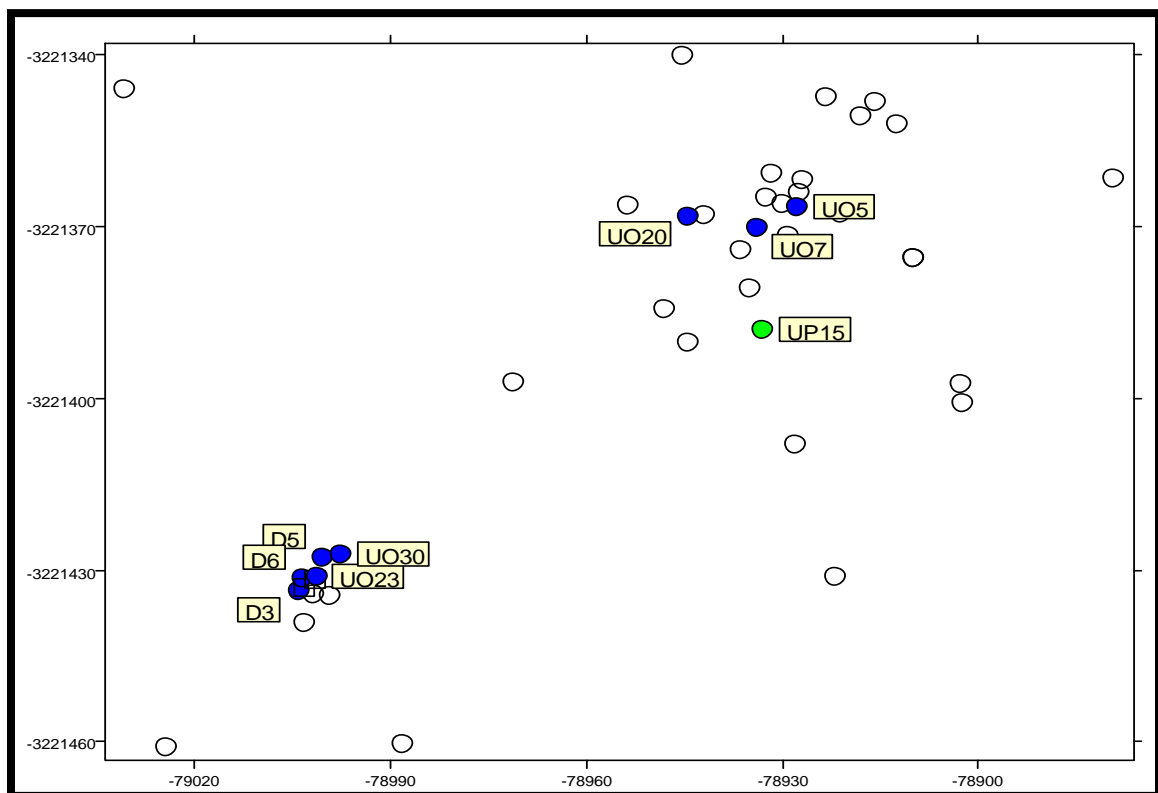


**Figure 7-2 Position of the selected for background information collection on the campus test site.**

A TLC meter was used for measuring FEC and temperature distribution in the borehole, by moving the probe up and down the borehole, while monitoring the

depth of the probe with a tape accurate to one millimetre. The FEC was logged at 0.5 meter intervals along the boreholes. Measurement at such resolution could not reveal accurately the actual position of the fracture, but, would rather help to localise the position of the most permeable zone in the borehole at an interval of 0.5 m. The objective of this step of our study was to confirm how anomalies on a borehole FEC profile can be related to the most conductive zones in a borehole.

As expected, all the boreholes that were previously identified as intersecting the main bedding-plane fracture zone yielded certain sudden and relatively significant changes (increases or decreases) in FEC values at depths previously identified as the locations of the bedding-plane fracture in the intersecting boreholes (D3, D6, UO5, UO7, UO20, UO23, and UP15). Anomalies were observed in the FEC profiles of nonintersecting boreholes at a depth that coincides with the geology of the bedding-plane fracture, as we can see in **Error! Reference source not found.** showing the eological, FEC, and temperature profiles along borehole D5.

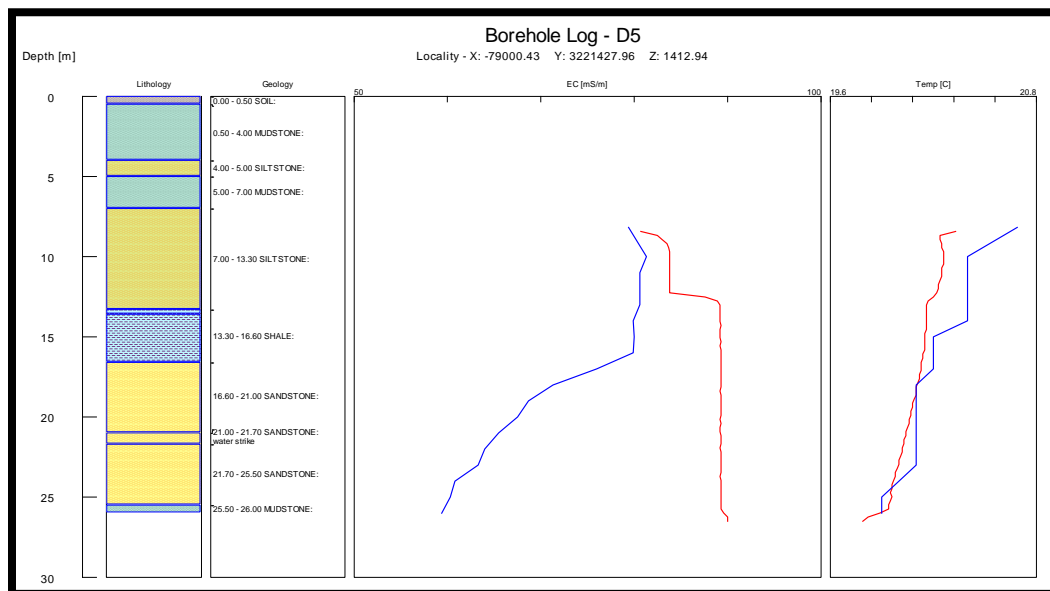


**Figure 7-3: Geology, FEC and Temperature Profiling of Borehole D5 at the IGS Campus test site (red curve: 2005; blue curve: 2010).**

In borehole UO30, a clear feed point is depicted at the bedding plane position in the sandstone layer. Previous work by Pretorius (2007) and Gebrekristos (2007) showed the existence of a fracture at 21.7 m bgs in this borehole, yet the same authors performed a pump test that dewatered the borehole UO30 in 20 minutes,

whereas the other boreholes that actually intersect the mode I fracture on the campus test site yield transmissivity values between 17 and 18 m<sup>2</sup>/day and also show the same drawdown behaviour. According to the conceptual model of Botha *et al.* (1998), the borehole intersects the fracture zone. But the slug test on borehole UO30 showed the same results as for the non-intersecting boreholes, and video camera inspection has not shown any fracture.

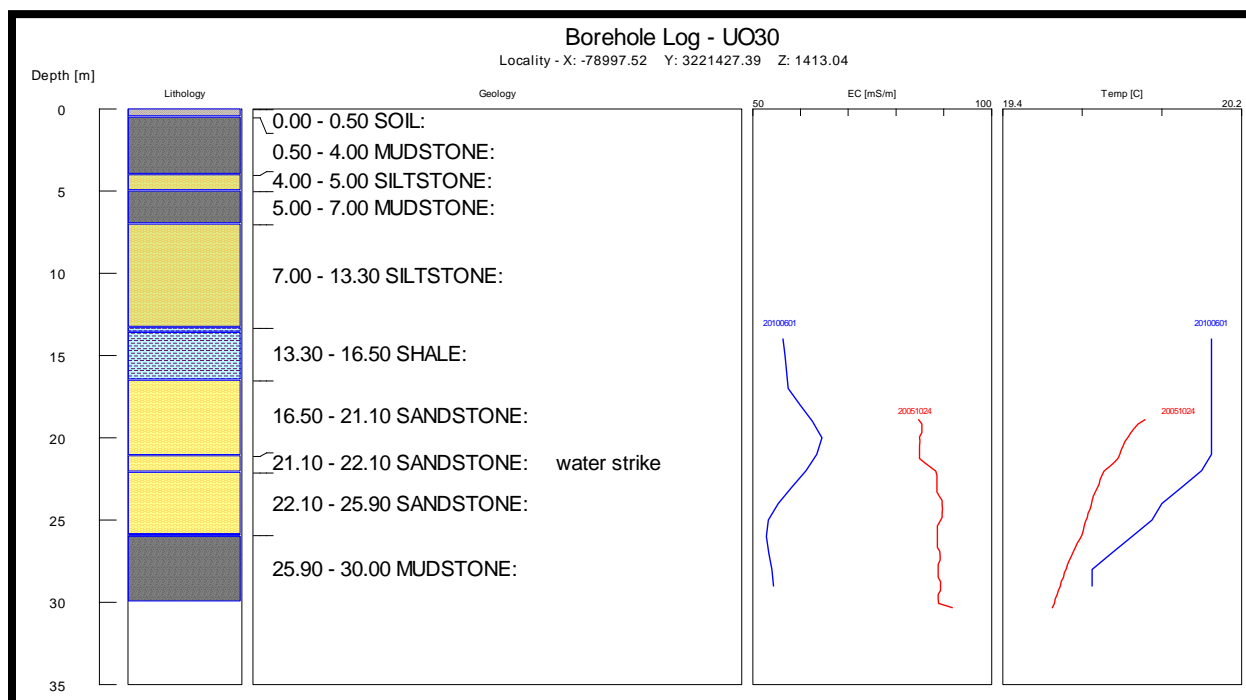


Figure 7-4 Geology, FEC and Temperature Profiling of Borehole UO30 at the IGS Campus test site (red curve: 2005; blue curve: 2010).

The estimated transmissivity value (1.2 m<sup>2</sup>day<sup>-1</sup>) of UO30 is lower than the one related to the mode I fracture (Pretorius, 2007). Pretorius (2007) concluded that the drawdown in the observation borehole OU30 when pumping from UP16 was mainly due to the fracture connectivity. Further work on the characterisation of this fracture zone in OU30 will certainly help confirm whether or not this borehole intersects the mode I fracture present on the campus test site. D5 was also considered as non- intersecting the mode I fracture according the results of the slug test, but in the present study yields an FEC profile that shows a general downward decrease of the FEC values from the top of the sandstone layer (Error! eference source not found.). This behaviour of the FEC profile in borehole D5 needs to



be confirmed, to conclude that fresher groundwater (FEC value of about 50 mS/m) is entering into the borehole somewhere in the sandstone layer.

According to the values of FEC, the boreholes were classified in two groups: the insignificant range of FEC values boreholes (UP15, UO23, D3, UO30, D5, and D6), and the significant range of FEC values boreholes (UO5, UO7, UO20). Table 7-1 and Table 7-2, below show the ranges of distribution of the readings made.

**Table 7-1 Ranges of distribution of the readings in Intersecting Boreholes**

	UO5		UO7		UP15		UO23		D3		UO20	
	EC (mS/m)	T <sub>⊙</sub>	EC (mS/m)	T <sub>⊙</sub>	EC (mS/m)	T <sub>⊙</sub>	EC (mS/m)	T <sub>⊙</sub>	EC (mS/m)	T <sub>⊙</sub>	EC (mS/m)	T <sub>⊙</sub>
Max Readings	254.7	19.4	378.6	19.5	70.9	20	89.2	20	82.9	20	214.7	19.9
Min Readings	70.7	19.2	56.3	19.4	53.9	19	73.4	20	55.1	20	57.6	19.5

**Table 7-2 Ranges of distribution of the readings in Non-Intersecting Boreholes**

	UO30		D5		D6	
	EC (mS/m)	T <sub>⊙</sub>	EC (mS/m)	T <sub>⊙</sub>	EC (mS/m)	T <sub>⊙</sub>
Max Readings	64.9	20	81.3	20	62.4	21
Min Readings	51.9	20	59.4	20	55.1	20

The significant range of FEC values is generally due to sudden and significant increases or decreases of the FEC values at different depths in the boreholes. All the boreholes that show significant ranges of vertical FEC variation intersect the dominant permeable sub-horizontal bedding-plane fracture, and show significant increases of FEC values below this fracture in the sandstone. Gebrekristos (2007) made the same observation by recording up to 290 mS/m of FEC values in the stagnant water of boreholes below the bedding-plane fracture, whereas the FEC in the bedding-plane fracture is 90 mS/m, which is indicative of fresh water recharging the aquifer. He explained the observed high values of FEC below the fracture zone, as the effect of the residual tracer solution that remained in the

aquifer and diffused into the rock matrix over time. The significant range of FEC values boreholes may be a confirmation of this explanation, since, UO20, UO5 and UO7 were used for tracer experiments in April 2010. The other monitored boreholes (boreholes UP15, UO23, and D3) that have insignificant range of FEC values, and intersect the mode I fracture, are situated upstream of the significant range of FEC values boreholes and therefore may not really be affected by the residual tracer.

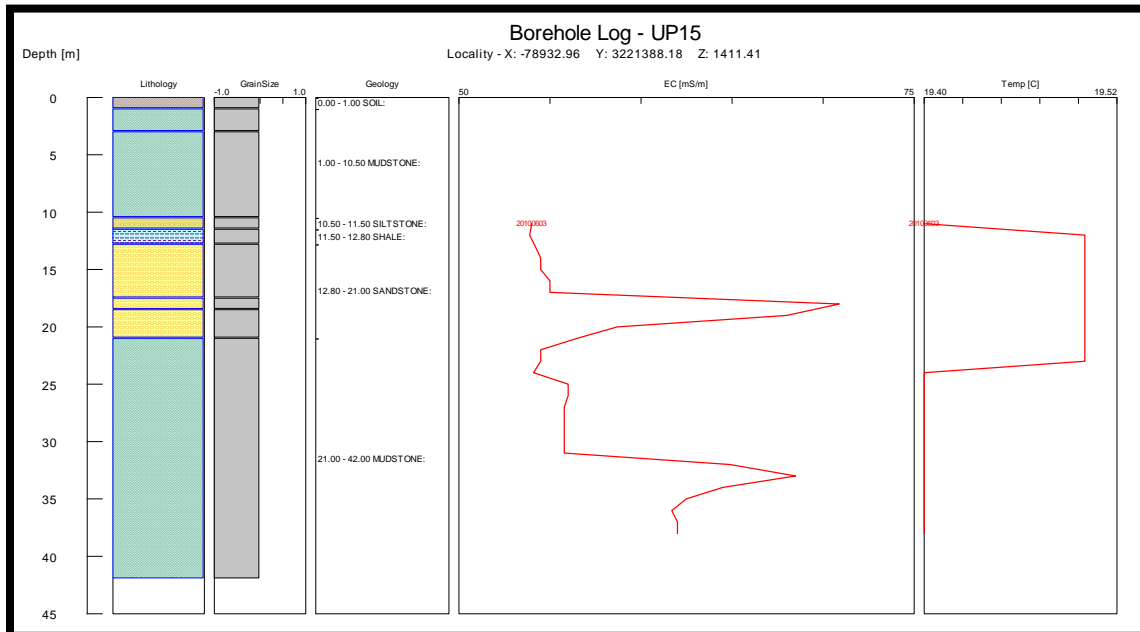


**Figure 7-5 Geology, FEC and Temperature Profiling of Borehole UP15 at the IGS Campus test site.**

### 7.1.3.2 Choice of the experimental borehole

Boreholes UO7 and UP05 were targeted for performing the experimental tests. It has been shown from previous work, and confirmed by the SFEC profiles in natural conditions, that borehole UO7 intersects one (1) flow zone (mode I fracture), while borehole UP15 intersects two (2) flow zones (

Figure 7-5). Borehole UP15 will allow assessment of the efficiency of the FEC-based dilution method in detecting multiple intersected fractures, and to weight their respective contribution to the flow of water from the aquifer to the well.

#### 7.1.4 Tracer tests

Static fluid electrical conductivity profiling was conducted on both boreholes UO7 and UP15 on 4 April 2010 and 23 August 2010, respectively. On UO7, a TLC was used to collect *in situ* FEC data. The average FEC of natural water in borehole UO7 was approximately  $194.83 \text{ mS m}^{-1}$ . After injection of the tracer, the average fluid electrical conductivity along the entire borehole at the beginning of the test was  $342.45 \text{ mS/m}$ , ranging between  $244.5 \text{ mS/m}$  and  $443.2 \text{ mS/m}$  at the beginning of the test. Five (05) FEC profiles were recorded unevenly at 30, 90, 150, 270, and 390 minutes in addition to the initial profiling, with an average rate of profiling of  $1.6 \text{ m/min}$ . The ambient FEC profiling depicts the known existing bedding-parallel fracture at 22.5 m from the top of the casing. A progressive upward widening of the dip shape at the point 22.5 m tends to indicate the existence of an upward flow from this point to an upper exit point (between 14 and 15 m). But this could also be the effect of diffusion coupled with a density effect along the part of the borehole situated above the bedding-parallel fracture. The relatively low dilution rate observed at the section situated below the mode I fracture, suggests that no flow occurs at this part of the borehole.

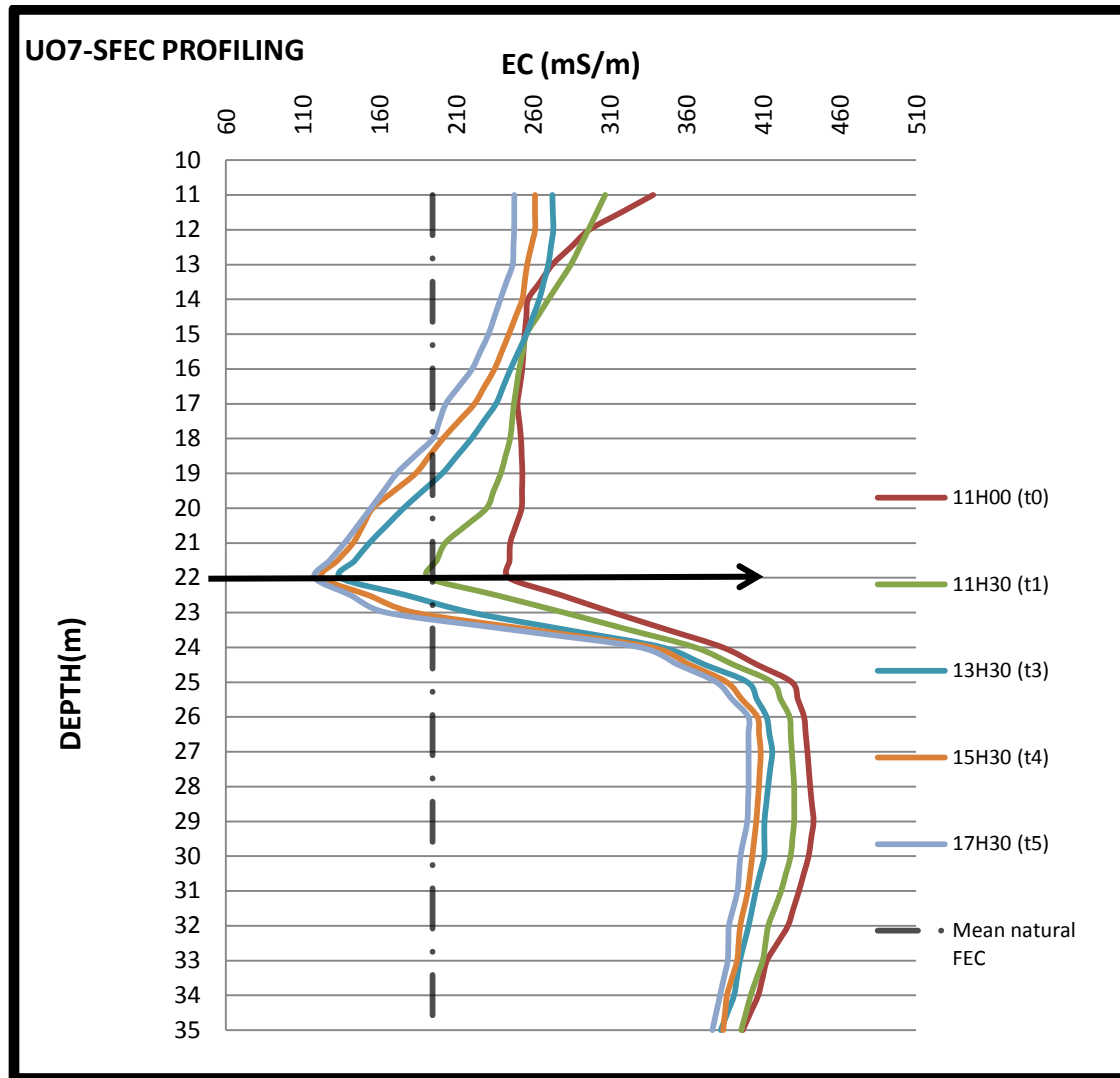


**Figure 7-6 Result of SFEC logging on borehole UO7. IGS Campus test site (UFS), The black arrow showing the detected flow point.**

Two pumping FEC tests were conducted on UP15 to confirm the existence of the two flow points. Two tests were run at respectively 4 L/min and 10 L/min. The bulk natural FEC in borehole UP15 was approximately 125.06 mS/m. By injecting the tracer, the natural bulk FEC was raised to 261.24 mS/m for the first FFEC, and to 257.08 mS. Four (4) FEC profilings were recorded at 3, 12, 23, and 63 minutes, with an average rate of profiling of 0.8 m/min for the first FFEC test (4 L/min). And five FEC profilings were recorded at 5, 32, 54, and 76 minutes in addition of the initial profiling, with an average rate of profiling of 0.8 m/min for the second FFEC test (10 L/min). The two known existing flow points (19 m and 24 m) were depicted on the two pumping FEC logs performed on UP15 (Figure 7-7 and Figure 7-8 and).

The two FFEC tests show clearly how in pumping conditions borehole UP15 sources its water mainly from the flow point at 19 m below casing, followed by the one at 24 m.

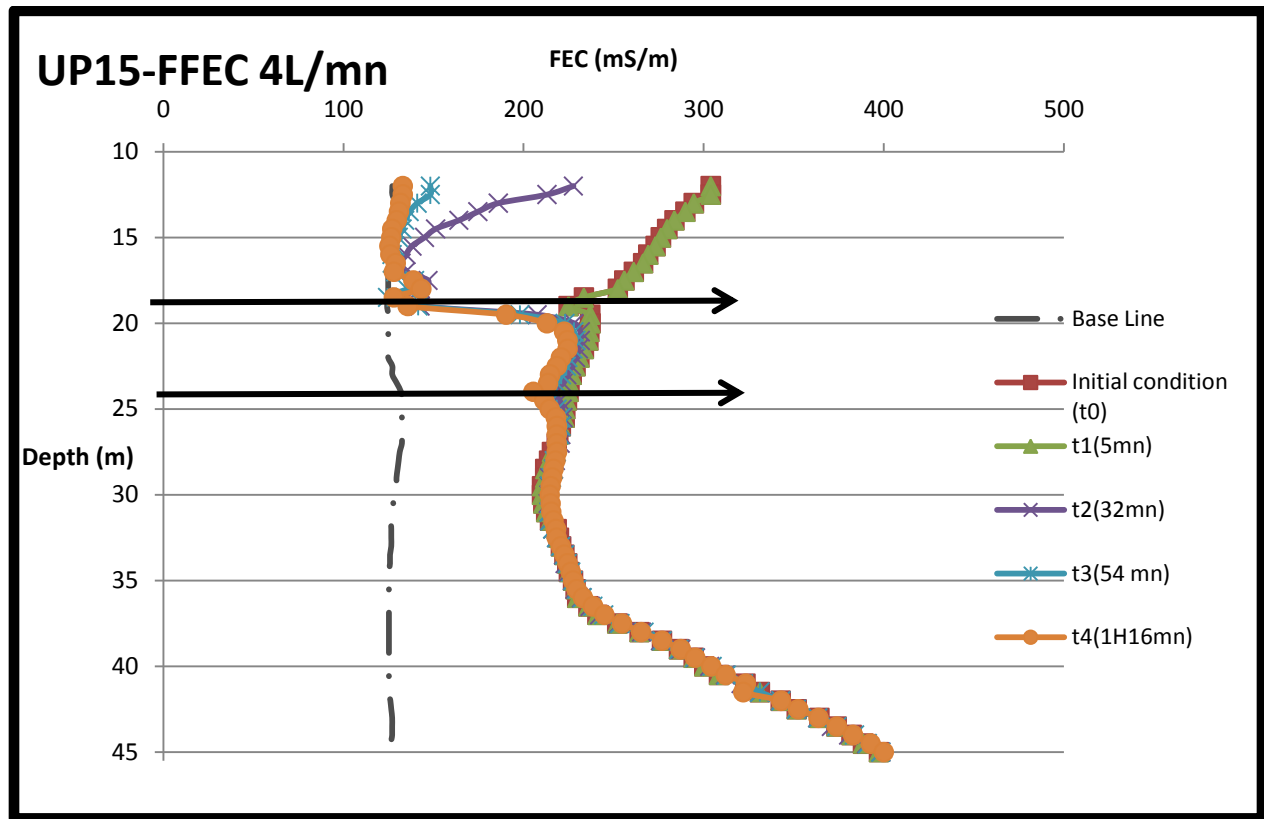


**Figure 7-7** Result of FFEC logging on borehole UP15. IGS Campus Test Site (UFS), the black arrows showing the detected flow points. (Pumping rate: 4 L/min)

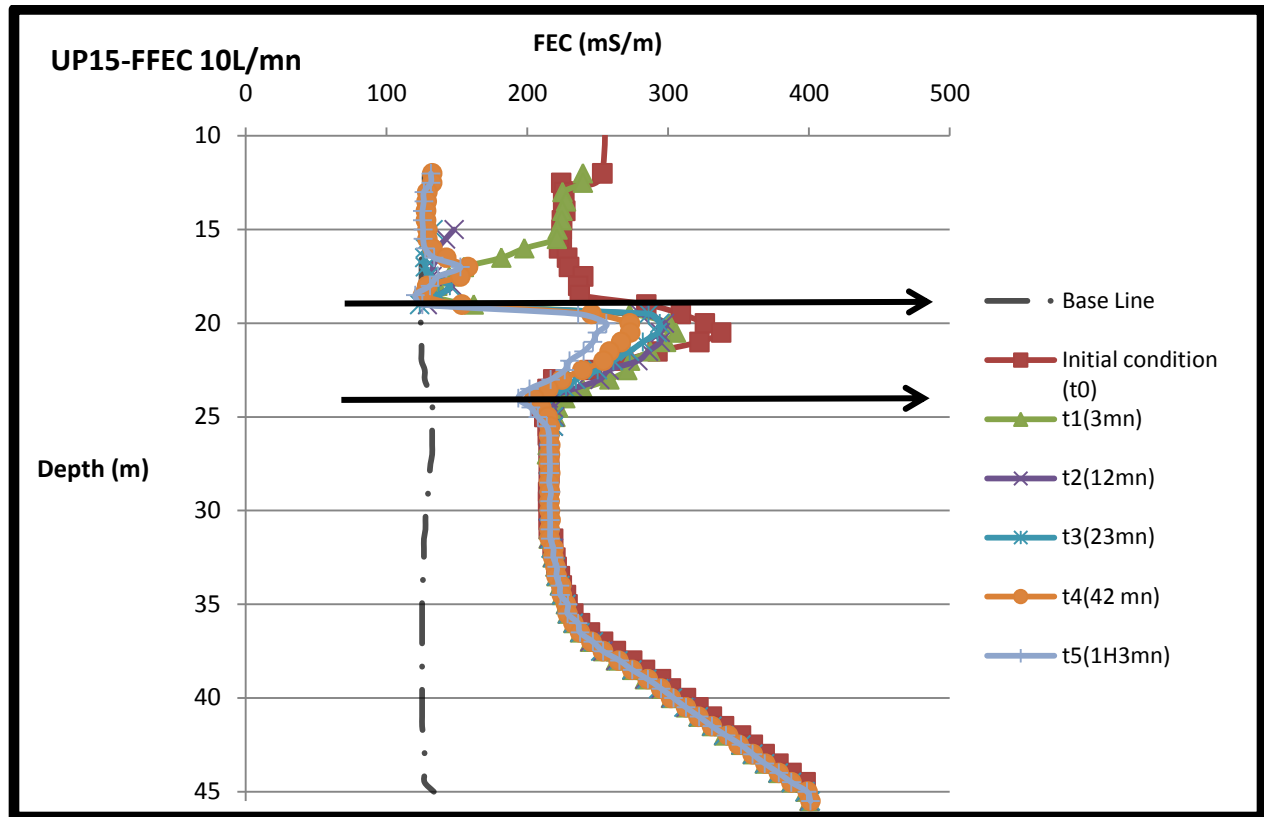


**Figure 7-8** Result of FFEC logging on borehole UP15. IGS Campus Test Site (UFS), the black arrows showing the detected flow points. (Pumping rate: 10 L/min)

#### 7.1.4.1 Data analysis

The analytical solution proposed by Drost *et al.* and suggested by Love *et al.* (2002) and Cook *et al.* (2001a) was applied to the concentration data (after conversion of EC measurements to tracer concentrations) for a semi-quantitative estimation of the groundwater flow.

Ambient groundwater flows were calculated for UO7, and range between 0.24 m/day (at the bedding plane fracture position) and 0.03 m/day (in the no-flow section). The estimated values decrease down and upward from the flow point position but are not symmetrical. This suggests the effect of diffusion surrounding the flow point and a density effect in the section above the flow point. Such estimated velocity values need to be adjusted. Also, assuming no natural occurrence of the tracer, the estimated values are found to underestimate the groundwater velocity compared to the case where the natural occurrence of the tracer in the groundwater is considered (Figure 7-9).

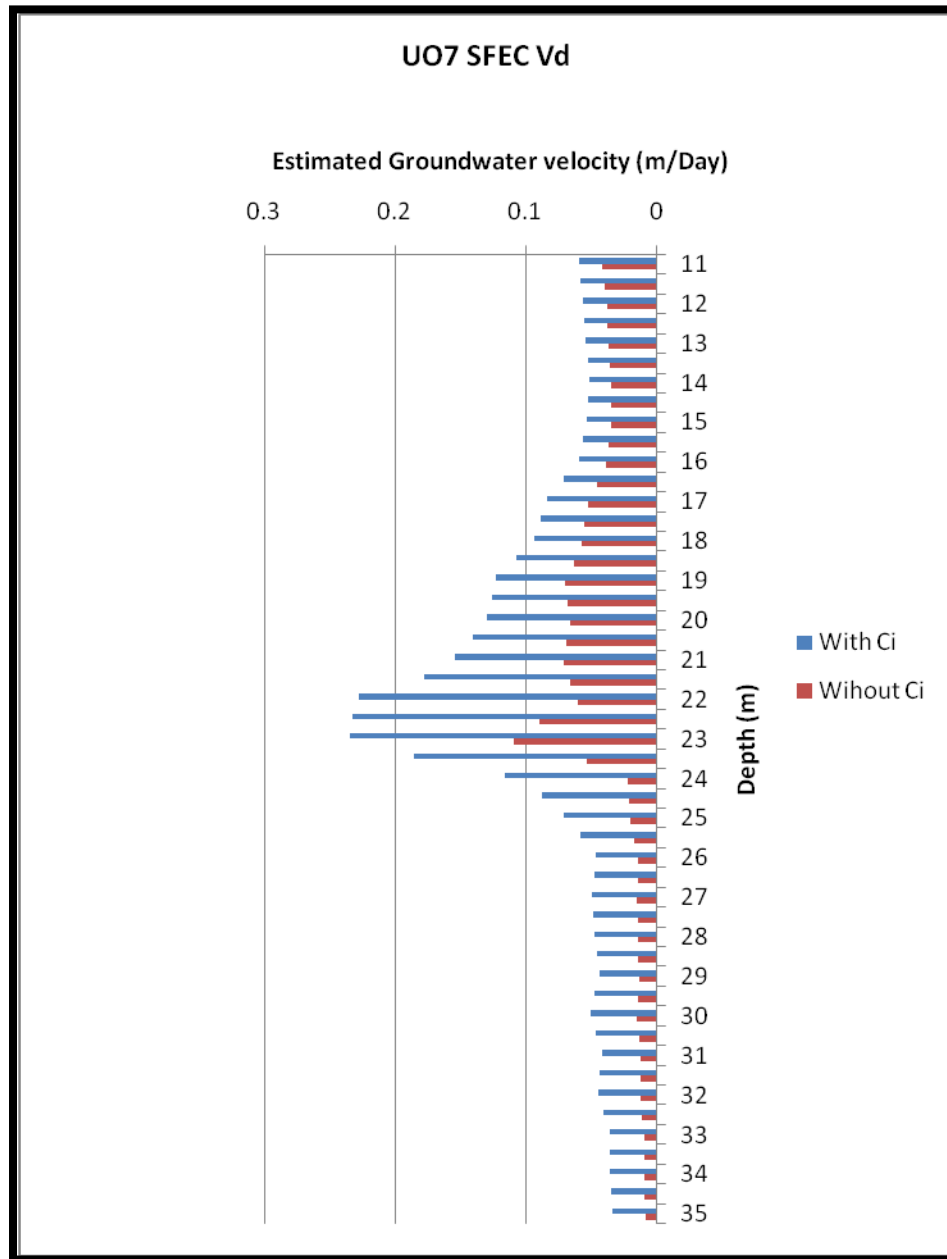


**Figure 7-9 Bulk groundwater flow estimated along U07 with the Drostian analytical solution.**

Forced groundwater flow of the main flow points that source groundwater for UP15 have been estimated for both of the two different pumping rates to check the variability of the contribution of the flow points under pumping conditions. The estimated groundwater velocity is 2.05 m/day and 5.87 m/day for the flow point at 19 m for respective pumping rates of 4 L/min and 10 L/min; whereas for the same respective pumping rates, the estimated groundwater velocities for the flow point at 24 m are respectively 0.27 m/day and 0.71 m/day (Figure 7-10).

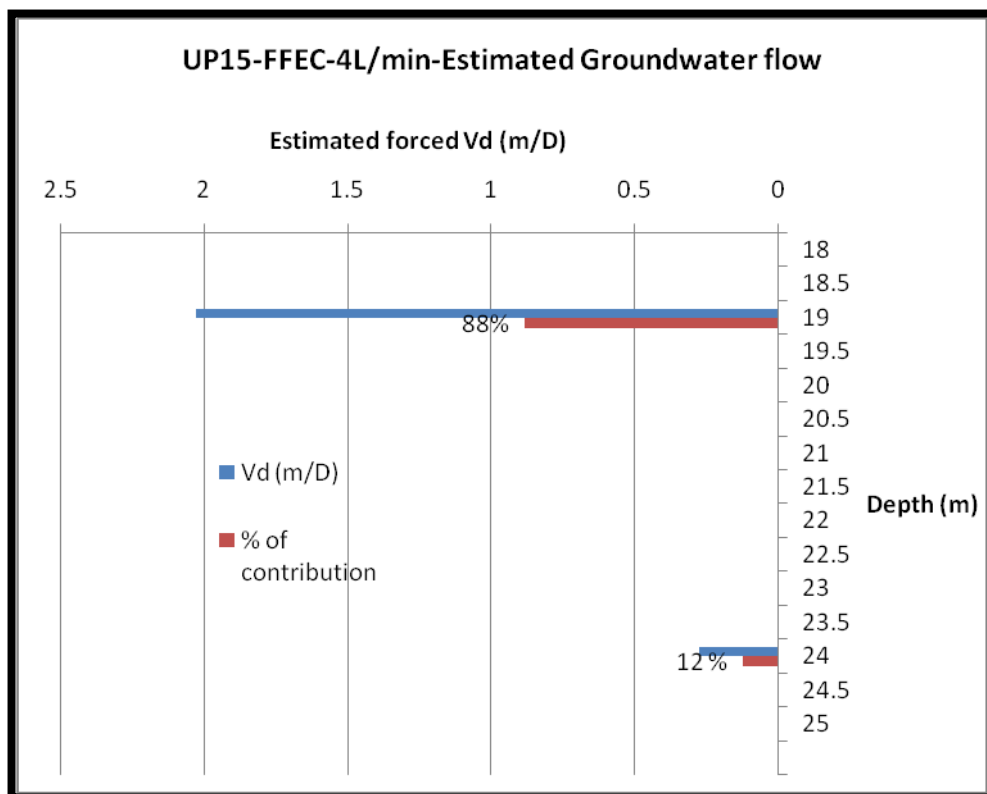


**Figure 7-10** Estimated forced groundwater flow at detected flow points in UP15 under a pumping rate of 4 L/min.

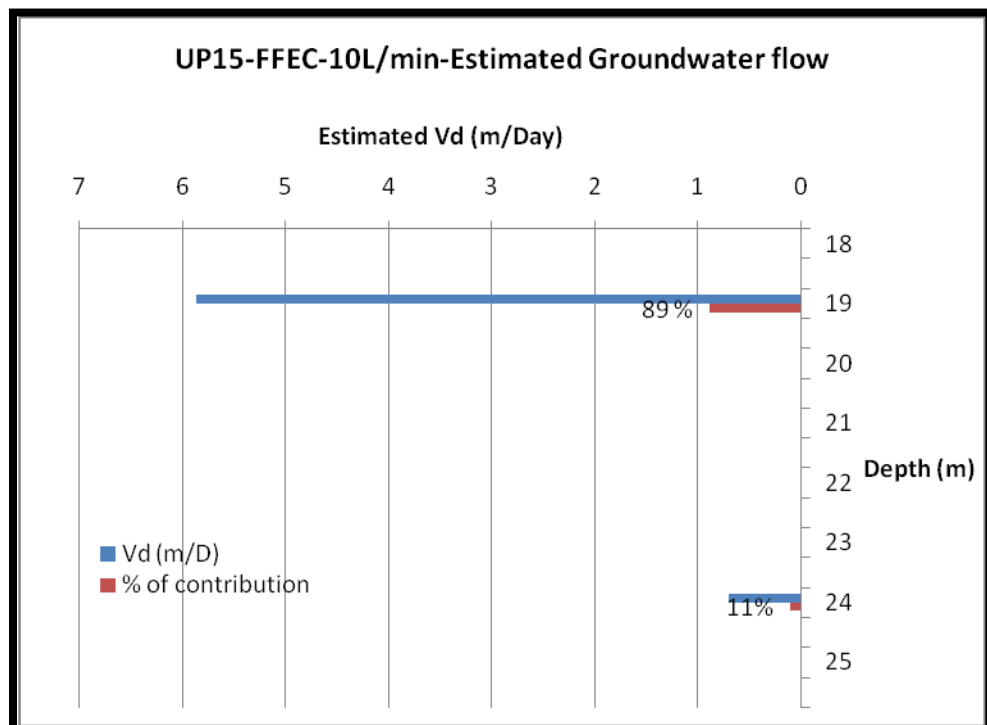


**Figure 7-11** Estimated forced groundwater flow at detected flow points in UP15 under a pumping rate of 10 L/min.



***Bore II attempts***

The numerical code BoreII has been used to attempt to calculate the time evolution of the FEC in the borehole. The model set up requires an initial concentration condition and model parameters need to be specified. The input parameters that are needed are:

- the depth interval being studied,
- the feed point characteristics ( $t_i$ ,  $q_i$ ,  $C_i$ ),
- the model simulation time (maximum length of the test),
- boundary conditions (maximum temperature  $T_{max}$  and maximum salinity  $FEC_{max}$ ),
- a coefficient for including of diffusion and dispersion (mixing in the borehole);
- and the C-to-FEC conversion factors.

The first most stable FEC profiling recorded after adding of salt is used as initial concentration condition in mS/m. The conversion factor are  $r_{gamma}=0$ ,  $r_{beta}=1$ , and  $r_{alpha}=0.1e-7$ . The coefficient for including of the diffusion and dispersion in the borehole is gotten by trial and error and ranges between  $1.e-6$  m<sup>2</sup>/s and  $1.e-4$  m<sup>2</sup>/s. The observed EC data is specified in appropriate data file (by rearranging the data in Excel worksheet and running a program called dataprep.exe). The data file contains observed values of FEC and temperature, and optionally may contain other fluid properties such as pH. The base line profile is used for very late time in the data file. A relatively large cable speed (profiling speed) is specified for the initial condition profile, because BOREII treats it as though it occurs all at  $t=0$ , rather than being measured gradually as the probe moves up or down the well. Detailed instructions for preparing the input and data file are given in the BORE II User guide (Doughty and Tsang, 2000-2004). The input and data files set up for UO7 and UP15 tests are presented in appendix D.

BOREII showed significant limitations for analysing the FEC based dilution test data. With the FEC based dilution test data, out-flow points are difficult to be diagnosed directly from the FEC profiles. But the code BOREII analysis requires the distinction between inflow points and out-flow points. Therefore out-flow points are assumed after trial and error. Steady concentration condition for each feed point does not allow to solving the observed time evolution of FEC in the borehole with the code.

Only transient concentration condition (that is not necessary real) has allowed the matching between model and observed time evolution FEC. The reason of this problem may be the density gradient that is not included in the code Bore II. The attempt (see result in appendix D) of the numerical inversion solution (Bore II) does not yields unique parameters set up for matching of model and observed data.

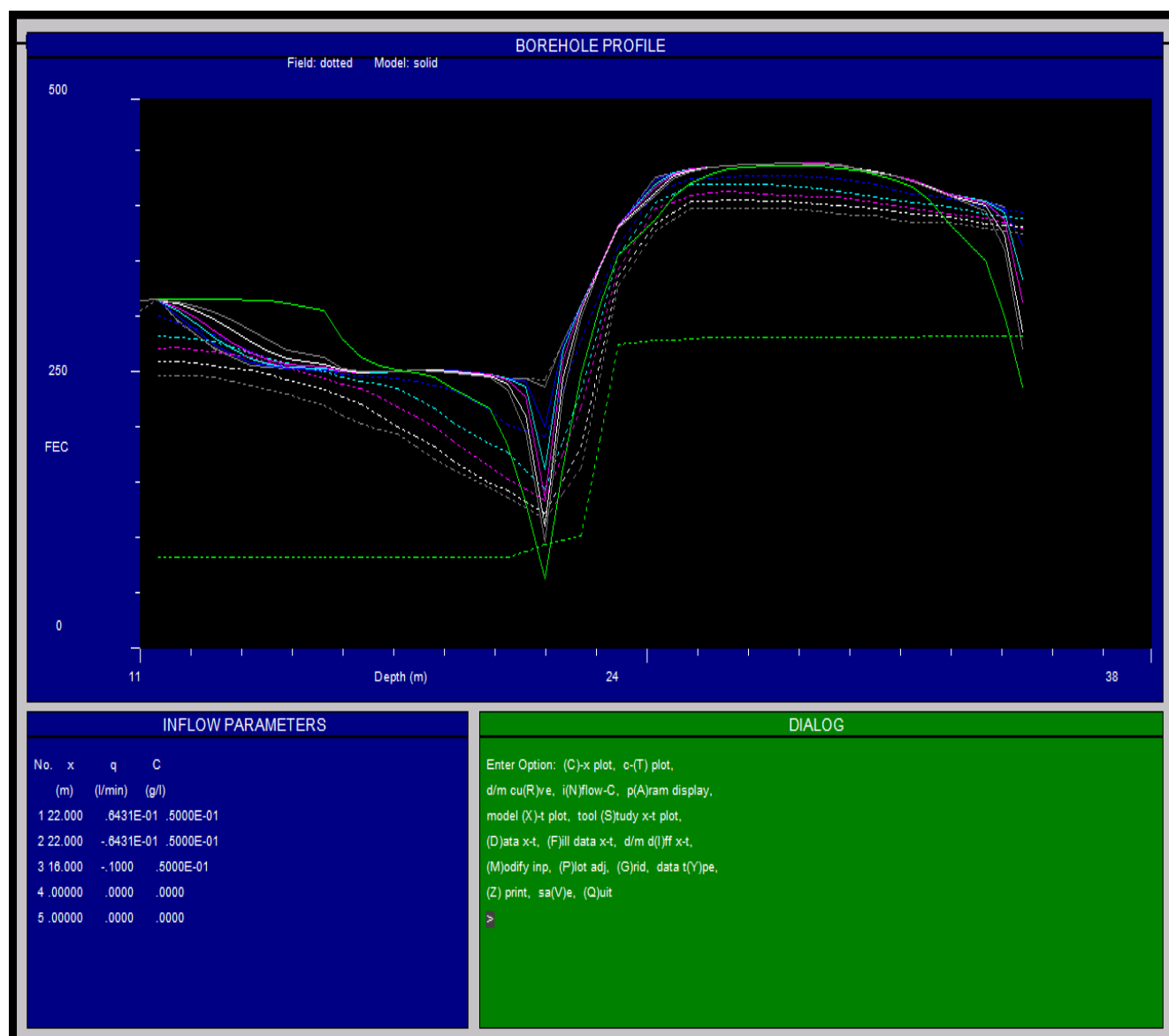


Figure 7-12 Example of BORE II results simulation for U07 (Model data do not match with the field data for early and late time simultaneously).

## **7.2 Paradys Proefplaas Farm**

### **7.2.1 Site Description**

IGS has been approached by the Faculty of Natural and Agricultural Sciences for implanting boreholes (with sustainable yield) to cover a need of 14 000 litres per hour. This need of water is estimated to serve for 8 hectares of Lucerne production and for agricultural research purposes. The Paradys experimental farm is situated nine (09) kilometres south-west of the centre of Bloemfontein (in 2926AA on South Africa topographic map).

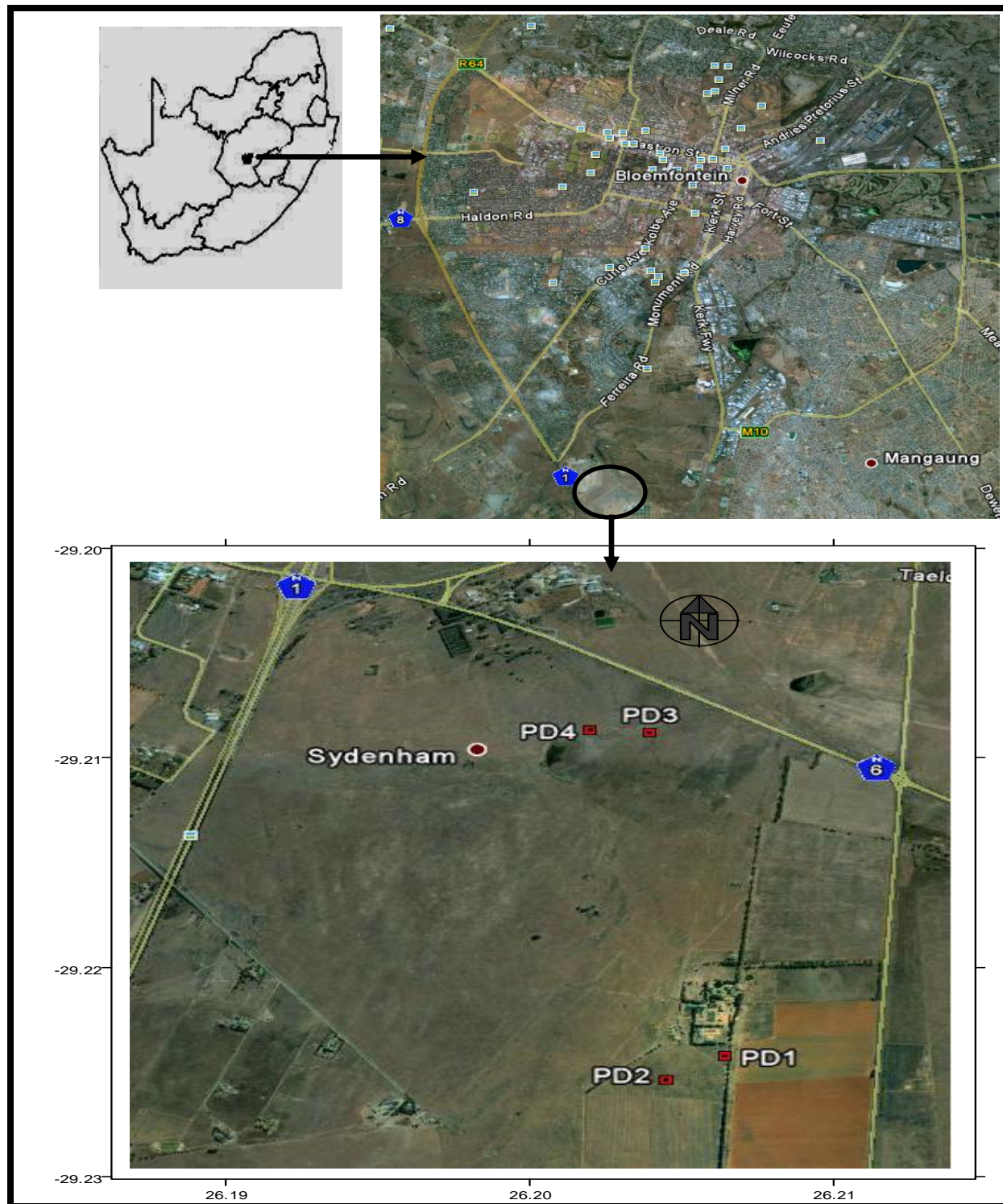
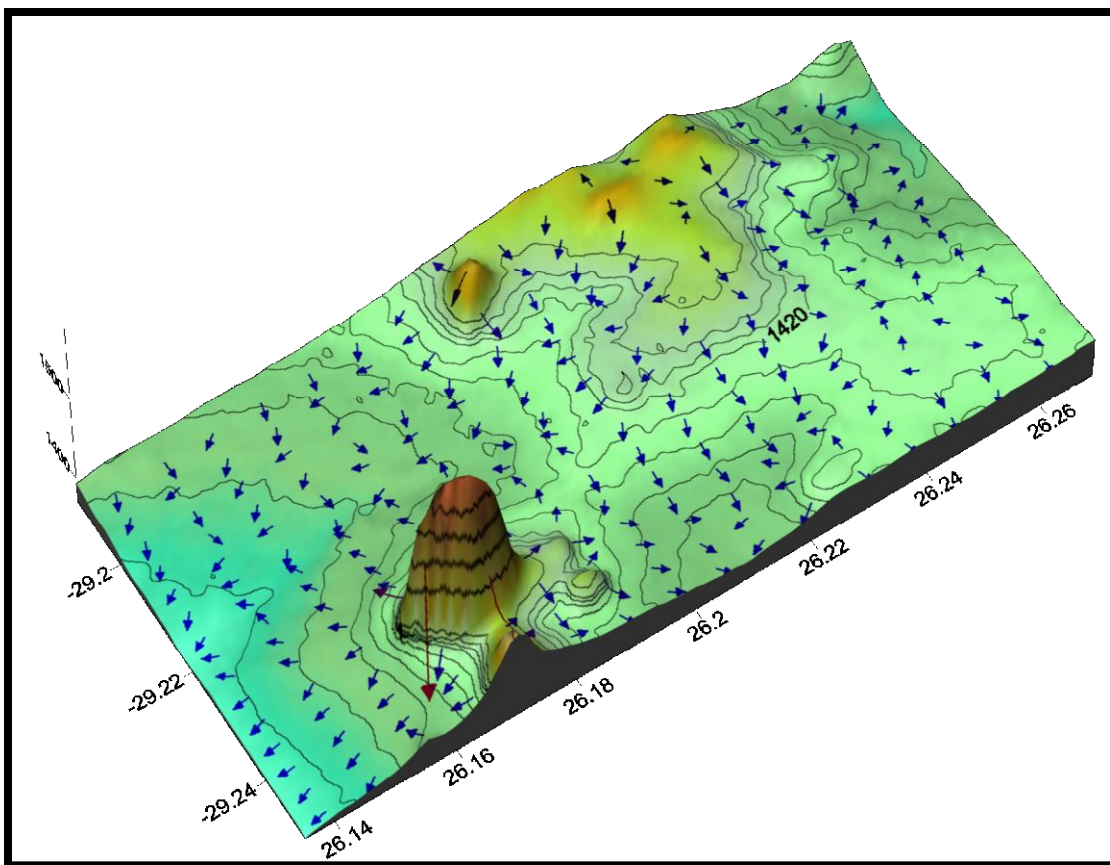


Figure 7-13 Location of the campus test site on an aerial photograph (Google Earth)

One important point that makes groundwater exploration challenging at this site is that the use of the new boreholes must not dry out four (4) other existing boreholes that supply water to the farmhouse, the workers and the animals on the farm. In addition, the site is known as a hydrogeologically difficult site, and the main preferential flow path of groundwater is difficult to identify. A campaign of borehole drilling was conducted by a previous owner, Mr Willie Dreyer (Dreyer Engineering Works), designer of the famous 'Dreyer stamper bore'. The drilled boreholes often intersect dolerite sills, without intersecting significant flowing fractures for irrigation purposes.



**Figure 7-14 Combined contours and vectors maps of Groundwater level in the Paradys Farm region.**

### **7.2.2 Local geology and geohydrology at the Paradys Proefplaas**

The main surface patterns that attract attention on the site are the two topographic highs that form ring-like outcrops, and may be associated with the occurrence of sill (Figure 7-15) intrusions in the country rock. The occurrence of sills has been



confirmed by the number of boreholes that intersect sills on the site. The site is situated in the Ecga (Danie and van Tonder., 2005) and its local geology consists predominantly of mudstone and silt-mudstone, which are generally covered by a clay layer of a thickness that ranges between 0.5 and 8 meters. This local geology is confirmed by geological borehole logs (Figure 7-24 and Figure 7-25) from drilling at the site.



*In situ* dolerite sill outcrop



Evidence of sill internal fracturing at surface on the site

**Figure 7-15 Surface evidence of dolerite intrusions in clay and mudstone formations at the Paradys farm (Bloemfontein)**

A census of the existing boreholes has given first local geohydrological information as resuming in Table 7-3.

Only two (2) of the existing boreholes (PD3 and PD4) have a relatively strong yield and are fitted with submersible pumps. The other existing boreholes yield less than 1 L/s.

**Table 7-3 Short summary of the borehole census at the PARADYS farm**

<b>Water Level (m bgl)</b>	<b>Average EC (<math>\mu\text{S}/\text{cm}</math>)</b>	<b>Boreholes Depths (m)</b>	<b>Boreholes Blow Yield (L/S)</b>	<b>Main water Strike Depth (m)</b>
11.5 – 13.5	950	20 - 50	10 – 15	12-23

### 7.2.3 Local groundwater chemistry at the Paradys Proefplaas

Danie and van Tonder (2005) classified the groundwater at Paradys farm as S1-C3 water (Figure 7-16) with a relatively high chloride values which may be related to the local geology (Ecca) but not to low recharge in the area. The detailed water quality at Paradys farm is resumed at Appendix E.

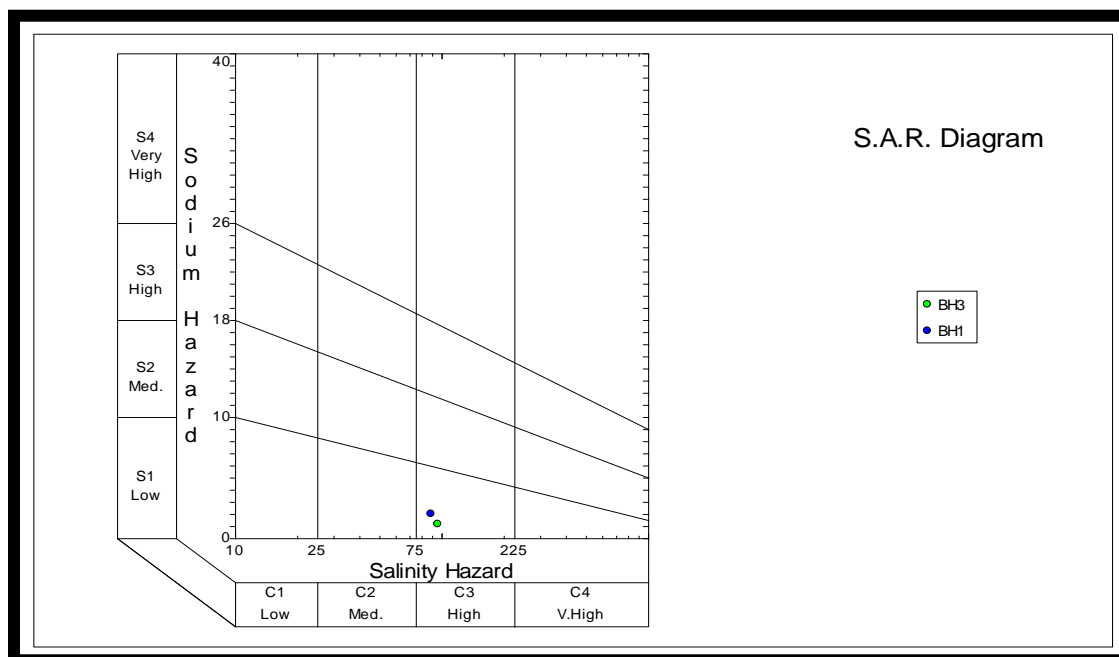


**Figure 7-16 SAR diagram of the water quality at Paradys (Danie and van Tonder.,2005). BH3 and BH1 represent respectively PD3 and PD1.**

### 7.2.4 Fieldwork performed

Owing to the main purpose (irrigation of the farm), the fieldwork conducted on Paradys Proefplaas followed the generally standard and simplified approach to aquifer characterisation as conducted within the main Karoo basin, with emphasis on the assessment of FEC-based dilution techniques for flow path (fracture)

characterisation through a single borehole. The fieldwork conducted can be grouped as follows:

- Surface geophysical survey (magnetic survey);
- Drilling of boreholes (10 boreholes);
- Hydraulics tests (slug and constant rate tests);
- Tracer tests (open borehole dilution test);
- Collection of background information (borehole census, use of water on the farm, geology, climatic information, etc.).

#### **7.2.4.1 Geophysical survey**

No fracture characterisation has been conducted previously on the site to describe the predominant types of fracture associated with any intrusion. But vertical jointing in the sediments above the sills or inclined sheet, bedding-parallel fractures (Botha *et al.*, 1998), or internal fracturing (vertical thermal columnar jointing, fractures parallel to the strike, and well-developed oblique or sub-horizontal open fractures) are suspected to constitute the main flow path for groundwater at the site. Also, fracturing at the junction between a feeder dyke/inclined sheet and a sill will be investigated.

From the study of satellite and air photos (Google Earth) and a site visit, a ground magnetic survey was carried out over the site with a 'G5 Proton Magnetometer', and the result processed and interpreted, for the siting of boreholes. Four traverses (T1 to T4) have been walked as shown on (Figure 7-17).



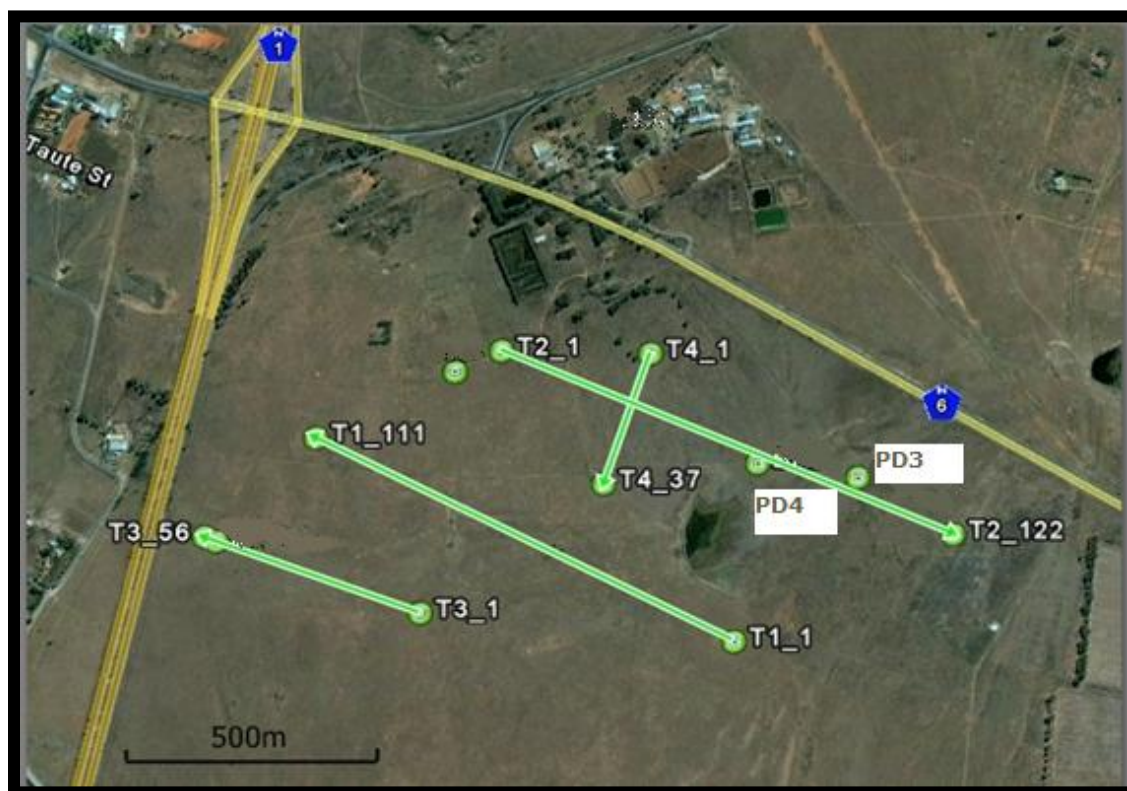


Figure 7-17 Magnetic survey traverses at Paradys farm

In addition to the presence of suspected sills (air photo, and visual patterns) on the farm, which the magnetic survey has confirmed, one wide dolerite dyke was depicted on traverse "T2" (Figure 7-18 and Figure 7-19 ). The strike of the dyke is found to be orientated SW-NE and the interpretation of the magnetic anomaly across the dyke shows a shallow, wide (about 24 m) dyke, which generally does not give a big possibility for intersecting significant flowing fractures or fracture zones (for strong boreholes), particularly in mudstone.

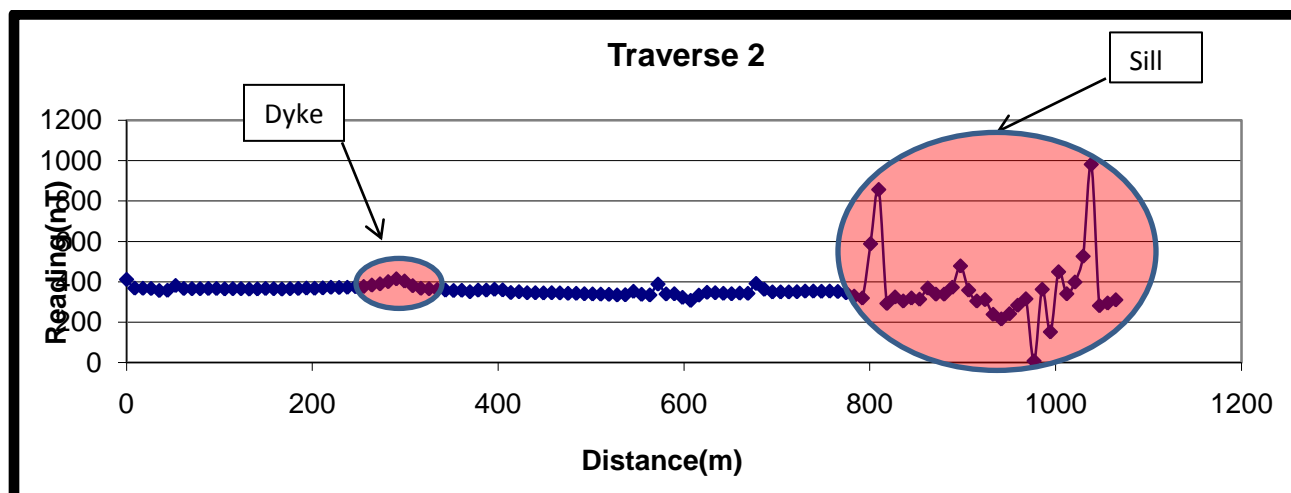


Figure 7-18 Magnetic survey at Paradys farm (traverse 2)

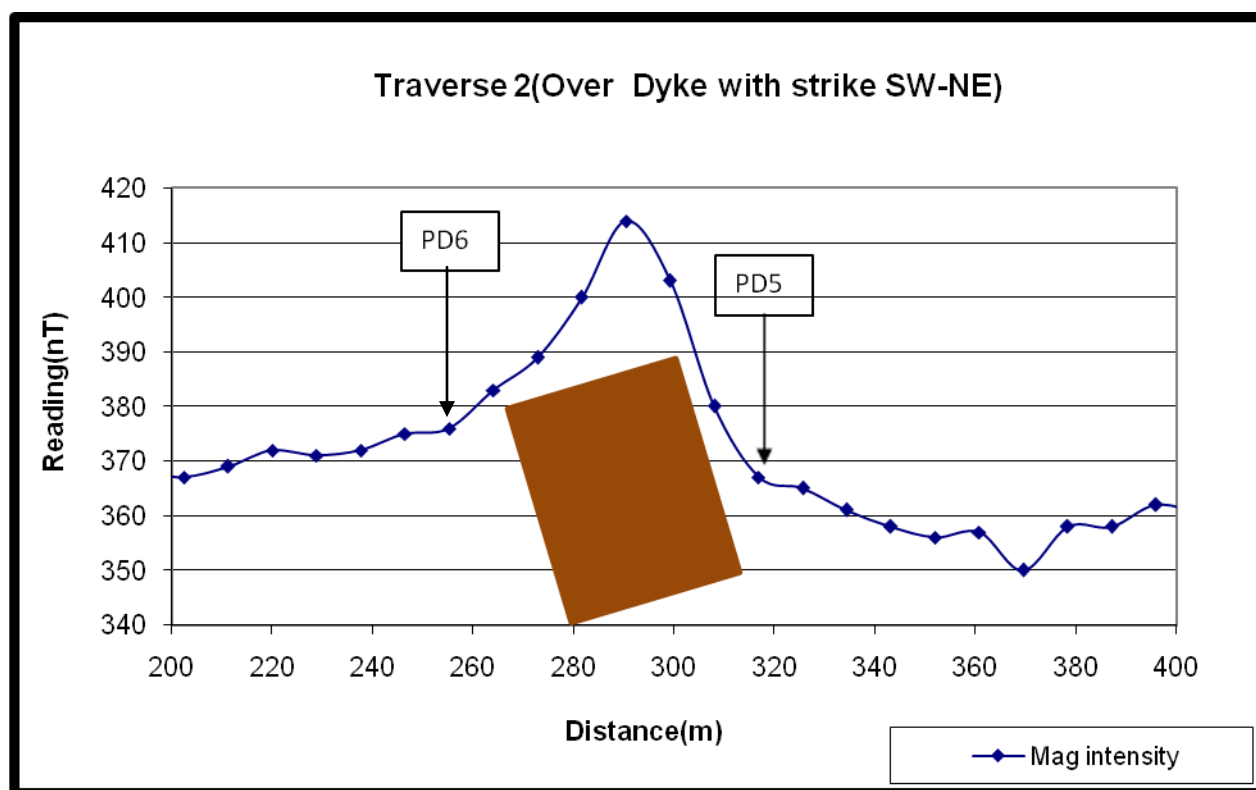


Figure 7-19 Magnetic anomaly and drilling positions and interpretation of the dip of the dyke with an interpreted dyke width of about 24 m.

Also the orientation of the strike of the dyke suggests a possible extending of the dyke towards a suspected sills anomaly on traverse 1, and therefore the possible existence of joint between the dyke and the sill.

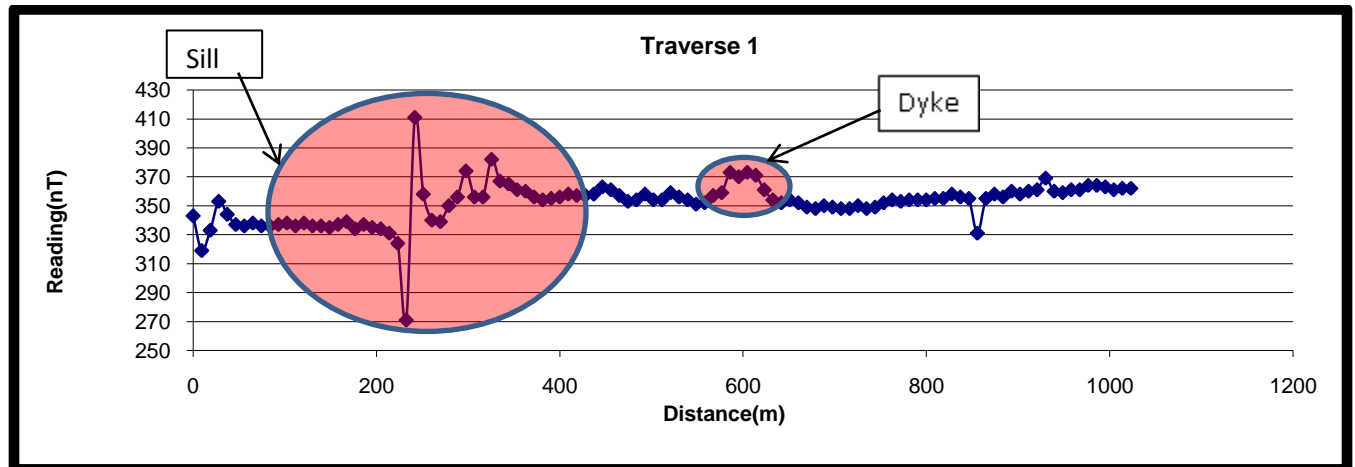


Figure 7-20 Magnetic survey at Paradys farm (traverse 1)

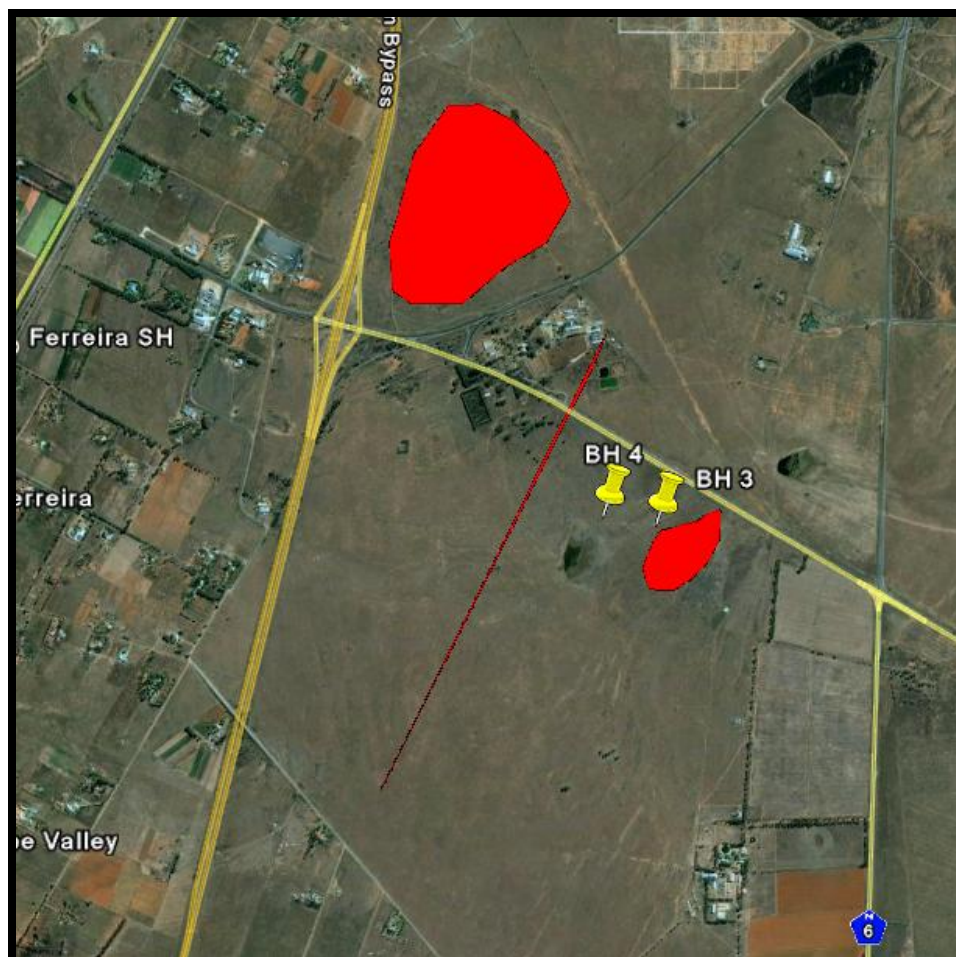
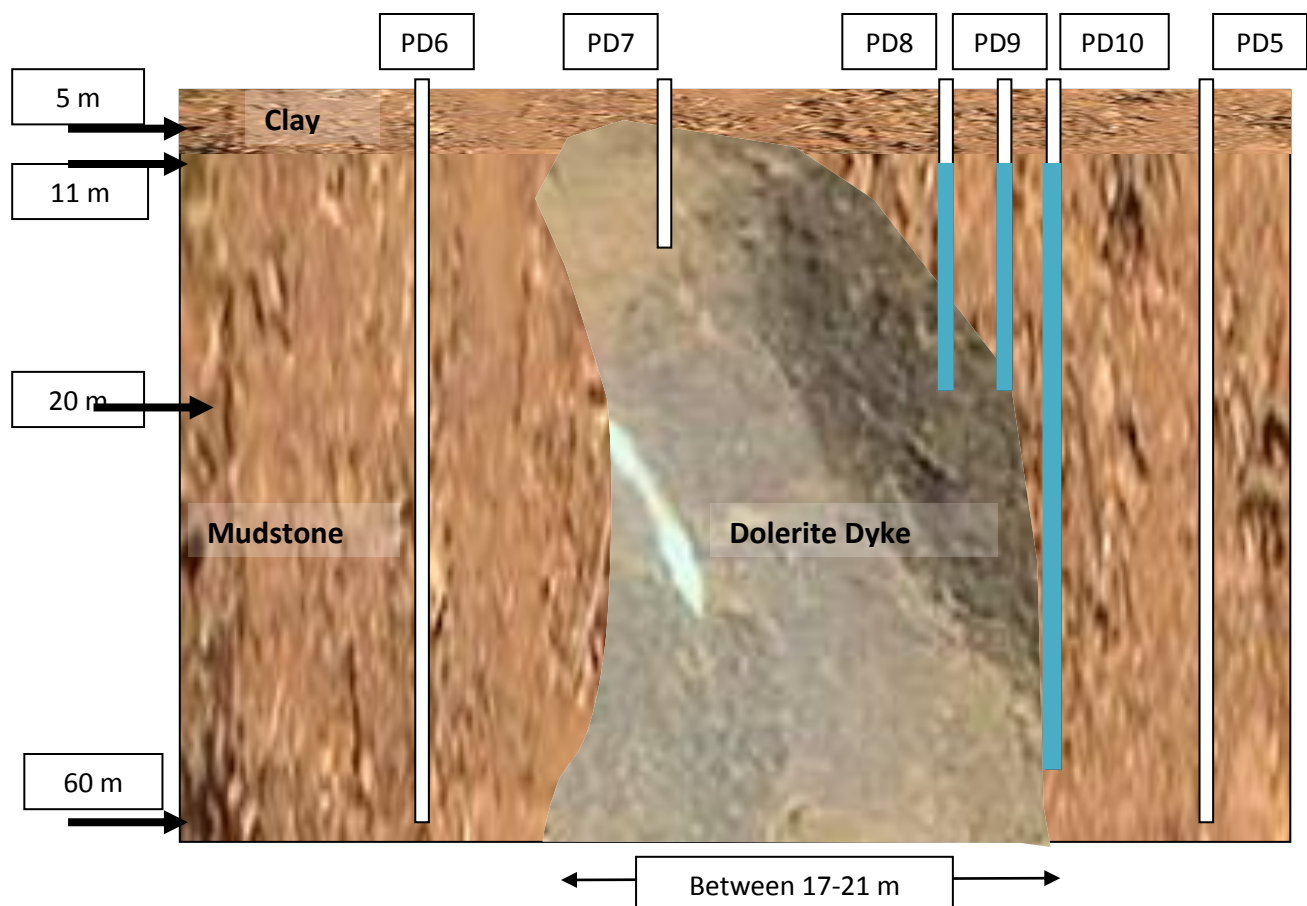


Figure 7-21 Location of the dyke (red line) and two sills (red area) at Paradys farm; BH3 and BH4 are also shown on the map.

### 7.2.4.2 Siting and drilling

In sum, thirteen (13) boreholes were sited with a magnetometer survey, and were drilled with the air compression method. The first implanting and drilling attempts were associated with the main dyke intrusion. As recommended by Murray for mudstone and shale formations, the closer side of the contact surface, in the dolerite, was targeted for finding significant flow paths (fractures) in the subsurface. Six boreholes (PD5, PD6, PD7, PD8, PD9, and PD10) were sited and drilled consecutively along the dyke. Only PD8, PD9 and PD10 gave very small water-strike (1 L/s at most) and the other boreholes were dry. The results of these drilling results emphasises that trying to drill for water along a wide dyke in mudstone is usually fruitless. The group of these six boreholes is termed "Dyke attempts".



**Figure 7-22 Conceptual picture of the intrusion of the dyke inferred from drilling associated with the dyke results: Boreholes PD6, PD7, PD8, PD9, PD9 and PD5.**



The lithology for the local geology surrounding the depicted wide dyke may be conceptualised as shown in Figure 7-22.

Five other boreholes (PD12, PD13, PD14, PD15, and PD16) were sited and drilled by looking for possible vertical jointing in the sediments above the sills, or bedding-parallel fractures. Borehole PD13 was drilled to investigate the possibility of the occurrence of groundwater flow zones at the suspected junction between the identified dyke and a sill, but no sign of dolerite intrusion contact (between dyke and sill) was found.

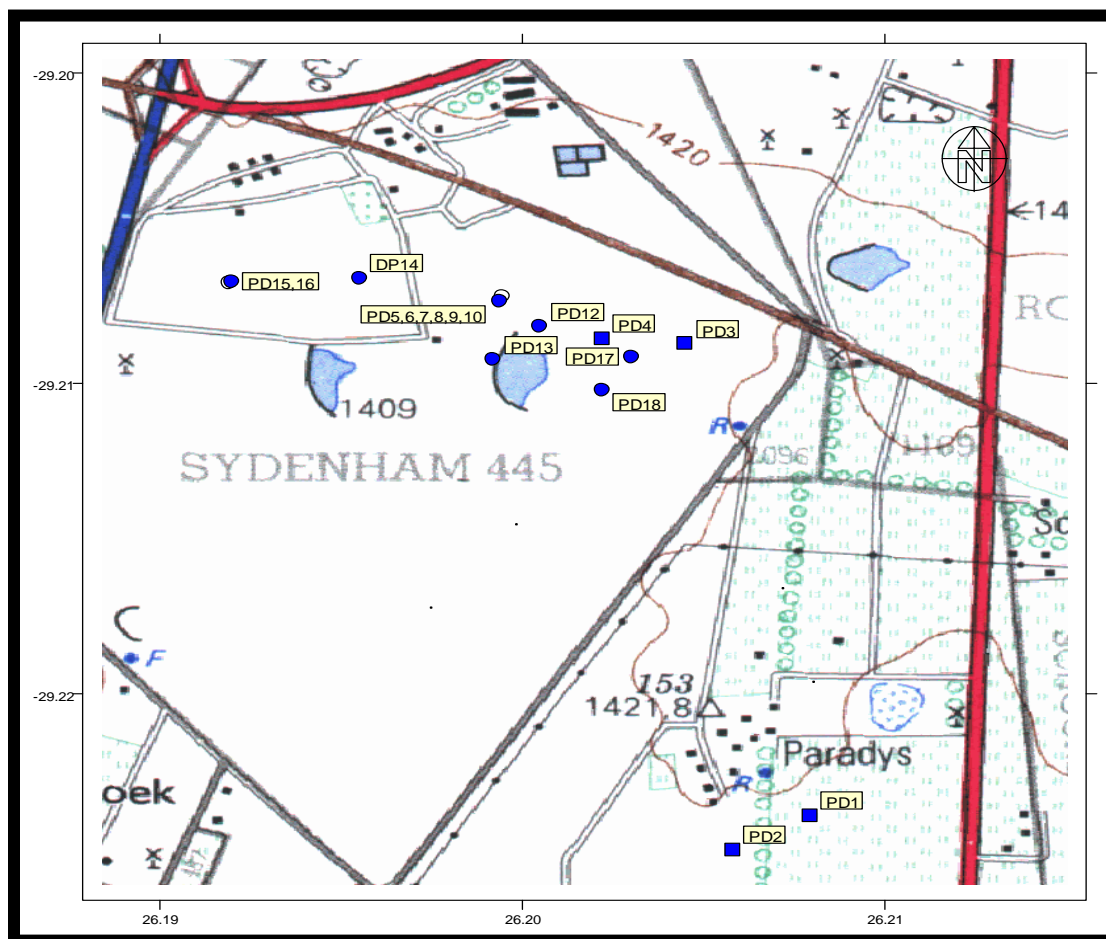


**Figure 7-23 Positions of the boreholes at Paradys Farm**

The two last attempts were PD17 and PD18, which yielded respectively 10 L/s and 0.8 L/s. Borehole PD17 was drilled in a sill and the borehole geology (Figure 7-24 and Figure 7-25) (from drilling cuttings) shows clearly a contact zone (sill and mudstone) of approximately 18 meters thickness under the near-surface sill sheet.

The driller estimated the main water strike at 21.6 meters below ground surface. The existing good boreholes, PD3 and PD4 (with yields in excess of 10 L/s) at the farm also intersect the sill and are located in the same area (Figure 7-23).

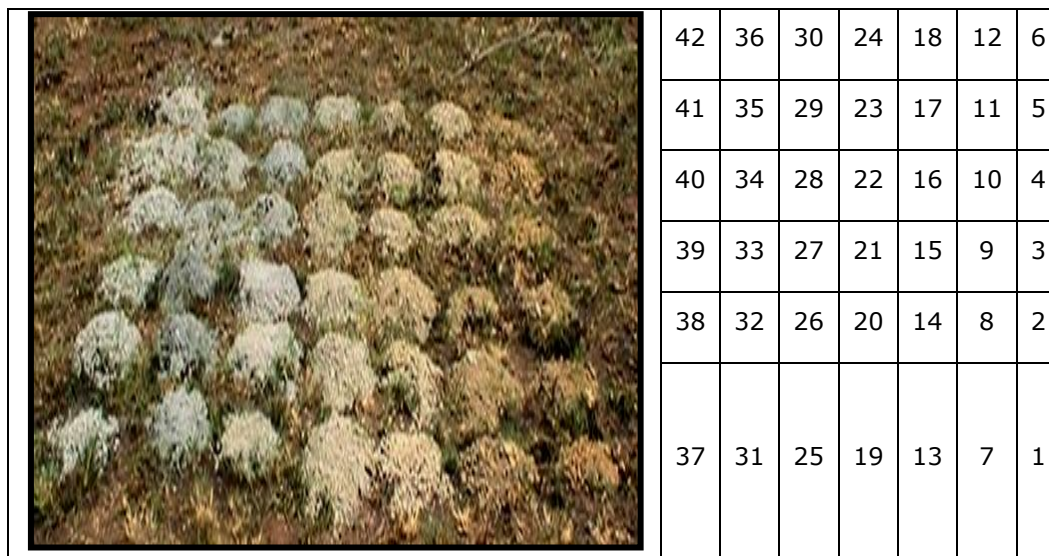


**Figure 7-24 PD17 Drilling cuts (Start from the bottom right corner and follow the numeric order in the cells at right to relate the corresponding depth of each cuts sampling)**

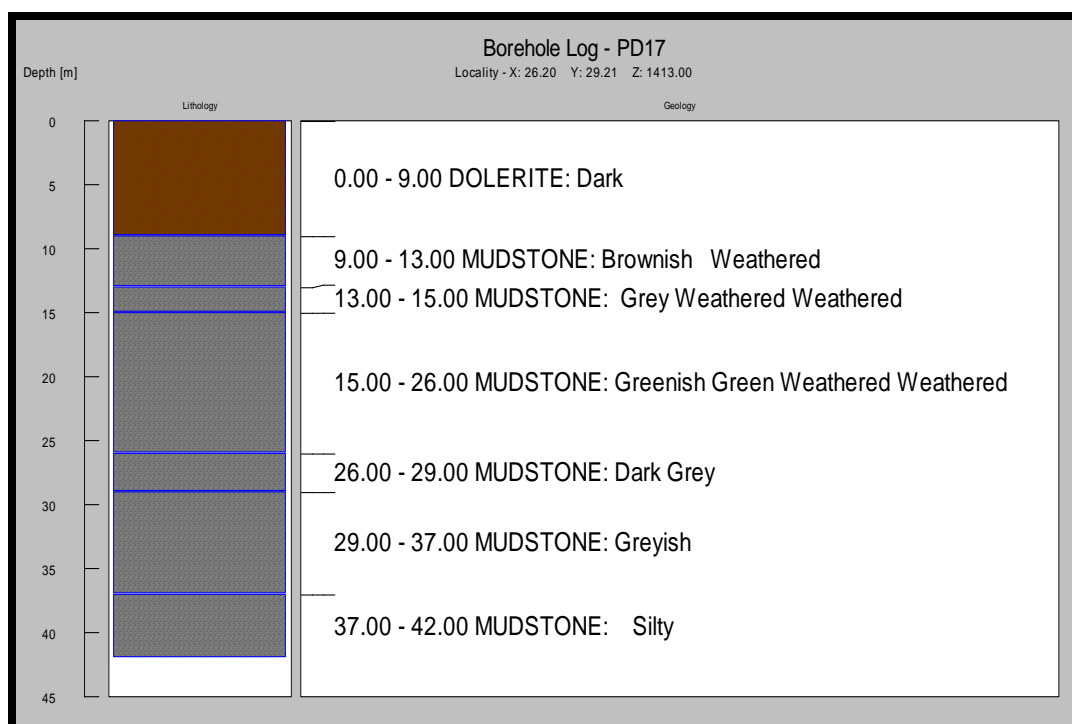


**Figure 7-25 Borehole PD17 geological log with the lithology.**

### 7.2.4.3 Hydraulics and tracer tests

After completing the drilling campaign, hydraulic (constant rate pumping test) and tracer tests (SFEC and 02 FFEC) have been performed to determine how strong the successful borehole (PD17) is and what may be the contribution of each intersected fracture for the production of the borehole. Also slug test have been carried out on PD5, PD8, PD12, PD15, PD16, PD14, PD17, and PD18.

#### **Slug tests**

The data of the slug tests that were performed have been analysed following the method proposed by Vivier (1994), and the results give the potential yield of the boreholes and a first idea of what the transmissivity of the system's borehole-aquifer could be, as resumed in Table 7-4.

**Table 7-4 Some parameters estimated from slug tests (Vivier method)**

Borehole name	Time (s)	Estimated Yield (l/s)	Sust_Q (l/s)	Formation T (m <sup>2</sup> /d)	Static water level (mbg)
BH5	39	1,4	0,27	3,4	8,7
BH8	65	0,9	0,18	2,2	10,4
BH12	45	1,2	0,24	3,0	11,1
BH15	9	4,5	0,91	11,0	13,4
BH16	48	1,1	0,23	3,0	13,1
BH14	26	1,9	0,38	4,74	10,8
BH17	3	11,2	2,25	28,0	11,3
BH18	55	1,0	0,20	2,6	10,6

The same data information has been used with the rule of THUMB and Swenson equation to estimate respectively the formation and the fractures transmissivity.

**Table 7-5 Some parameters estimated from slugs tests (rule of THUMB and Swenson equation)**

<b>Borehole name</b>	<b>Time (s)</b>	<b>Estimated Yield (ℓ/s)</b>	<b>T (m/D) Rule of THUMB</b>	<b>T (m/D) Swenson equation</b>
BH5	39.00	1.40	7	79.40
BH8	65.00	0.90	4.5	47.64
BH12	45.00	1.20	6	68.81
BH15	9.00	4.50	22.5	344.06
BH16	48.00	1.10	5.5	64.51
BH14	26.00	1.90	9.5	119.10
BH17	3.00	11.20	56	1032.19
BH18	55.00	1.00	5	56.30

The estimated fracture transmissivity values calculated with the Swenson equation are overestimated and seem unrealistic.

### ***Constant pumping rate***

On 13 September 2010, BH17 was pumped at a constant rate of 5.5 l/s for 210 minutes (3.5 hours), followed by a recovery (2 hours) measurement. The data from this test were processed with the programme FC (developed by IGS) and the results are shown below (Figure 7-26)



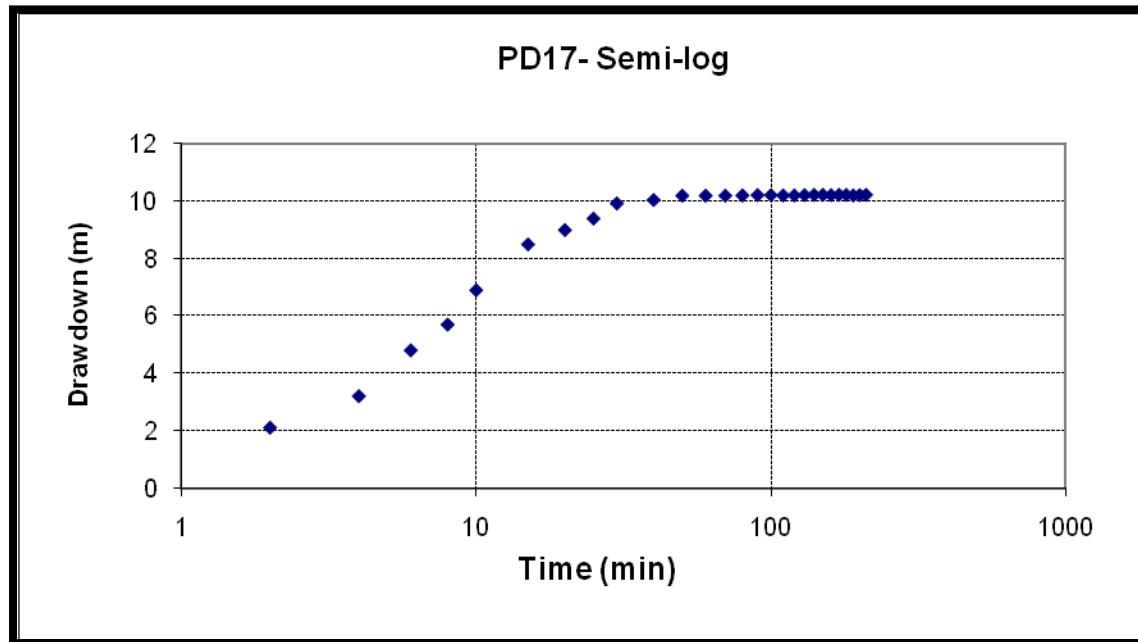


**Figure 7-26 PD17-Constant pumping (5.5 L/s) test result on Semi-log**

The time drawdown on the log-log curve (Appendix B ) shows a slope between 1 and 0.5, characteristic of fracture storage for linear flow, followed by a very short time period of bi-linear flow (slope between 0.25 and 1) before the flattening of the curve. The derivative plot (Appendix B), clearly shows a dewatering of the fracture (decrease of the derivative curve), followed by an effect of recharge boundary (further decrease of the derivative curve). The dam at approximately 100 meters downstream of PD17 could constitute this recharge boundary, or the reach of a connected and more transmissive fracture zone (or fracture network) at some distance from the borehole may also result of this behaviour. Analysis of the derivative curve indicates a fracture position at 21.5 m (30 minutes from the beginning of the test) from the top of casing. This fracture position needs to be confirmed with other fracture detection method. The length of the pumping test is of concern (less than four hours), since a longer test will sample more volume of the aquifer system and therefore a better diagnostic of groundwater flow could be inferred.

A transmissivity value may be determined with the Cooper-Jacob method by fitting the curve at the transition between the linear part and the flat part of the semi-log curve. This transmissivity value ( $20 \text{ m}^2/\text{day}$ ) corresponds well with the one

obtained from the recovery measurement ( $20.2 \text{ m}^2/\text{day}$ ). The estimated transmissivity value (based on relatively late time drawdown) is representative of the entire aquifer-borehole system (Riemann 2002). It is indicated for the determination of the sustainable yield of the borehole (management purposes). Only knowledge of the fractures and fracture networks geometries could help to determination accurately of how transmissive the aquifer system is. Accurate flowing-fractures' transmissivities or fracture zone transmissivity determination from a constant rate pumping test, requires the flowing section to be isolated (with packers), and its responses to be collected from corresponding piezometers.

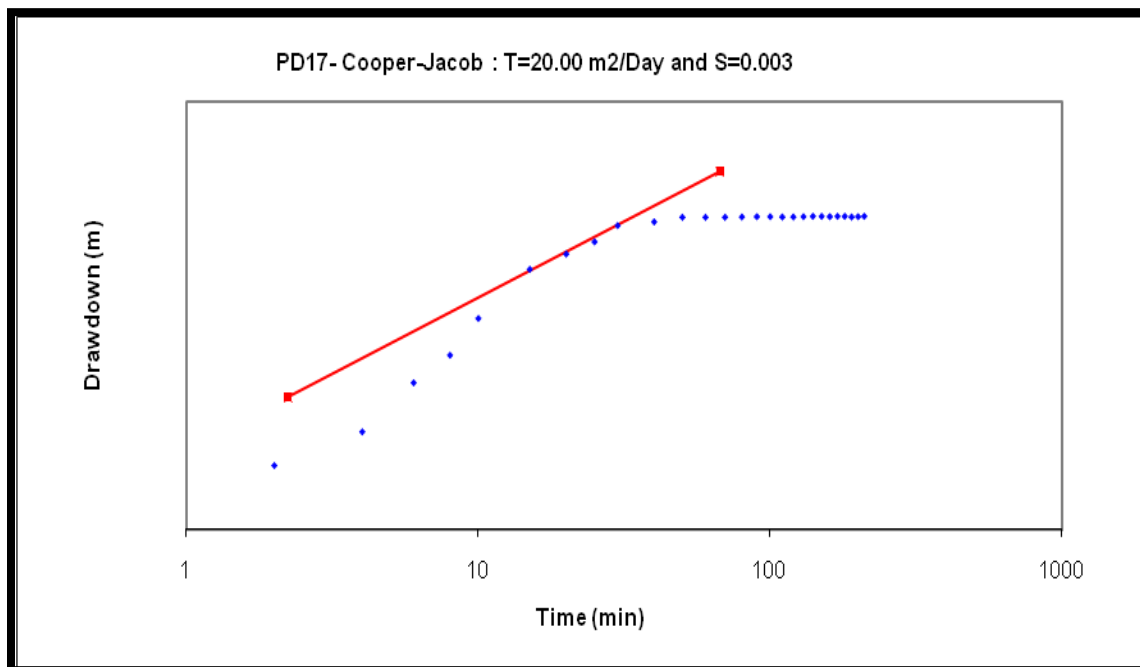


**Figure 7-27 PD17- Cooper-Jacob: T=20.00 m<sup>2</sup>/Day and S=0.003**

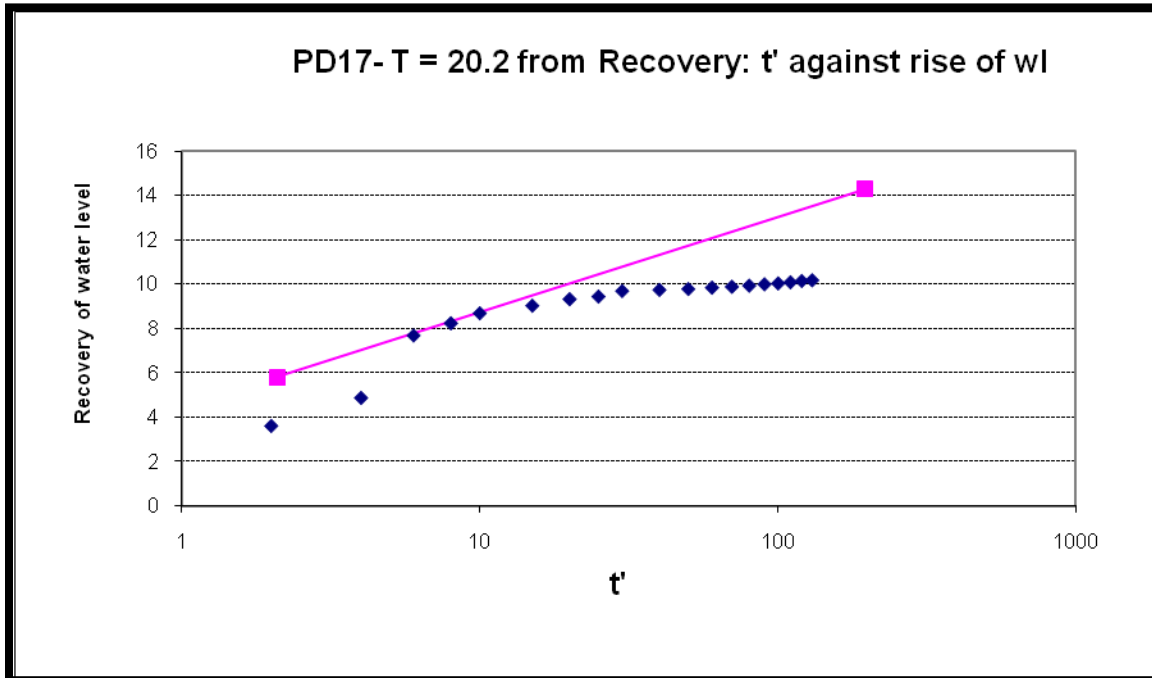
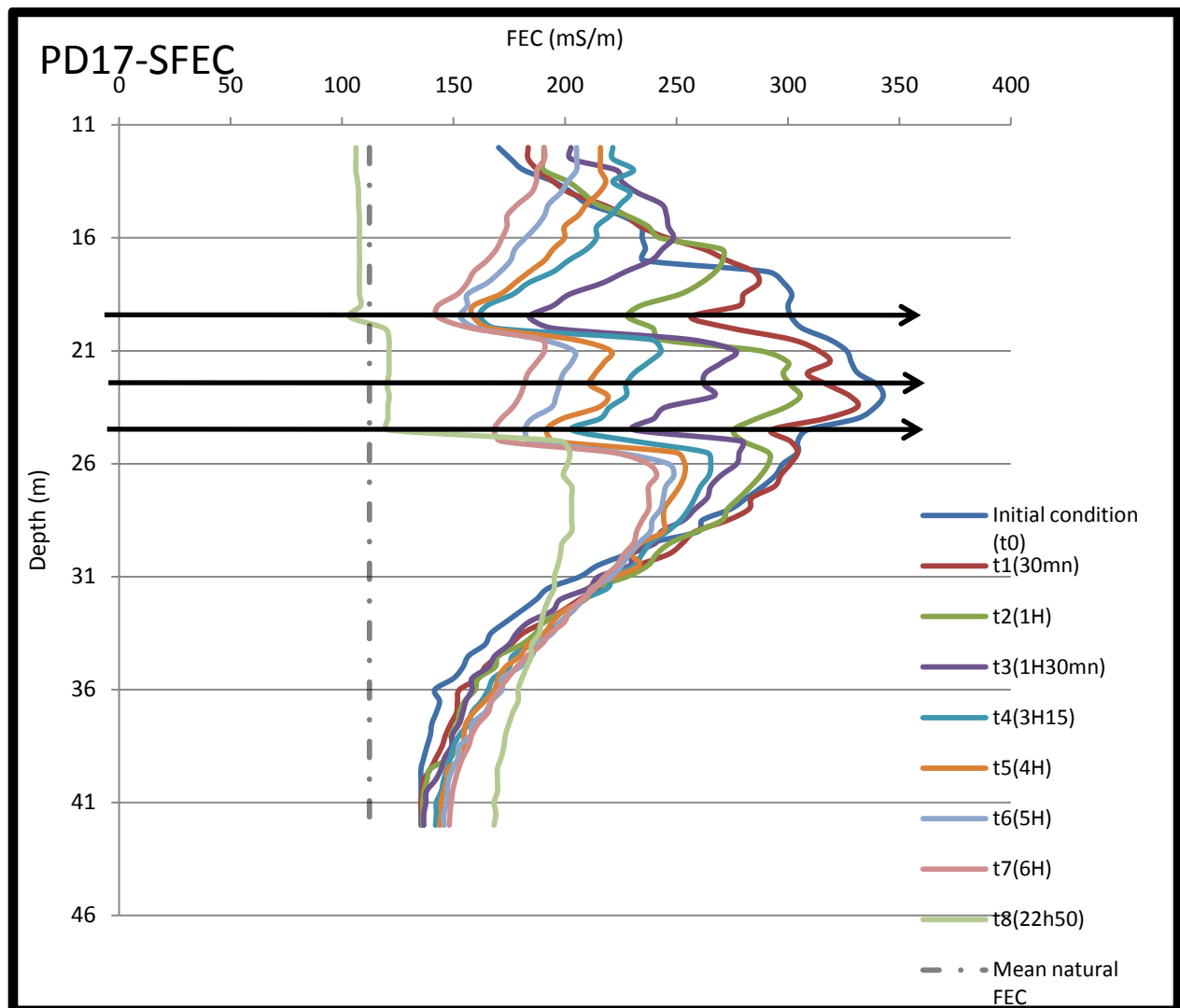


Figure 7-28 PD17- T = 20.2 from Recovery:  $t'$  against rise of wl for sustainable yield.

### Tracer tests

One ambient (SFEC) and two pumping (FFEC) tracer tests were conducted on borehole PD17 to detect the locations of its main flow points and the intra-well flow condition. The results of the data will be used to determine the groundwater flow rate into the borehole at the main flow points. Salt was injected by moving a pouch of known mass of sodium chloride (NaCl) up and down, until complete dilution of the salt in the borehole was obtained. The amount of salt for each test was calculated based on the natural salinity in the borehole water, which is assumed to represent the natural condition in the aquifer surrounding the borehole. The method of calculation was described previously in the section 6.2.2.

For the ambient FEC logging, the natural groundwater average FEC at the site was approximately  $112.33 \text{ mS m}^{-1}$ . The injection of salt took approximately two (2) minutes. After injection of the tracer, the initial recorded fluid electrical conductivity along the entire borehole ranged between  $135.4 \text{ mS/m}$  and  $342.7 \text{ mS/m}$  with an average of  $226.88 \text{ mS/m}$ . FEC profiling was recorded unevenly at 30, 60, 90, 195, 240, 300, 360, and 1370 minutes after injection of the salt, with a rate of profiling ranging between 0.26 and 0.35 m/min. At the end the test, the bulk dilution of the tracer was about 72 % with a mean of  $155 \text{ mS/m}$ .



**Figure 7-29 Steady state FEC-based dilution logging at Paradys farm (Bloemfontein)**

The ambient FEC profiling results show clearly three (03) main points with relative high rate of dilution, indicative of flowing of water at 19.5m, 22m, and 24.5m as measured from the top of the casing. The most significant zone is depicted at 19.5m followed by the point at 24.5m. The flowing point (21.50 m) suspected on the derivative plot of the constant rate pumping test data, may be related to the one depicted with the tracer test at 22m, or may be just the effect of the entire flow zone between 19.5 m and 24.5 m. The symmetrical shape of the dip observed on the time evolution concentration curves at 19.5m and 24.5m reveal that groundwater flow through the borehole at these positions do not circulate into the borehole, but are horizontal. But as time passing a slow widening of the dip

observed at the position 22m may be due to a low vertical circulation of water from this point to the point 24.5m where it exiting the borehole. The flattening of the profile between the two points at t8 (late time: 22h50mn after tracer injection) confirms the vertical circulation between the two points.

The two FFEC (2.32 L/min and 9.47 L/min) results confirm the existence of the three main flow points in the borehole at their respective positions (19.5 m; 22 m; 24.5 m) as depicted in the SFEC test. This suggests that in either ambient or pumping conditions, the bulk of water from the borehole is supplied firstly by the flow point at 19.5 m followed the 24.5 m. By observing the response of the flow point at 22 m under the two different pumping rates it can be seen that under very low pumping rates this point may not be contributing significantly to groundwater supply.

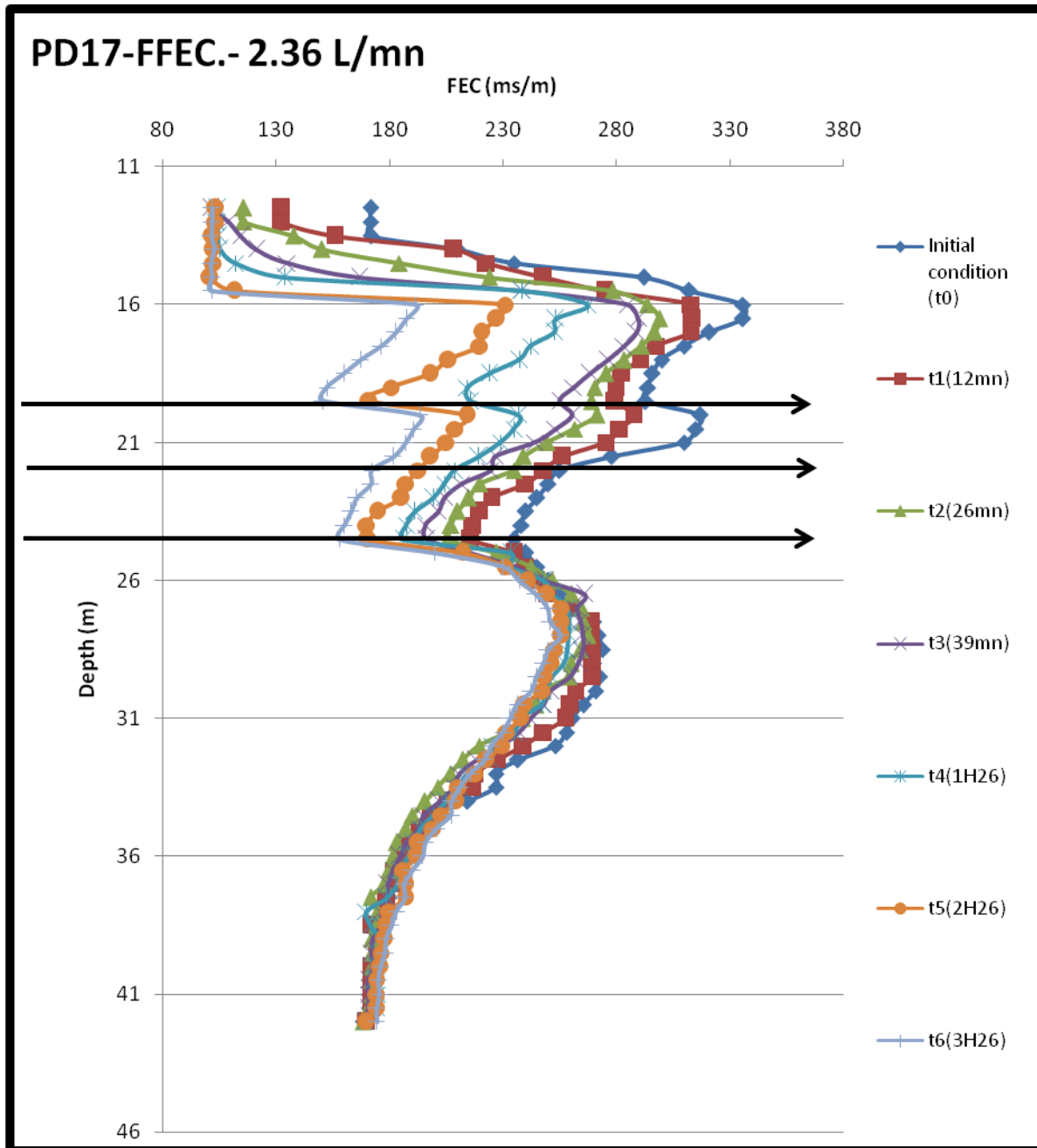


**Figure 7-30 Pumping FEC-based dilution logging (pumping rate: 2.36L/mn) at Paradys farm (Bloemfontein)**

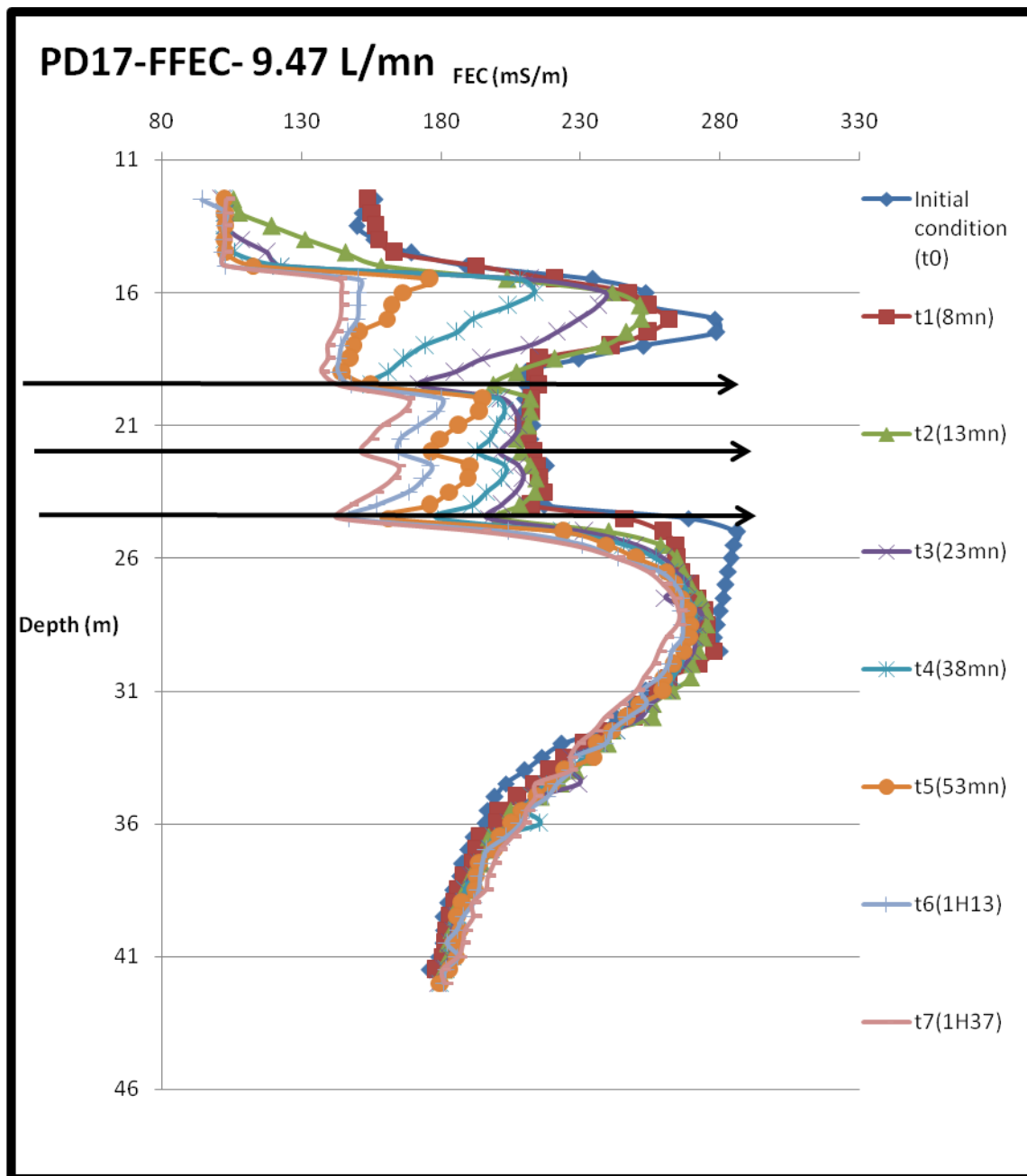


**Figure 7-31 Pumping FEC-based dilution logging (pumping rate: 2.36L/mn) at Paradys farm (Bloemfontein)**

- **Conceptual model**

The conceptual model on which the semi-quantitative analysis of the data will be based is illustrated by Figure 7-32

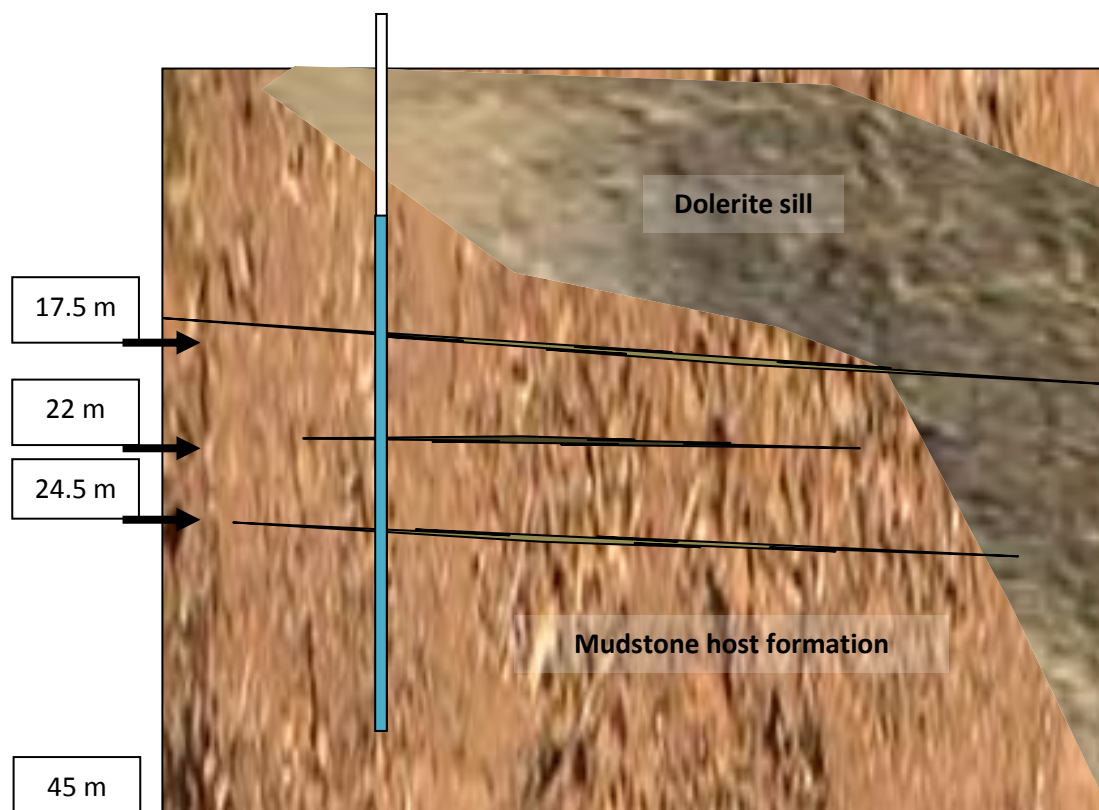


**Figure 7-32** Conceptual model of the borehole-aquifer system showing the main flow path intersected at the mudstone-sill contact zone under the sill (Paradys farm, Bloemfontein)

- **Data analysis**

The collected data were converted into concentration profiles for a semi-quantitative estimation of the groundwater flow along the borehole, with a special focus on the main flow points that source groundwater for the studied well. The estimated semi-quantitative values will be compared to weight the contribution of each flow point to flow naturally or at different specific pumping rates. The Drostian analytical solution was applied for that purpose.

Flow rates were estimated to range from between 0.28 m/day and 0.39 m/day at the flow point locations but generally fluctuating below 0.1 m/day at other points along the borehole. Figure 7-33 shows the estimated groundwater flow velocities at the flow points' positions with their respective estimated percentage of contribution. The graph of the estimated values along the borehole is shown in Appendix C.



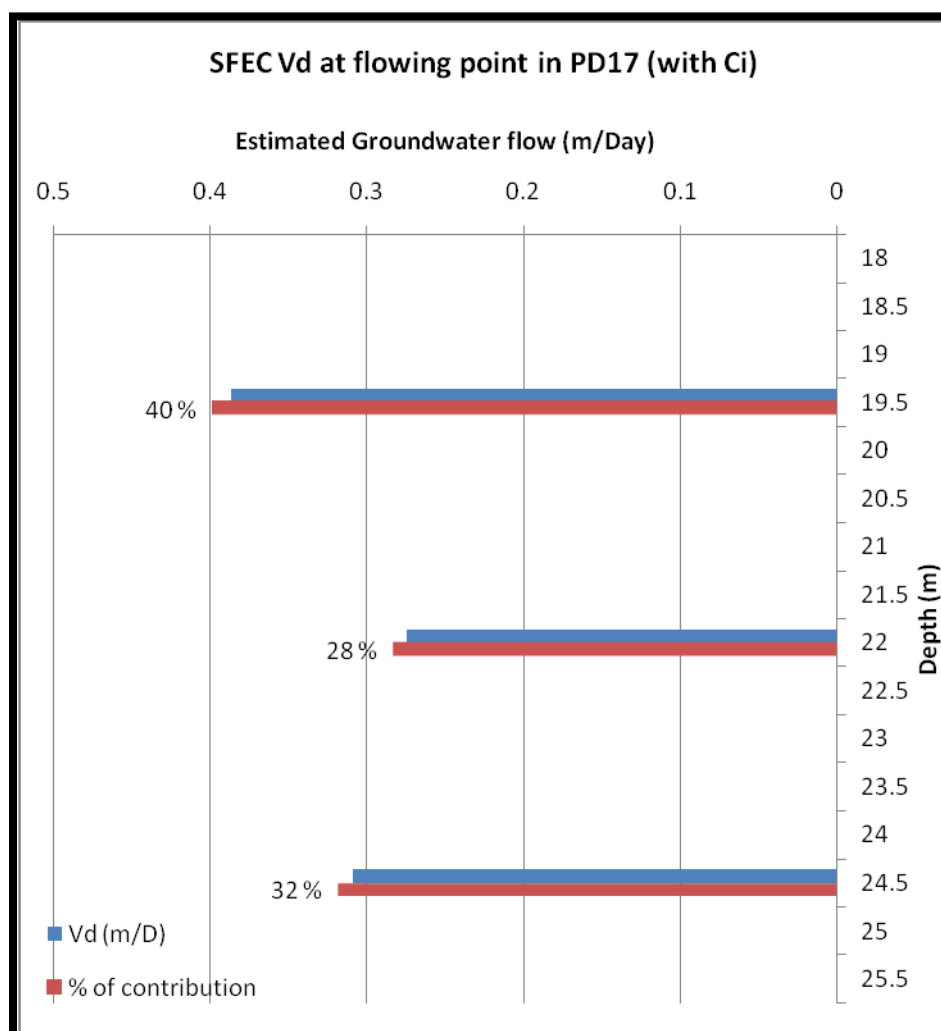


**Figure 7-33 Estimated groundwater velocity at different flow points (19.5m, 22m, and 24.5 m), applying Drostian analytical solution to SFEC profiling in borehole PD17 (Paradys farm, Bloemfontein).**

The estimated flow velocity values confirm the point at 19.5 m as the main flow, with 40 % of relative contribution to the total fast flow, followed by the point at 24.5 m, with 32 % of relative contribution to the total fast flow. The relative contributions of the different flow points have been noticed to change under stress conditions (pumping) and according to the rate of abstraction. This can be seen clearly in Figure 7-34 and Figure 7-35. This result suggests that under high pumping rates, the relative contributions of the flow points at 19.5 m and 22.5 m may be closer to each other.

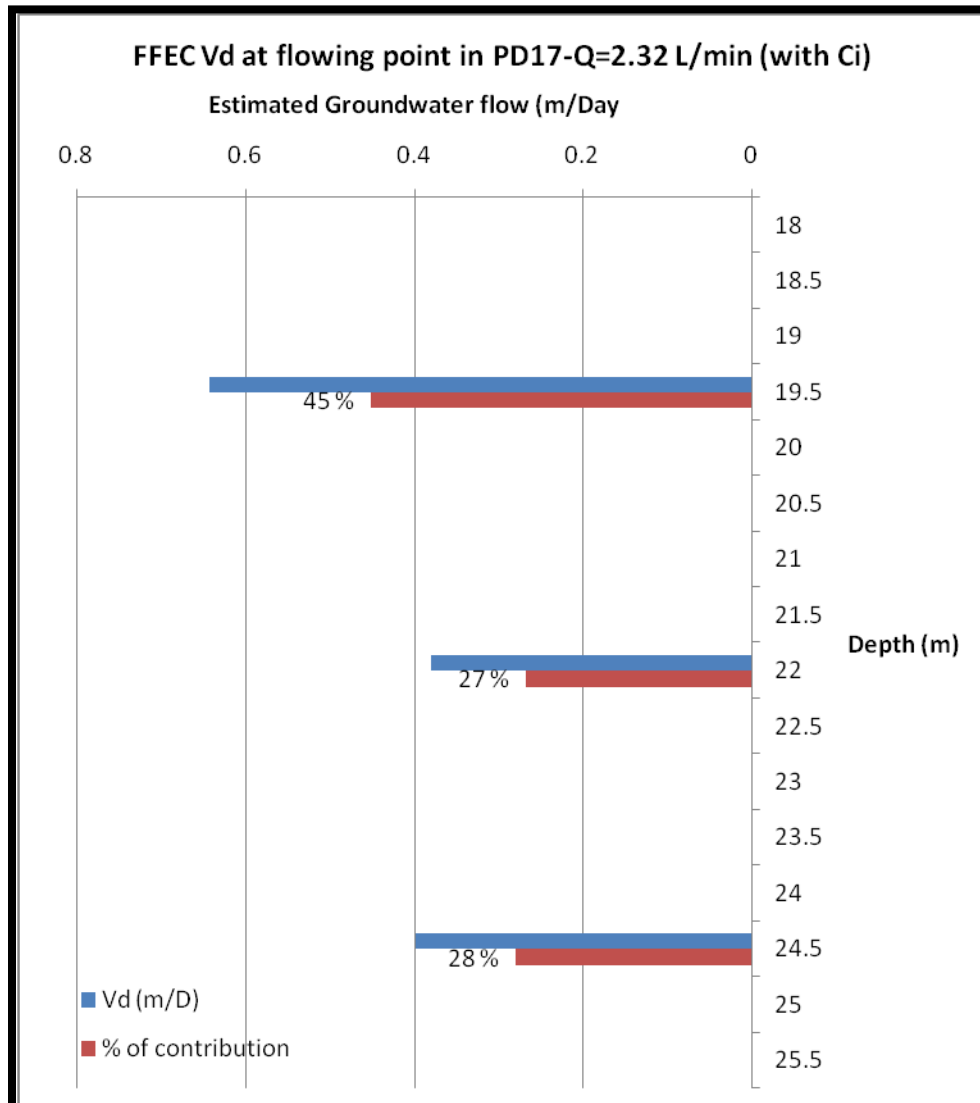


**Figure 7-34 Estimated groundwater velocity at different flow points (19.5 m, 22 m, and 24.5 m), applying Drostian analytical solution to FFEC profiling in borehole PD17 at 2.32 L/min of pumping. (Paradys farm, Bloemfontein)**

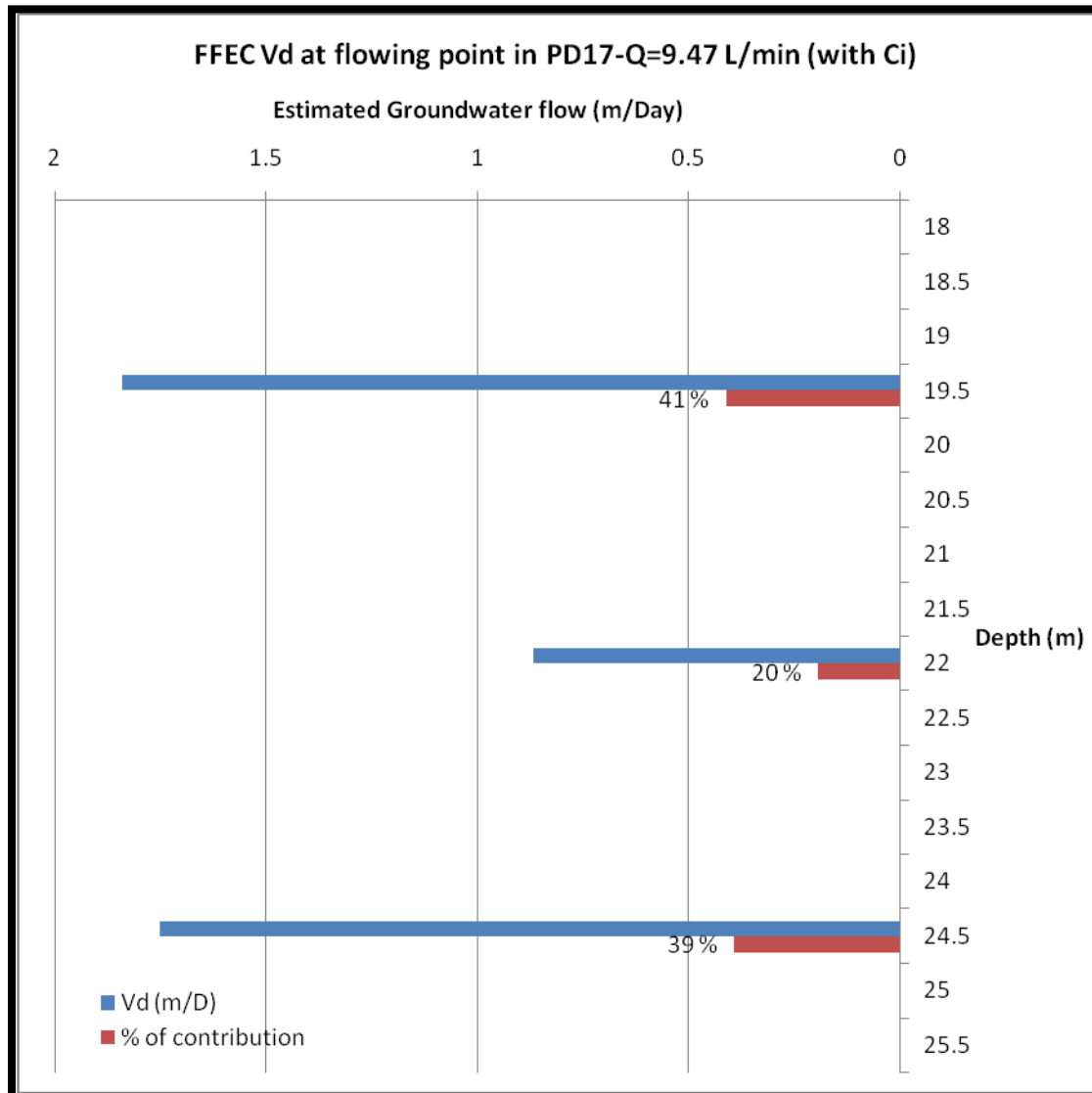


**Figure 7-35** Estimated groundwater velocity at different flow points (19.5 m, 22 m, and 24.5 m), applying Drostian analytical solution to FFEC profiling in borehole PD17 at 9.47 L/min of pumping. (Paradys farm, Bloemfontein)

## 8 CONCLUSION AND RECOMMENDATIONS

Different aspects involved in fracture characterisation have been presented in the present study, with special focus on Karoo aquifers. Valuable information on the kinds of fractures that tend to form in the different geological settings of the main Karoo and their commonly associated patterns has been documented from laboratory and field investigations. This information is key and should help in decision making when flowing fractures have to be identified, located and quantitatively evaluated (geometry, flow and transport).

Whereas a fracture's geological and physical characters describe the geometry of the fracture, its location, and its general physical presentation, its hydraulic and mass transport character control respectively the flow and mass transport processes (behaviour) under natural or stressed conditions. Laboratory and field studies of fracture properties, and geophysical, hydraulic and tracer testing can be carried out to help determine these parameters. Each of these developed tools has its own benefits and limitations.

Surface and underground based geophysical tools (single borehole, cross-borehole, and channel) are designed for detecting heterogeneity and anisotropy in the subsurface that may be associated with fractures, but they trace mainly the fracture's mechanics or electrical properties and not its geohydrological properties. Hydraulic and tracer tests are designed to infer flow or transport properties from a given response of the aquifer system to a perturbation (pumping or tracer), but the inversion process may suggest different distributions of heterogeneity for the same hydrological response and are restricted to small-scale field studies.

At the small scale (in a radius of approximately 150 m) a combination of the fracture's surface mapping, geophysical surveys or logs, and hydraulics and tracer tests can provide an understanding of the possible locations and the hydrological and mass transport properties of main flow paths in the subsurface. At a larger scale, the resolution of the geophysical survey becomes problematic, hydraulics test responses are no longer detectable, and tracer test lengths are not practicable. Large-scale studies usually involve monitoring the response (spatial variation of

groundwater age, and temporal variation of the heads) of the groundwater system to natural perturbations (recharge and discharge) and long-term human disturbances (water production, manmade chemical tracing) to characterise the large-scale flow of groundwater.

The temporal and spatial variability of the fractures' characters that control flow and mass transport through transmissive fractures, require fracture characterisation studies to be an iterative sequence of characterisation, scenario testing, evaluation, and comparison. Modelling is a powerful approach for scenario testing, whereas *in situ* fieldwork research facilities are important to evaluate the accuracy of the characterisation results. Additional *in situ* facilities should be developed in the Karoo aquifer system for fracture characterisation purposes.

Among the small-scale appropriated tools, the FEC-based techniques, mainly the single-borehole based ones are found to be increasingly applicable for fracture characterisation, particularly in Karoo aquifers where multiple available boreholes are scarce and groundwater projects are constrained by lack of funding. This technique is attractive in South Africa because of the simple and relatively cost-effective equipment it involves. The FEC-based dilution technique (well dilution) has been applied in two different fractured systems (bedding-plane fracturing and sill-intrusion fracturing). The method is found to be efficient in the detection of flow points and for the study of intra-borehole flow. In pumping conditions, the method may also detect low transmissive flow points intersected by a borehole. The FEC method, when well designed, may be used to classify intersected flowing fractures in terms of relative contribution to the general flow, either in ambient conditions or in stressed conditions.

With the FEC based dilution test data, out-flow points are difficult to be diagnosed. Therefore out-flow points are assumed after trial and error, when attempting to simulate concentration evolution in a borehole numerical code "BORE II". Also, the code "BORE II" does not take into account density gradient along the borehole, and does not yield unique parameters set up for matching of model and observed data.

The adaptation of the analytical solution proposed by Drost, for calculating intersected fractures' groundwater velocity into the borehole, based on well dilution test data certainly remains of concern due to non-ideal conditions of the test. However, its application yields a semi-quantitative value that can be used as a first estimation. There are two main points that need to be refined in the application of dilution tests for accurate fracture flow velocity determination. Field procedures need to be refined to ensure that a tracer is as well mixed as possible for homogeneity in the borehole column water. An appropriate methodology also needs to be developed to account for the mass circulation that may be associated with density gradients in the well and with adjacent aquifer.

New technologies (recirculation systems), have been developed to insure homogeneity in the borehole column water, but they need to be simplified for practical reasons and more importantly for economic reasons. Also, during these tests, one has to insure that no pumping from the studied aquifer that might affect the data is occurring, mainly when performing ambient logging. Such interference may yield inaccurate data, and therefore misunderstanding of the behaviour of the aquifer system.

## REFERENCES

1. Abelin, H., L. Birgersson, J. Gidlund, and I. Neretnieks. (1991a) . A large-scale flow and tracer experiment in granite 1. Experimental design and flow distribution. *Water Resources Research*, 27(12):3017–3117.
2. Abelin, H., L. Birgersson, L. Moreno, H. Widen, T. Agren, and I. Neretnieks. (1991b). A large-scale flow and tracer experiment in granite 2. Results and interpretation. *Water Resources Research*, 27(12):3019–3135.
3. Abram Erasmus Van Wyk. (1998). Tracer Experiments in Fractured-Rock Aquifers. M.Sc. Thesis. Faculty of Science, Department of Geohydrology at the University of the Orange Free State. South Africa.
4. AC Woodford and L Chevallier. (2002). Hydrogeology of the Main Karoo Basin: Current Knowledge and Future Research Needs. WRC Report No. TT 179/02 November 2002.
5. Alcamo, J., P. Döll, T. Henrichs, F. Kaspar, B. Lehner, T. Rösch and S. Siebert, (2003a): Development and testing of the WaterGAP 2 global model of water use and availability. *Hydrol. Sci. J.*, 48, 317–338.
6. Andreoli M.A.G., Doucouré M., Van Bever Donker J., Brandt D. And Andersen N.J.B. (1996): Neotectonics of Southern Africa - A review. *Africa Geoscience Review*, Vo.3, No1, 1-16.
7. Archie, G. E. (1942). The electrical resistivity log as an aid in determining some reservoir characteristics. *Transactions of the American Institute of Mechanical Engineering*, 146:54–62.
8. Asgian, M. 1989. A numerical model of fluid flow in deformable naturally fractured rock masses. *International Journal of Rock Mechanics and Mining Science and Geomechanics. Abstracts*, 26:(3/4) 317–328.
9. Atekwana, E.A, Sauck, A., Douglas, D and Werkema, Jr. (1998). Investigations of geoelectrical signatures at a hydrocarbon contaminated site. *J. Applied Geophysics*: vol. 44, pp 167 – 180.
10. Bahat, D. (1988). Fractographic determination of joint length distribution in chalk. *Rock Mechanics and Rock Engineering*, 21:79–94.

11. Bangoy, L.M., P. Bidaux, C. Drogue, R. Plegat, and S. Pistre (1992). A new method of characterizing fissured media by pumping test with observation wells. *Journal of Hydrology* 138, pp. 77-88.
12. Bardenhagen, I., (1999). TPA software, Test Pumping Analysis for fractured and non fractured aquifers. Published in Van Tonder et al. (2001)
13. Barton C.C. (1996) Characterizing bedrock fractures in outcrop for studies of groundwater hydrology: an example from Mirror Lake, Grafton County, New Hampshire, In: Morganwalp D. and Aronson D.A. (ed.) U.S. Geological Survey Toxic Substances Program, U.S. Geological Survey, Water Resources Investigations Report 94-4015, 81-87.
14. Barton N. and Choubey V. (1977). The shear strength of rock joints in theory and practice. *Rock Mechanics*, 10:1-54.
15. Bauer, G.D. and J.J. LoCoco, (1996). Hydrogeophysics determines aquifer characteristics, *International Ground Water Technology*, Vol. 2, No. 7, pp. 12-16,
16. Barenblatt, G.I., Yu.P. Zheltov, and I.N. Kochina (1960). Basic Concepts in the Theory of Seepage of Homogeneous Liquids in Fissured Rocks. In *Well Testing in Heterogeneous Formations*. An Exxon Monograph. T.D. Streltsova. John Wiley & Sons, New York, 413 p.
17. Barker, R.D. (1989). Depth of investigation of collinear symmetrical four electrode arrays. *Geophysics*, 54:1031- 1037.
18. Barker, J.A., (1988). A Generalized Radial Flow Model for Hydraulic Tests in Fractured Rock. *Water Resources Res.*, Vol. 24, No. 10, pp. 1796 – 1804.
19. Belanger, D. W., G. A. Freeze, J. L. Lolcama, and J. F. Pickens. (1988). Interpretation of hydraulic testing in crystalline rock at the Leuggernb orehole, Nagra Tech. R ep. NTB 87-19, Nagra, B aden, Switzerland, December 1988.
20. Beukes, N. J., (1969): Die Sedimentologie van die Etage Holkranssandsteen, Sisteem Karoo. Unpublished M.Sc. Thesis. Department of Geology, P.O. Box 339, Bloemfontein.
21. Binnie and Partners (1971) from Alan
22. Binley, A., Cassiani, G., Middleton, R. and Winship, P. (2002). Vadose zone flow model parameterisation using cross-borehole radar and resistivity imaging. In:



- Samoueliana, A., Cousina, I., Tabbaghc, A., Bruandd, A. and Richarde, G. 2005. Electrical resistivity survey in soil science: a review. *Soil & Tillage Research* 83:173–193.
- 23.Botha, J. F., Verwey, J. P., Tredoux G.,Moodie J.W. and Hodgkiss, M. (1990). Modelling Groundwater Contamination in the Atlantist Aquifer. WRC Report N 175/1/90. Water Research Commission, P.O. Box 824 Pretoriat 0001.
- 24.Botha, J. F., J.P. Verwey, I. Van der Voort, J.J.P. Vivier, J. Buys, W.P. Colliston and J.C. Looch,. (1997). Karoo aquifers: Their geology, geometry and physical properties. Report to the Water Research Commission of South Africa..
- 25.Botha, J. F., Verwey, J. P., Van der Voort, I., Vivier, J. J. P., Colliston, W. P. and Looch, J. C. (1998). Karoo Aquifers. Their Geology, Geometry and Physical Behaviour. Water Research Commission. South Africa.
- 26.Bregman, N. D., R. C. Bailey, and C. H. Chapman. (1989). Crosshole seismic tomography. *Geophysics*, 54:200–215.
- 27.Brown, S.R. (1987). Fluid flow through rock joints: effects of surface roughness. *J. of Geophysical Research* 92(B2), 1337–1347.
- 28.Brown, S. R., and C. H. Scholz. (1986). Closure of rock joints. *Journal of Geophysical Research*, 91:4939–4948.
- 29.Brown, S. R., R. L. Kranz, and B. P. Bonner. (1986). Correlation between the surfaces of natural rock joints. *Geophysics Research Letter*, 13:1430–1433.
- 30.Campbell, G.D.M., (1975). Groundwater Investigation at Beaufort West, Technical Report Gh3235, Directorate: Geohydrology, Department Water Affairs & Forestry, Pretoria.
- 31.Chevallier L., Goedhart, M. and Woodford A.C. (2001). Influence of dolerite ring-structures on the occurrence of groundwater in Karoo Fractured Aquifers: a morpho-tectonic approach, Project Number K937, Water Research Commission, Pretoria.
- 32.Chevallier L. and Woodford A.C. (1999). Morpho-tectonics and mechanism of emplacement of the dolerite rings and sills of the Western Karoo, South Africa., *S.Afr.J.Geol.*, Vol. 102 (1), pp. 43-54.
- 33.Chevallier, L., (1997): Distribution and tectonics of kimberlites; a craton / off craton study from South Africa. In: N.V. Sobolev and R.H. Mitchell Eds,

- Proceedings of the sixth International Kimberlite Conference, Novosibirsk, Russia, Vol.2.
- 34.Chevallier, L. (1998): Karoo dolerites to Drakensberg basalts: structure, volcanics and seismicity. In: Melis and Duplessis consulting Engineers (eds), Review of the current stage of knowledge of the seismotectonic setting of Lesotho and its significance in predicting seismic design parameters for the Katse and Mohale Dams and further phases of the LHWP. Lesotho Highlands Water Project contract No 1028. Workshop in Maseru,. 17pp.
- 35.Cinco-Ley, H. and F. Samaniego (1981). Pressure Transient Analysis for Naturally Fractured Reservoirs. SPE 11026. Society of Petroleum Engineers of AIME. Paper presented at the 57th Annual Fall Technical Conference and Exhibition of the Society of Petroleum Engineers of AIME held in New Orleans, Luisiana, 26 – 29 September 1982.
- 36.Cinco, H., F. Samaniego, and N. Dominguez (1978). Transient pressure behaviour for a well with a finite-conductivity vertical fracture. Society of Petroleum Engrs JI, pp. 253-264.
- 37.Coetsee, D.S., (1983): The deformation style between Meirings Poort and Beaufort West. In: A.P.G. Söhnge and I.W. Hälbig (eds), Geodynamics of the Cape Fold Belt. Geol. Soc. S. Afr. Spec. Publ., No 12, 101 - 113.
- 38.Cole, D.I., Labuschagne L.S., Söhnge, Stettler E.H. and Scheinder G.I.C., (1991). Aeroradiometric survey for uranium and ground follow-up in the Main Karoo Basin.Geol. Surv., Memoir 76, 172 pp + map.
- 39.COLVIN C, LE MAITRE D and HUGHES S (2003) Assessing Terrestrial Groundwater Dependent Ecosystems in South Africa. WRC Report No. 1090-2/2/03. Water Research Commission, Pretoria, South Africa.
- 40.Cook P.G., Solomon D.K., Sanford W.E., Busenberg E., Plummer L.N. and Poreda R.J. (1996) Inferring shallow groundwater flow in saprolite and fractured rock using environmental tracers. Water Resour. Resear., 32(6):1501–1509.
- 41.Cook P.G., Herczeg A.L. and McEwan K.L (2001) Groundwater recharge and stream baseflow, Atherton Tablelands, Queensland. CSIRO Land and Water, Tech.Rep. 08/01.

42. Cook G. P. (2003). A guide line to regional groundwater in fractured rock aquifers. National Library of Australia Cataloguing. ISBN 1 74008 233 8. CSIRO Land and Water, Glen Osmond, SA, Australia
43. Cooper H.H. and C.E. Jacob (1946). A Generalized Graphical Method for Evaluating Formation Constants and Summarizing Well Field History. *Am. Geophys. Union Transactions*, Vol. 27, pp. 526 – 534.
44. Cosma, C., P. Heikkinen, and S. Pekonen. (1991). Improvement of high resolution seismics: Part I, Development of processing methods for VSP surveys; Part II, Piezoelectric signal transmitter for seismic measurements. *Stripa Project TR 91-13*. Stockholm: Swedish Nuclear Fuel and Waste Management Co.
45. Crampin, S. (1991). A decade of shear-wave splitting in the earth's crust. *Geophysical Journal International*, 107(3):387–408.
46. Dahlin, T. (2001). The development of DC resistivity imaging techniques. *Computers & Geosciences*, Volume 27:1019-1029.
47. Danie Vermeulen and Gerrit van Tonder. 2005. Groundwater borehole report at Paradys Experimental Farm, Bloemfontein. Rprt N: 2005/03/PDV (Fevrier). IGS.
48. Darcy, H. 1856. *Les fontains publiques de la ville de Dijon*. Victor Dalmont, Paris.
49. Dawson J.B. (1962). Basutoland kimberlites. *Geol. Soc. Am. Bull.*, v.73, 545 560.
50. DeGraff, J. M., and A. Aydin. (1993). Effect of thermal regime on growth increments and spacing of contraction joints in basaltic lava. *Journal of Geophysical Research*, 98:6411–6430.
51. De Lange, S.S. (1999). Environmental impact of point pollution sources. Unpublished M.Sc.thesis, University of the Free State, Bloemfontein, South Africa.
52. Delaney, P. T., D. D. Pollard, J. I. Ziony, and E. H. McKee. (1986). Field relations between dikes and joints: emplacement processes and paleostress analysis. *Journal of Geophysical Research*, 91:4920–4938.

- 53.Dey, A., W. H. Meyer, H. F. Morrison, and W. M. Dolan. (1975). Electric field response of two- dimensional inhomogeneities to unipolar and bipolar configurations. *Geophysics*, 40:615–632.
- 54.Doughty, C., Tsang, C.-F. (2000). BORE II—A code to compute dynamic wellbore electrical conductivity logs with multiple inflow/outflow points including the effects of horizontal flow across the well, Rep. LBNL-46833, Lawrence Berkeley\ National Laboratory, Berkeley, CA (available on-line at <http://www-library.lbl/docs/LBNL/468/33/PDF/LBNL-46833.pdf>).
- 55.Doughty, C., Tsang, C.-F. 2002. Inflow and outflow signatures in flowing wellbore electrical-conductivity logs, Rep. LBNL- 51468. Berkeley, CA: Lawrence Berkeley National Laboratory (available on-line at <http://www-library.lbl.gov/docs/LBNL/514/68/PDF/LBNL-51468.pdf>).
- 56.Doughty, C., Tsang, C.-F. (2004).(revised version of 2000) BORE II—A code to compute dynamic wellbore electrical conductivity logs with multiple inflow/outflow points including the effects of horizontal flow across the well, Rep. LBNL-46833, Lawrence Berkeley\ National Laboratory, Berkeley, CA (available on-line at <http://www-library.lbl/docs/LBNL/468/33/PDF/LBNL-46833.pdf>).
- 57.Doughty Christine, Shinji Takeuchi, Kenji Amano, Michito Shimo, and Chin-Fu Tsang. (2005). Application of multirate flowing fluid electric conductivity logging method to well DH-2, Tono Site, Japan. *WATER RESOURCES RESEARCH*, VOL. 41, W10401.
- 58.Doughty Christine, Barry Freifeld, Stefan Finsterle. (2006). Preliminary Estimates of Specific. Discharge and Transport Velocities near Borehole NC-EWDP-24PB. Earth Sciences Division. Lawrence Berkeley National Laboratory.
- 59.Doughty, C, C-F, Tsang, Hatanaka, K, and Yabuuchi S. (2008). Application of direct-fitting, Mass Integral, and Multirate method of analysis of flowing fluid electrical conductivity logs from Horonobe, Japan, *Water Resources Reservoirs.*, Vol 44.
- 60.Dyer, B. C., and M. H. Worthington. 1988a. Seismic reflection tomography—a case study. *First Break*, 6:354–365.

- 61.Dyer, B., and M. H. Worthington. (1988). Some sources of distortion in tomographic velocity images. *Geophysical Prospecting*, 36:209–222.
- 62.Drost W., Klotz D., Koch A., Moser H., Neumaier F. and Rauert W. (1968) Point dilution methods of investigating ground water flow by means of radioisotopes. *Water Resour, Resear.*, 4(1):125–146.
- 63.Drost, W., H. Moser, F. Neumaier, and W. Rauert. (1972). Isotope methods in ground water science. In *European atomic energy commission report EURISOTOP 61*, ser. 16, ed. P. Fritz and J.C. Fontes, 1–178. Brussels, Belgium: Bureau EURISOTOP.
- 64.Drost, W. and F. Neumaier (1974). Application of single borehole methods in groundwater research. In *Proceedings, Symposium on Isotope Techniques in Groundwater Hydrology*, Vienna, pp. 241 254.
- 65.Du Toit, A.L. (1905). Geological survey of Glen Grey and parts of Queenstown and Woodehouse, including the Indwe area. Geological Commission of the Cape of Good Hope, tenth annual report, 95-140.
- 66.Du Toit, A.L. (1920) The Karoo Dolerites- a study in Hypabyssal Intrusion. *Trans. Geol. Soc. S. Afr.*, V23, pp1-42.
- 67.Dvorkin, J., and A. Nur. 1992. Filtration fronts in pressure compliant reservoirs. *Geophysics*, 57:1089-1092.
- 68.Engelder, T. 1993. *Stress Regimes in the Lithosphere*. Princeton, N.J.: Princeton University Press, 457 pp.
- 69.Fetter, C.W. (1999). *Contaminant Hydrogeology*. Second Edition. Prentice Hall, Upper Saddle River, N.J., 500 pp.
- 70.Freeze, R.A. and J.A. Cherry (1979). *Groundwater*. Prentice-Hall, Englewood Cliffs, N.J., 604 pp.
- 71.Garotta, R. (1989). Detection of azimuthal anisotropy. Pp. 861–863 in *European Association of Exploration Geophysicists, 51st Annual Meeting Extended Abstracts*, Zeist, Holland.
- 72.Gebrekristos Robel Amine. (2007). *Site Characterisation Methodologies for DNAPLs in Fractured South African Aquifers*. PhD thesis. Promoter: Dr. B.H. Usher. Institute for Groundwater Studies at the University of the Orange Free State, Bloemfontein, South Africa.

73. Gelhar, L.W. (1986). Stochastic subsurface hydrology from theory to applications. *Water Resources Res.*, Vol. 22, No. 9, pp. 135S-145S
74. Gentier, S., and J. Ries. (1990). Quantitative description and modeling of joint morphology. Pp. 375– 382 in *Rock Joints, Proceedings of the International Symposium on Rock Joints*, Loen, Norway, W. Barton and E. Stephansson, eds. Rotterdam: A. A. Balkema.
75. Grace W. Su<sup>1</sup>, Nigel W.T. Quinn<sup>2</sup>, Paul J. Cook, and William Shipp. (2006) Miniaturization of the Flowing Fluid Electric Conductivity Logging Technique. (2006) *National Ground Water Association*. Vol. 44, No. 5—GROUND WATER—(pages 754–757).
76. Greeff, G.J. (1968): Fracture systems and the kimberlite intrusions of Griqualand West. M.Sc. Thesis, Stellenbosch Univ., 126 p.
77. Gringarten, A.C., H.J. Ramey, and R. Raghavan (1974). Unsteady-state pressure distributions created by a well with a single infinite-conductivity vertical fracture. *Society of Petroleum Engrs JI*, August, pp. 347-360.
78. Gringarten, A.C. and H.J. Ramey Jr. (1974). Unsteady-State Pressure Distribution Created by a Well with a Single Horizontal Fracture, Partial Penetration, or Restricted Entry. *Society of Petroleum Engineers of AIME. Transactions*, Vol. 257, pp. 413 – 426.
79. Hälbig, I.W. and Swart, J., (1983): Structural zoning and dynamic history of the cover rocks of the Cape Fold Belt. In: A.P.G. Söhne and I.W. Hälbig (eds), *Geodynamics of the Cape Fold Belt*. *Geol. Soc. S. Afr. Spec. Publ.*, No 12, 75 - 100.
80. Halevy, E., H. Moser, O. Zellhofer, and A. Zuber. (1967). Borehole dilution techniques: A critical review. In *Proceedings of the symposium on Isotopes in Hydrology*, 531–564. Vienna, Austria: I.A.E.A
81. Handcock, P.L. and Engelder, T., (1989): Neotectonic joints. *Soc. Am. Bull.*, V101, 1197 - 1208.
82. Hans Gehrels and Ambro S.M. Gieske. (2003). *Aquifer Dynamics*. In: Ian Simmers. *Understanding Water in a Dry Environment: Hydrological Processes in Arid and Semi-arid Zones*. IAH Int Contrib Hydrogeol 23. A.A. Balkema, Tokyo, ISBN 90 5809 618 1. pp 211-250.

- 83.Hartnady, C.J.H. and Woodford, A.C., (1996): A feasibility investigation of the relationship between near-surface neotectonic crustal stress and groundwater occurrence in a Karoo fractured-rock aquifer. Research proposal to the Water Research Commission.
- 84.Haxby, W.F. and Turcotte, D.L., (1976): Stresses induced by the addition or removal of overburden and associated thermal effects. *Geology*, 4, N03, 181-184.
- 85.Hess, A. E. (1986). Identifying hydraulically conductive fractures with a slow-velocity borehole flowmeter. *Canadian Geotechnical Journal*, 23(1):69-78.
- 86.Ingrid Dennis, J. Pretorius, G. Steyl. 2010. Effect of fracture zone on DNAPL transport and dispersion: a numerical approach. *Environ Earth Science*. DOI 10.1007/s12665-010-0468-8.
- 87.Ivansson, S. (1986). Seismic borehole tomography—theory and computational methods. *Proceedings of the Institute of Electrical and Electronic Engineers*, 74:328–338.
- 88.Johnsen, H. K. (1977). A man/computer interpretation system for resistivity soundings over a horizontally stratified earth. *Geophysical Prospecting*, 25:667–691.
- 89.Johns, R.A. and P.V. Roberts (1991). A Solute Transport Model for Channelized Flow in a Fracture. *Water Resources Res.*, Vol. 27, No. 8, pp. 1797-1808.
- 90.Kafritsas, J. (1987). Coupled flow/deformation analysis with the distinct element method. Ph.D. thesis, Massachusetts Institute of Technology, Cambridge.
- 91.Katz, A.J., Thompson, A.H., (1986). Quantitative prediction of permeability in porous rock. *Phys. Rev. B* 34 (11), 8179–8181.
- 92.Katz, A.J., Thompson, A.H., (1987). Prediction of rock electrical conductivity from mercury injection measurements. *J. Geophys. Res.* 92 (B1), 599–607.
- 93.Kazemi, H. (1969). Pressure Transient Analysis of Naturally Fractured Reservoirs with Uniform Fracture Distribution. SPE 2156A. Society of Petroleum Engineers. Paper Presented at the 43rd Annual Fall Meeting held in Houston, Texas, 29 September – 2 October 1969.

94. Kazumasa Ito, Naoto Takeno, Yoji Seki, Kazuki Naito, Yoshio Watanabe. 2006. AIST, Research Center for Deep Geological Environment. 1-1-1 Higashi Tsukuba, Ibaraki, 305-8567, Japan. PROCEEDINGS, TOUGH Symposium 2006 Lawrence Berkeley National Laboratory, Berkeley, California, May 15–17, 2006.
95. Kelly WE, Reiter PF (1984) Influence of anisotropy on relations between electrical and hydraulic properties. *J Hydrol* 74:311–321.
96. Ketola, M., and M. Puranen. (1967). Type curves for the interpretation of Slingram (horizontal loop) anomalies over tabular bodies. Report of Investigations #1. Espoo: Geological Survey of Finland.
97. Keuper BH, Wealthall GP, Smith JWN, Leharne SA. And Lerner DN., 2003. An illustrated handbook of DNAPL transport and fate in the subsurface. Environment agency R&D Publication, 133 EA, Bristol.
98. Kirchner, J and G.J. van Tonder (1995). Proposed guidelines for the execution, evaluation and interpretation of pumping tests in fractured-rock formations. *Water SA*, Vol. 21(3), South Africa.
99. Kornelius Riemann. (2002). Aquifer Parameter Estimation in fractured-Rock Aquifers using a Combination of Hydraulic and Tracer Tests. PhD, Thesis. Faculty of Natural and Agricultural Sciences, Department of Geohydrology at the University of the Free State, Bloemfontein, South Africa.
100. Kosinski WK, Kelly EW (1981) Geoelectric sounding for predicting aquifer properties. *Ground Water* 19:163–171.
101. Kruseman, G P, and N A de Ridder. Analysis and Evaluation of Pumping Test Data. Wageningen: International Institute for Land Reclamation and Improvement, 1994.
102. Lacy, L. L., and X. Smith. (1989). Fracture azimuth and geometry determinations. Pp. 357–375 in SPE Monograph 12: Recent Advances in Hydraulic Fracturing. Richardson, Tex.: Society of Petroleum Engineers.
103. Lasher Candice et al. (2009). Comparison between conventional methodology and Fluid Electrical Conductivity logging to characterize hydraulic properties of fractures rock Aquifer. 2009 Biental Groundwater Conference “Pushing the limit”. 16-18 November 2009. NH The Lord Charles Somerset West South Africa.



104. La Pointe P.R. and Hudson J.A. (1985) Characterization and interpretation of rock mass joint patterns. Geological Society of America Special Paper 199. Geological Society of America, 37pp.
105. Long, J.C.S. and P.A. Witherspoon (1985). The Relationship of the Degree of Interconnection to Permeability in Fracture Networks. J. of Geophysical Research, Vol. 90, No. B4, pp. 3087 – 3098.
106. Louis, C.L., and Y. Maini (1970), Determination of in situ hydraulic parameters in jointed rock, in: Proc. 2nd Int. Congr. Rock Mechanics, Belgrade, Inst. Dev. Water Resour., vol. I, 235-245.
107. Love A.J., Cook P.G., Harrington G.A. and Simmons C.T. (2002) Groundwater flow in the Clare Valley. Department for Water Resources, South Australia. Report DWR02.03.0002, 43pp.
108. Magnusson, K. A., S. Carlsten, and O. Olsson. (1987). Crosshole investigations—physical properties of core samples from boreholes F1 and F2. Stripa Project IR 87-10. Stockholm: Swedish Nuclear Fuel and Waste Management Company (SKB).
109. Majer, E. L., R. H. Chapman, W. D. Stanley, and B. D. Rodriguez. (1992). Monograph on The Geysers Geothermal Field, Special Report 17, Geothermal Resources Council, Davis, Calif.
110. Maske S., (1966): The petrography of the Ingeli Mountain Range. Annale Universiteit van Stellenbosch, Vol. 41, 108 pp.
111. Meyer, R. en van Zijl, J.S.V., (1980): Die ontwikkeling en evaluasie van tegnieke vir die bepaling van die ontginningspotensiaal van grondwaterbronne in die Doornberg-breuksone. Finale verslag Deel 2(b): Venterstad-omgewing - Geofisiese studies. Water Research Commission Project K5/28.
112. Michalsky A., G.D. Klepp. (1989). Characterization of transmissive fracture by simple tracing of internal flow in well. Manuscript submitted to groundwater.
113. Milan Radulović, Dragan Radojević, Neda Dević, Milica Blečić. (2008). Discharge Calculation of Spring Using Salt Dilution Method- Application Site BOLJE SESTRE SPRING (MONTENEGRO). BALWOIS 2008-Orhid, Republic of Macedonia.

114. Miller, S. M., P. C. McWilliams, and J. C. Kerkerling. (1990). Ambiguities in estimating fractal dimensions of rock fracture. Pp. 471–478 in *Rock Mechanics Contributions and Challenges, Proceedings of the 31th U.S. Symposium on Rock Mechanics*, W. A. Hustrulid and G. A. Johnson, eds. Rotterdam: A. A. Balkema.
115. Miroslav Kobr, Stanislav Mares and Frederick Paillet. 2005. *Borehole Geophysics for Hydrogeological studies: Principles and applications*. Y. Rubin and S. S. Hubbard (eds.), *Hydrogeophysics*, 291–331. © 2005 Springer. Printed in the Netherlands.
116. M. Pitrak, S.Mares, and M. Kobr. (2007). A Simple Borehole Dilution Technique in Measuring Horizontal Ground Water Flow. No. 1 GROUND WATER-Vol. 45, (pages 89–92).
117. Modreck Gomo. (2009). *Site Characterisation of LNAPL – Contaminated Fractured - Rock Aquifer*. M.Sc. Institute for Groundwater Studies. Faculty of Natural- and Agricultural Sciences. University of the Free State.
118. Moench, A.F. (1984). Double-Porosity Models for a Fissured Groundwater Reservoir with Fracture Skin. *Water Resources Res.*, Vol. 20, No. 7, pp. 831 – 846.
119. Mohr Samuel and van Biljon Willem. (2009). The application of fluid electrical conductivity profiling and discrete level low flow sampling in the refinement of a site conceptual model for an LNAPL affected fractured rock aquifer. 2009 Bional Groundwater Conference “Pushing the limit”. 16-18 November 2009. NH The Lord Charles Somerset West South Africa.
120. Molz, F. J., and S. C. Young. (1993). Development and application of borehole flowmeters forenvironmental assessment. *The Log Analyst*, 34(1):13–23.
121. Momii, K., K. Jinno, and F. Herein. (1993). Laboratory studies on a new LDV system for horizontal groundwater velocity measurement in a borehole. *Water Resources Research*, 29:283–291.
122. Morris, B. L, Lawrence, A. R. L, Chilton, P. J. C, Adams, B, Calow, R. C. and Klinck, B. A. (2003) *Groundwater and its Susceptibility to Degradation: A Global Assessment of the Problem and Options for Management*. Early Warning and

- Assessment. Report Series, RS. 03-3. United Nations Environment Programme, Nairobi, Kenya.
123. National Research Council Committee on Fracture Characterization and Fluid Flow, 1996. Rock fractures and fluid flow: contemporary understanding and applications, National Academy Press, Washington, DC.
124. Newton, A.R., (1993): Thrusting on the northern margin of the Cape Fold Belt, near Laingsburg. *S.Afr.J.Geol.*, 96 (1/2), 22 - 30.
125. Nixon P.H., Boyd F.R. and Boctor N.Z. (1983) East Griqualand kimberlites. *Trans. Geol. Soc. S. Afr.*, 86, 221 - 236.
126. Nixon P.H. and Kresten P. (1973) Butha-Buthe swarm and associated kimberlite blows. In: P.H. Nixon Ed., *Lesotho kimberlites*. Lesotho National Development Corporation. 197 - 206.
127. Nordqvist, A.W., Y.W. Tsang, C-Fu Tsang, B. Dverstorp, and J. Andersson (1996). Effects of high variance of fracture transmissivity on transport and sorption at different scales in a discrete model for fractured rocks. *Journal of Contaminant Hydrology* 22, pp. 39-66.
128. Norman J.L., Price N.J. and Petres E.R. (1977) Photogeological fracture trace study of controls of kimberlite intrusion in Lesotho basalts. *Mining and Metallurgy*, May 1977, 78 - 90.
129. Novakowski, K. S., and P. A. Lapcevic. (1994). Field measurements of radial solute transport in fractured rock. *Water Resources Research*, 30(1):37-44.
130. Andreoli M.A.G., Doucouré M., Van Bever Donker J., Brandt D. And Andersen N.J.B. (1996): Neotectonics of Southern Africa - A review. *Africa Geoscience Review*, Vo.3, No1, 1-16.
131. Olsson, O., P. Anderson, and E. Gustafsson. (1991). Site characterization and validation—monitoring of saline tracer transport by borehole radar measurements. Final report, Stripa Project TR 91-18. Stockholm: Swedish Nuclear Fuel and Waste Management Co.
132. Olsson, O., ed. (1992). Site characterization and validation. Final report, Stripa Project, TR 92-22. Stockholm: Swedish Nuclear Fuel and Waste Management Co.

133. Paillet, F. L. (1991a). Use of geophysical well logs in evaluating crystalline rocks for siting of radioactive waste repositories. *The Log Analyst*, 33(2):85–107.
134. Patten, E.P., and G.B. Bennet. (1962). Methods of flow measurements in well bores. U.S. Geol. Surveys water supply paper 1544-C. US. Gov. Printing Office, Washington D.C., pp D40-D45.
135. Paterson, M. S. (1983). The equivalent channel model for permeability and resistivity in fluid- saturated rocks—a reappraisal. *Mechanics and Materials*, 2(4):345–352.
136. Patterson, M. S. (1958). Experimental deformation and faulting in Wombeyan marble. *Geological Society of America Bulletin*, 69:465–476.
137. Prem V. Sharrma, (1997). *Environmental and engineering geophysics*, Press Syndicate of the University of Cambridge, Cambridge University Press, Cambridge, United Kingdom.
138. Pedler, W.H., C.L. Head, and L.L. Williams, *Hydrophysical logging: A new wellbore technology for hydrogeologic and contaminant characterization of aquifers*, National Outdoor Action Conference, National Ground Water Association, Las Vegas, Nevada, 1992.
139. Perkins, T. K., and J. A. Gonzalez. (1985). The effect of thermoelastic stresses on injection well fracturing. *Society of Petroleum Engineers Journal*, Feb., pp. 78–88
140. Pyrak-Nolte, L.J., and J.P. Morris (2000), Single fractures under normal stress: The relation between fracture specific stiffness and fluid flow, *Int. J. Rock. Mech. Min. Sci.*, 37:245-262.
141. Olsson, O., L. Falk, O. Forslund, L. Lundmark, and E. Sandberg. (1992). Borehole radar applied to the characterization of hydraulically conductive fracture zones in crystalline rock. *Geophysical Prospecting*, 40:109–142.
142. Raghavan, R., J. D. T. Scorer, and F. G. Miller. (1972). An investigation by numerical methods of the effect of pressure-dependent rock and fluid properties on well flow tests. *Society of Petroleum Engineers Journal*, 12:267–275.

143. Richard Ayuk II Akoachere and Gerrit van Tonder. (2009). Two new methods for the determination of hydraulic fracture apertures in fractured-rock aquifers. Revised version. Water SA Vol. 35 No. 3 April 2009. ISSN 0378-4738. ISSN 1816-7950: Water SA (on-line). Available on website <http://www.wrc.org.za>.
144. Robain, H., Descloitres, M., Ritz, M. and Atangana, Q.Y. (1996). A multiscale electrical survey of a lateritic soil system in the rain forest of Cameroon. In: Samoueliana, A., Cousina, I., Tabbaghc, A., Bruandd, A. and Richarde G. 2005. Electrical resistivity survey in soil science: a review. Soil & Tillage Research 83:173–193.
145. Roberts, R.M., R.L. Beauheim, and J.D. Avis (2001). nSIGHTS (n-dimensional Statistical Inverse Graphical Hydraulic Test Simulator), software for hydraulic test interpretation in low permeable aquifers. Unpublished beta-version. Sandia National Laboratory, Albuquerque.
146. Rogers, A.W. and Du Toit A.L. (1903). Geological Survey of parts of the divisions of Ceres, Sutherland and Calvinia. Ann. Report of Cape Geol. Comm., 36-43.
147. Rowsell, D.M. and de Swart, A.M.J., (1976): Diagenesis in Cape and Karoo sediments, South Africa and its bearing on their hydrocarbon potential. Trans. geol. Soc. S. Afr., pp81-145.
148. Sami, K, I Neumann, D Gqiba, G de Kock, and G Grantham. Groundwater Exploration In Geologically Complex And Problematic Terrain - Guidelines (Volume 1). WRC Report No.966/1/02, Pretoria: Water Research Commision, 2002.
149. Sandberg, E. V., O. L. Olsson, and L. R. Falk. (1991). Combined interpretation of fracture zones in crystalline rock using single-hole, cross-hole tomography and directional borehole-radar data. The Log Analyst, 32(2):108–119.
150. Sebastien Lamontagne, John Dighton, and William Ullman.(2002). Estimation of groundwater velocity in riparian zones using point dilution test. CSIRO Land and Water. Technical Report 14/02. May 2002.

151. Sen, P. N., C. Scala, and M. H. Cohen. (1981). A self-similar model for sedimentary rocks with application to the dielectric constant of fused glass beads. *Geophysics*, 46:781–795.
152. Shapiro, A. M., and P. A. Hsieh. (1994). Overview of research at the Mirror Lake site: use of hydrologic, geophysical and geochemical methods to characterize flow and transport in fractured rock. In U.S. Geological Survey Toxic Substances Hydrology Program— Proceedings of the Technical Meeting, Colorado Springs, Colorado, September 20-24, 1993, D.W. Morganwalp and D.A. eds. USGS Water Resources Investigation Report 94-4015, U.S. Geological Survey, Reston, Va.
153. Shapiro, A.M. (2001). Effective matrix diffusion in kilometer-scale transport in fractured crystalline rock. *Water Resources Res.*, Vol. 37, No. 3, pp. 507-522.
154. Shedlovsky, T., and L. Shedlovsky. (1971). Conductometry, technique of chemistry, in *Physical Methods of Chemistry*, IIa, Electrochemical method, vol. 1, edited by A. Weissberger and B.W. Rossiter, pp. 164-171, John Wiley, New York.
155. Schlumberger, Ltd, (1984). Log interpretation charts, New York.
156. Singhal B.B.S. and Gupta R.P. (1999) *Applied Hydrogeology of Fractured Rocks*. Kluwer, Dordrecht, 400pp.
157. Sihvola, A. H. (1989). Self-consistency aspects of dielectric mixing theories. *IEEE Transactions on Geoscience and Remote Sensing*, 27:403–415.
158. Simandoux, P. (1963). Mesures dielectrique en milieux poreux, application a mesure des saturations en eaux, etude du comportement des massifs argileux. *Rev. de l'institut Francais du Petrole*, (Suppl.).
159. SINGHAL BBS and GUPTA RP (1999) *Applied Hydrogeology of Fractured Rocks*. Kluwer, Dordrecht. 400 pp.
160. Snow, D.T. (1965), A parallel plate model of fractured permeable media, PhD Thesis, University of California, Berkeley.
161. STEELE A, REYNOLDS DA, KUEPER BH and LERNER DN (2006) Field determination of mechanical apertures, entry pressure and relative permeability of fractures using NAPL injection. *Geotech.* 56 (1) 27-38.

162. Stear, W.M., (1980): Sedimentary environment of the Beaufort West Group uranium province in the vicinity of Beaufort West, South Africa. PhD thesis, Univ. Port Elizabeth (unpubl.).
163. Suppe, J. (1985). *Principals of Structural Geology*. Englewood Cliffs, N.J.: Prentice-Hall, p. 537.
164. Swan, G. (1981). Tribology and the characterization of rock joints. Pp. 402–407 in *Proceedings of the 22nd U.S. Symposium on Rock Mechanics*. Cambridge: Massachusetts Institute of Technology.
165. Theis, C.V. (1935). The Relation Between the Lowering of the Piezometric Surface and the Rate and Duration of Discharge of a Well Using Ground-Water Storage. *American Geophysical Union, Transactions. Reports and Papers, Hydrology – 1935*.
166. Thomas, T. R. (1982). *Rough Surfaces*. New York: Longman.
167. Tsang C.F., and C. Doughty, Detailed validation of a liquid and heat flow code against field performance, paper presented at the Eighth SPE Symposium on Reservoir Simulation, Soc. of Petrol. Eng., Dallas, Tex., Feb. 10-13, 1985.
168. Tsang, C. F. (1985) Lessons learned in the verification and validation studies of a coupled heat and fluid flow code, paper presented at the Symposium on Groundwater Flow and Transport Modeling for Performance Assessment of Deep Geologic Disposal of Radioactive Waste: A Critical Evaluation of the State of the Art. Albuquerque, New Mexico.
169. Tsang, Y. W., and C. F. Tsang. (1987). Channel model of flow through fractured media. *Water Resources Research*, 23(3):467–479.
170. Tsang C.F. and F. V. Hale. (1988). A code to compute borehole fluid conductivity profiles with multiples feed points. LBL-24928. Lawrence Berkeley Laboratory, Berkeley.
171. Tsang, Y. W., and C. F. Tsang. (1989). Flow channeling in a single fracture as a two-dimensional, strongly heterogeneous permeable medium. *Water Resources Research*, 25(9):2076–2080.
172. Tsang C.F., Hufschmied P. and Hale F.V. (1990) Determination of fracture inflow parameters with a borehole fluid conductivity logging method. *Water Resour. Resear.*, 26(4):561–578.

173. Tsang, Y.W., 1992. Usage of "equivalent apertures" for rock fractures as derived from hydraulic and tracer tests. *Water Resources Research*. Vol 28, n 5, pp 1451-1455.
174. Tsang, C.-F., Doughty, C., (2003). Multi-rate flowing fluid electric conductivity logging method. *Water Resour. Res.* 39 (12), 1354.10.1029/2003WR002308.
175. UN, 2006: World Water Development Report 2: Water, a Shared Responsibility. UNESCO, Paris, 601 pp.
176. Van der Kamp G. (1992) Evaluating the effects of fractures on solute transport through fractured clayey aquitards. *Proc. 1992 Conf. of the International Association of Hydrogeologists, Canadian National Chapter, Hamilton, Ontario.*
177. Van der Voort (2001). Risk based decision tool for managing and protecting groundwater resources. Ph.D. Thesis, University of the Free State, Institute for Groundwater Studies, Bloemfontein, S.A.
178. Vandoolaeghe, M.A.C., (1979): Middelburg geohydrological investigation., Unpublished Technical Report GH3072, Directorate:Geohydrology, Department of Water Affairs, Cape Town.
179. Vandoolaeghe, M.A.C., (1980): Queenstown geohydrological investigation., Unpublished Technical Report GH3135, Directorate:Geohydrology, Department of Water Affairs, Cape Town.
180. Van Tonder, G.J., I. Bardenhagen, K. Riemann, J. van Bosch, P. Dzanga, and Y. Xu (2001). Manual on Pumping Test Analysis in fractured-Rock Aquifers. Final Report, WRC Project, Pretoria
181. Van Tonder, G, I Bardernhagen, K Riemann, J van Bosch, P Dzanga, and Y Xu. Manual on Pumping Test Analysis in Fractured-rock Aquifers. Pretoria: Water Research Commision Report No. 1116/1/02, 2002.
182. Van Wyk, W.L., (1963): Groundwater studies in northern natal, zuland and surrounding areas, Memoir 52, Geological Survey of South Africa, pp133.
183. Verwey, J. P., and Botha, J. F. (1992). A Comparative Study of Two and Three-Dimensional Groundwater Models. WRC Reports N 271/1/92. Water Research Commission, P.O. Box 824, Pretoria 0001.



184. Verweiji, H.J.M. and J.A. Barker (1999). Well Hydraulics and Yield Analysis In Water Resources of hard rock aquifers in arid and semi-arid zones. UNESCO Publication 58, Edited by J.W. Lloyd, Paris.
185. Voss, C. F., and L. R. Shotwell. (1990). An investigation of the mechanical and hydraulic behavior of tuff fractures under saturated conditions. Pp. 825–834 in High-Level Radioactive Waste Management. La Grange Park, Ill.: American Nuclear Society.
186. Wall, J., A. Nur, and J. Dvorkin. (1991). A slug test method in reservoirs with pressure sensitive permeability. Pp. 95–105 in Proceedings of the 1991 Coalbed Methane Symposium, May 13-16, University of Alabama, Tuscaloosa.
187. Walsh, J.B., Brace, W.F., (1984). The effect of pressure on porosity and the transport properties of rock. J. Geophys. Res. 89 (B11), 9425–9431.
188. Ward, S. H. (1990). Resistivity and induced polarization methods. Pp. 147–189 in Geotechnical and Environmental Geophysics, vol. 1, S. H. Ward, ed. Tulsa, Okla.: Society of Exploration Geophysicists.
189. Warren, J.E. and P.J. Root (1963). The behavior of naturally fractured reservoirs. Society of Petroleum Engrs JI, Vol. 3, pp. 245-255.
190. Warpinski, N. R. (1991). Hydraulic fracturing in tight, fissured media. Journal of Petroleum Technology, Feb., p. 146.
191. Waxman, M. H., and L. J. M. Smits. (1968). Electrical conductivities of oil-bearing shaley sands. Transactions of the Society of Petroleum Engineers, 243:107–115.
192. Weaver JMC, Talma AS, Cave' LC (1999) Geochemistry and isotopes for resource evaluation in the fractured rock aquifers of the table mountain group, Water Research Commission, South Africa.WRC Report No. 1999 481/1/99
193. Wei, L., J. Hadwin, E. Chaput, K. Rawnsley, and P. Swaby (1998). Discriminating Fracture Patterns in Fractures Reservoirs by Pressure Transient Tests. SPE 49233. Society of Petroleum Engineers. Paper presented at the 1998 SPE Annual Technical Conference and Exhibition held in New Orleans, Luisiana, 27 – 30 September 1998.
194. Welty, D., and L. W. Gelhar. (1989). Evaluation of longitudinal dispersivity from tracer test data. Report 320, Ralph M. Parsons Laboratory for Water

- Resources and Hydrodynamics, Massachusetts Institute of Technology, Cambridge.
195. Willis, H. A., G. L. Rethford, and E. Bielouski. (1986). Azimuthal anisotropy: occurrence and effect on shear-wave data quality. Pp. 470–481 in Society of Exploration Geophysicists (SEG) Convention Expanded Abstracts. Tulsa, Okla.: Society of Exploration Geophysicists.
196. Wyllie, M.R.J., Rose, W.D., (1950). Some theoretical considerations related to the quantitative evaluation of the physical characteristics of reservoir rock from electrical log data. Trans. Am. Inst. Mech. Eng. 189, 105–118.
197. Yadav GS, Abolfazli H (1998) Geoelectric soundings and their relationship to hydraulic parameters in semi arid regions of Jalore Northwestern India. J Appl Geophys 39:35–51.
198. Zhou, W., Beck, B.F. and Adams, A.L. (2002). Effective electrode array in mapping karst hazards in electrical resistivity tomography. Environmental Geology (2002) 42:922–928.
199. Zhou, Q.Y., Shimada, J. and Sato, A. (2001). Three-dimensional spatial and temporal monitoring of soil water content using electrical resistivity tomography. In: Samoueliana, A., Cousina, I., Tabbaghc, A., Bruandd, A. and Richarde G. 2005. Electrical resistivity survey in soil science: a review. Soil & Tillage Research 83:173–193.

**APPENDIXES**

## APPENDIX A

## Magnetic survey at Paradys farm

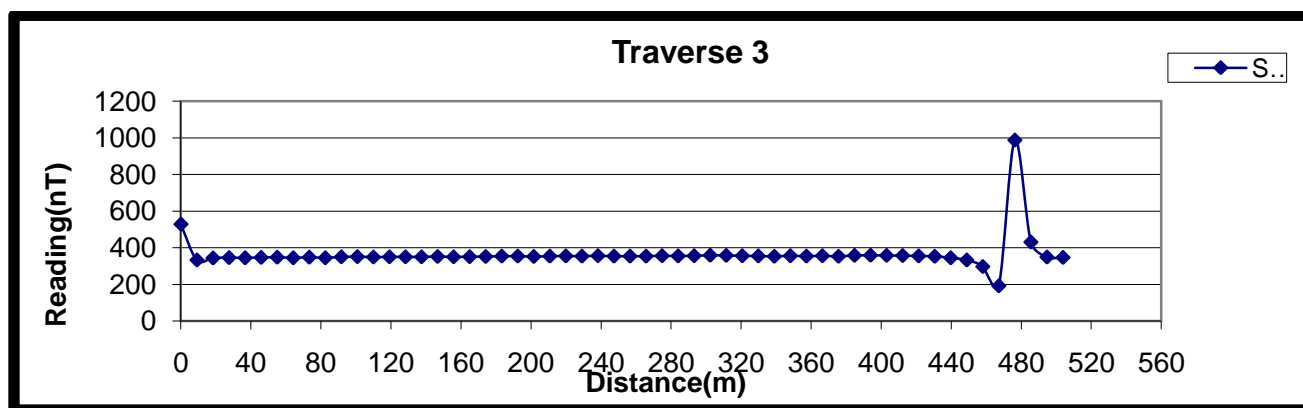


Figure 0-1PD17- Magnetic survey at Paradys (traverse 3)

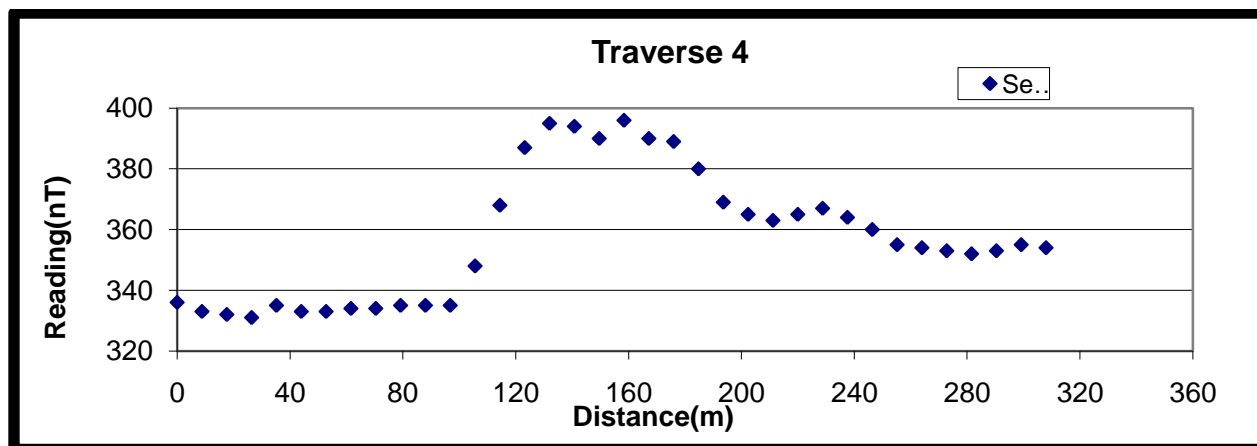
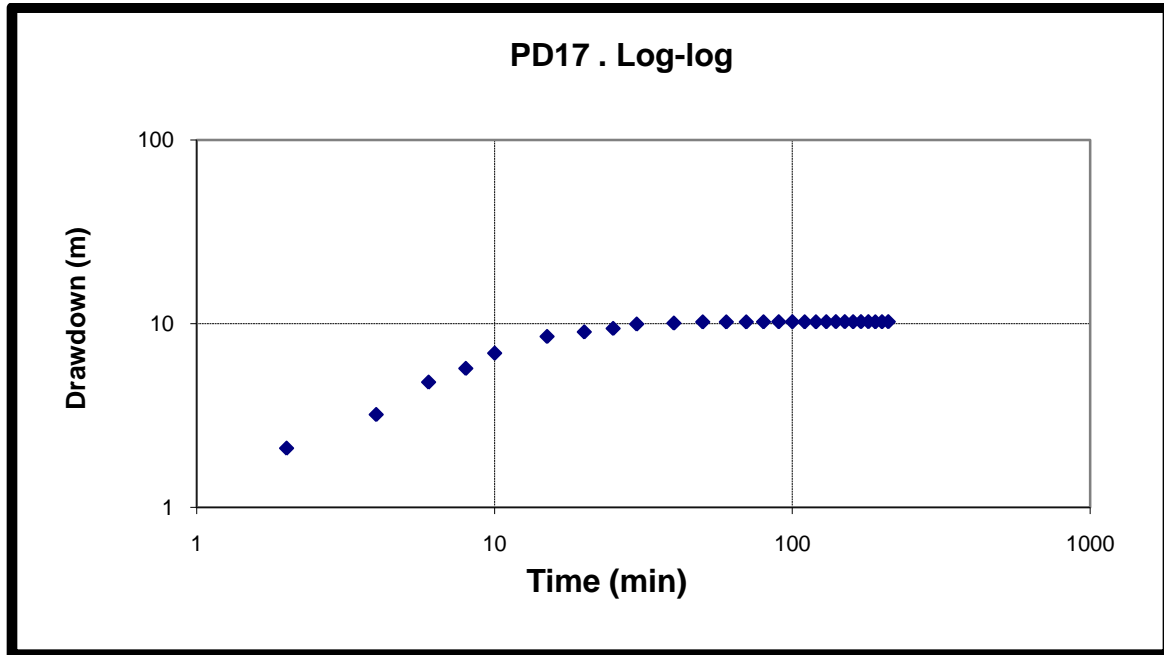
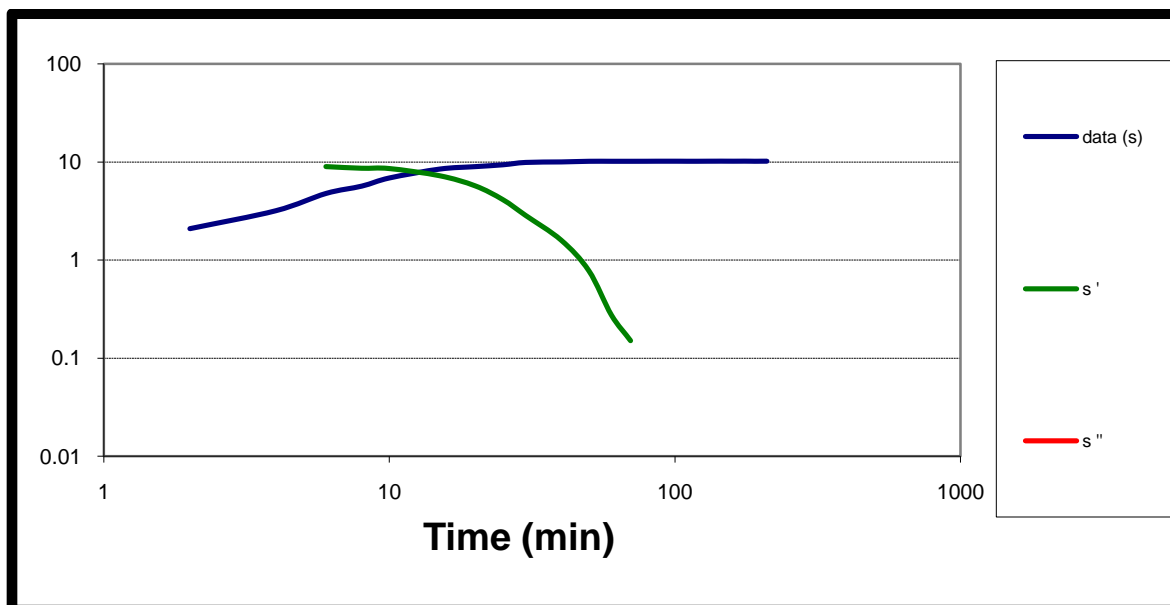


Figure 0-2PD17- Magnetic survey at Paradys (traverse 4)

## APPENDIX B

## Constant rate Pumping test at Paradys farm

Figure 0-3PD17-Constant pumping (5.5L/S) test result on **Log-log**Figure 0-4PD17-Constant pumping (5.5L/S) test result on **Derivative plot ( $S'$ )**

## APPENDIX C

Semi-quantitative estimated ground water velocity into PD17 under different conditions

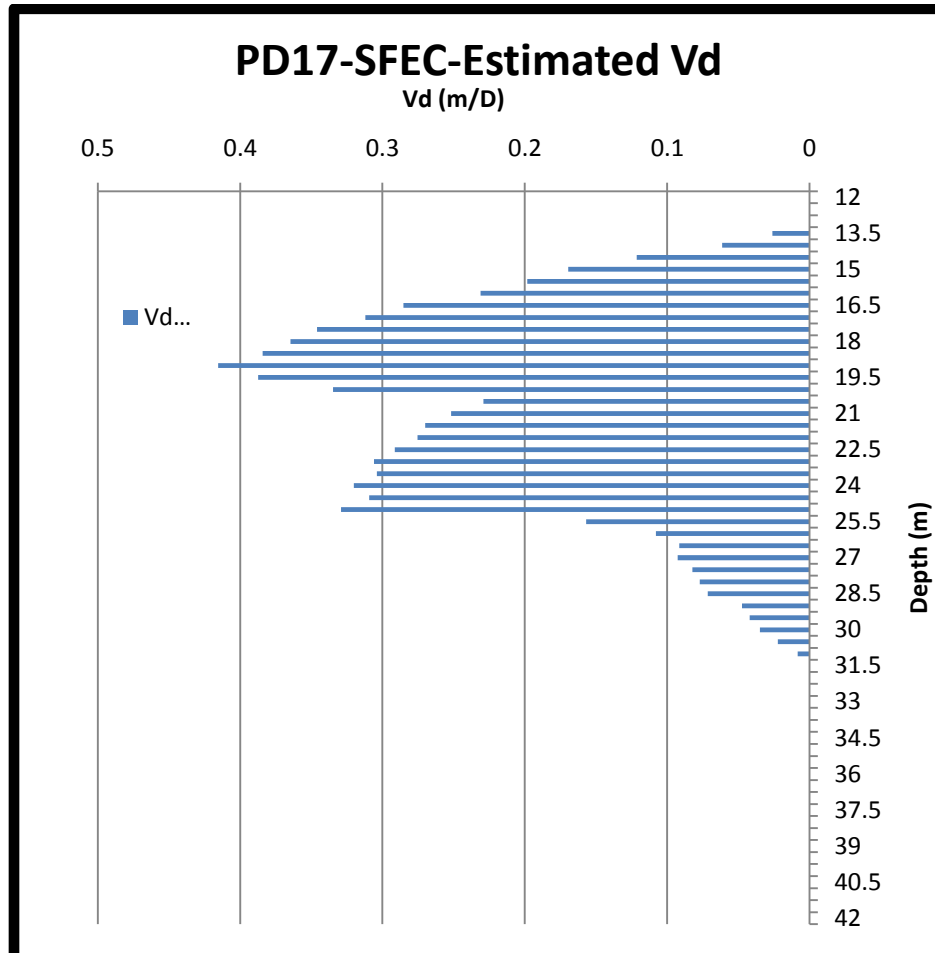


Figure 0-5 Estimated groundwater velocity along the PD17 in ambient condition, applying Drostian analytical solution. (Paradys farm, Bloemfontein)

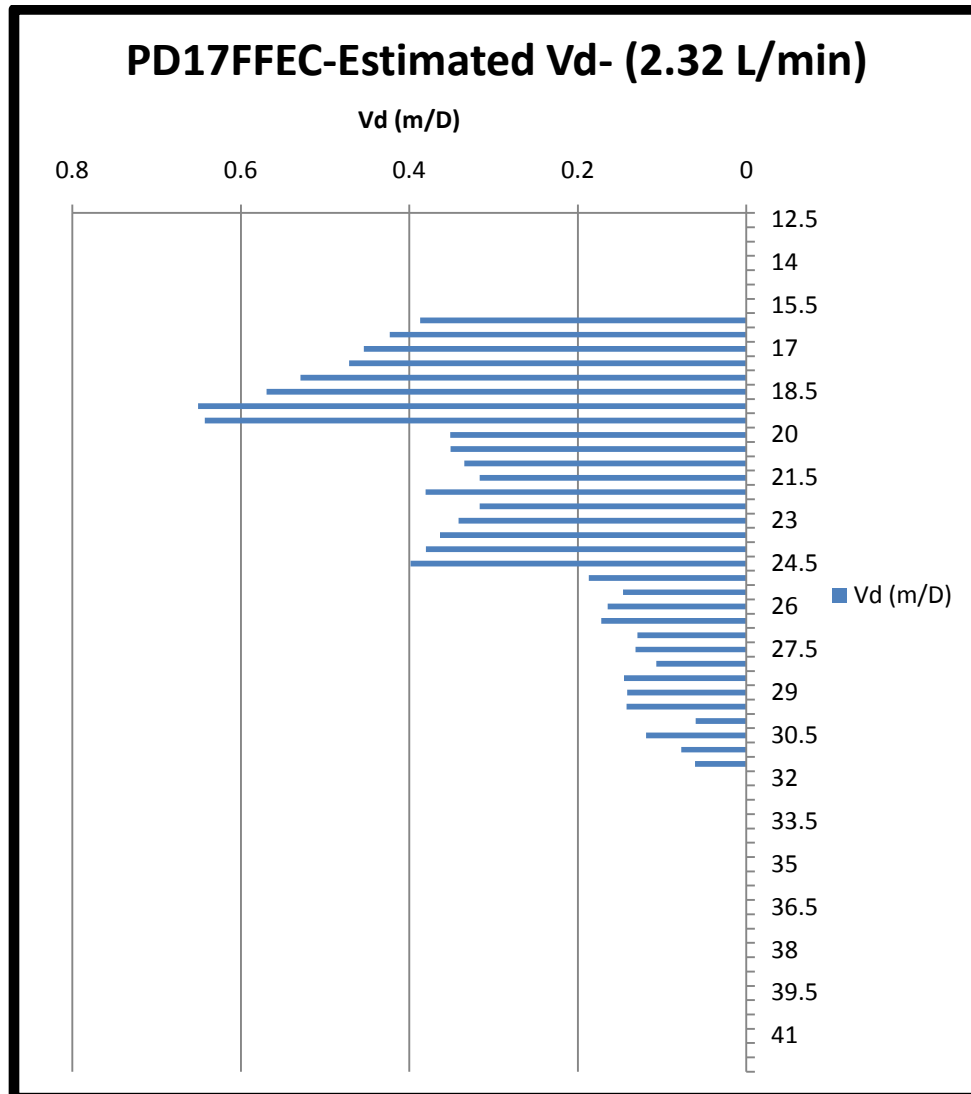


Figure 0-6 Estimated groundwater velocity along PD 17 at 2.32 L/min of pumping, applying Drostian analytical solution. (Paradys farm, Bloemfontein)

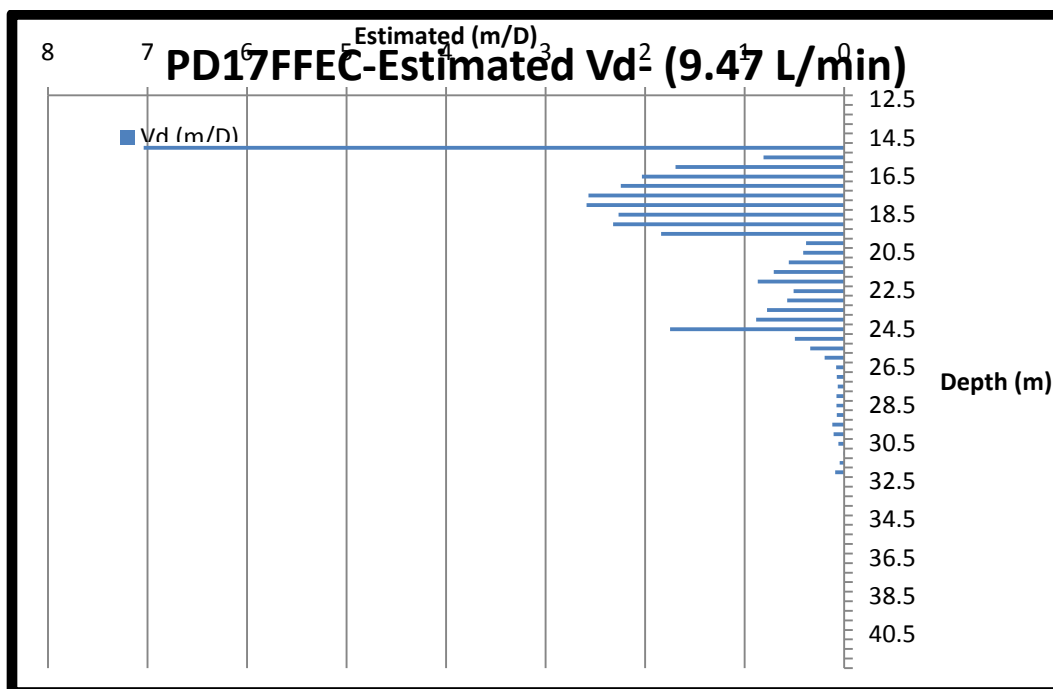


Figure 0-7 Estimated groundwater velocity along PD 17 at 9.47 L/min of pumping, applying Drostian analytical solution. (Paradys farm, Bloemfontein)

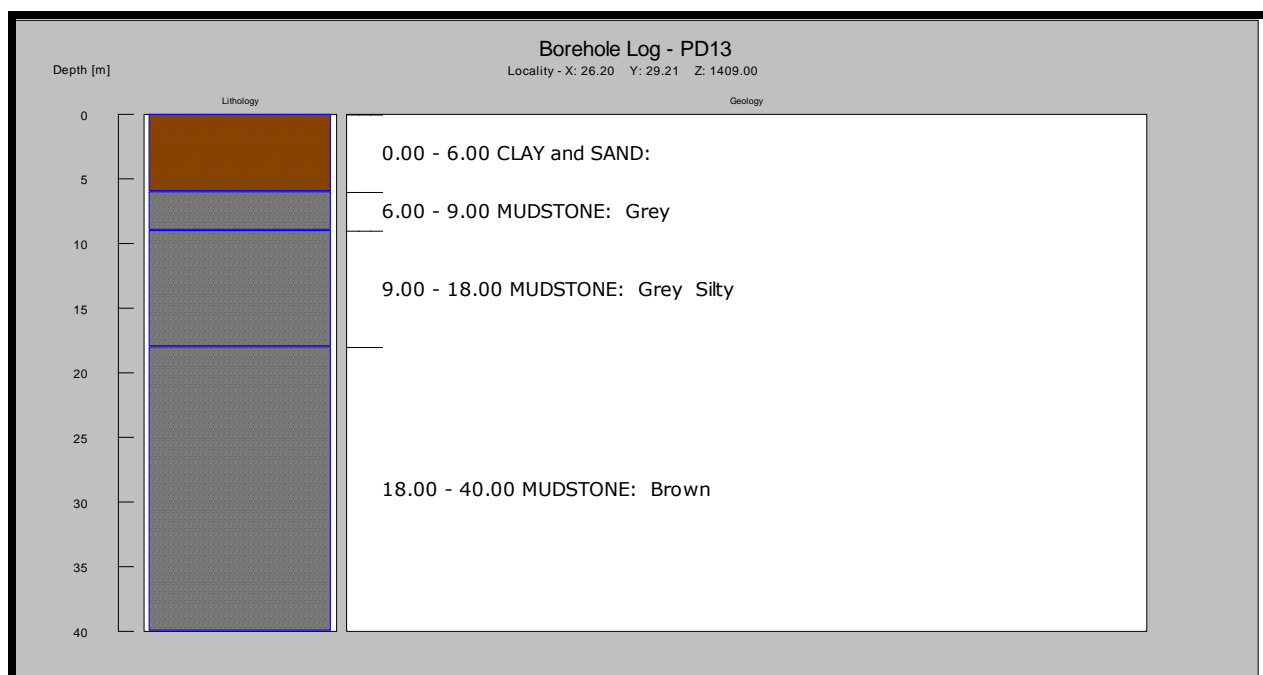


Figure 0-8 PD13 Borehole log

## APPENDIX D

## BORE II attempts on OU7 and UP15

```

XMIN(m)      XMAX(m)      DIAM(cm)      iBORn
11.00         38.50         16.50         49
QW(L/min)     HALPHA       !QW=flow from below; HALPHA=hor. flow constriction
.0000         2.500
#FEED_PTS     VARIABLE_FLOWRATE_IDENTIFIER
3             999
DEPTH(m)      Q(L/min)      C(g/L)         T0(hr)         Q/V_FLAG      !vd(m/day)
16.0          -000.10        0.0500         .0000         0
22.0          000.40         0.0500         .0000         1
22.0          -000.40        0.0500         .0000         1
TMAX(hr)      FECMAX        DIFFUSION_COEF.(m2/s)
25            500.0          1E-05
RGAMMA         RBETA         RALPHA         !FEC = RGAMMA + C*RBETA + C*C*RALPHA
.0000          1.000         .1000E-07
IC0FLAG        !If 0, c0=0; If <0, read one C0; If >0,read IC0FLAG (X,C0) pairs
49
X(m)           C0(g/L)              !#entries is IC0FLAG
11             338.6
11.5           317.8
12             297
12.5           284.95
13             272.9
13.5           264.95
14             257
14.5           255.9
15             254.8
15.5           254
16             253.2
16.5           251.65
17             250.1
17.5           251.25
18             252.4
18.5           252.85
19             253.3
19.5           253.05
20             252.8
20.5           249.1
21             245.4
21.5           244.95
22             244.5
22.5           278.5
23             312.5
23.5           348.2
24             383.9
24.5           406.45
25             429
25.5           433
26             437

```

Figure 0-9 Example of BORE II input file set up for UO7



	A	B	C	D	E	F	G	H	I
1	YM	data	u07.txt						
2	FEC	has	been	corrected	for	temp			
3	Depth	in	m	FEC	in	micro	Siemens	per	cm
4	line	4							
5	line	5							
6	line	6							
7	line	7							
8	line	8							
9	11	338.6	20	0	0	0	0	0	
10	11.5	317.8	20	0	0	0	0	0	
11	12	297	20	0	0	0	0	0	
12	12.5	284.95	20	0	0	0	0	0	
13	13	272.9	20	0	0	0	0	0	
14	13.5	264.95	20	0	0	0	0	0	
15	14	257	20	0	0	0	0	0	1
16	14.5	255.9	20	0	0	0	0	0	1
17	15	254.8	20	0	0	0	0	0	1
18	15.5	254	20	0	0	0	0	0	1
19	16	253.2	20	0	0.001	0	0	0	1
20	16.5	251.65	20	0	0.001	0	0	0	2
21	17	250.1	20	0	0.001	0	0	0	2
22	17.5	251.25	20	0	0.001	0	0	0	2
23	18	252.4	20	0	0.001	0	0	0	2
24	18.5	252.85	20	0	0.001	0	0	0	2
25	19	253.3	20	0	0.001	0	0	0	3
26	19.5	253.05	20	0	0.001	0	0	0	3
27	20	252.8	20	0	0.001	0	0	0	3
28	20.5	249.1	20	0	0.001	0	0	0	3
29	21	245.4	20	0	0.001	0	0	0	3

Figure 0-10 Example of BORE II data file set up for U07

```

!FEED sample type: 1=flow from below; 2=horizontal flow; 3=variable flow
XMIN(m)      XMAX(m)      DIAM(cm)      iBORN
15.00      45.50      16.50      62
QW(L/min)    HALPHA      !QW=flow from below; HALPHA=hor. flow constriction
0.00      2.5
#FEED_PTS    VARIABLE_FLOWRATE_IDENTIFIER
2          999
DEPTH(m)     Q (L/min)     C(g/L)      T0(hr)      Q/V_FLAG
19.0      .060      0.36      .0000      0 !1st 2 feed pts-hor. flow
24.0      .013      0.36      .0000      0 !final feed pt
TMAX(hr)    FECMAX      DIFFUSION_COEF.(m2/s)
25.000      500.      5E-05
RGAMMA      RBETA      RALPHA      !FEC = RGAMMA + C*RBETA + C*C*RALPHA
.0000      1.000      .1000E-07      !default values will be used
IC0FLAG      !If 0, C0=0; If <0, read one C0; If >0, read IC0FLAG (X,C0) pairs
62
X(m)      C0(g/L)      !#entries is IC0FLAG
15      224.6
15.5      224.4
16      224.5
16.5      222.5
17      228.2
17.5      229.6
18      239.6
18.5      236
19      237.2
19.5      284.5
20      309
20.5      326
21      337.6
21.5      322.2
22      292.4
22.5      268
23      246
23.5      218.5
24      214.2
24.5      212.6
25      209.8
25.5      212.1
26      214.5
26.5      214.5
27      215.1
27.5      215.3
28      215.3
28.5      215.6
29      215.3
29.5      214.8
30      214.8

```

Figure 0-11 Example of BORE II input file set up for UP15

A1		YM							
	A	B	C	D	E	F	G	H	I
1	YM	data	UP15.txt						
2	FEC	has	been	corrected	for	temp			
3	Depth	in	m	FEC	in	micro	Siemens	per	cm
4	line	4							
5	line	5							
6	line	6							
7	line	7							
8	line	8							
9	12.5	253.2	20	0.017	0.017	0	1	0	
10	13.5	226.2	20	0.017	0.017	0	1	1	
11	14.5	227	20	0.017	0.018	0	1	3	
12	15.5	224.4	20	0.017	0.018	0	1	5	
13	16	224.5	20	0.017	0.019	0	1	6	
14	16.5	222.5	20	0.017	0.019	0	1	7	
15	17	228.2	20	0.017	0.019	0	1	8	
16	17.5	229.6	20	0.017	0.019	0	1	9	
17	18	239.6	20	0.017	0.02	0	1	10	
18	18.5	236	20	0.017	0.02	0	1	11	
19	19	237.2	20	0.017	0.02	0	1	12	
20	19.5	284.5	20	0.017	0.02	0	1	13	
21	20	309	20	0.017	0.021	0	1	14	
22	20.5	326	20	0.017	0.021	0	1	15	
23	21	337.6	20	0.017	0.021	0	1	16	
24	21.5	322.2	20	0.017	0.022	0	1	17	
25	22	292.4	20	0.017	0.022	0	1	18	
26	22.5	268	20	0.017	0.022	0	1	19	
27	23	246	20	0.017	0.022	0	1	20	
28	23.5	218.5	20	0.017	0.023	0	1	21	
29	24	214.2	20	0.017	0.023	0	1	22	

Figure 0-12 Example of BORE II data file set up for UP15

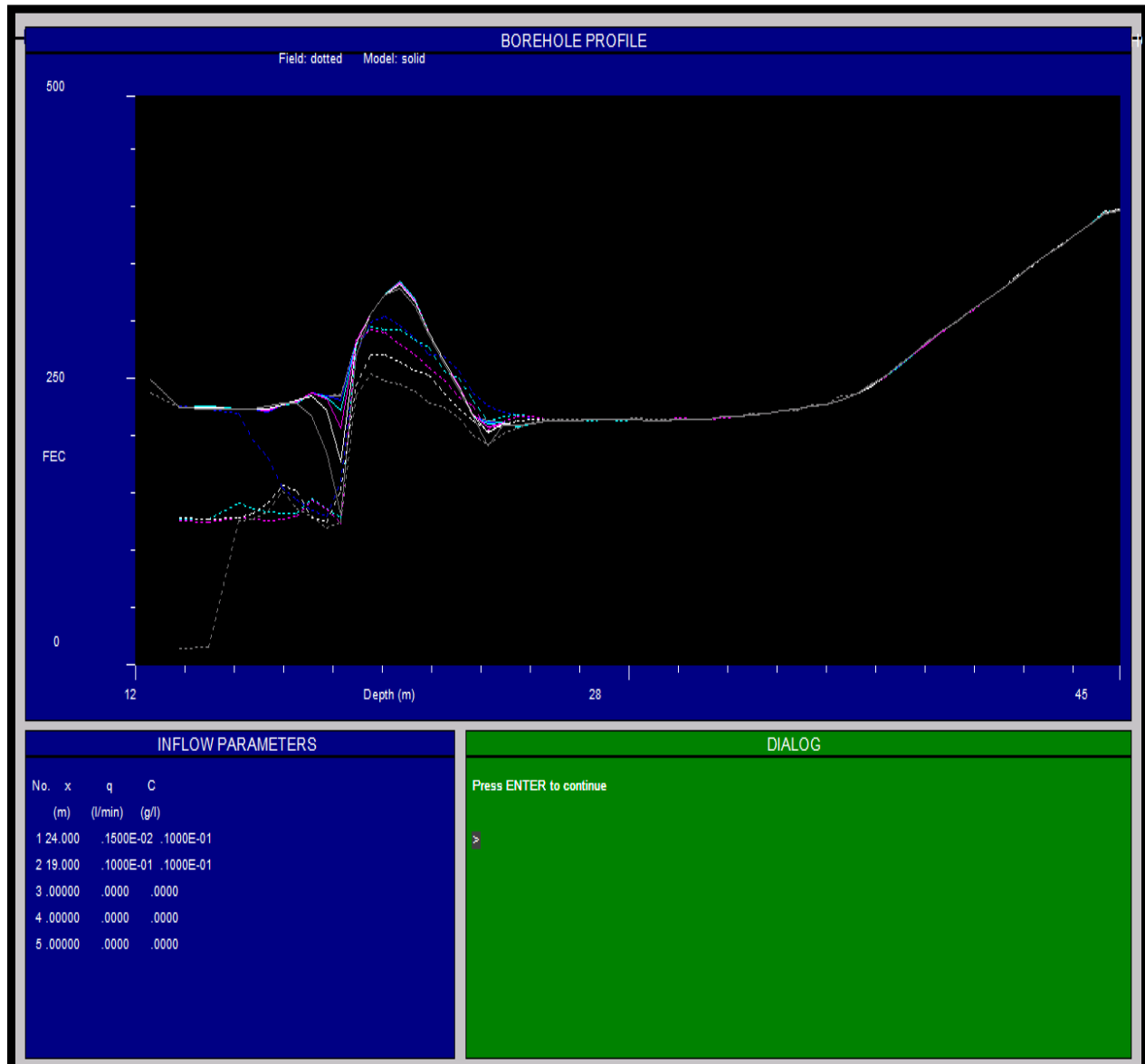


Figure 0-13 Example of BORE II results simulation for UP15

## APPENDIX E

## WATER QUALITY AT PARADYS

Site Name	pH	EC (mS/m)	TDS (mg/ℓ)	Ca (mg/ℓ)	Mg (mg/ℓ)	Na (mg/ℓ)	K (mg/ℓ)	PALK (mg/ℓ)
BH1	7,51	89	625	67	26	76	8,74	0
Bh3	7,43	96	671	86	42	52	2,36	0
Site Name	MALK (mg/ℓ)	Cl (mg/ℓ)	SO <sub>4</sub> (mg/ℓ)	NO <sub>3</sub> (mg/ℓ)	Al (mg/ℓ)	Fe (mg/ℓ)	Mn (mg/ℓ)	NH <sub>4</sub> (mg/ℓ)
BH1	288	70	33	12,45	<0,004	0,012	0,002	0,30
BH3	274	88	113	2,86	0,010	0,023	0,005	0,020
Site Name	As (mg/ℓ)	Cd (mg/ℓ)	Cu (mg/ℓ)	Pb (mg/ℓ)	Zn (mg/ℓ)	<i>E.coli</i> (mg/ℓ)	Total coliforms (mg/ℓ)	SAR
BH1	<0,006	<0,001	0,008	<0,015	0,009	<1	2	1,997
BH3	<0,006	<0,001	0,008	<0,015	0,010	<1	>200,5	1,149

## SUMMARY

Fractures are mechanical ruptures in rocks, form by stress (lithostatic, tectonic, and thermal stresses and high fluid pressures) concentrations around flaws, heterogeneities, and physical discontinuities at a variety of scales. In groundwater reservoirs, mainly in those formed within relatively less permeable or hard rocks, connected fractures may form privileged conduits for fluid flow and solute through the rock, and therefore needs to be located and quantitatively (geometry, permeability, and ability to transport solute) appreciated for a better understanding of water flow and mass transport processes in the subsurface. Many techniques have been adapted from petroleum applications to address these issues and are reviewed in the present study with after an overview on geological and geo-mechanical features that evolve fracturing.

Very few existing tools are cost-effective and easy to be performed on the field. The FEC (Fluid Electrical Conductivity) based techniques; mainly the single borehole based ones involve often, relatively cost effective equipments and are simple. The present study focus also on the applicability of "Flowing Fluid Electrical conductivity logging" (Tsang et al., 1990; Doughty et al., 2005) and the FEC based dilution test (well dilution) for fracture characterization in the Karoo aquifer. The FFEC is found to be a promising technique for local fracture characterization, mainly in contamination studies (investigation and scenario testing), like in mine environments; and is recommended to be experienced in South-Africa, particularly in the meta-sediments of the Karoo environment. The FEC based dilution test (well dilution) is gaining interest in fracture characterization in South Africa (Mohr Samuel and van Biljon Willem., 2009; Lasher Candice et al., 2009) and has been assessed on two experimental fields in the Karoo Aquifer. The technique is found to constitute a powerful tool for detection of flowing fractures and for qualitative interpretation. The Drost et al (1968) analytical solution suggested for the analysis of the test data (Cook et al., 2001a; Love et al., 2002) have been applied and yielded semi-quantitative values that can be used as first estimation of the groundwater velocity from flowing points into the studied boreholes. However, due to non ideal condition, refinements are still needed mainly for the field procedure

and for the consideration of the mass circulation that may be associated with density gradient along the borehole.

**Key words:** Karoo, fractures, Characteristics, Electrical conductivity, Tracer concentration, dilution.